NRL Memorandum Report 1513

MEASUREMENTS ON FREE-FLOODED MAGNETOSTRICTIVE RINGS

J. Chervenak

SOUND DIVISION

March 17, 1964

U. S. NAVAL RESEARCH LABORATORY
Washington, D.C.

CONTENTS

ABSTRACT

Magnetostrictive ring transducers are rugged and relatively insensitive to hydrostatic pressure when used in a free-flooded condition. Therefore, arrays of this type of transducer are ideally suited for deep submergence applications provided acoustic beam directionality is not required.

This report is concerned with measurements which show how spacing between free-flooded coaxially mounted rings in a line array affects acoustic beam patterns, bandwidth, and efficiency. Information on individual rings is provided as an aid to a better understanding of some measurements made on the array.

PROBLEM AUTHORIZATION

SF 001-03-18-8047 and RF 001-03-44-4051
NRL Problem 55S02-06

PROBLEM STATUS

This is an interim report on one phase of the project.
Work is continuing.

INTRODUCTION

One solution to the problem of reliable deep submergence transducer arrays may be the use of magnetostrictive rings arranged in an array configuration that will provide directional acoustic beams without the use of pressure release materials or reflectors. Magnetostrictive ring transducers are rugged, simple in design, and insensitive to hydrostatic pressure when used in a free-flooded condition. However, both experimental data and mathematical formulations necessary for rapid development of directional ring arrays are just in the acquisition stage. Preliminary measurements[1] indicate that efficiency, bandwidth, and beam patterns may be varied within certain limits by arrangement of transducer elements. Data presented in this report show how the operating characteristics of a line array of ring transducers change as the spacing between rings is varied. Some of the beam patterns obtained for the array had an asymmetry that might be ascribed to some spurious mode of vibration of the rings. Therefore, measurements were made of the modes of vibration of each ring and some unexpected results were obtained. This information should be useful to the designer in devising better ring fabricating techniques, to the mathematician in deriving equations for a more realistic model, and to the reader in comprehending some of the data presented.

Measurements reported are divided into four parts. Part I includes all the data obtained for the magnetostrictive rings operating in air and consists of impedance circle information and modes of vibration for each ring. Part II includes preliminary measurements made at the U. S. Naval Ordnance Laboratory, Brighton Dam Facility on free-flooded rings and rings with ends sealed to enclose an air cavity. Information is given on 1 to 4 rings in various arrangements. Parts III and IV contain data obtained at the U. S. Naval Research Laboratory Lake Seneca Transducer Calibration Platform. Two different transducer arrays of free-flooded, coaxially mounted, magnetostrictive rings were used in these measurements. In Part III, the length of the array was held constant and the number of rings was varied from 2 to 12. In Part IV, the number of rings was held constant at 12 and the length of the array was allowed to vary.

MEASUREMENTS ON FREE-FLOODED MAGNETOSTRICTIVE RINGS

Part I

This section contains a description of the magnetostrictive rings and information on measurements made when the rings were operated in air. The magnetostrictive rings were scroll wound from 0.005 inch thick cobalt-nickel strip consolidated with an epoxy resin and wound with a single layer of 195 turns of a No. 18 copper wire which was then covered with a layer of epoxy resin. The final waterproofing covering of each ring was a brushed-on coating of a rubber compound. Overall dimensions of each ring were: Inside diameter 5-3/8 inches, radial thickness 0.5 inch and axial length 5/8 inches.

In Part II of the measurements, two different lengths of rings were used; one was the 5/8 inch length of the ring element described above and one was a 1-7/8 inch length obtained by bonding three of the ring elements together. Impedance circle data on both sizes of rings operating in air were generally similar. However, the mechanical Q for the longer ring was less. This was due to the increase in mechanical losses caused by bonding together three slightly dissimilar rings. Impedance circle information on each of twelve 5/8 inch long rings operating in air is given in Table I. Maximum variation in resonant frequency is 325 cycles per second or approximately 3.8% of the lowest frequency. A variation of approximately 100% in the mechanical Q indicates considerable non-uniformity in the fabrication process. This could be due to a single or a combination of such factors as processing of the core material of the ring, consolidating the scroll, or applying the electrical winding. The variation in the potential efficiency based on the maximum value of 79% is 7.2% and the change measured in the effective coefficient of electromechanical coupling varies from 0.23 to 0.31 or approximately 26% of the higher value. Clamped reactances and complex impedances of the rings are also tabulated so that the variations may be noted.

TABLE I

Impedance Circle Data for Single Magnetostrictive Rings Operating in Air

D.C. = 0.5 Amps.

Ring No.	f_r	f_1	f_2	Q	P.E.	K	x_c	Z_r
1	8750	8680	8870	46.0	77.5	.30	88	360-j46
2	8920	8848	8985	65.0	76.4	.26	87	377-j38
3	8880	8800	8960	55.5	76.0	.28	87	362-j44
4	9040	8980	9090	82.0	78.0	.24	70	317-j22
5	8895	8820	8970	59.2	77.0	.27	79	346-j28
6	8758	8670	8840	51.5	79.0	.31	75	366-j39
7	9012	8960	9060	90.0	78.0	.24	60	322-j12
8	8797	8705	8887	48.2	73.3	.30	85	365-j50
9	8823	8755	8885	68.0	76.5	.25	90	379-j42
10	8742	8648	8840	45.5	78.0	.30	92	371-j47
11	9075	9020	9130	82.5	76.0	.23	72	312-j25
12	8857	8760	8952	46.0	79.0	.30	85	339-j38

Where

f_r = Resonant frequency in cycles per second

f_1 = Lower quadrantal frequency in cps

f_2 = Upper quadrantal frequency in cps

Q = Mechanical Q in air, $Q = \frac{f_r}{f_2 - f_1}$

K = Effective Coefficient of electromechanical coupling

x_c = Ohms clamped reactance of electromechanical system

Z_r = Ohms impedance at resonance

P.E. = Potential Efficiency in percent

Arrangement of Rings in 12 Ring Arrays	8742 ~	8758 ~	8823 ~	8880 ~	8920 ~	9075 ~	9040 ~	9012 ~	8895 ~	8857 ~	8797 ~	8750 ~
	No. 10	No. 6	No. 9	No. 3	No. 2	No. 11	No. 4	No. 7	No. 5	No. 12	No. 8	No. 1

Modes of vibration of rings operating in air were investigated by means of accelerometer probes and sand patterns. In the former method, one accelerometer was located on a fixed spot while the other was used to probe around the ring. Both accelerometer outputs were displayed simultaneously in proper phase relationship on a Tektronix scope. It was noted that the radial displacements over a wide frequency range (4000 to 9000 cps) were in phase. Accelerometer probings over the same frequency range but taken along the annular or end section of the ring disclosed flexural vibrations which varied from complicated patterns to those which could be represented by as high as 5 phase reversals of displacements. Information on some flexural vibrations are given in Table II. During the course of measurements on various array arrangements operating in water, peak transmitting current responses occurred at frequencies ranging from 6000 to 8400 cps. These frequencies are among those for which flexural modes of vibration were recorded.

Table II shows that not all 12 rings had the same number of phase reversals at the same frequency or, in fact, near the same frequency. These variations which may be due to differences in material and fabrication techniques may be responsible for some of the asymmetric beam patterns obtained in measurements made in water. The variation in the radial resonant frequency noted at the bottom of Table I can also generate asymmetric beam patterns.

Differences in flexural modes of vibration are also indicated by the sand patterns of Figures 1 and 2 for magnetostrictive rings number 2 and 4 respectively. The sharpness of the sand pattern is represented by the sharpness of the sketch. Where the patterns were drawn sharp and clear cut there was very little movement of sand at the nodes. Less sharp patterns indicate more movement of sand in the node area. Nodes represented by dots indicate considerable movement of sand in a direction perpendicular to the plane of the ring. Arrows on the patterns of Figure 2 indicate the direction of sand movement before the formation of the nodes. Unsymmetric patterns indicate unsymmetric stresses or spurious modes of vibration which would contribute partly or wholly to break-down at high driving powers.

TABLE II

Accelerometer Data on Flexural Vibrations of Magnetostrictive Rings

Ring No.	Number of phase reversals observed around the side of a ring. For frequencies of: 4000 cps	6000 cps	7000 cps	8000 cps	8200 cps	8400 cps	8800 cps	9000 cps
1	4	4	3	5	5	5	0	0
2	4	0	2	3	4	4	0	0
3	4	2	4	3	5	5	0	5
4	4	2	4	5	5	5	3	3
5	0	2	4	3	0	5	5	3
6	4	1	2	3	4	4	0	3
7	4	0	2	3	4	4	5	5
8	4	0	4	5	4	5	5	5
9	4	4	2	3	4	5	5	0
10	4	1	2	3	4	5	5	5
11	4	0	2	3	4	5	5	5
12	4	2	4	3	4	5	5	5

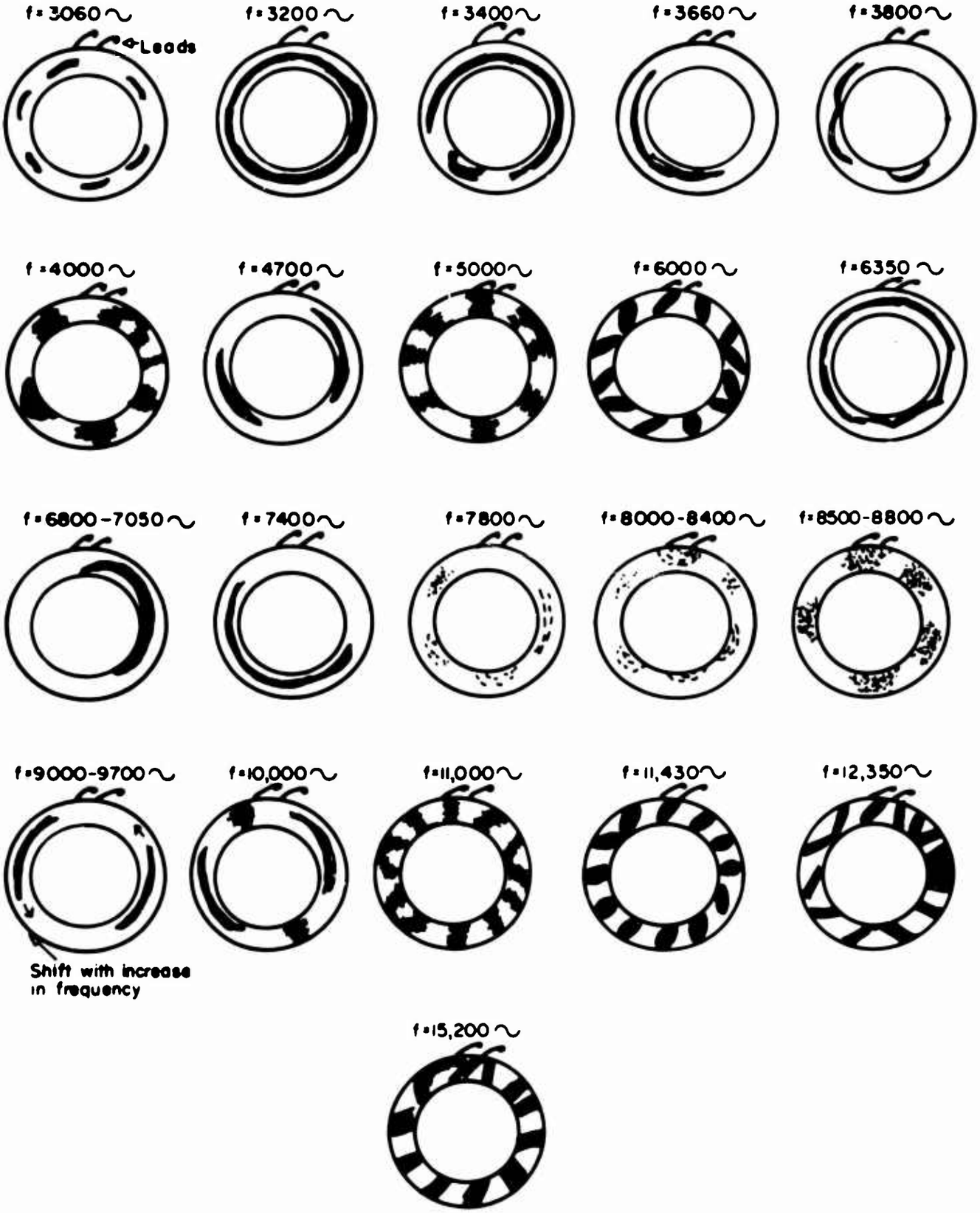

Figure 1 - Sand Patterns Ring No. 2

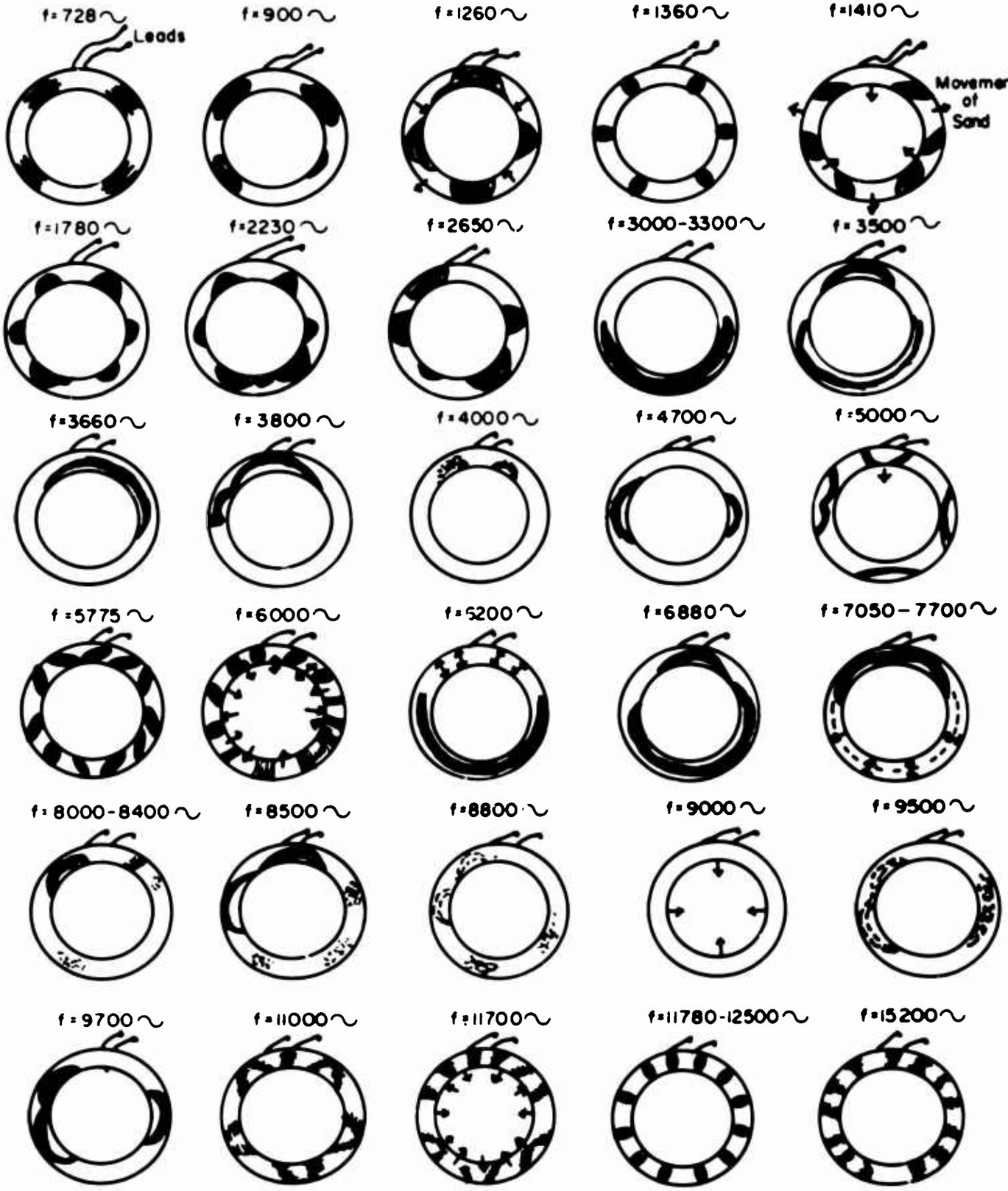

Figure 2 - Sand Patterns Ring No. 4

In summary, the measurements of Part I show how the dynamic characteristics of 12 magnetostrictive rings vary. Measurements made in air indicate that a fundamental radial mode of vibration is coupled with a higher order flexural mode at frequencies which produce peak acoustic responses in water. The flexural mode of vibration is complicated by a spurious mode tendency induced by fabrication differences in individual ring structures.

Spurious modes of vibration should be eliminated by improving fabricating techniques. Optimum efficiency could be realized by changing the ring design to separate higher orders of flexural modes from the fundamental radial mode of vibration or alternatively, the rings might be used in a configuration in which the two modes would complement each other to produce a desired acoustic beam pattern.

Part II

Preliminary measurements on a few magnetostrictive rings were made at the U. S. Naval Ordnance Laboratory Transducer Calibration Station located at Brighton Dam, Maryland. All measurements were made at a depth of 21 feet, in water 46 feet deep. Two lengths of magnetostrictive rings were used: a short or 5/8" length and a long or 1-7/8 inch length which was obtained by rigidly consolidating three of the 5/8 inch long rings. Data was obtained on long rings which:

1) Were free-flooded and closely stacked,
2) contained air cavities and were closely stacked,
3) contained air cavities and were separated by baffles 3/4 wavelength long.

Data was also obtained on closely stacked, free-flooded, short rings and on short rings which were separated by a 1/4 wavelength distance. Air cavities for long rings were formed by bonding a circular sheet of rubber 1/16 inch thick to each side of the ring and then bonding a 1/16 inch thick aluminum plate over the rubber. The plates were sufficiently rigid to maintain the cavity in water and the rubber was sufficiently elastic to permit radial vibration of the ring without undue damping by the plates.

Results of measurements made are given in Table III. The meaning of the symbols heading the columns of this table are as follows:

S = Transmitting Current response in db vs 1μbar per ampere at 1 meter.

f = Frequency in cycles per second at peak response.

R = Ohms resistance of array at peak response.

B.W. = Bandwidth in cycles per second between two points which are 3 db down from peak response and are located on the transmitting current response curve.

D.I. = Directivity Index in db.

Eff. = Efficiency in percent.

Bandwidth is used in preference to mechanical Q in water in these measurements because the impedance circles for various arrangements are distorted and contain spurious loops. Therefore, mechanical Q as obtained from impedance circles and the relationship $Q = \frac{f_r}{f_2 - f_1}$ would be difficult to determine and would not correspond to the mechanical Q's obtained from response curves. Values of resistance at peak transmitting response were obtained from measurements made on a General Radio Z-Y Bridge.

Efficiencies were calculated from the following standard equation.[2],[3]

$$\text{Eff} = \frac{\text{Acoustic Power}}{\text{Electric Power}} = \frac{4\pi r^2 . p^2 / Z / 2 \, 10^{-7}}{\rho c . R. / E / 2 \, (D.F.)} \qquad (1)$$

$$\text{Eff} = \frac{4\pi r^2 . p^2 . 10^{-7}}{(\rho c) . I^2 . R. (D.F.)} \qquad (2)$$

$$10 \log \text{Eff.} = S - 10 \log R - \text{D.I.} - 70.6$$

For fresh water, $\rho c = 1.45 \times 10^5$ gms/cm^2 sec.

r = 1 meter or 100 centimeters

p = Pressure on principal acoustic axis corrected to a distance of 100 centimeters.

ρc = Specific acoustic resistance of water

I = Current at input terminals

D.F. = Directivity factor(3)

The first section of Table III contains data on 1, 3, and 4 long magnetostrictive rings operating free-flooded and with air cavities. As the number of rings, in either case, is decreased the transmitting current response drops but the directivity index and resistance also drops to give maximum efficiency when a single long ring is used. The operating bandwidth in water for the free-flooded condition varies most and is highest for a single long ring. Figure 3 shows a smooth transmitting current response curve for one long ring with an air cavity. Figure 4 shows a horizontal beam pattern which was taken at the frequency of peak response. The acoustic energy radiated along the principal or broadside axis (labeled $\theta = 0°$ on the patterns) is 2 db less than along the ring axis. Radial patterns for this, and all other ring arrangements were essentially circular. Figure 5 shows a transmitting current response curve for a long single free-flooded ring. The curve has a double peak which may be due to mechanical differences between the three bonded rings comprising that element. The beam pattern in Figure 6 was taken at 5900 cps and is for the response peak at the lower frequency. Two minor lobes located on the ring axis are 10 db down from the principal lobes. The beam pattern for the response peak at 8300 cps is of dipole form as shown in Figure 7. No minor lobes are evident and the acoustic energy along the ring axis is 20 db down.

TABLE III

Measurements Made At Brighton Dam

No. of Long Rings	S db	B.W. cps	D.I. db	R ohms	f_r cps	Eff. %	Rings Stacked
Air Cavity Center							
4	94.4	3600	4.9	260	8300	29.5	Close
3	92.8	3450	4.4	190	8400	31.6	"
1	86.8	2650	1.4	68	7500	44.6	
Free-Flooded Center							
4	94.3	1800	2.6	335	8300	38.0	"
3	91.2	2450	2.9	210	8300	28.0	"
1	86.7	3900	3.0	48	6000	42.7	2 Peaks
	86.1	4100	0.9	58	8300	50.0	
No. of Short Rings Free-Flooded							Rings Stacked
3	85.8	3900	1.1	40	7000	65.0	Close
3	91.5	1050	2.9	102	7700	63.0	2" Apart
1	87.5	850	1.0	70	7500	55.0	
No. of Long Rings with Air Cavities and 3/4 λ Baffles							
3 (Driven in phase)	95.2	1400	5.0	260	7250	35.0	
3 (Drive to center)	84.4	1000	0.95	90	5750	32.0	2 Peaks
3 (Ring Reversed)	82.0	4850	?.7	190	8000	13.0	

Note: Short rings are 5/8" long (axial length).

Long rings are 1-7/8" long = 3 short rings cemented together.

Transmitting current response curves and beam patterns for 3 and 4 large rings operating with air cavities and in a free-flooded condition are made available in Figures 8, 9, 10, 11, 12, 13, 14, and 15. Additional data is given in Table III. No special comments concerning these figures will be made except to note that differences between rings and differences in the resonant structure of a given ring show up as dissymmetries in the beam patterns.

When three short rings are loosely stacked to form one long ring, a smooth transmitting current response curve (Figure 16) is obtained for free-flooded operation. The bandwidth in water is 3900 cps and compares favorably with the 3900 and 4100 cps value given in Table III for the double humped response curve for one long free-flooded ring. The calculated efficiency of 65% is higher than the 50% value for the long ring. The beam pattern which is shown in Figure 17 is of dipole form and is similar to the pattern of Figure 7.

Response of three short coaxially mounted and free-flooded rings with a 2-inch separation between rings is shown in the curve of Figure 18. The bandwidth in water is 1050 cps compared to 3900 cps for the previous arrangement. The beam pattern of Figure 19 is similar to the preceding beam pattern but is not symmetrical along the ring axis. Calculated efficiency is 63%. The accuracy of this calculation as well as of the efficiency calculation for the following ring arrangement may be less than the other values given because the frequency of peak response as determined from the uncorrected transmitting current response curve was 500 cycles too high. The frequency of peak response turned out to be 7700 cps and the beam pattern was taken at 8200 cps.

Data on one short free-flooded ring as given in Table III shows that the bandwidth is only slightly less than for 3 short rings with a 2" separation between rings but considerably less than for 3 short rings stacked close together. Efficiencies for all measurements on the short rings are better than for the long rings. The transmitting current response curve for a short free-flooded ring is shown in Figure 20 and the beam pattern in Figure 21.

Concluding measurements for Part II were made as a spot check on calculations made by R. E. Faires concerning beam pattern formation by out-of-phase operation of point sources. For this test, three long magnetostrictive rings with air cavities were used in an arrangement where the rings were separated by 3/4 λ long baffles. The baffles were solid cylinders of aluminum with a diameter equal to the outside diameter of the rings. In the first measurement, the three rings were connected in series and driven in phase. Figure 22 shows the transmitting current response curve. A primary response peak occurs at 7250 cps and a subdued secondary peak at 10,000 cps. Pertinent information is given in Table III. An eight lobed beam pattern for this arrangement is shown in Figure 23. For the second part of the measurement, only one condition was changed; the center ring was driven 180° out-of-phase relative to the two end rings. The transmitting current response curve is shown in Figure 24. The principal response peak has retained the sharpness of the peak for the previous run but occurs at 5750 cps instead of 7250 cps. Efficiencies at both frequencies are essentially the same at 32 and 35%. The secondary response peak for the curve of Figure 24 is saddle shaped or double humped and the bandwidth of 4850 cps is much greater than the 1000 cps value measured for the principal peak, however, the efficiency of 13% is less than half of the 32% efficiency calculated at the maximum transmitting current response which occurred at 5750 cps. Beam patterns for response peaks at the lower and upper frequencies are shown in Figures 25 and 26 respectively.

In summary, measurements made in Part II indicate that as the number of closely stacked long magnetostrictive rings is decreased the efficiency increases. For long rings with air cavities, the bandwidth in water decreases as the number of rings are decreased. However, for long free-flooded rings the bandwidth increases as the number of rings is decreased. Data given in Table III on short rings suggests that it may be possible to arrange short free-flooded rings in a line array which will operate at high efficiency and broad bandwidth.

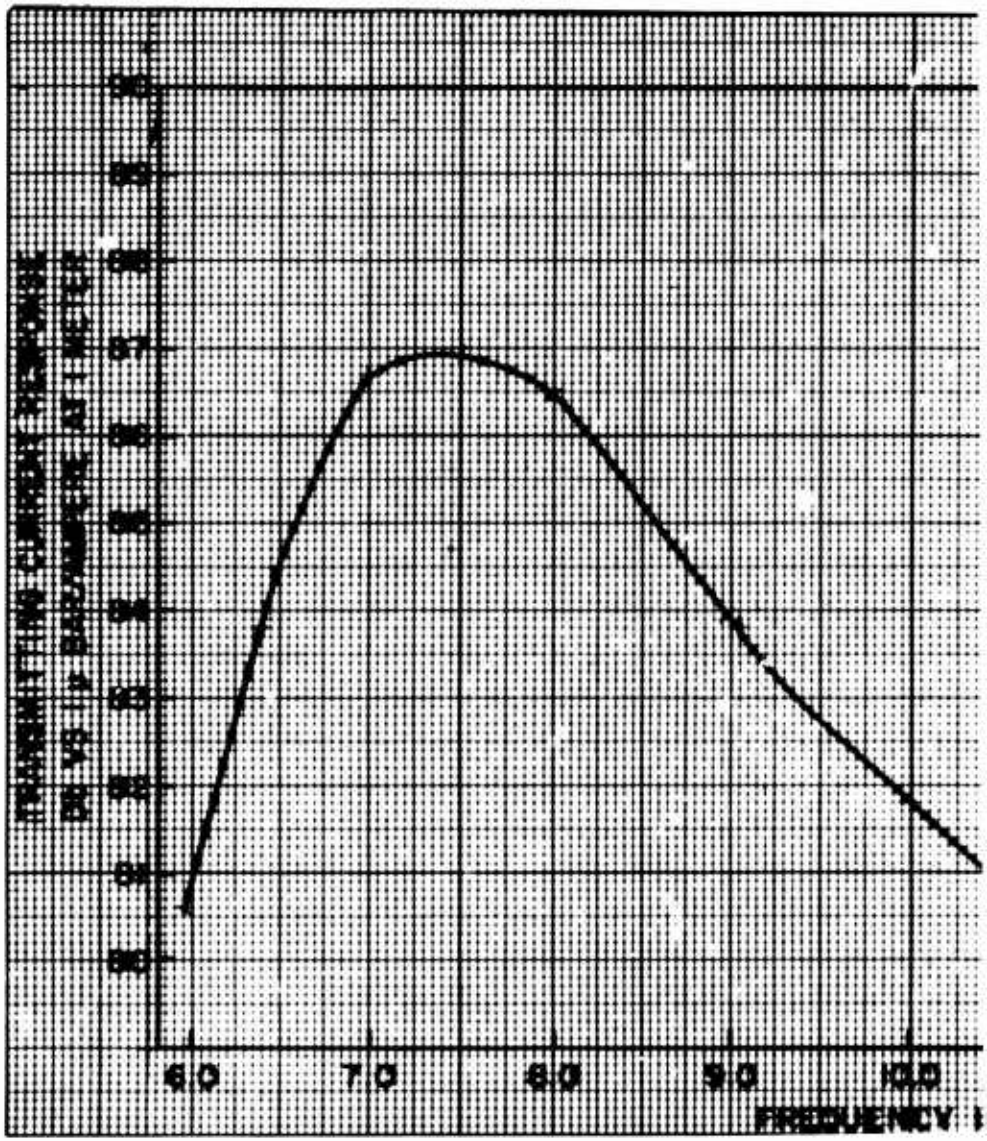

Figure 3. Transmitting Cur
1 Long Magnetostrictive Ri
Center.

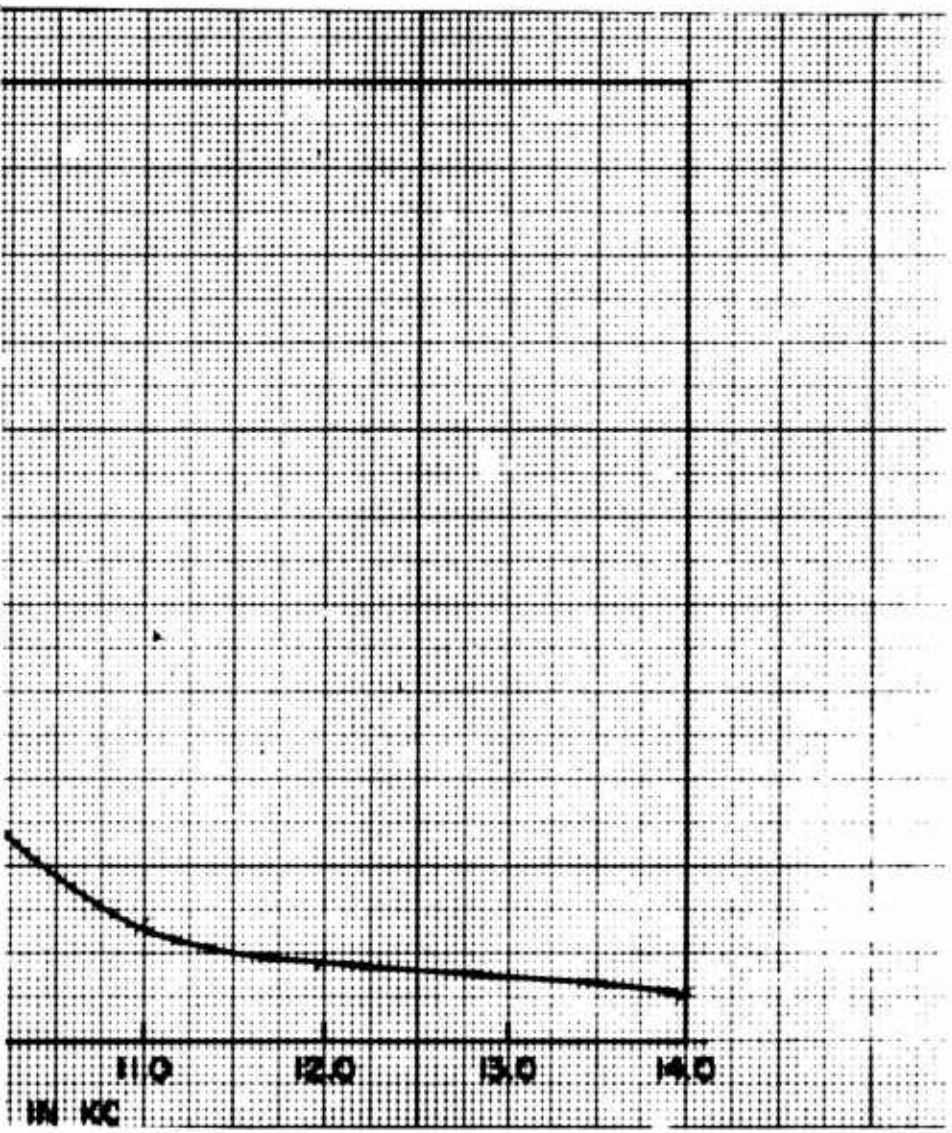

urrent Response Curve.
Ring with an Air Cavity

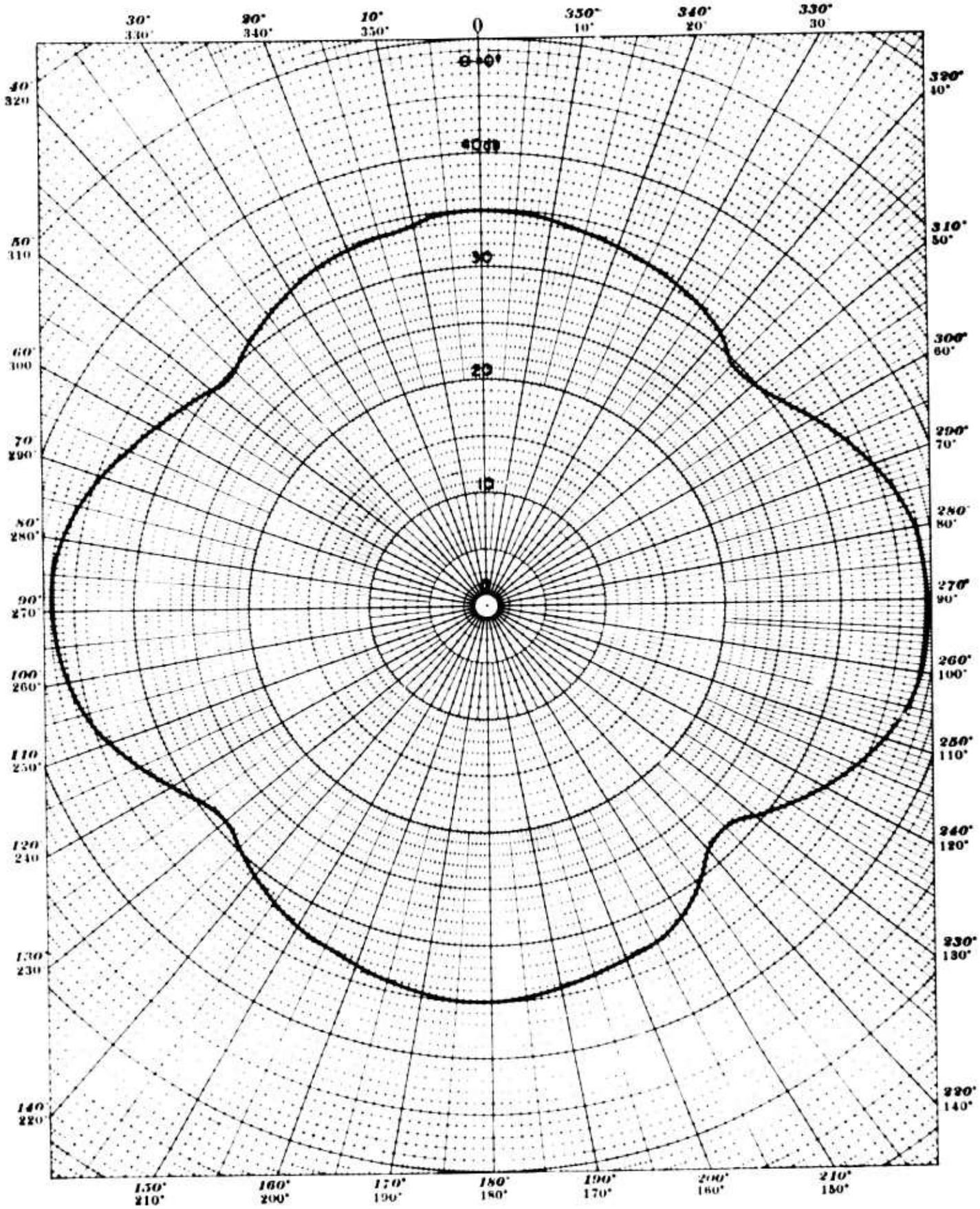

Figure 4. Directivity Pattern - 1 Long Magnetostrictive Ring with an Air Cavity Center

Frequency: 7400 cps—Test Distance: 1 Meter—Depth: 6.4 Meters

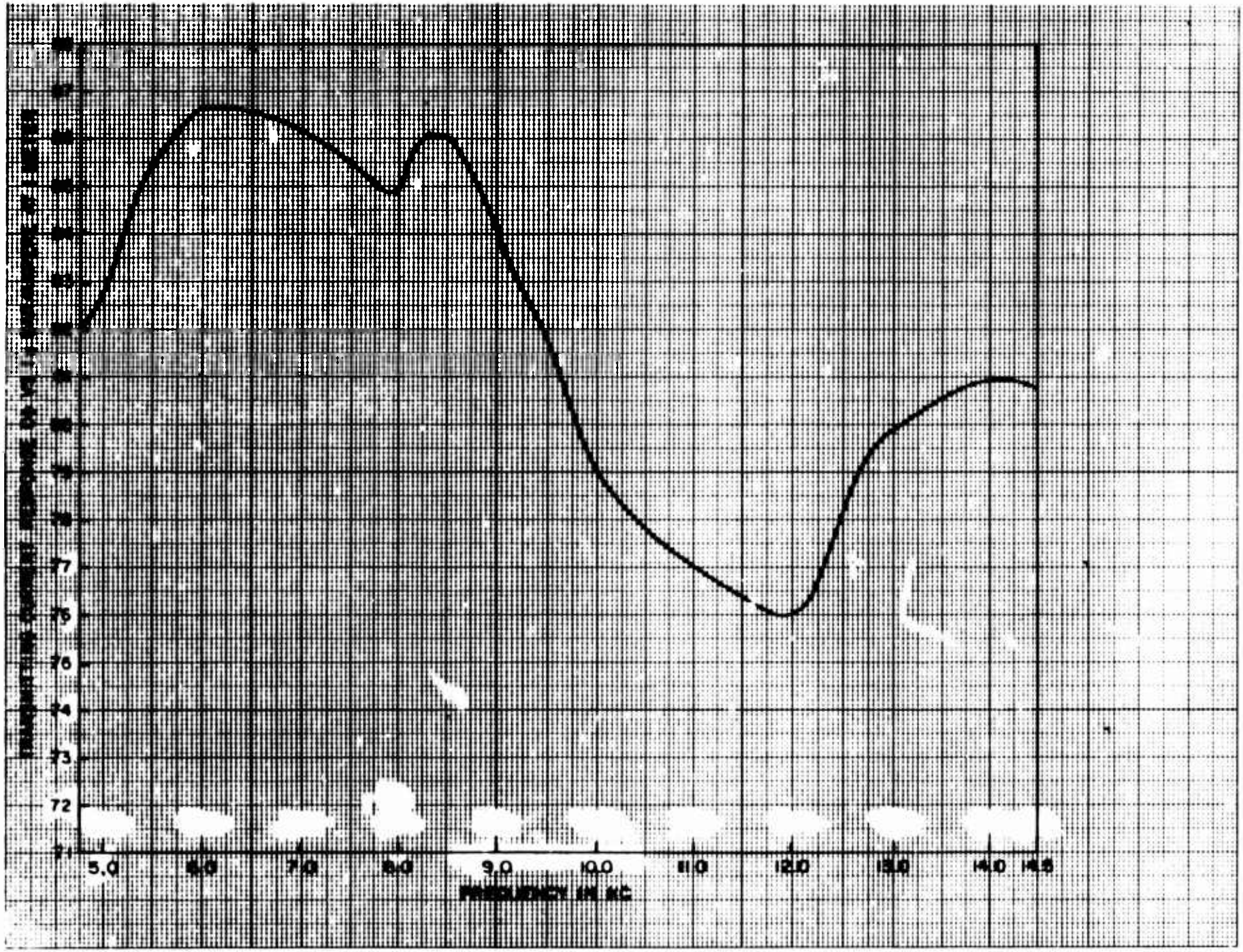

Figure 5. Transmitting Current Response Curve. 1 Long Magnetostrictive Ring with Free-Flooded Center.

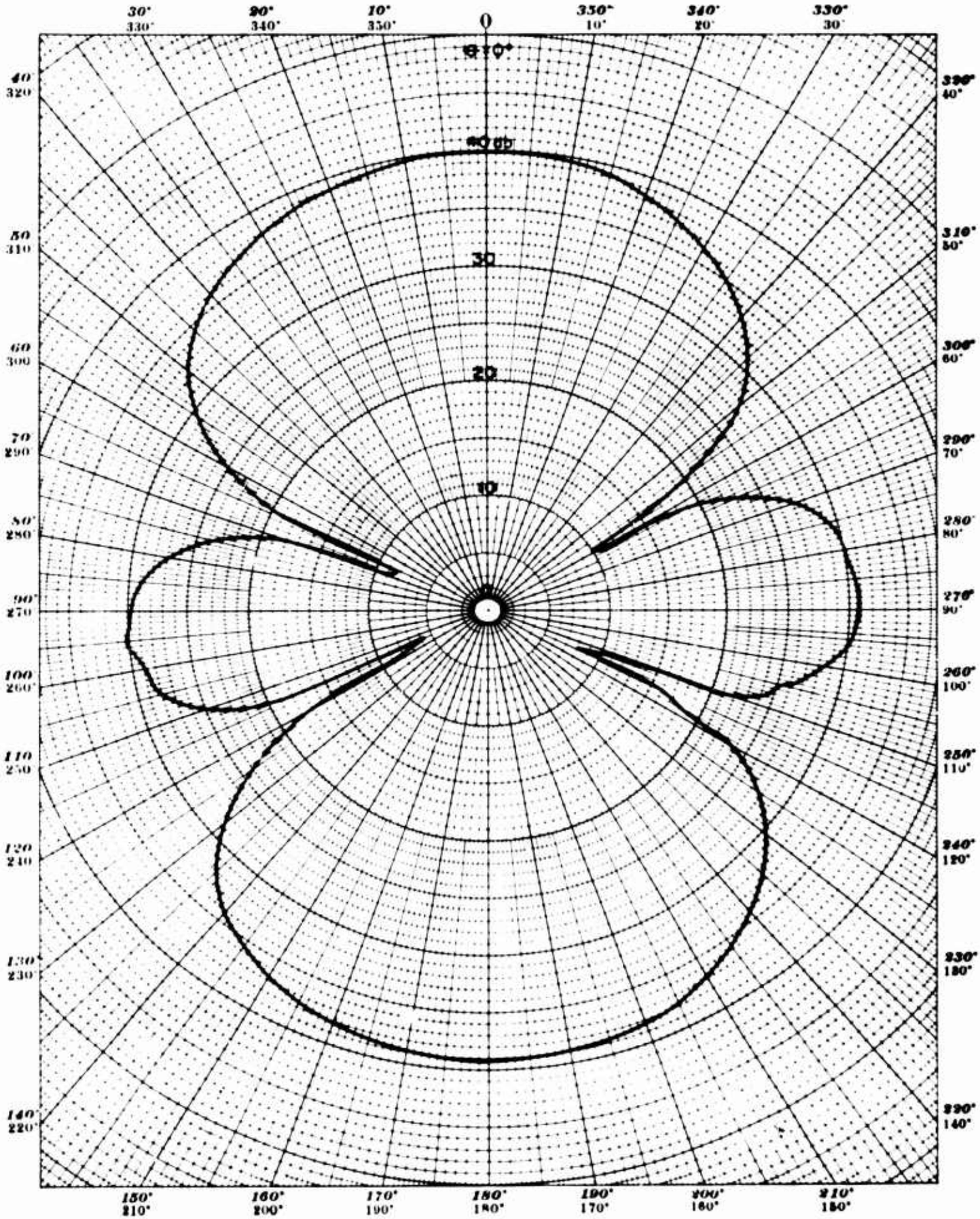

Figure 6. Directivity Pattern - 1 Long Magnetostrictive Ring with a Free-Flooded Center

Frequency: 5900 cps—Test Distance: 1 Meter—Depth: 6.4 Meters

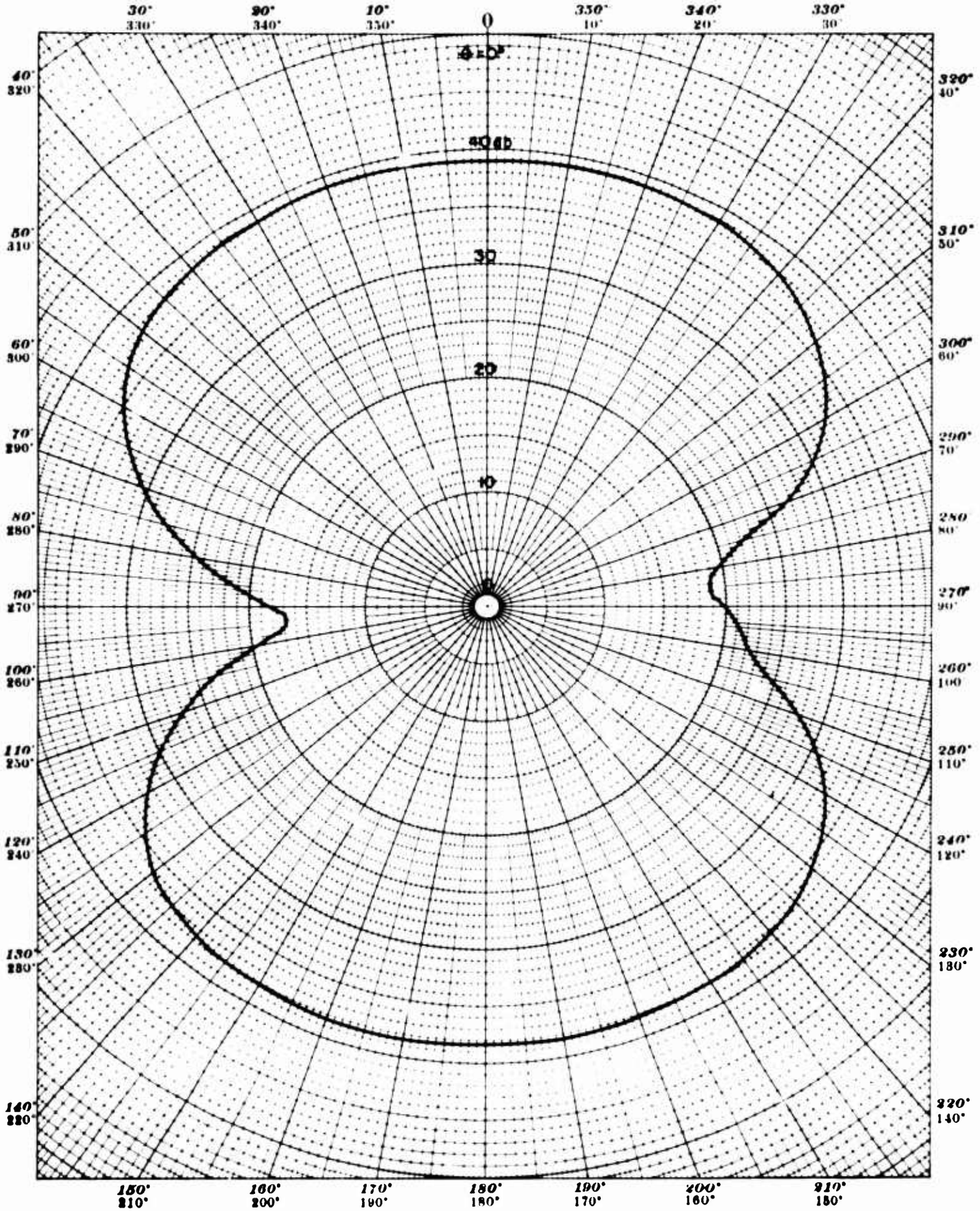

Figure 7. Directivity Pattern - 1 Long Magnetostrictive Ring with a Free-Flooded Center

Frequency: 8300 cps—Test Distance: 1 Meter—Depth: 6.4 Meters

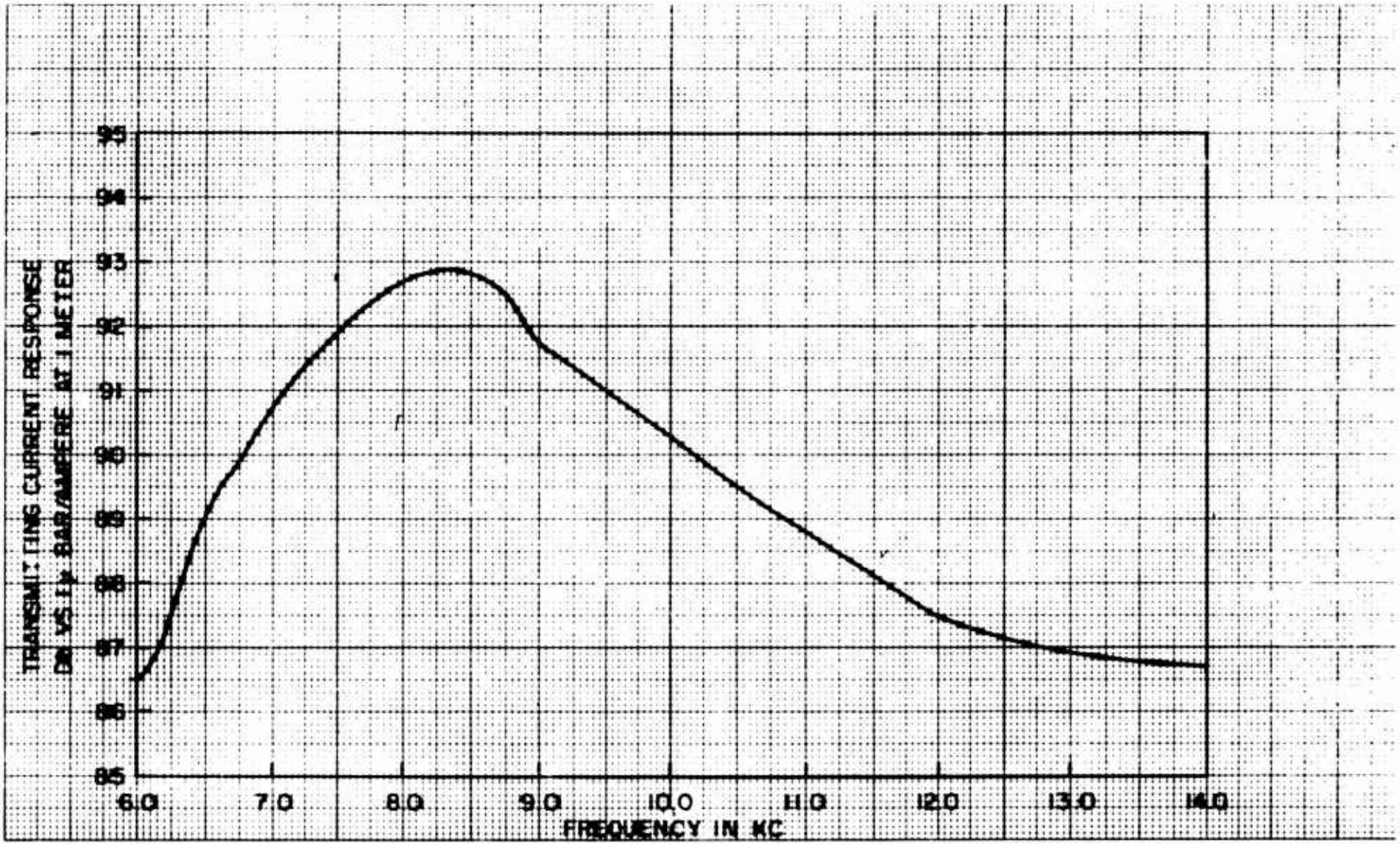

Figure 8. Transmitting Current Response Curve. 3 Long Magnetostrictive Rings with Air Cavity Centers. Rings Stacked Close Together.

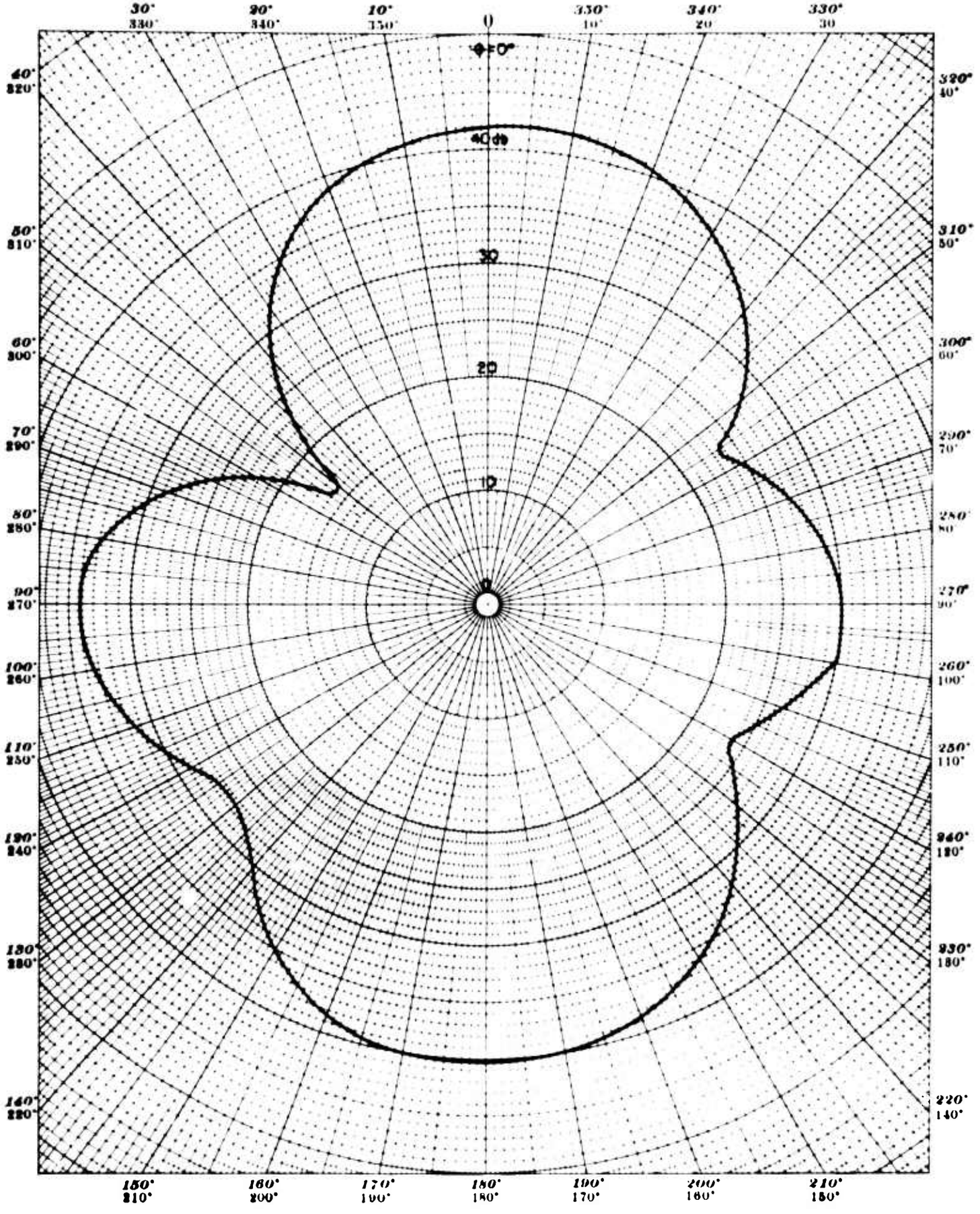

Figure 9. Directivity Pattern - 3 Long, Closely Stacked Magnetostrictive Rings with Air Cavity Centers

Frequency: 8200 cps—Test Distance: 1 Meter—Depth: 6.4 Meters

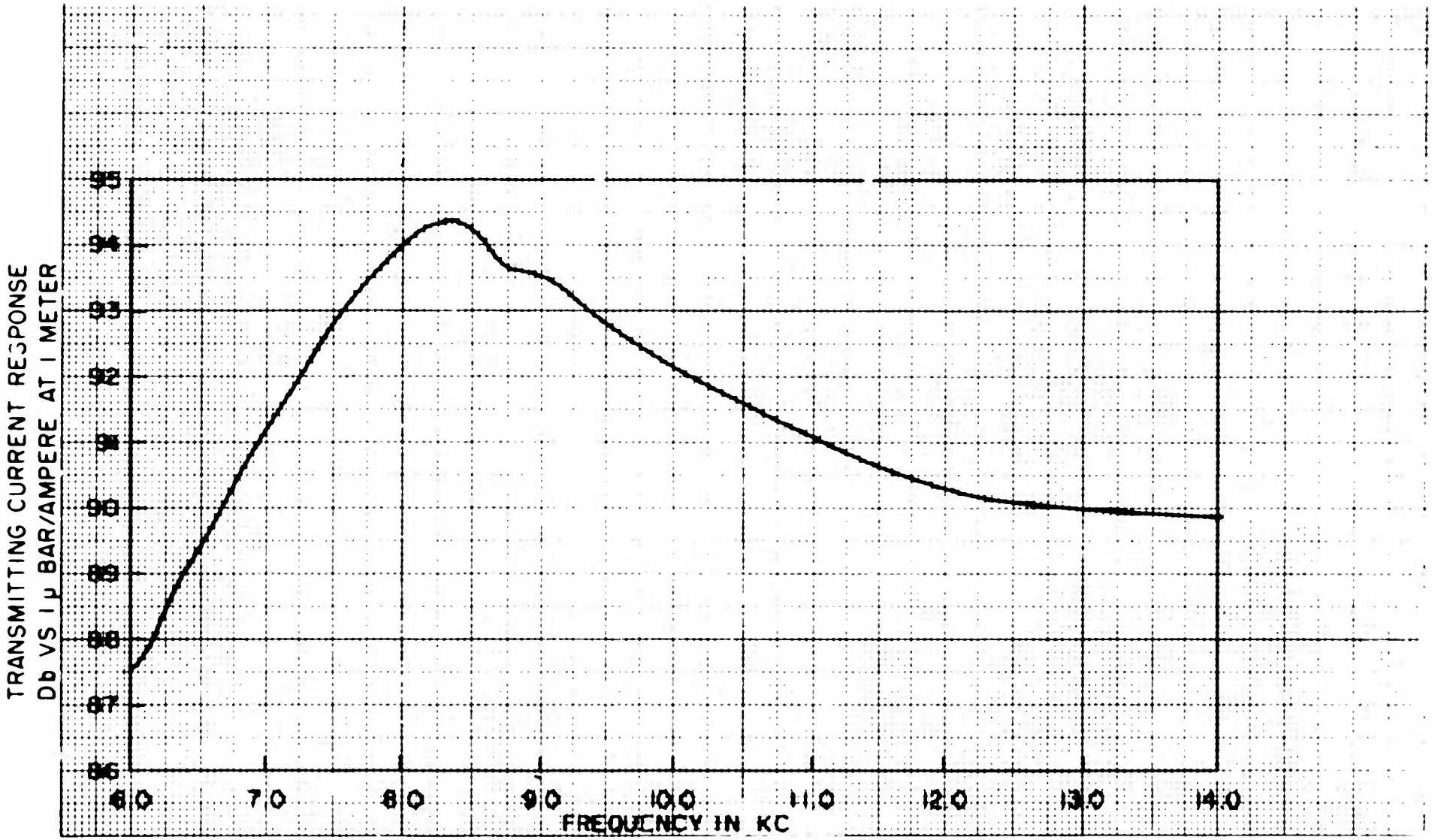

Figure 10. Transmitting Current Response Curve. 4 Long Magnetostrictive Rings with Air Cavity Centers. Rings Stacked Close Together.

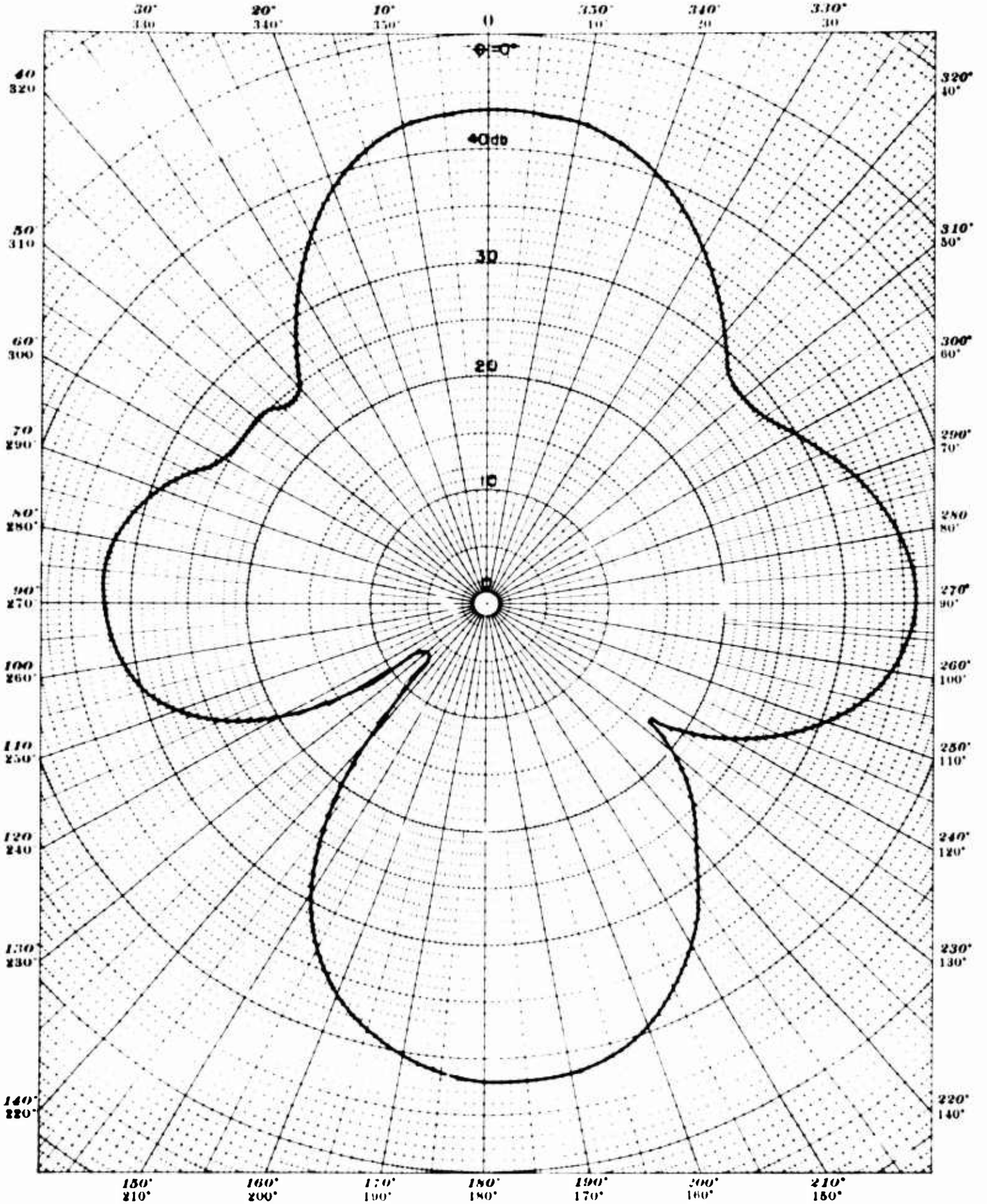

Figure 11. Directivity Pattern - 4 Long, Closely Stacked Magnetostrictive Rings with Air Cavity Centers

Frequency: 8300 cps—Test Distance: 1 Meter—Depth: 6.4 Meters

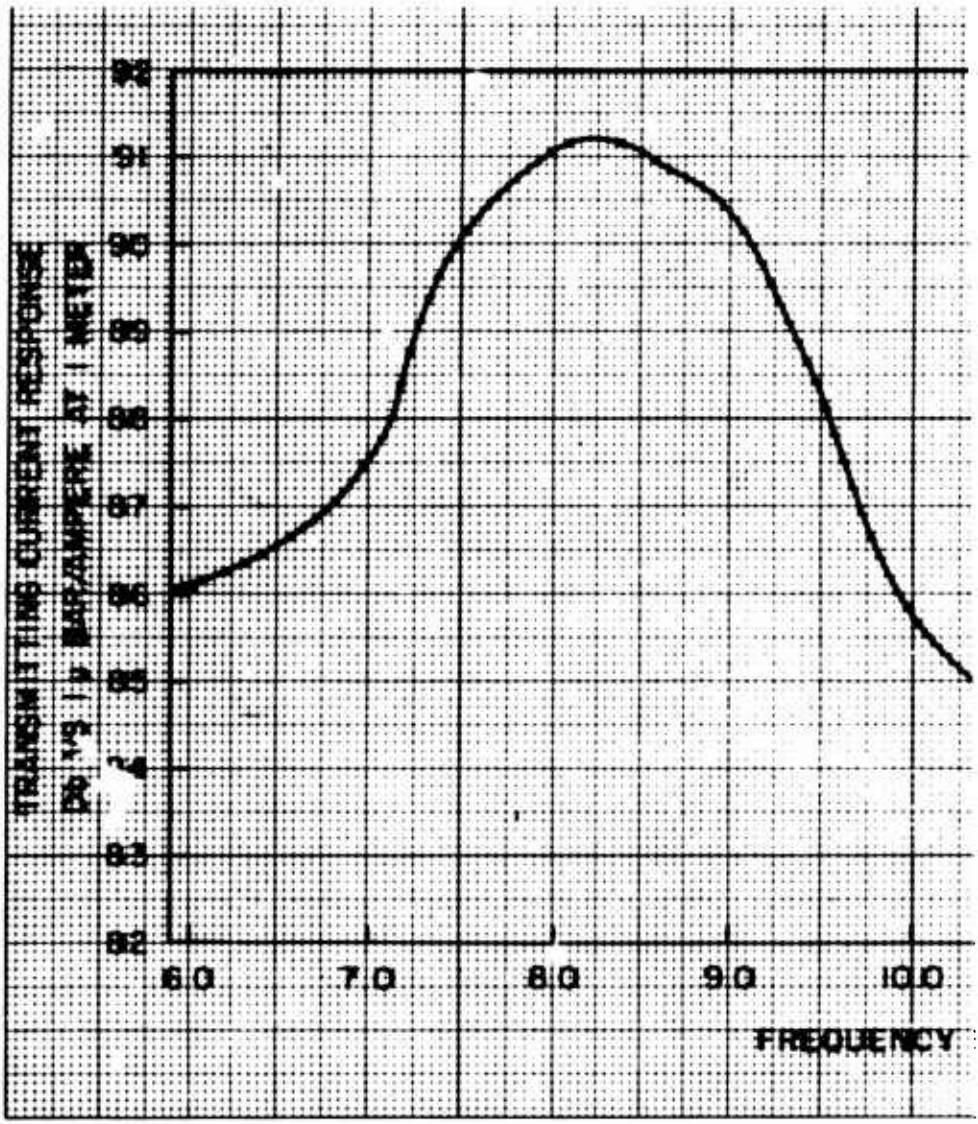

Figure 12. Transmitting C
3 Long Magnetostrictive R
Centers. Rings Stacked Cl

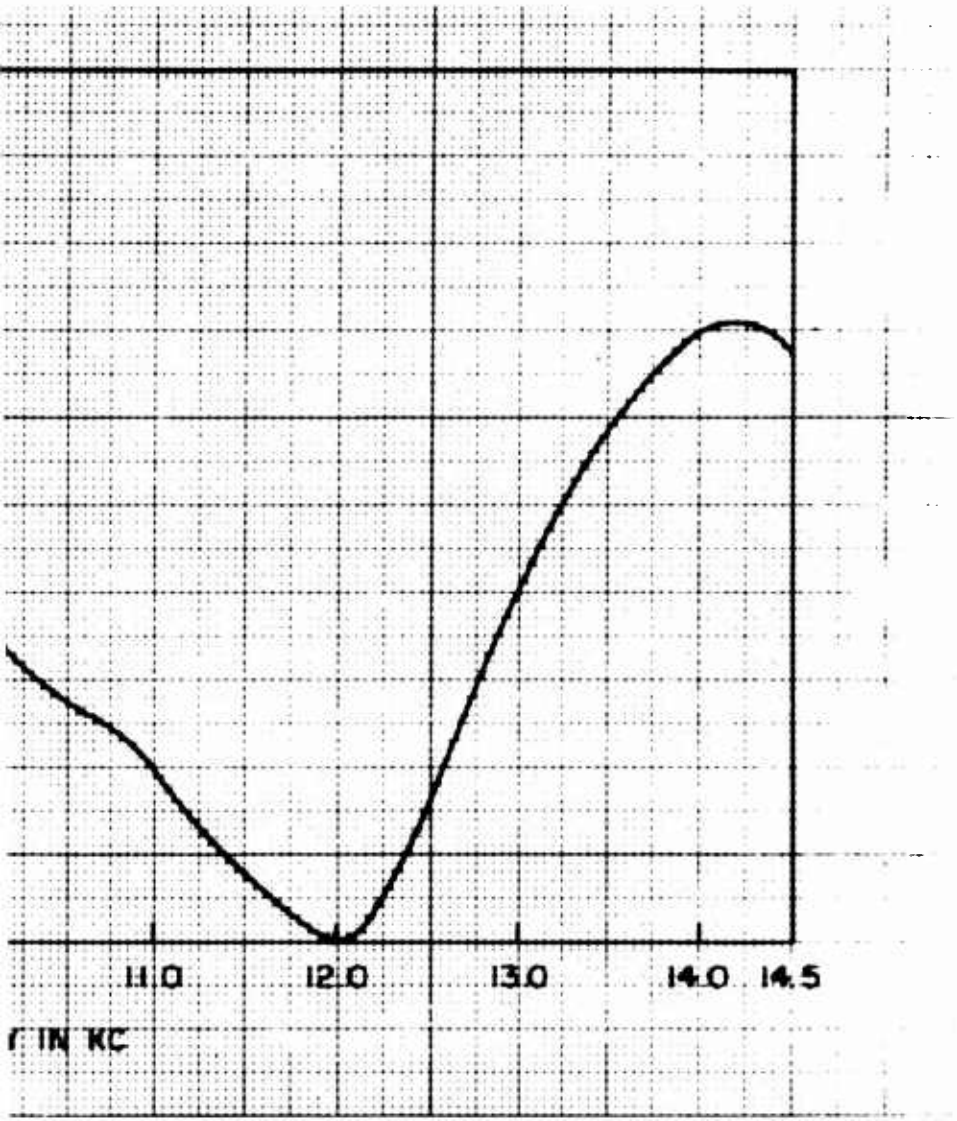

Current Response Curve.
Rings with Free-Flooded
Close Together.

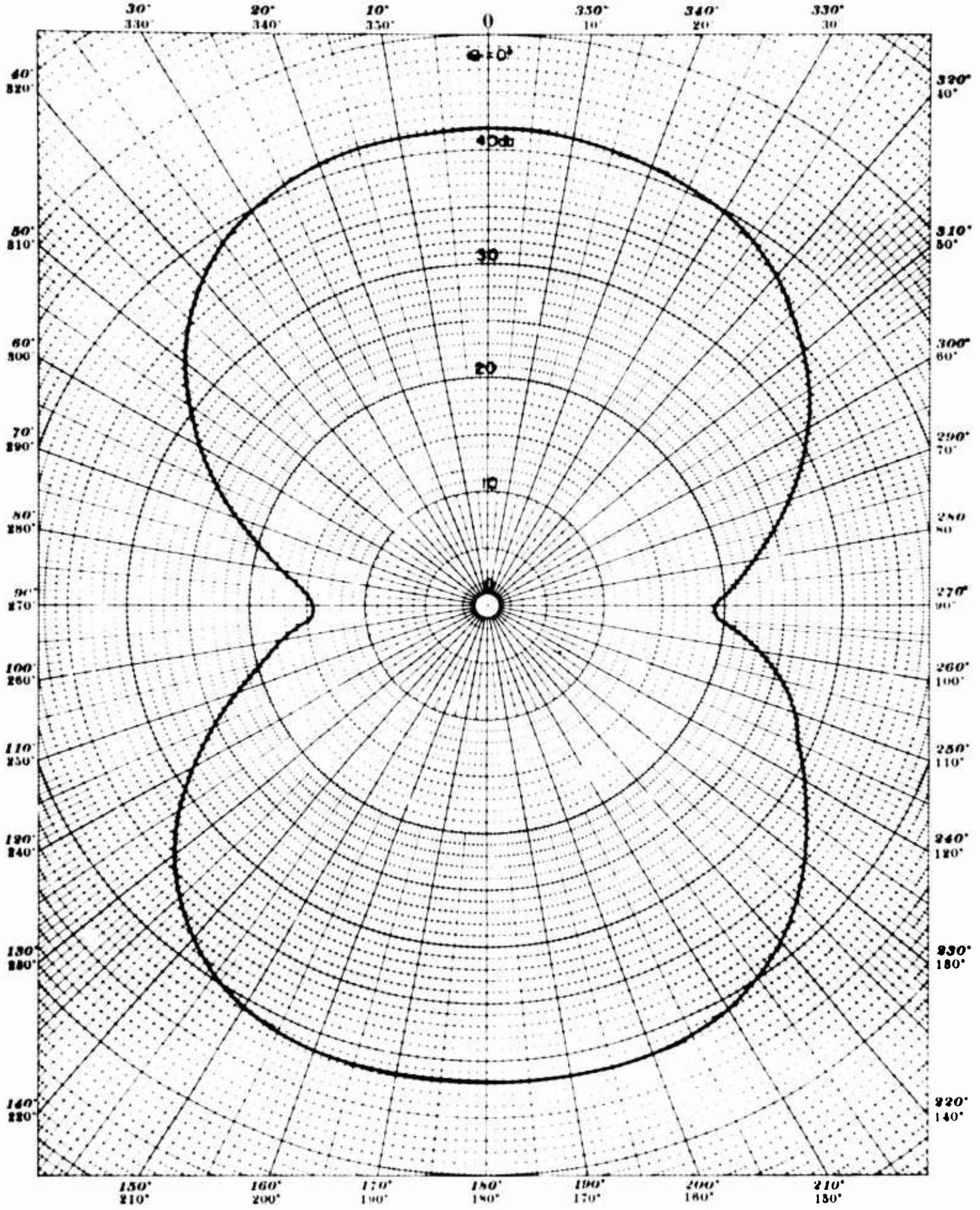

Figure 13. Directivity Pattern - 3 Long, Closely Stacked Magnetostrictive Rings with Free-Flooded Centers

Frequency: 8300 cps—Test Distance: 1 Meter—Depth: 6.4 Meters

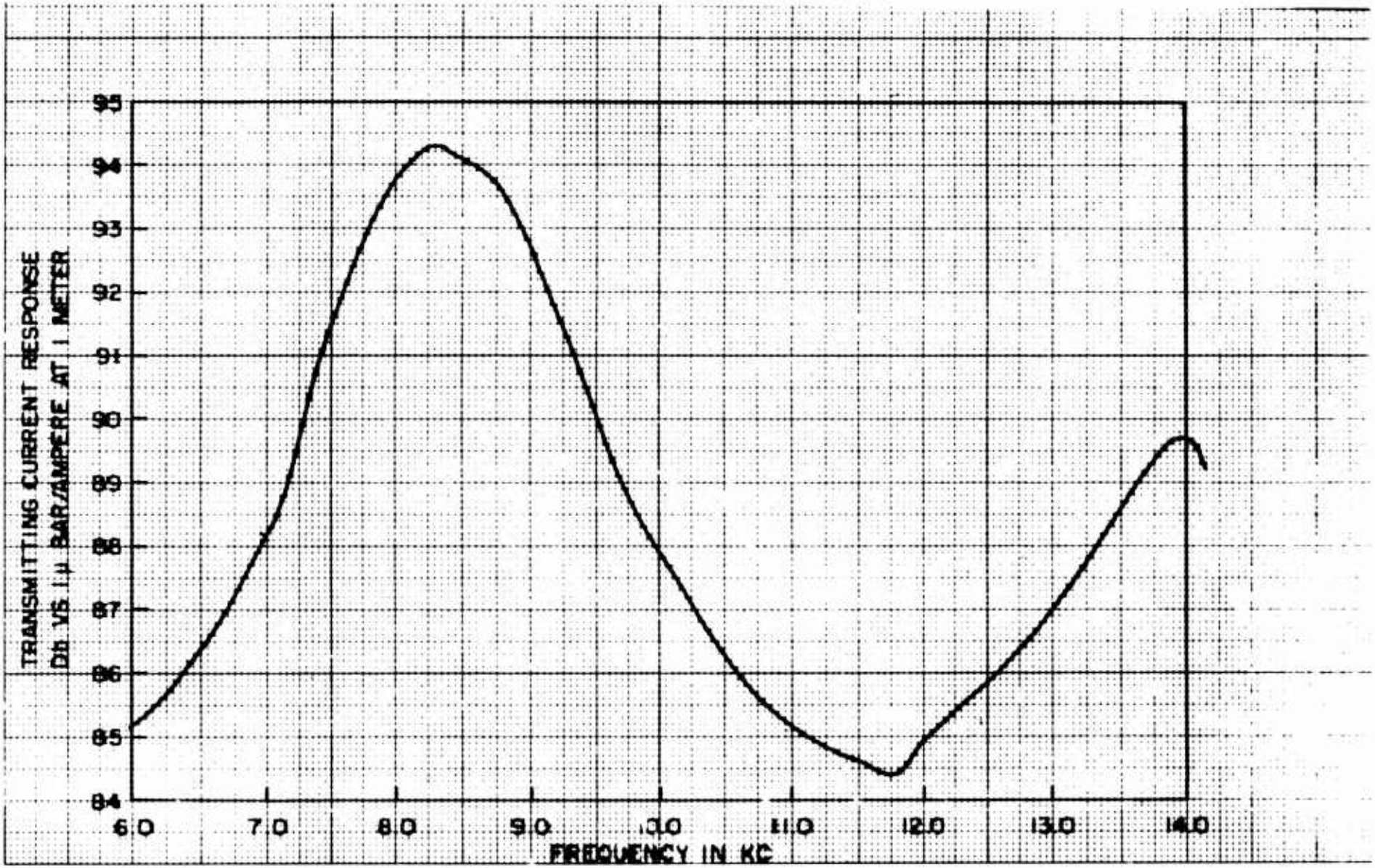

Figure 14 - Transmitting Current Response Curve. 4 Long Magnetostrictive Rings with Free-Flooded Centers. Rings Stacked Close Together.

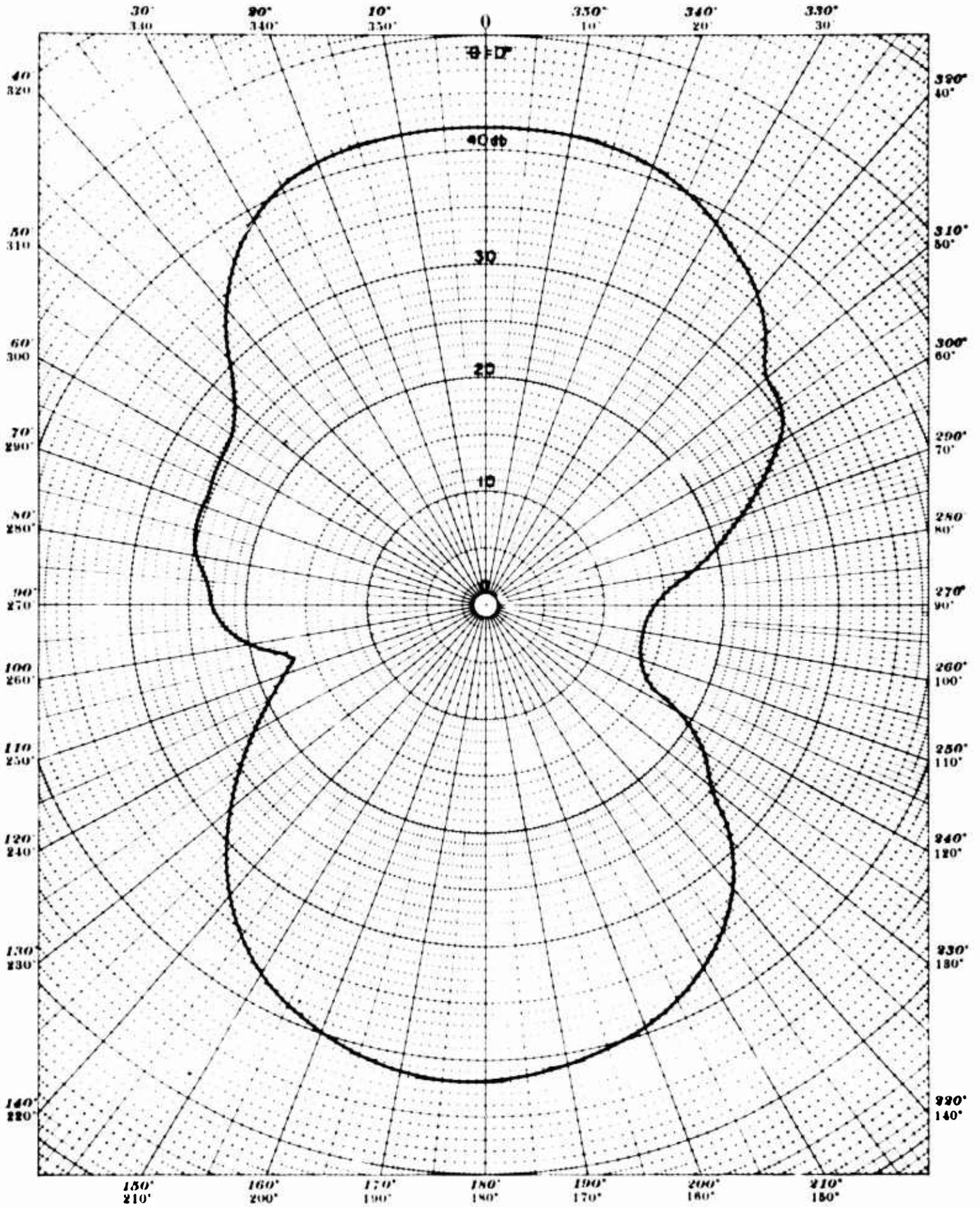

Figure 15. Directivity Pattern - 4 Long, Closely Stacked Magnetostrictive Rings with Free-Flooded Centers

Frequency: 8300 cps—Test Distance: 1 Meter—Depth: 6.4 Meters

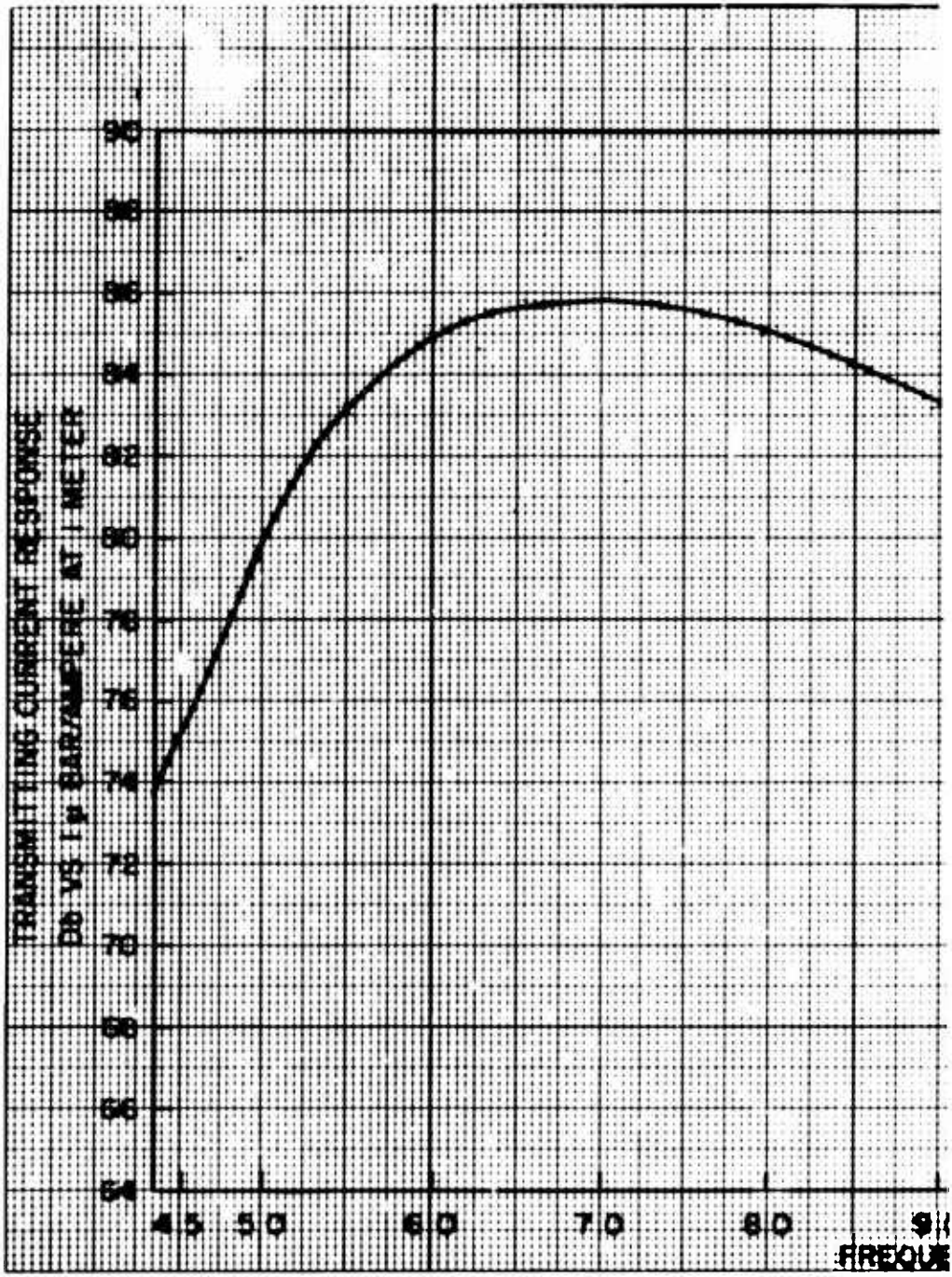

Figure 16. Transmittin
3 Short Magnetostrictiv
Centers. Rings Stacked

3 short ring

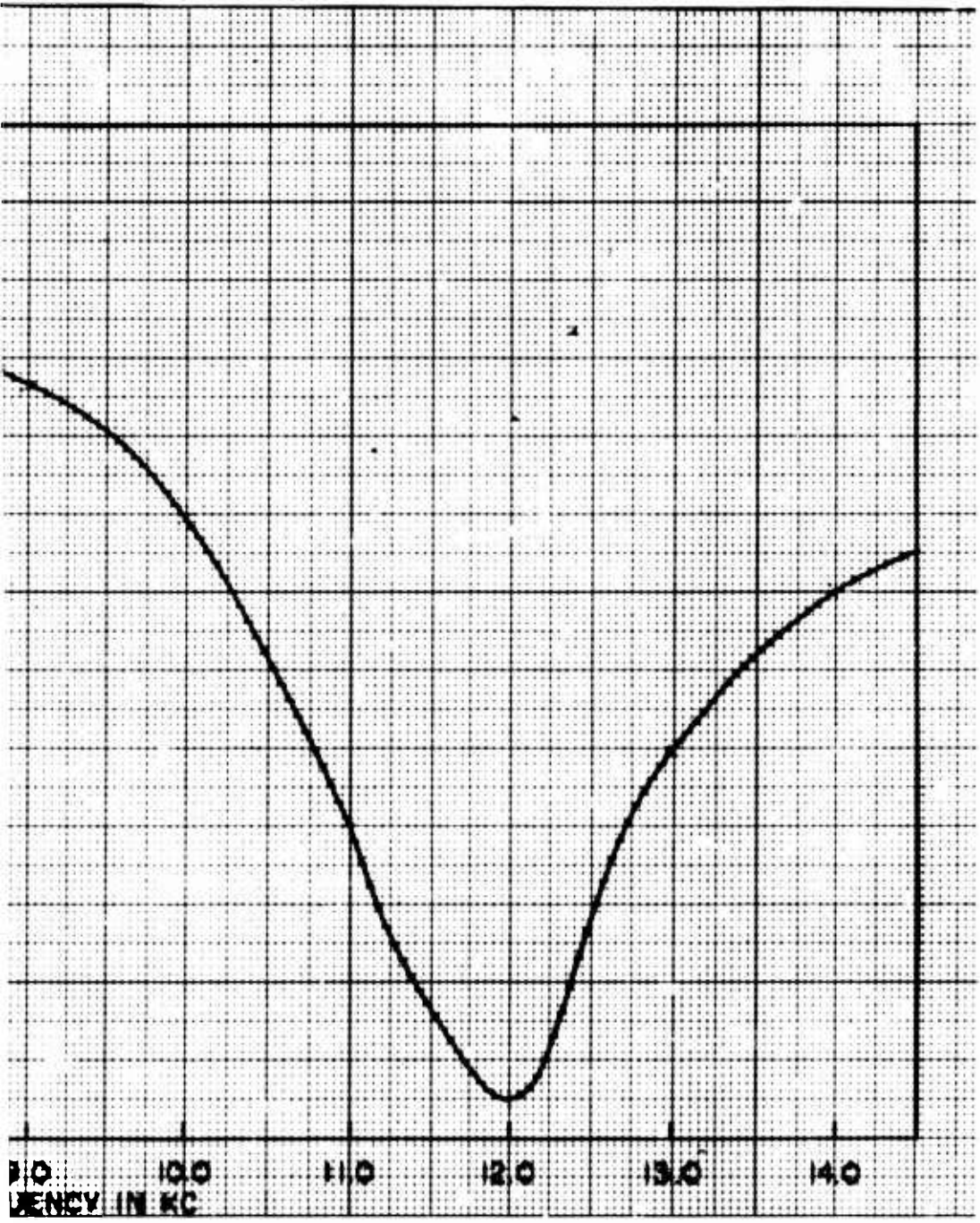

ing Current Response Curve.
ive Rings with Free-Flooded
ed Close Together.

ngs = 1 long ring

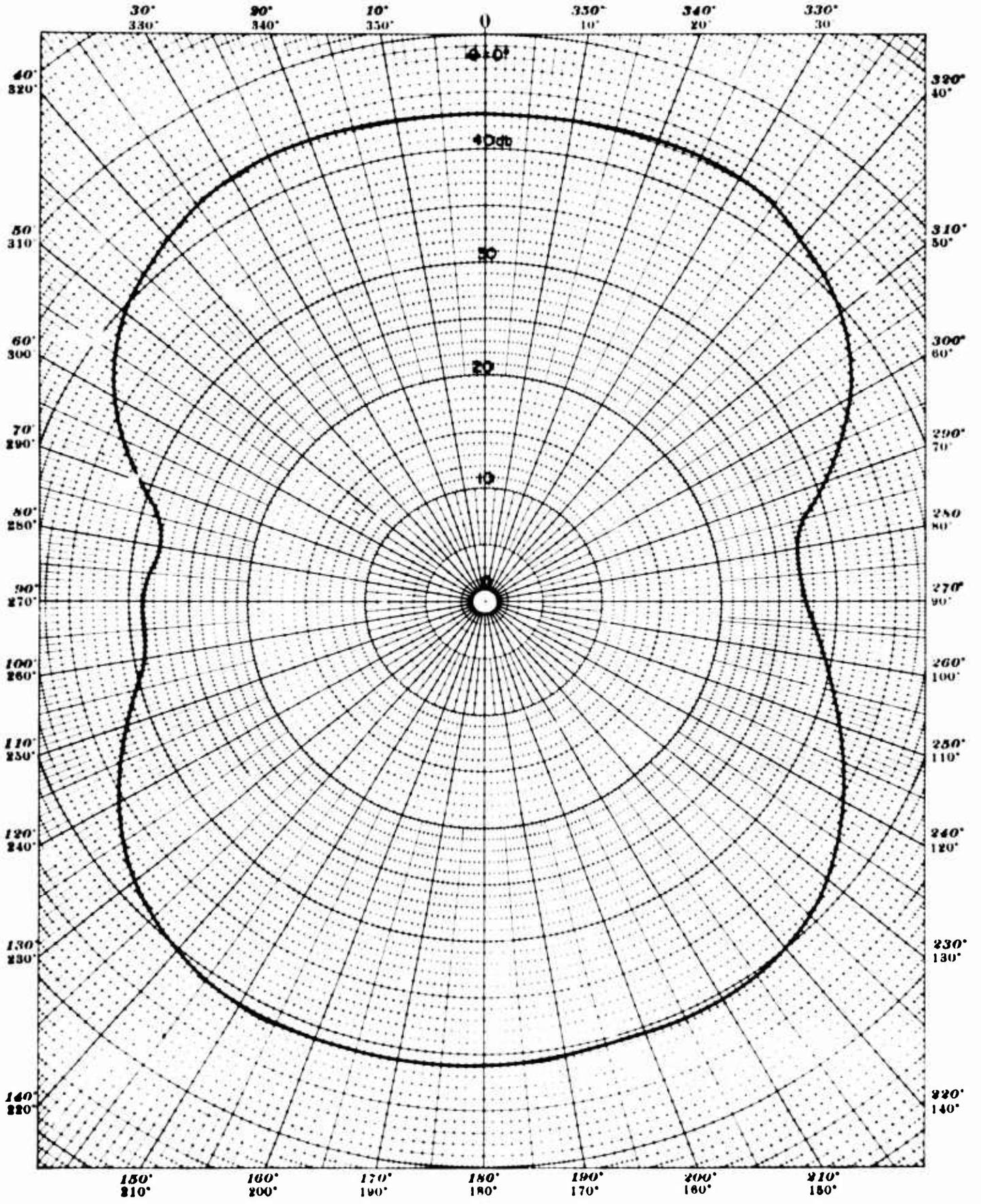

Figure 17. Directivity Pattern - 3 Short, Closely Stacked Magnetostrictive Rings with Free-Flooded Centers

Frequency: 8000 cps—Test Distance: 1 Meter—Depth: 6.4 Meters

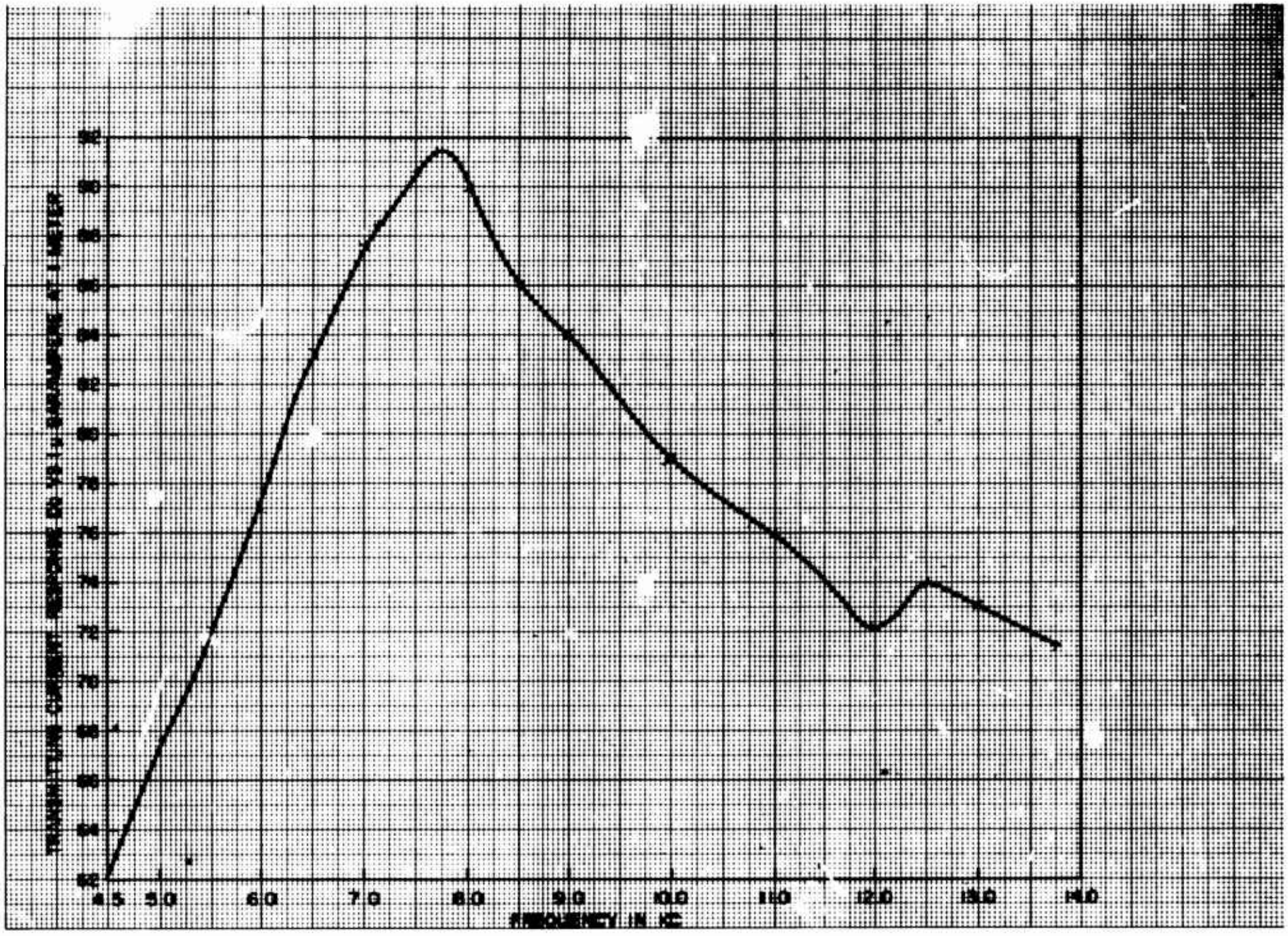

Figure 18. Transmitting Current Response Curve. 3 Short Magnetostrictive Rings with Free-Flooded Centers. 2-inch Separation Between Rings.

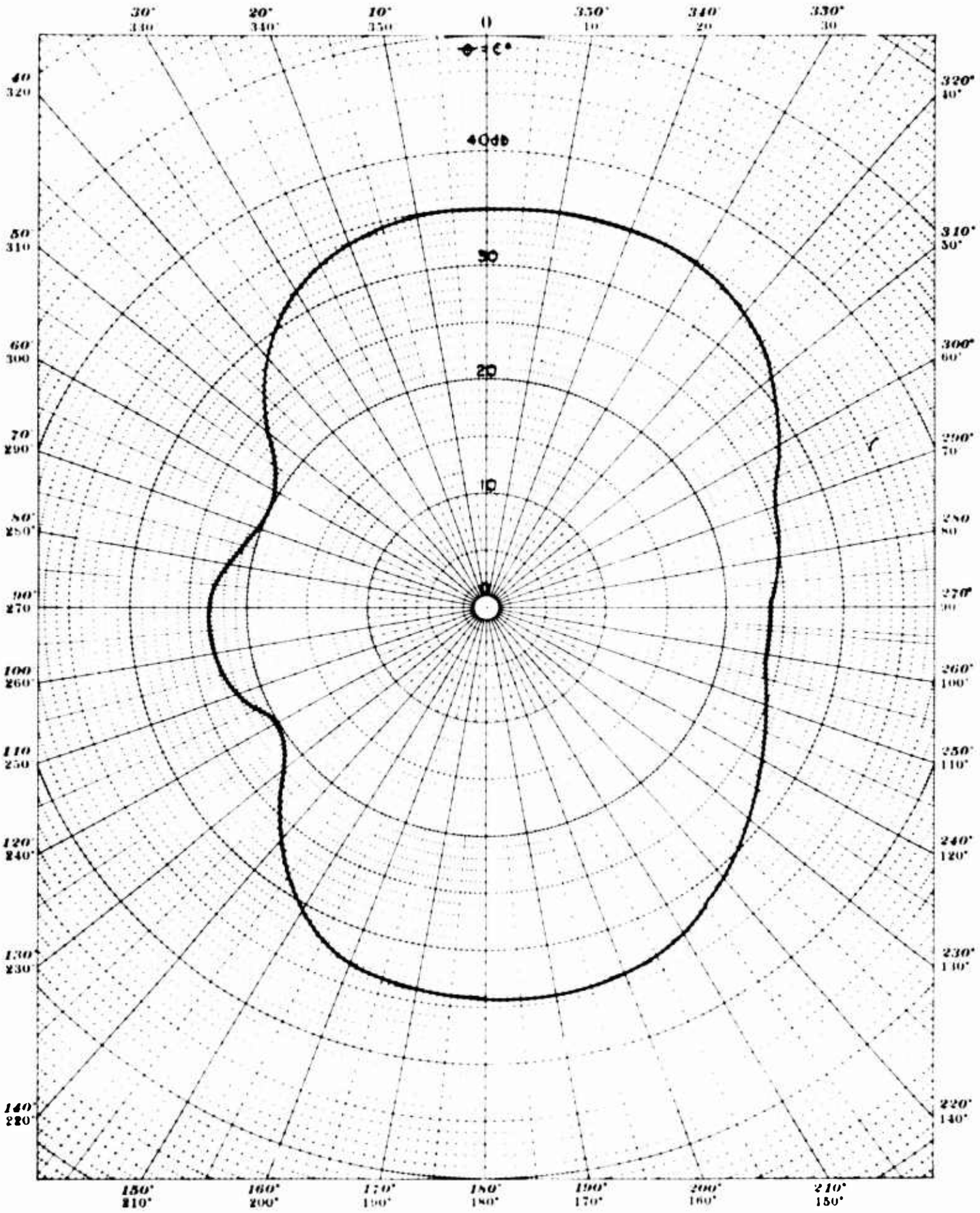

Figure 19. Directivity Pattern - 3 Short Magnetostrictive Rings with Free-Flooded Centers, 2 Inch Separation Distance between Rings

Frequency: 8200 cps—Test Distance: 1 Meter Depth: 6.4 Meters

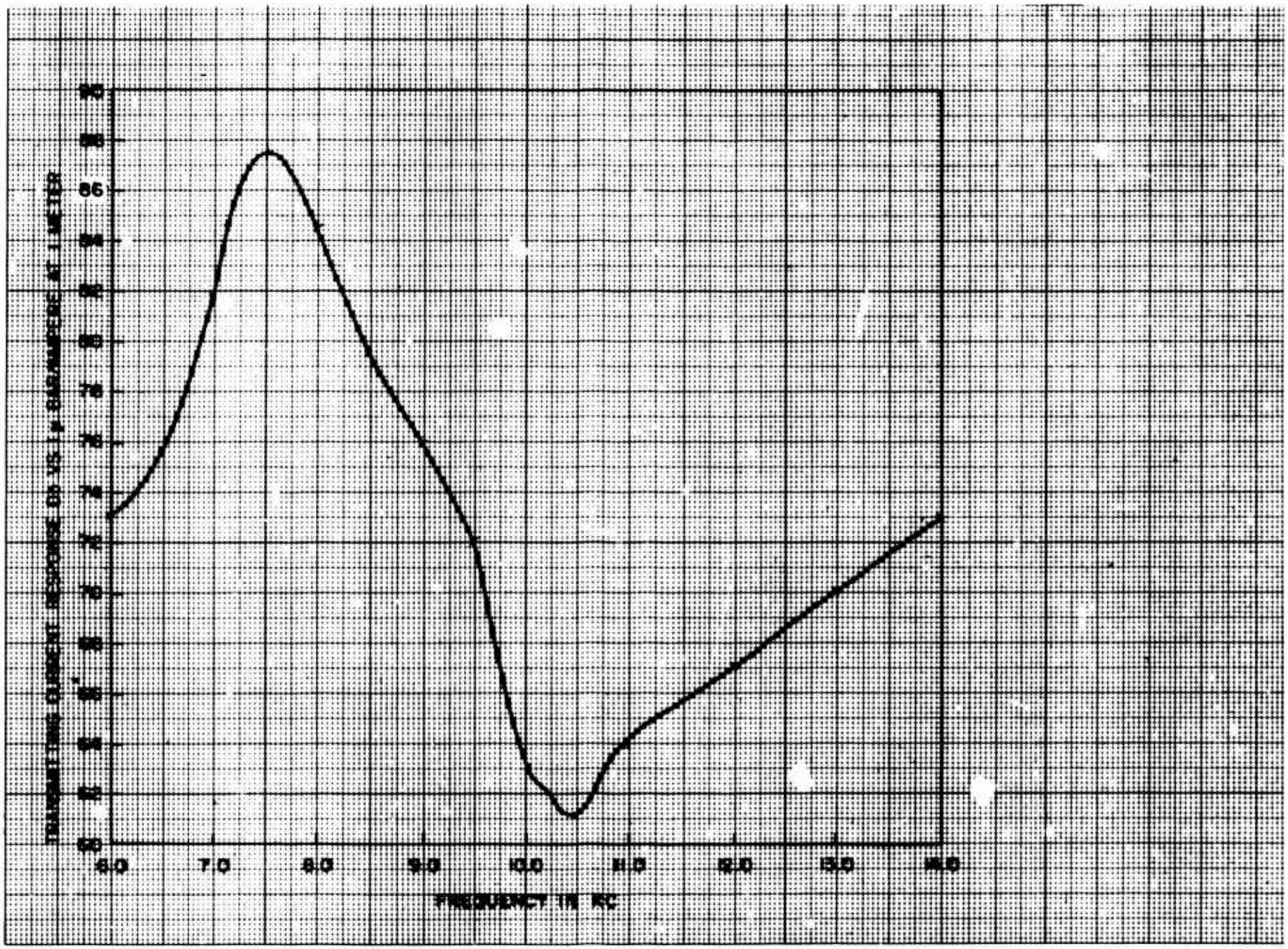

Figure 20. Transmitting Current Response Curve. 1 Short Magnetostrictive Ring with a Free-Flooded Center.

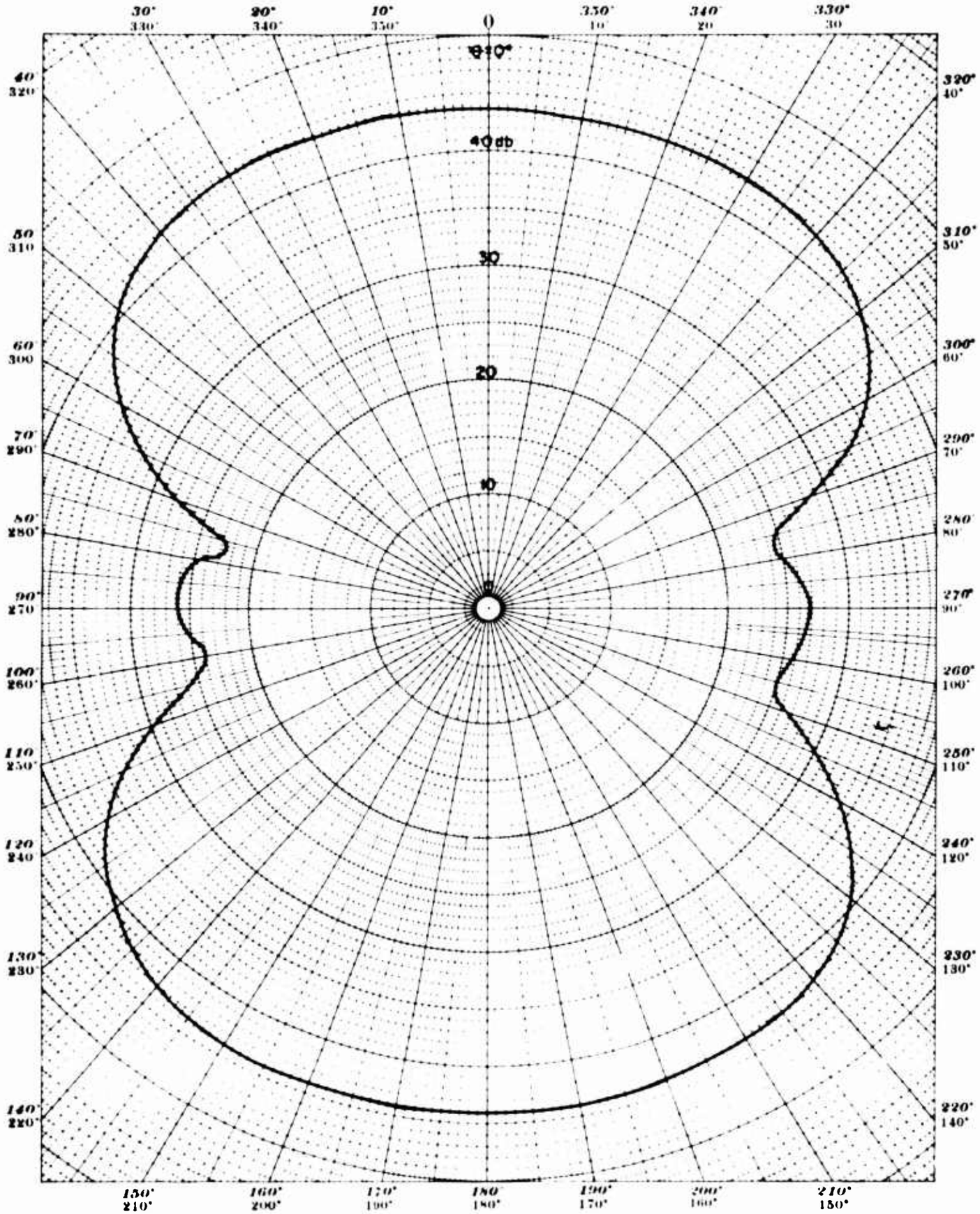

Figure 21. Directivity Pattern - 1 Short Magnetostrictive Ring with a Free-Flooded Center

Frequency: 8000 cps—Test Distance: 1 Meter—Depth: 6.4 Meters

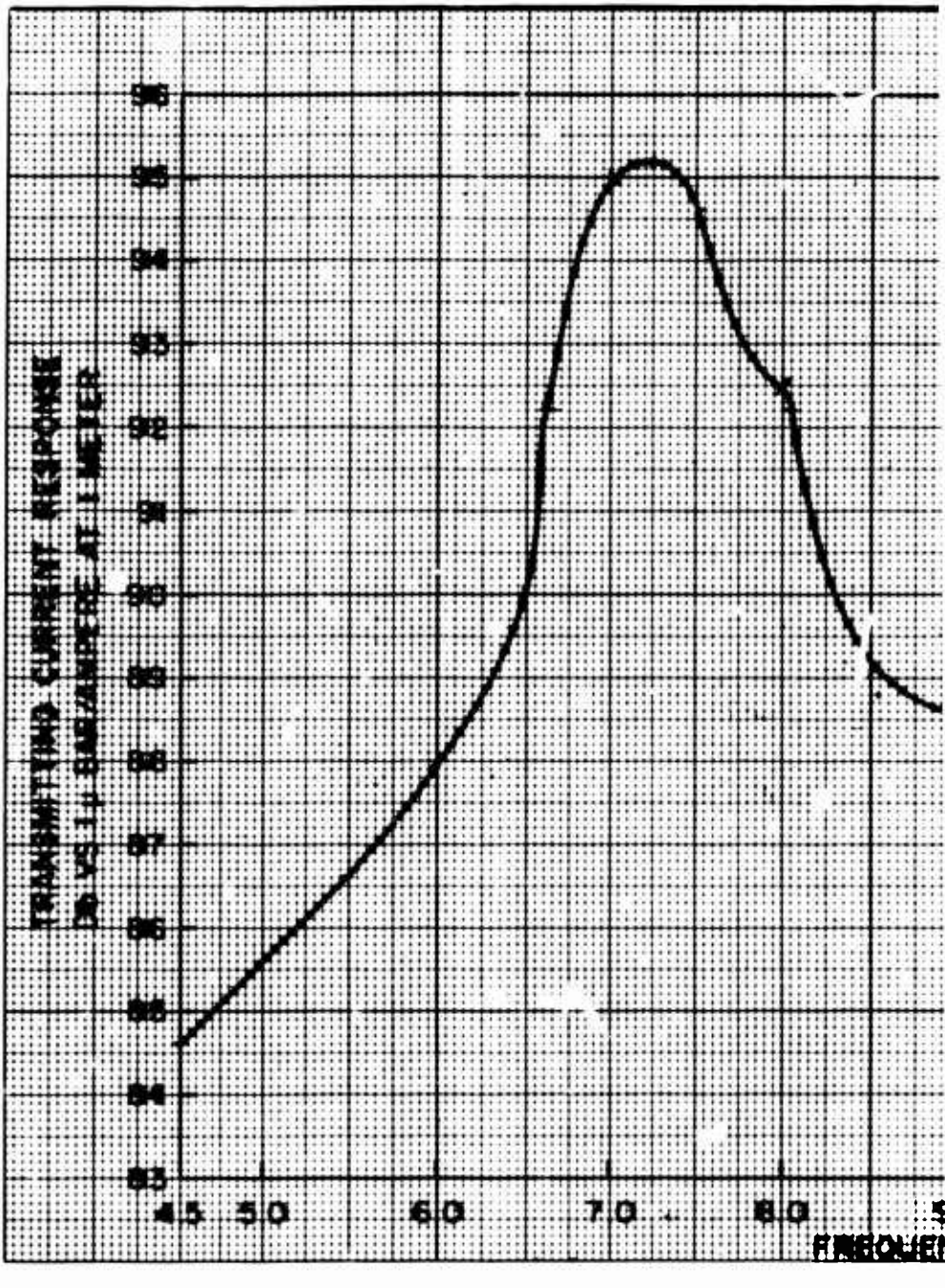

Figure 22. Transmitting Cur
3 Long Magnetostrictive R
Centers. 3/4 Wavelength B
All Rings Driver in Phase.

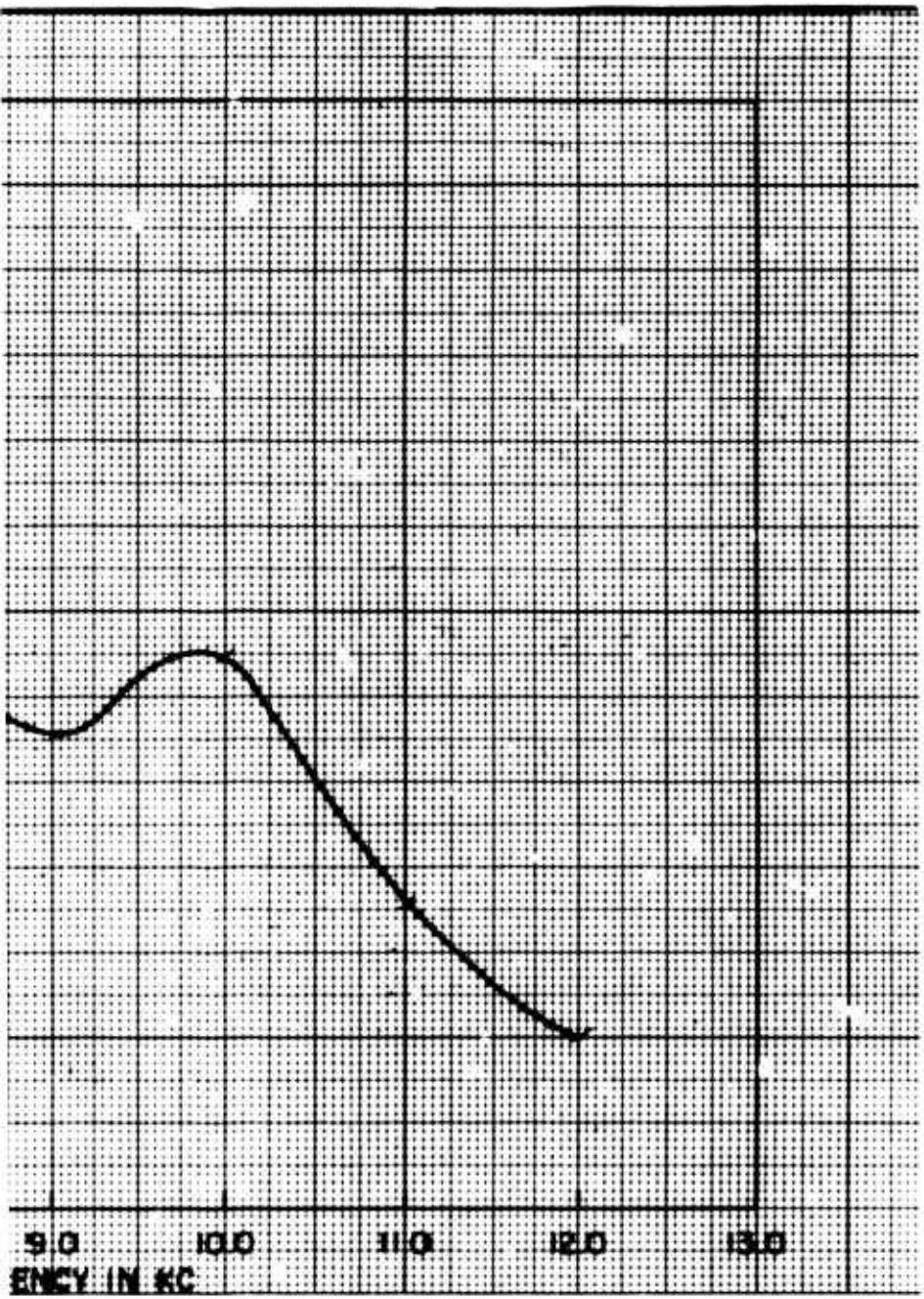

'urrent Response Curve.
Rings with Air Cavity
Baffles between Rings.

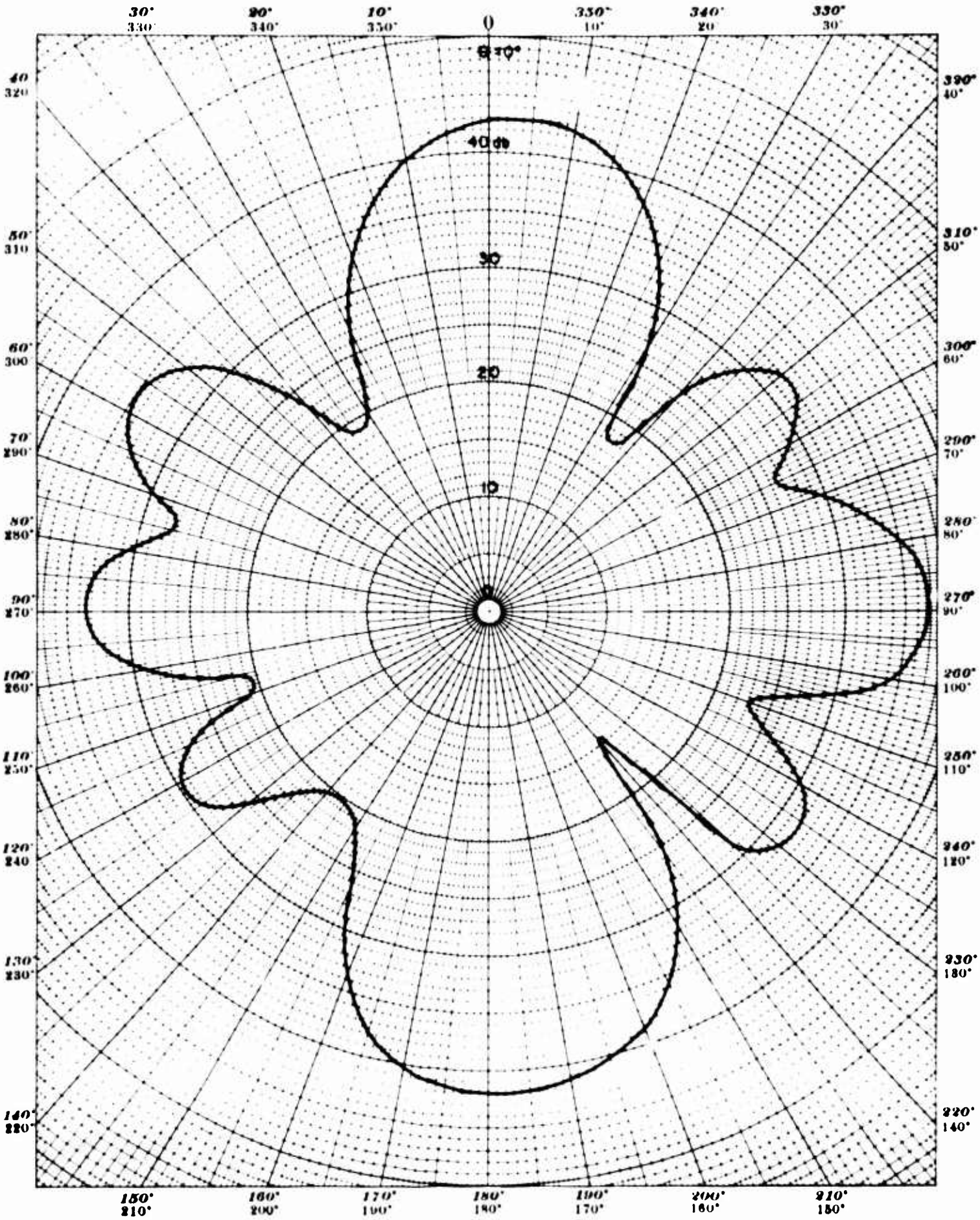

Figure 23. Directivity Pattern - 3 Long Magnetostrictive Rings with Air Cavity Centers, Rings Separated by 3/4 λ Baffles, All Rings Driven in Phase

Frequency: 7600 cps—Test Distance: 1 Meter—Depth: 6.4 Meters

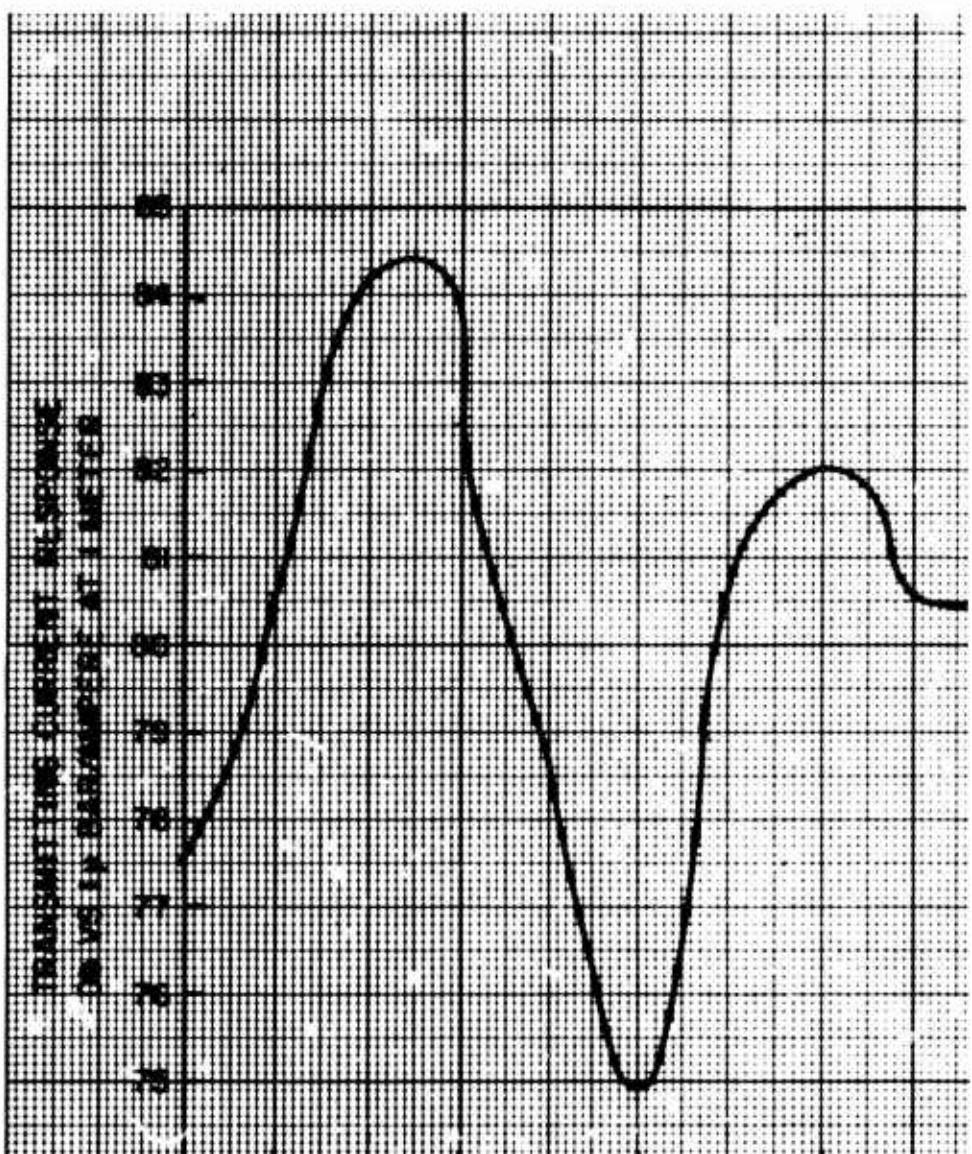

Figure 24. Transmitting C
3 Long Magnetostrictive
Centers. 3/4 Wavelength
Phase of Input Voltage to Ce

Current Response Curve.
Rings with Air Cavity
h Baffles between Rings.
Center Ring was Reversed.

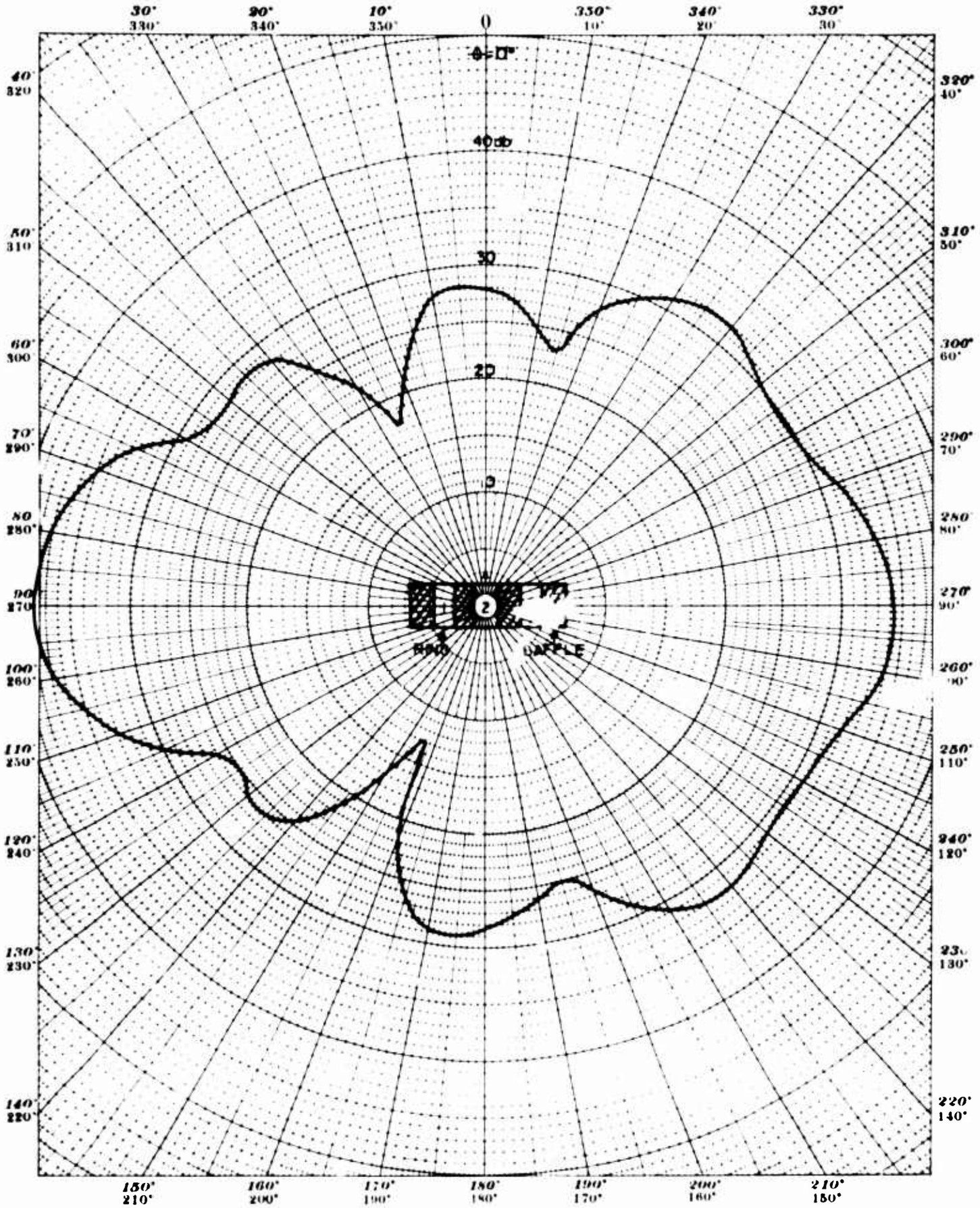

Figure 25. Directivity Pattern - 3 Long Magnetostrictive Rings with Air Cavity Centers, Rings Separated by 3/4 λ Baffles, Center Ring Driven 180 Out-of-Phase with End Rings

Frequency: 5900 cps—Test Distance: 1 Meter—Depth 6.4 Meters

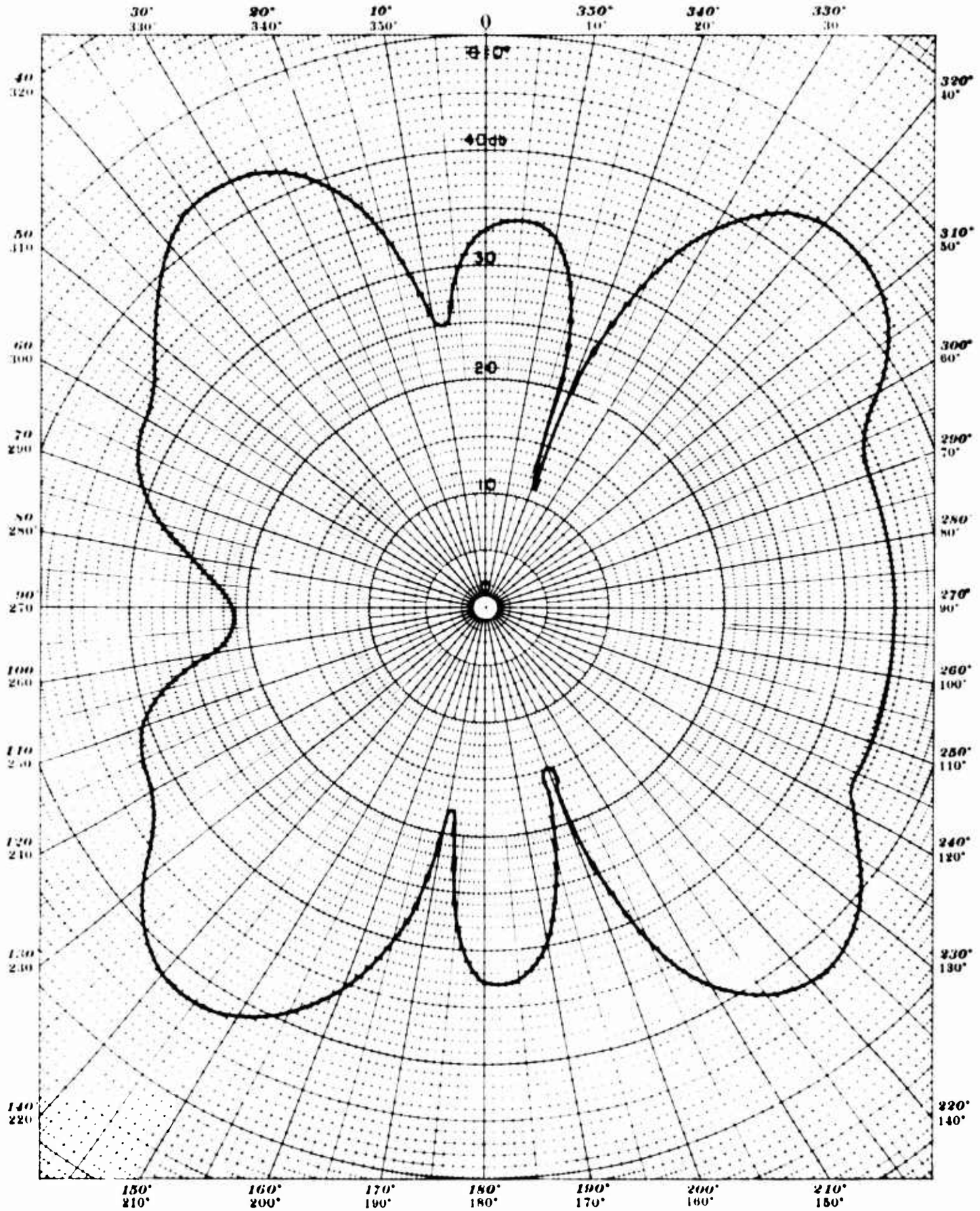

Figure 26. Directivity Pattern - 3 Long Magnetostrictive Rings with Air Cavity Centers, Rings Separated by 3/4 " Baffles, Center Ring Driven 180° Out-of-Phase with End Rings

Frequency: 8200 cps—Test Distance: 1 Meter—Depth: 6.4 Meters

Part III

Measurements presented in Parts III and IV were obtained at the NRL Transducer Calibration Platform, Lake Seneca, New York. The experimental array used in Part III is shown in Figure 27. Initially 12 short, free-flooded, magnetostrictive rings were closely stacked on a holding frame. The separation distance between end rings was 6.75 inches and this distance was maintained throughout the experiment. Then as one ring at a time was removed, the separation distance between the remaining rings was made uniform. Rings of the array were connected electrically in series and polarized by gradually increasing the direct current to 5 amperes and then decreasing the current to a fixed value of 0.5 ampere.

Table IV shows how the array characteristics varied with the number of rings used and the spacing between them. A graphical representation of the same data is shown in Figure 28. Since the separation distance between the 3 and 2 ring arrangements extends over more than 50% of the abscissa scale of the graph, the curves between these points are drawn with dashed lines to indicate that experimental values were not obtained for intermediate separations. Curves of Figure 28 show that as the number of rings was reduced, the efficiency curve rose to a peak value and then decreased. A maximum efficiency of 78% was measured when the number of rings was reduced to four and the separation distance between rings was approximately 1.8 inches or slightly more than 1/4 wavelength at the frequency of peak response for this arrangement. The corresponding bandwidth at the 3 db down points from the peak of the transmitting current response curve is shown to be 900 cps or less than half of the maximum bandwidth recorded. Although the curves indicate that efficiency, bandwidth, and transmitting current response do not peak at the same abscissa values of the graph, a good combination of the three parameters was obtained for a five-ring arrangement in which the separation distance between rings was approximately 1.2 inches or roughly 1/6 of a wavelength at the frequency of peak response. For this arrangement, the indicated efficiency is 68%, bandwidth is 1900 cps, and

the transmitting current response is 97.8 db vs 1μbar per ampere at 1 meter. When the number of rings was changed from 4 to 5 the response increased but the increase in resistance was sufficiently large to decrease the efficiency.

Directivity indexes were obtained from beam patterns taken at the frequency of peak response. The dipole form of pattern shown in Figure 41 is for the 4-ring array. Beam angle of the principal lobes at the 10 db down points is approximately 55 degrees and the directivity index is 5.1 db. Minor lobes at 60, 120, 260, and 300 degrees are from 12 to 18 db below the principal lobe and the asymmetry about the ring axis may indicate the presence of a spurious mode of vibration. Acoustic pressure on the ring axis is 20 db lower than on the principal acoustic axis. A beam pattern taken at the frequency of peak response for a five-ring array is shown in Figure 47. Minor lobes similar to those noted in the previous pattern are noticeable but greatly suppressed. The beam angle of the principal lobe has increased to 74 degrees and the directivity index has dropped to 4.3 db. Acoustic pressure on the ring axis is approximately 25 db lower than on the principal axis. The beam patterns discussed above were taken in a plane including the ring axis. Patterns taken in a plane perpendicular to the ring axis were circular and are not shown.

Although all the pertinent information obtainable from the transmitting current response curves is given in Table IV, the curves are included in the report for the convenience of those who may want to observe the response transition from one array arrangement to another or to study secondary response peaks which may be found in the curves for 9 and 12 ring arrays. Many beam patterns are also included in the report. Patterns for each ring arrangement were taken at several different frequencies which were determined by response curve information or by impedance circles which were displayed on the scope of a "Vector Impedance Locus Plotter". Both response curves and beam patterns are labeled and numbered. The Figure numbers start at 29 and end at 66.

In summary, measurements made in Part III, as graphically illustrated in Figure 28, show that values for the array parameters do not peak at the same abscissa value. However, a good combination of large bandwidth, good transmitting response and efficiency are obtained for 5 rings when the separation distance between rings is approximately 1.2 inches.

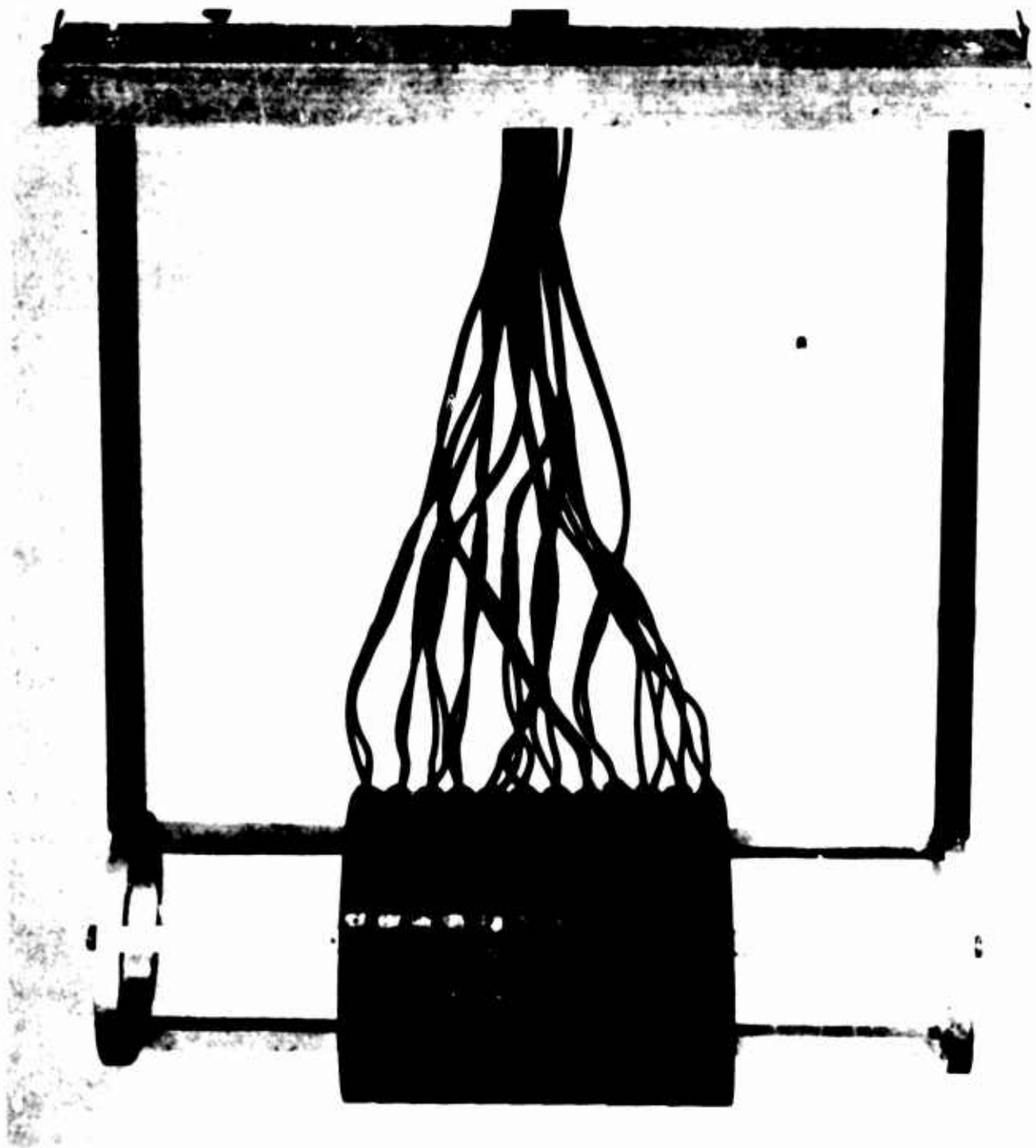

Figure 27. Array of Closely Stacked Rings

TABLE IV

Array of 2 to 12 Magnetostrictive Rings

Lake Seneca Measurements Sept. 16-20, 1963

No. Rings in Series	Separation In Inches	S db	R ohms	f_r cps	D. I. db	Eff. %	B. W. cps
2	6.75	92.0	93	8000	4.7	50	1000
3	3.0625	93.7	100	8200	4.4	74	840
4	1.833	96.2	145	8400	5.1	78	900
5	1.218	97.8	287	8300	4.3	68	1900
6	0.850	98.3	459	8200	4.4	47	1360
9	0.297	98.8	585	7200	4.6	39	780
12	0.045	91.9	300	6600	4.3	16	1200

S = Current Transmitting Response in db vs 1 μ bar per ampere at 1 Meter. (Taken at f_r)

R = Resistance in ohms at frequency of peak response.

f_r = Frequency in cps at peak response

D. I. = Directivity Index

B. W. = Bandwidth in Cps at 3 db down points from f_r.

Separation between rings was kept uniform in all arrangements and distance between end rings was kept constant at 6.75 inches. Ring thickness was 5/8 inch.

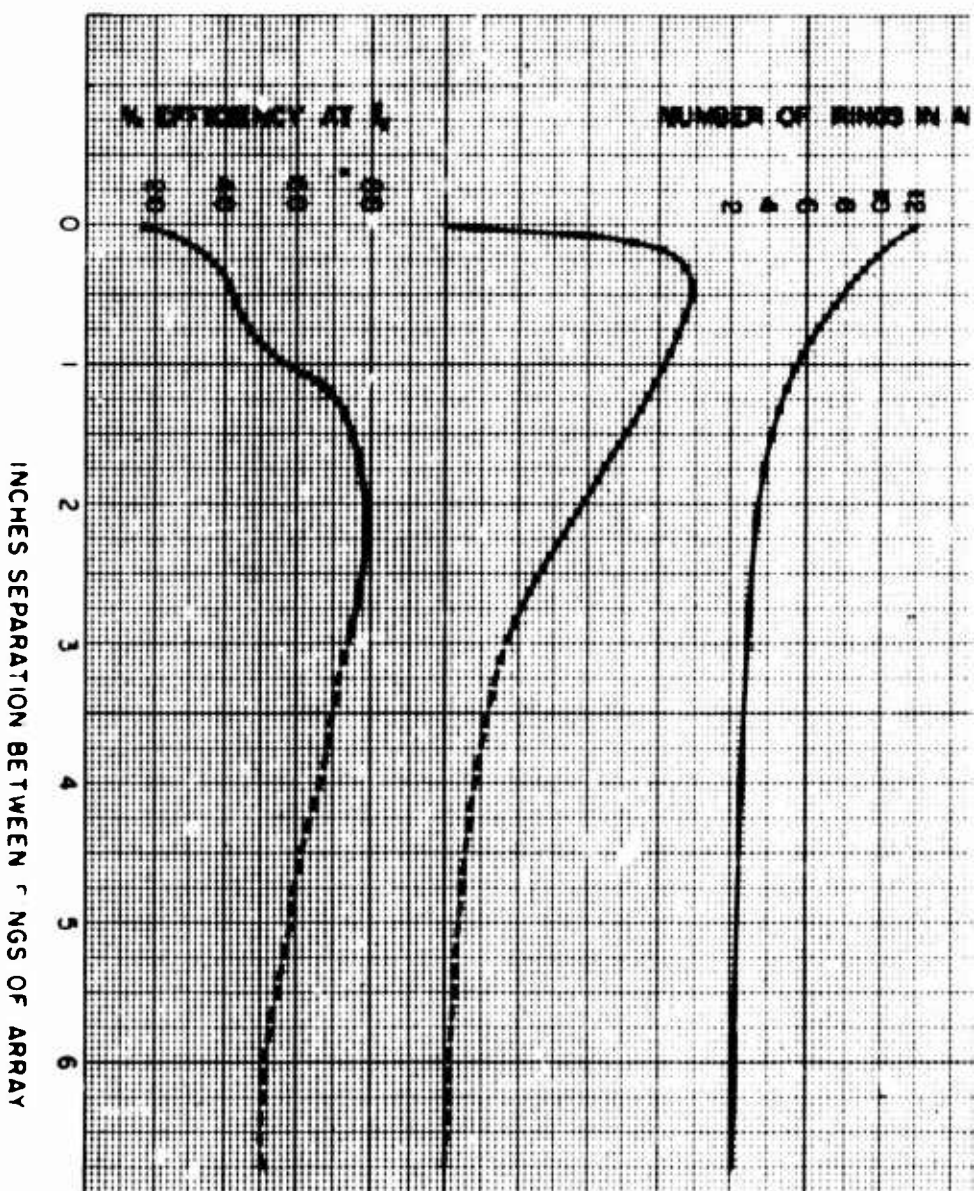

Figure 28. Array of 2 to 12 Magn
Between End Rings of Array H

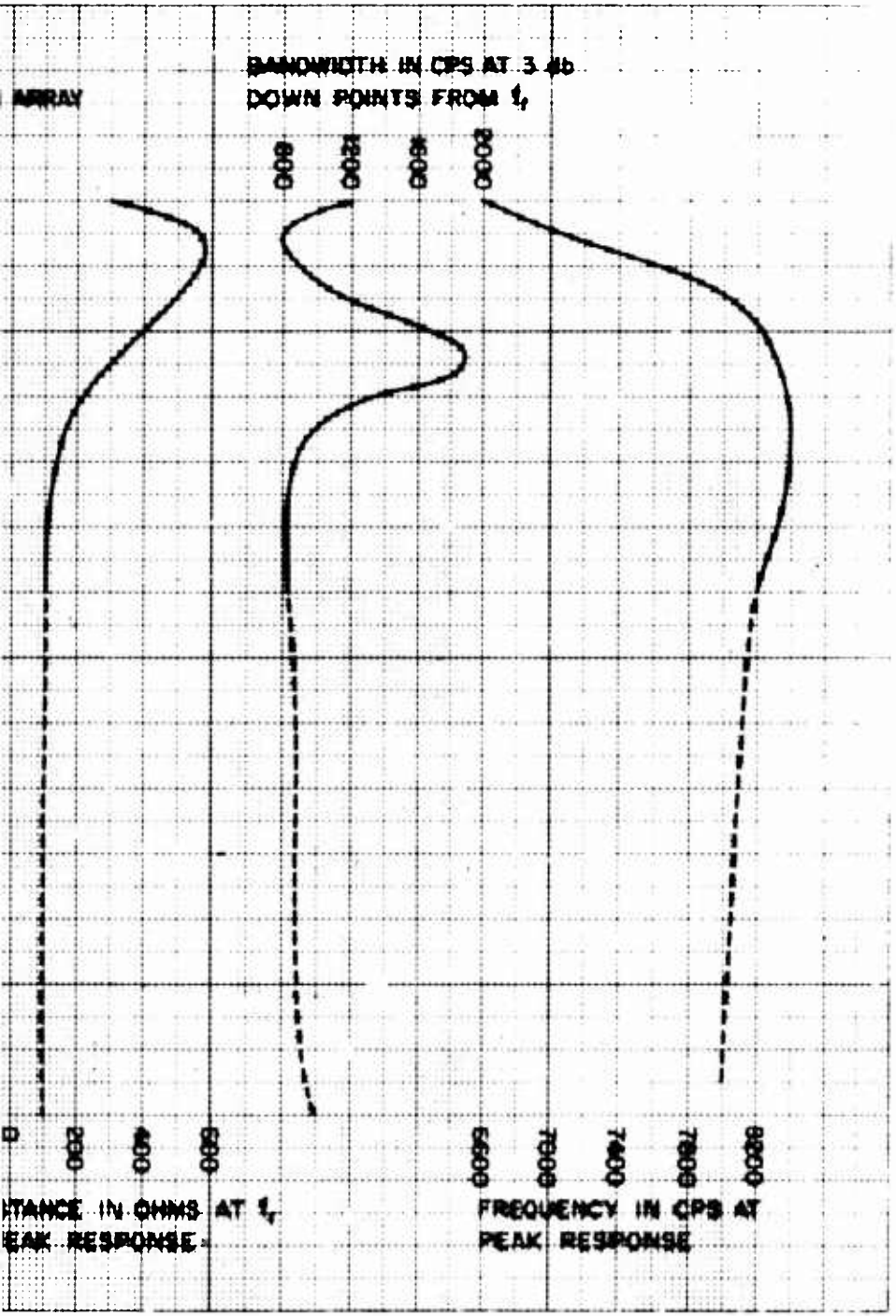

gnetostrictive Rings. Separation
Held Constant at 6.75 Inches.

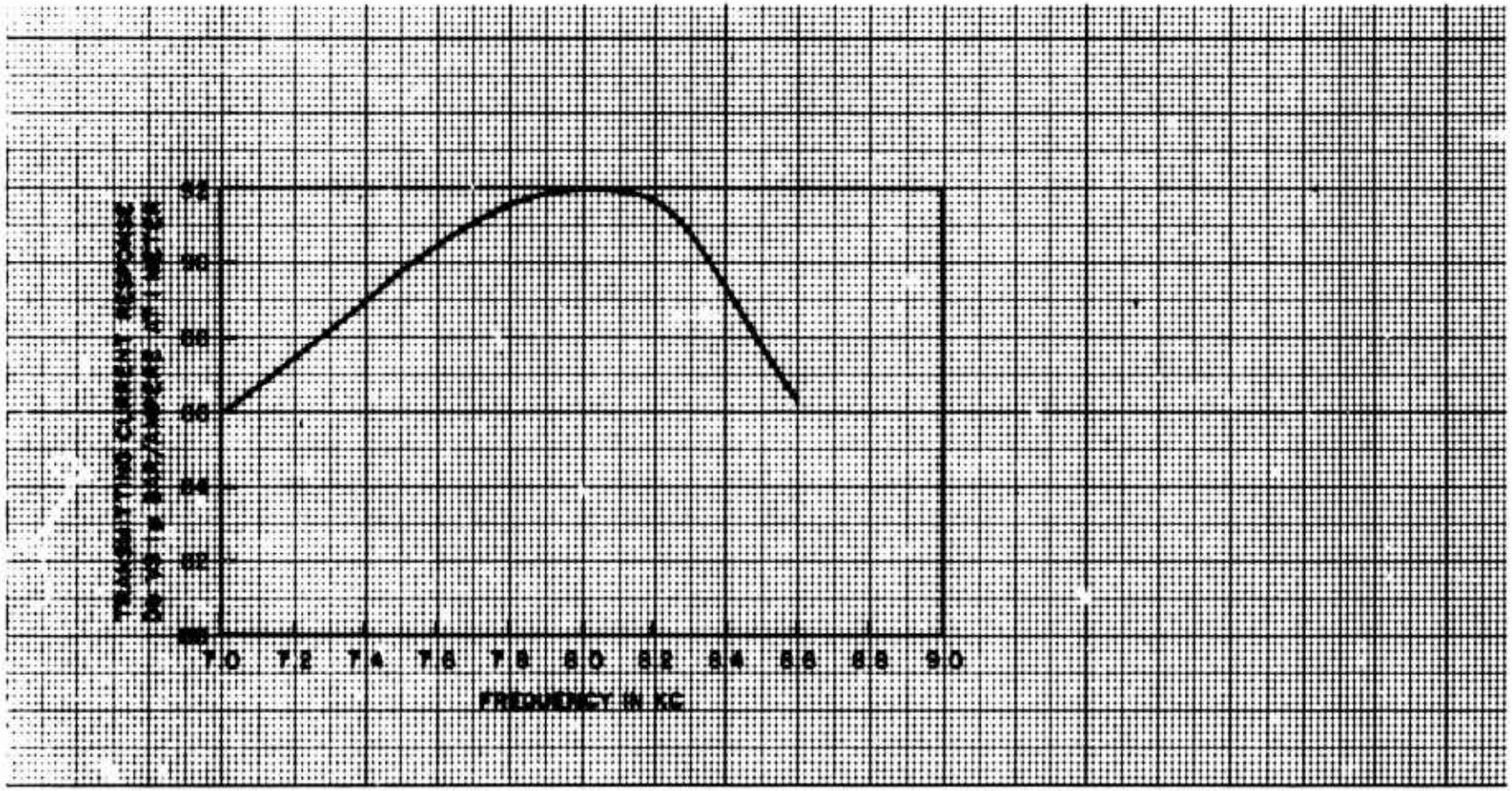

Figure 29. Transmitting Current Response Curve, Array of 2 Magnetostrictive Rings in Series. D.C. = 0.5 Amperes, 87-foot depth. (Distance between rings = 6.75 inches).

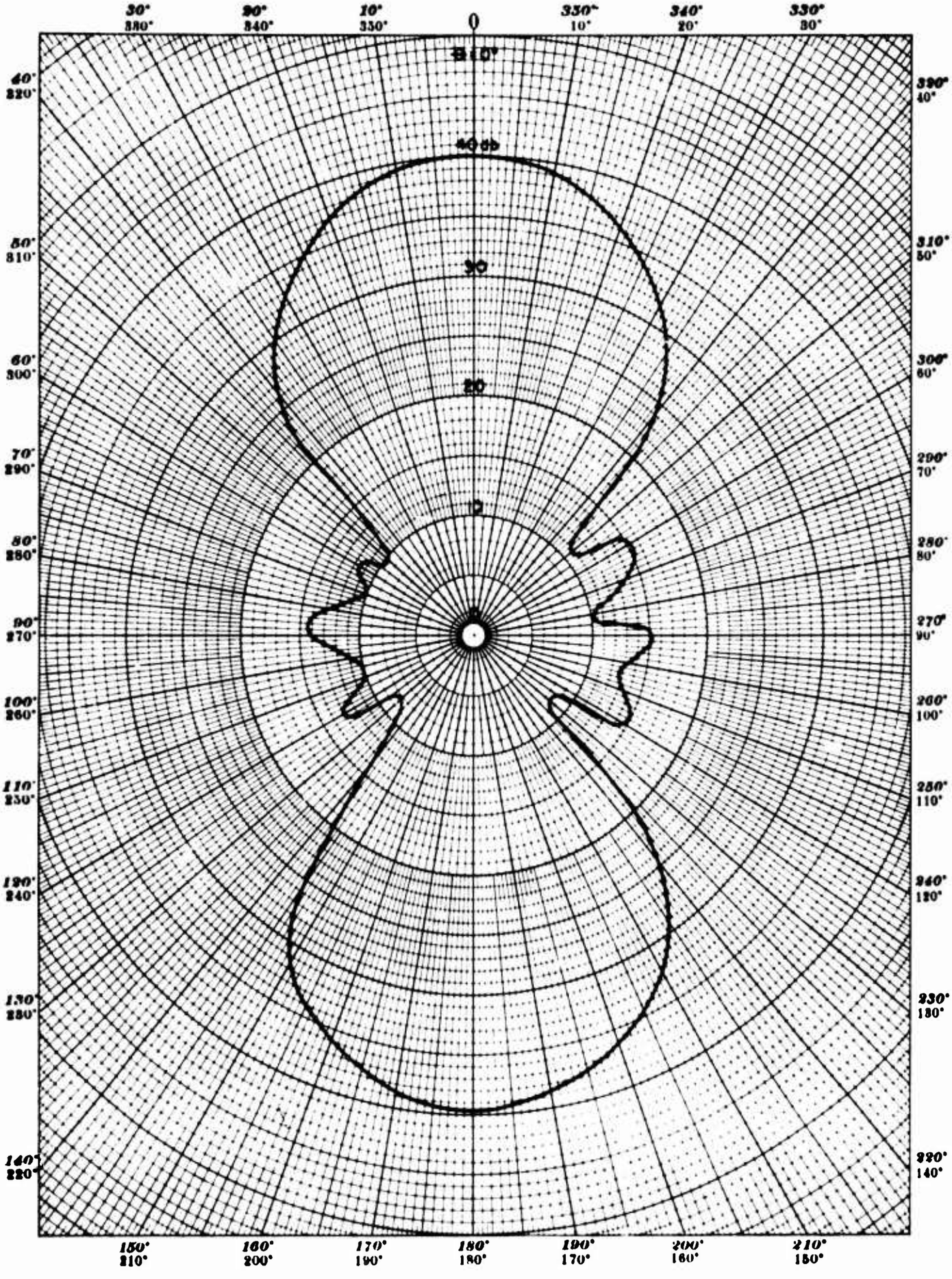

Figure 30. Directivity Pattern - Constant Length Array, 2 Free-Flooded Magnetostrictive Rings

Frequency: 5000 cps—Test Distance: 5 Meters—Depth: 26.5 Meters

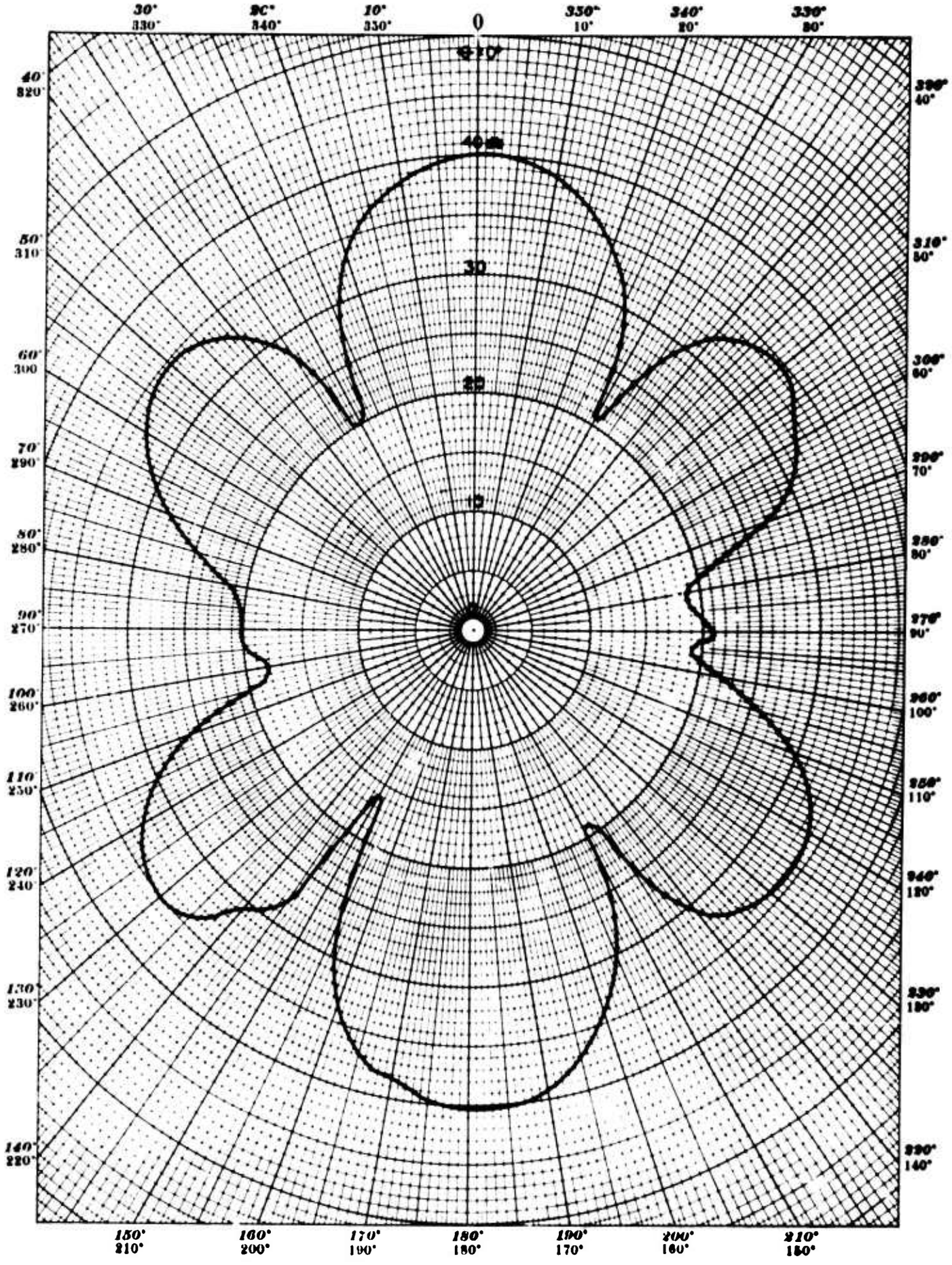

Figure 31. Directivity Pattern - Constant Length Array, 2 Free-Flooded Magnetostrictive Rings

Frequency: 8000 cps—Test Distance: 5 Meters—Depth: 26.5 Meters

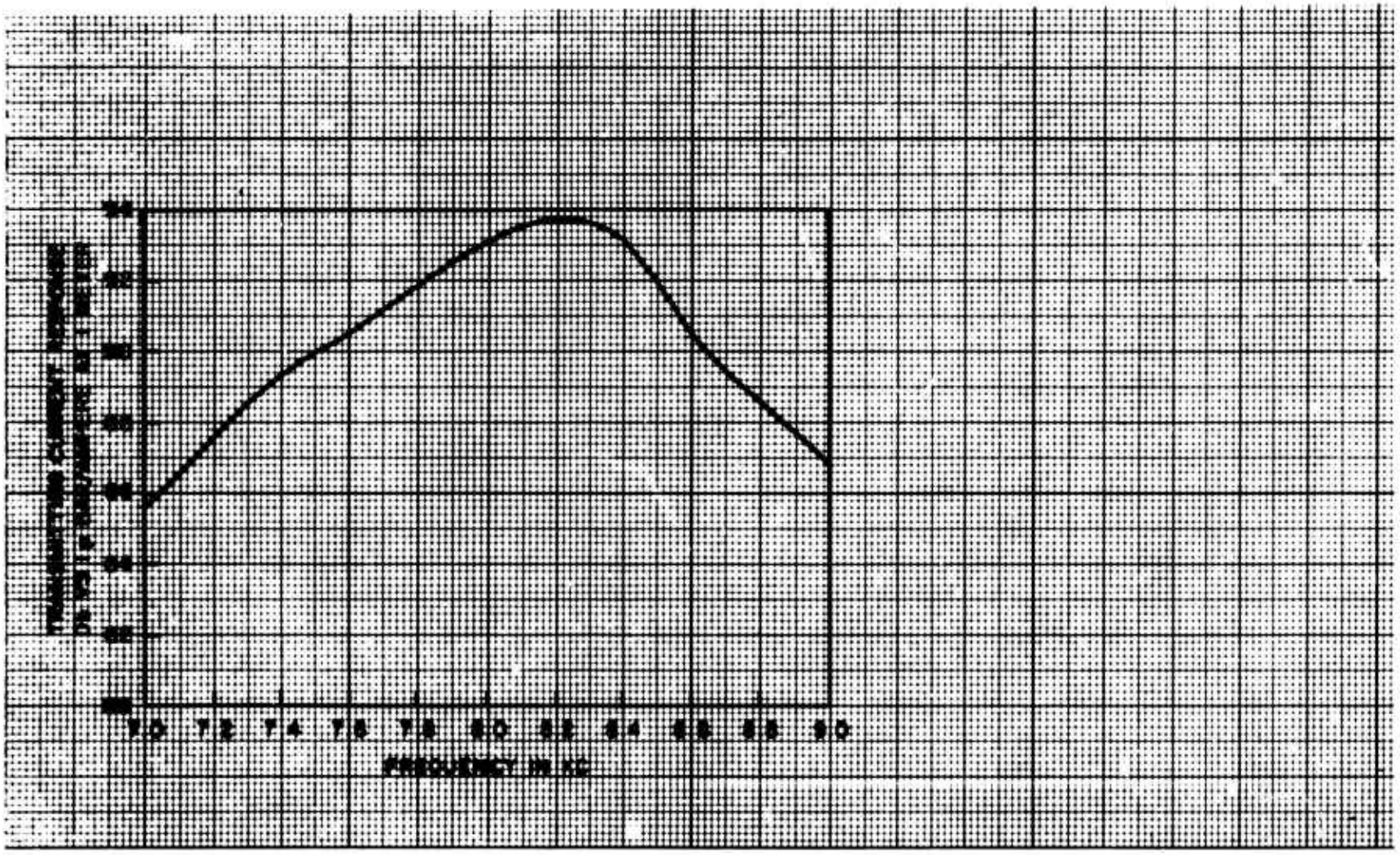

Figure 32. Transmitting Current Response Curve, Array of 3 Magnetostrictive Rings in Series. D.C. = 0.5 Amperes, 87-foot depth. (Distance between rings = 3.0625 inches).

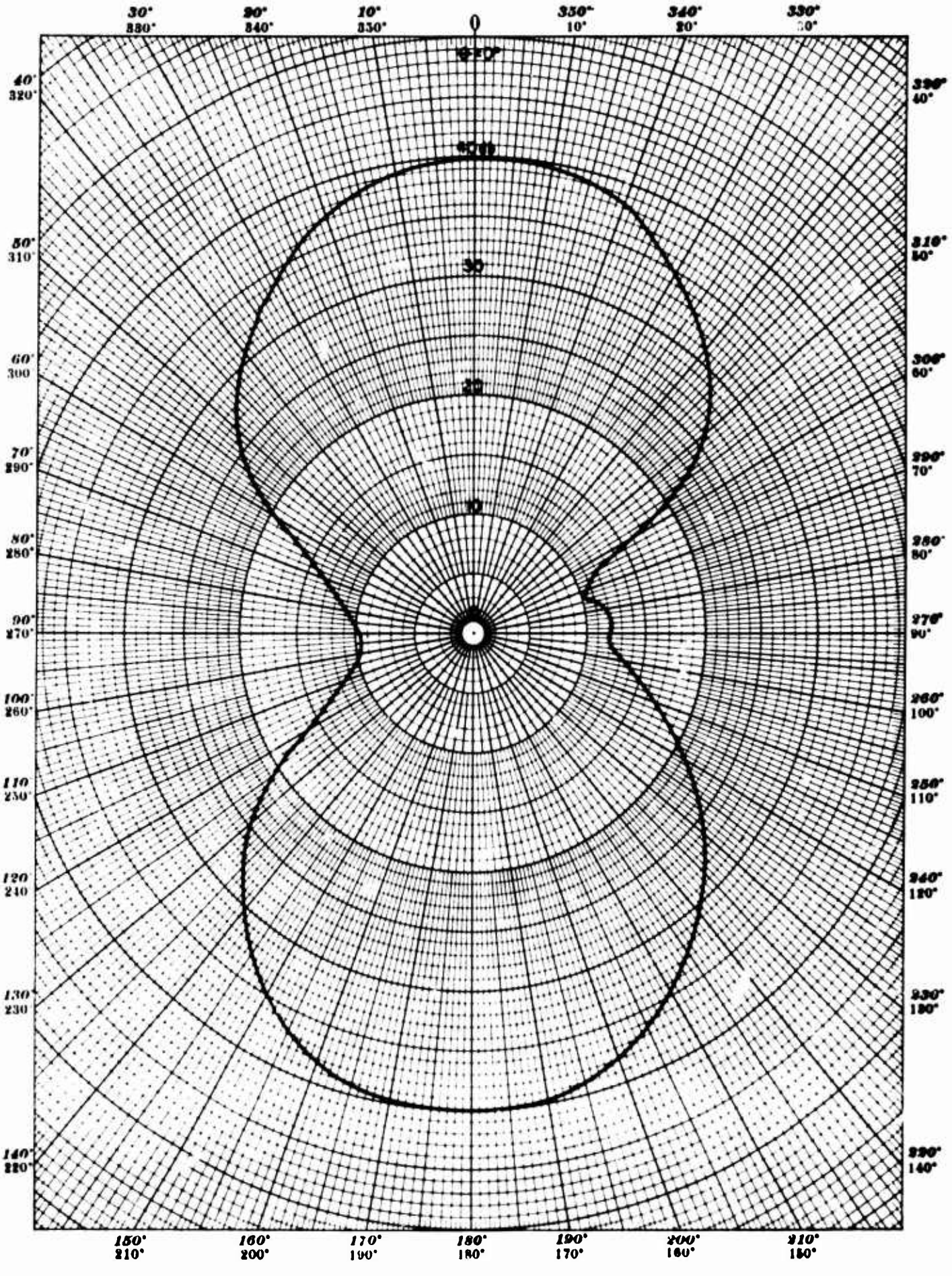

Figure 33. Directivity Pattern - Constant Length Array, 3 Free-Flooded Magnetostrictive Rings

Frequency: 5000 cps—Test Distance: 5 Meters—Depth: 26.5 Meters

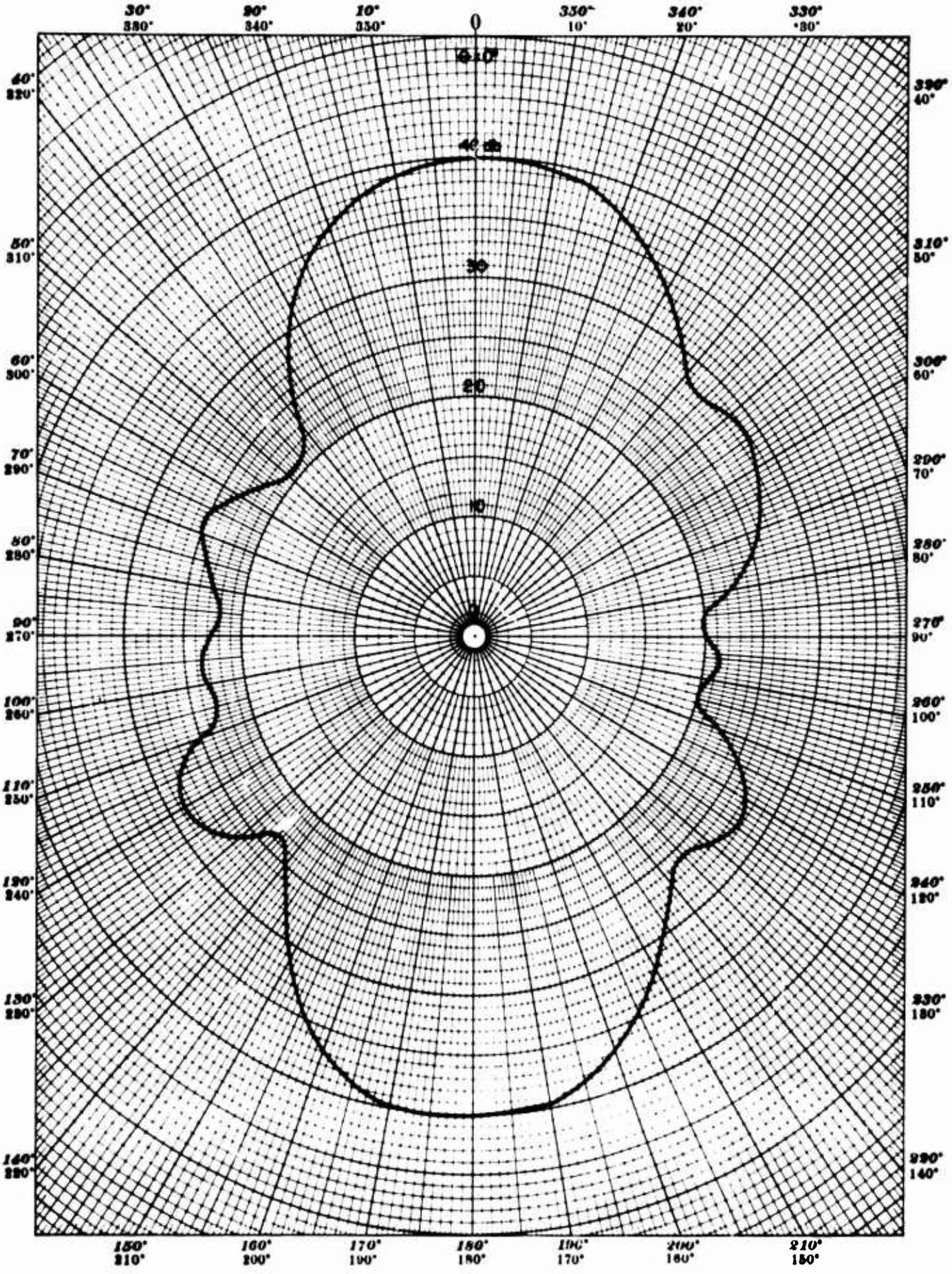

Figure 34. Directivity Pattern - Constant Length Array,
3 Free-Flooded Magnetostrictive Rings

Frequency: 7600 cps—Test Distance: 5 Meters—Depth: 26.5 Meters

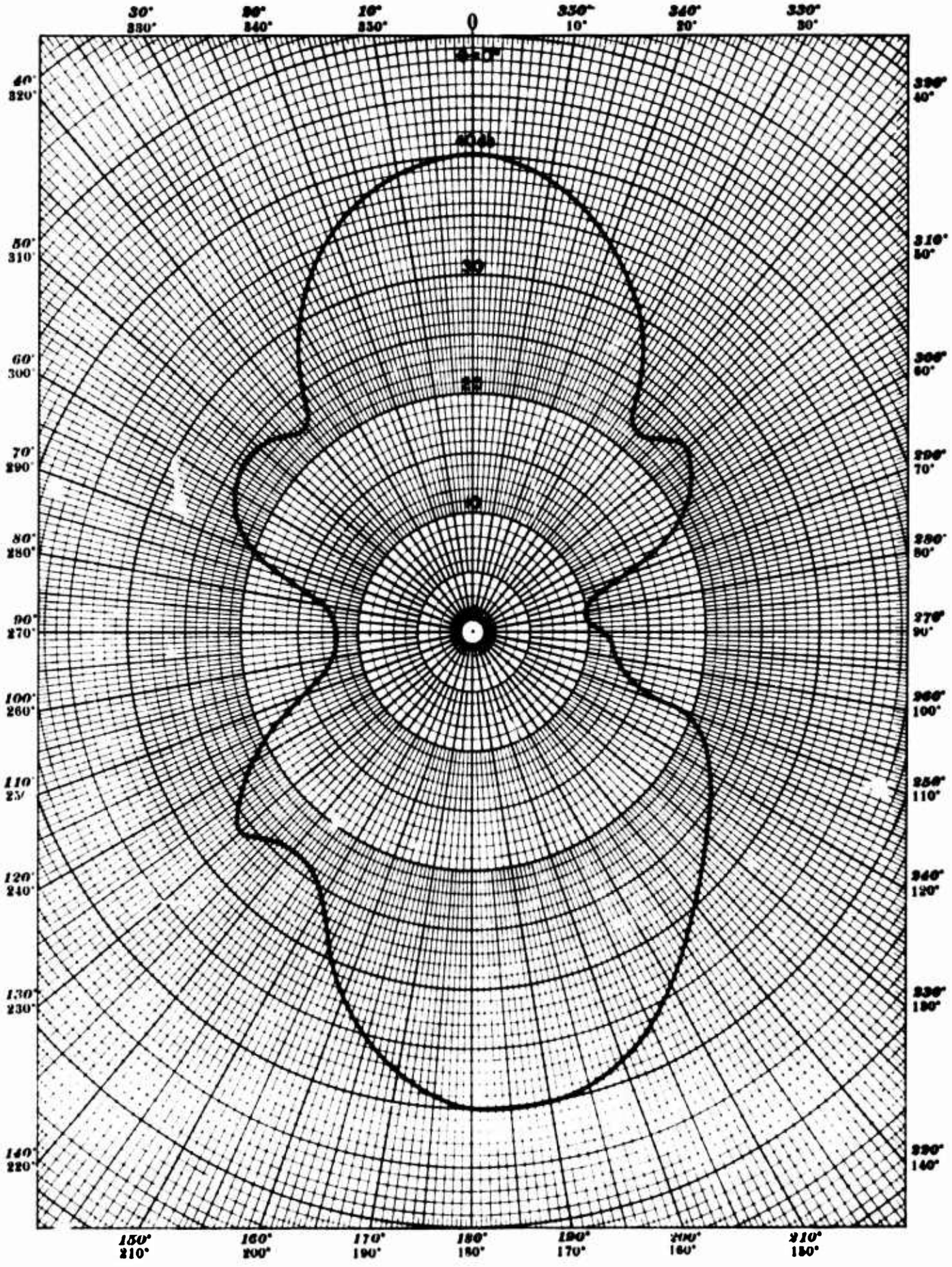

Figure 35. Directivity Pattern - Constant Length Array,
3 Free-Flooded Magnetostrictive Rings

Frequency: 8000 cps—Test Distance: 5 Meters—Depth: 26.5 Meters

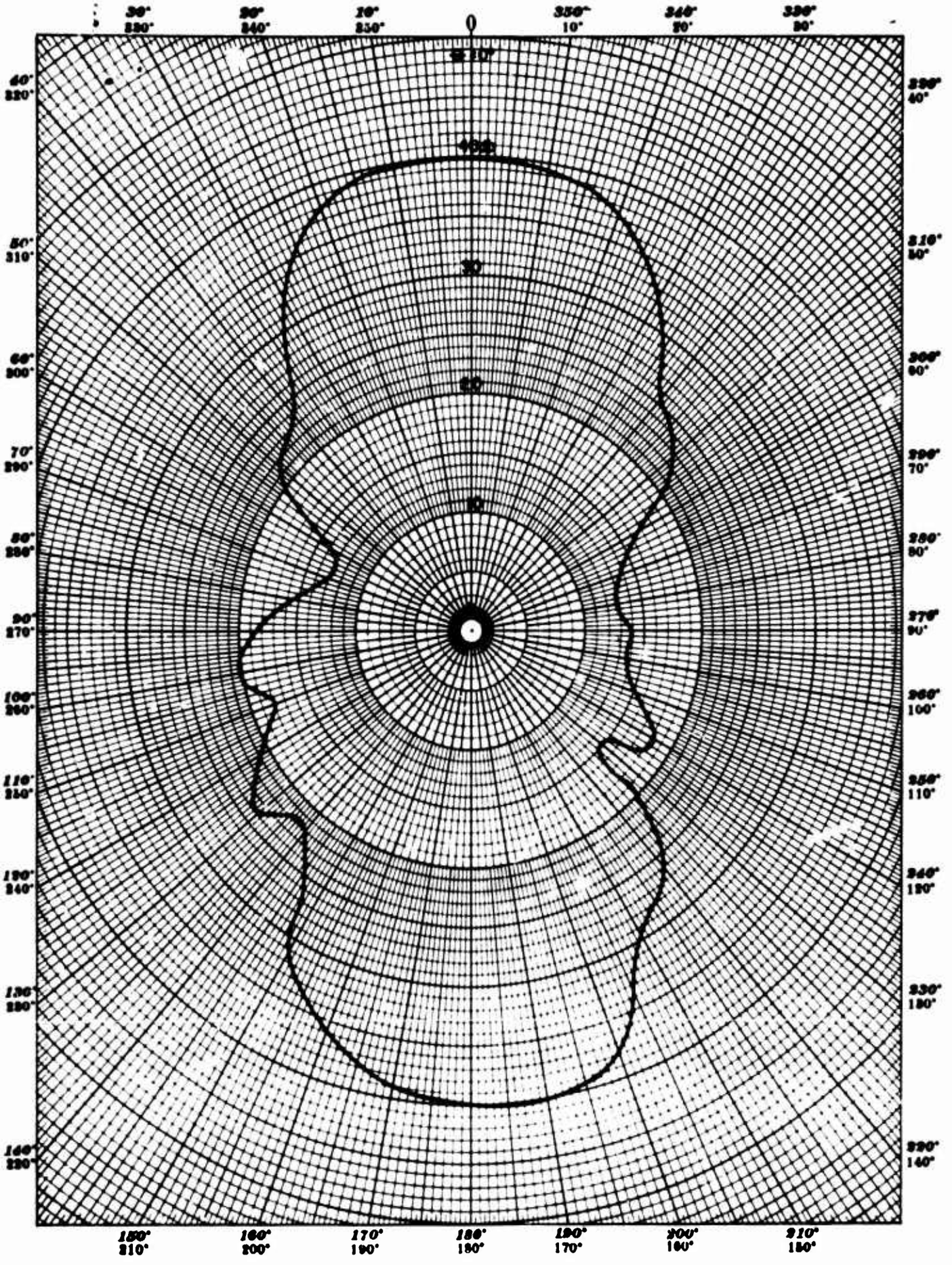

Figure 36. Directivity Pattern - Constant Length Array,
3 Free-Flooded Magnetostrictive Rings

Frequency: 8200 cps—Test Distance: 5 Meters—Depth: 26.5 Meters

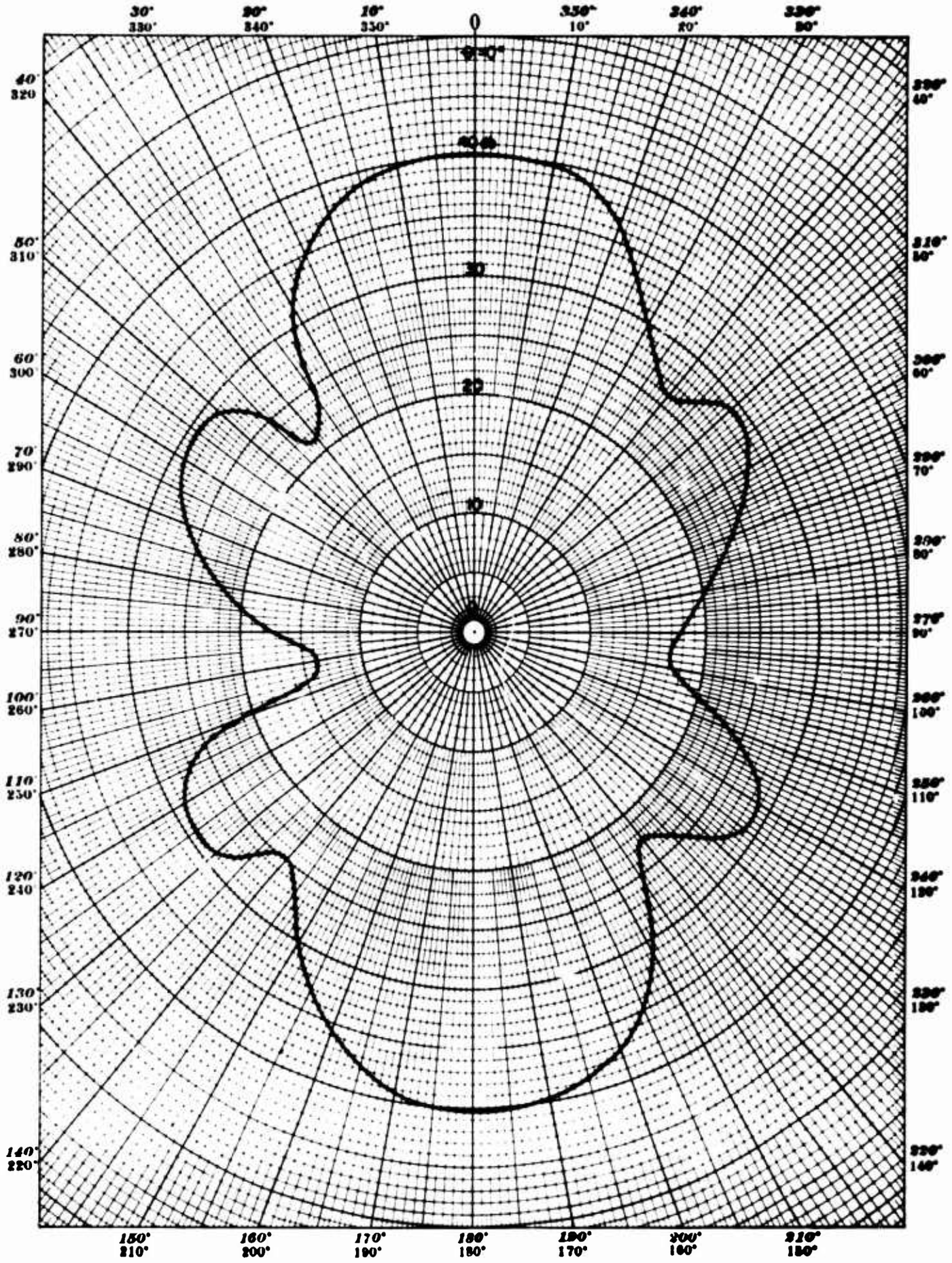

Figure 37. Directivity Pattern - Constant Length Array,
3 Free-Flooded Magnetostrictive Rings

Frequency: 8400 cps—Test Distance: 5 Meters—Depth: 26.5 Meters

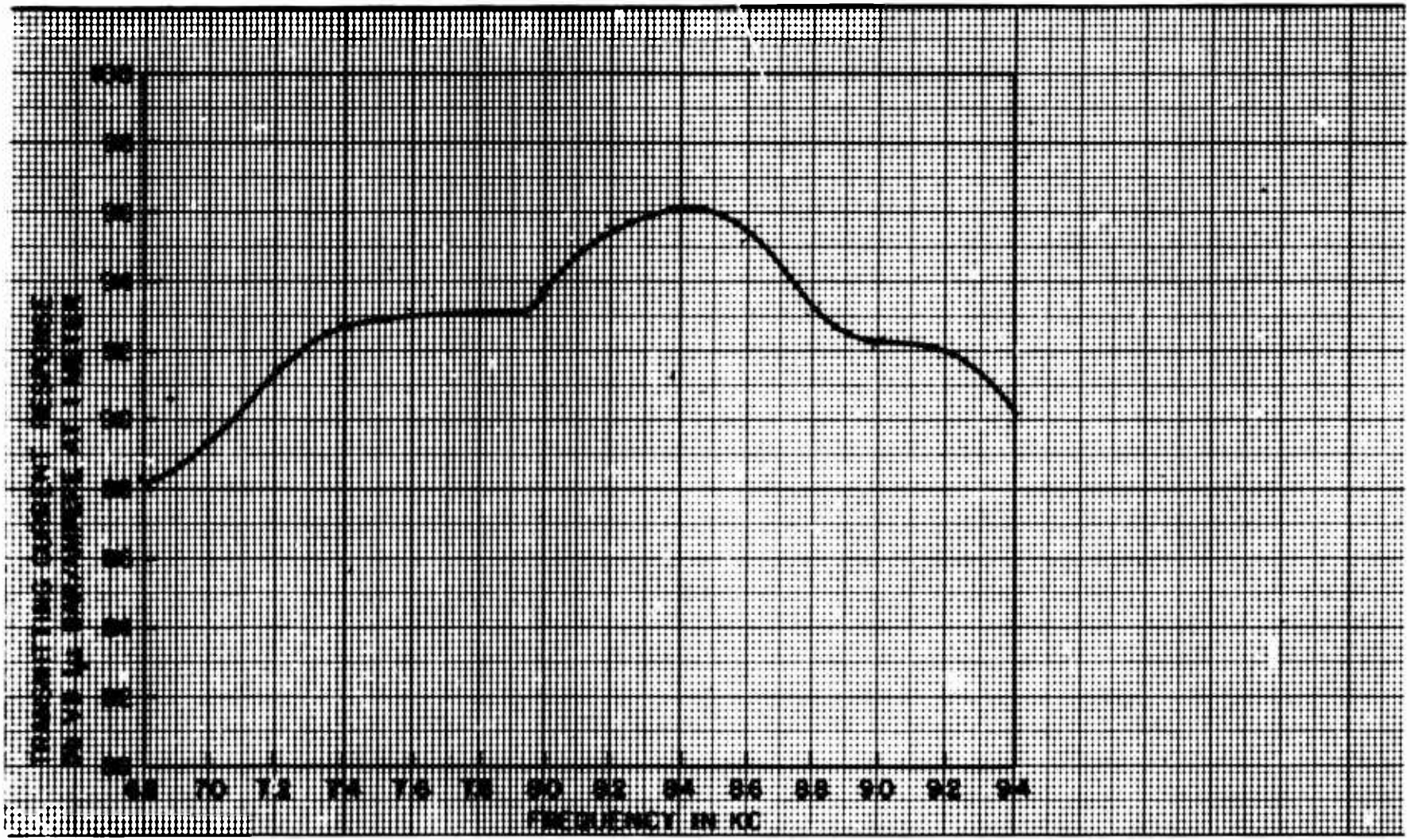

Figure 38. Transmitting Current Response Curve, Array of 4 **Magnetostrictive Rings** in Series. D.C. = 0.5 Amperes, 87-**foot depth. (Distance** between rings = 1.833 inches).

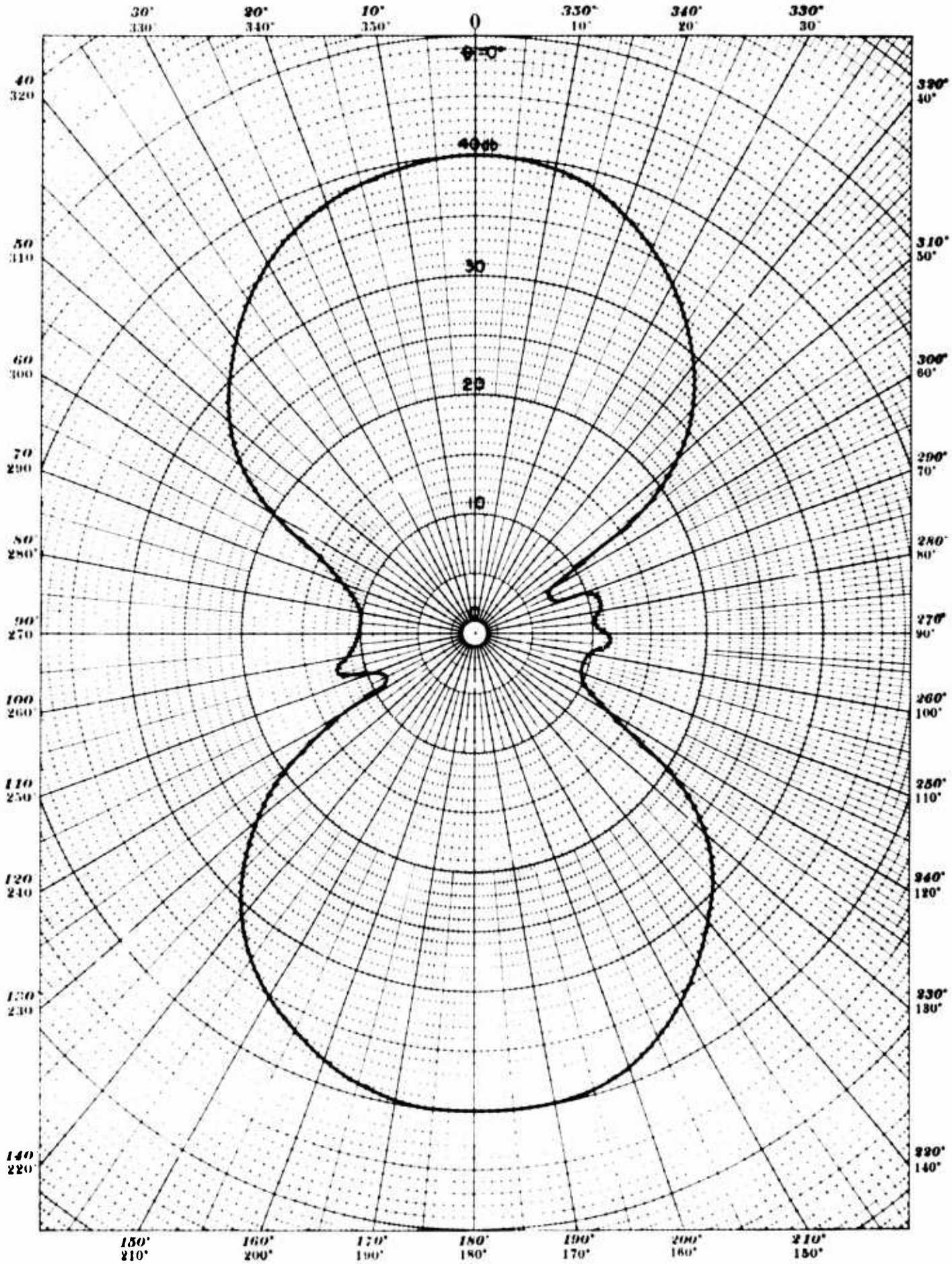

Figure 39. Directivity Pattern - Constant Length Array, 4 Free-Flooded Magnetostrictive Rings

Frequency: 5000 cps—Test Distance: 5 Meters—Depth: 26.5 Meters

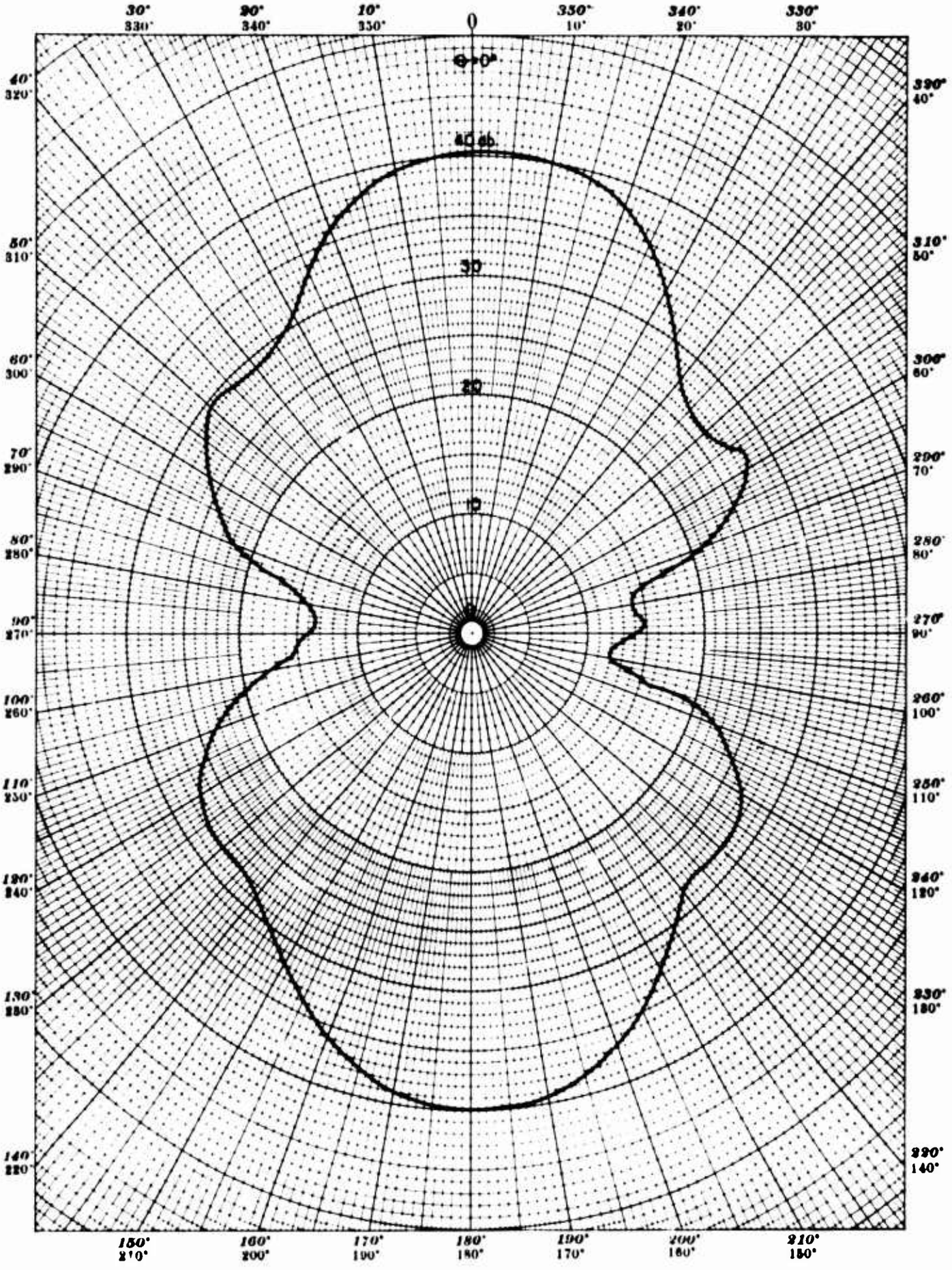

Figure 40. Directivity Pattern - Constant Length Array, 4 Free-Flooded Magnetostrictive Rings

Frequency: 8000 cps—Test Distance: 5 Meters—Depth: 26.5 Meters

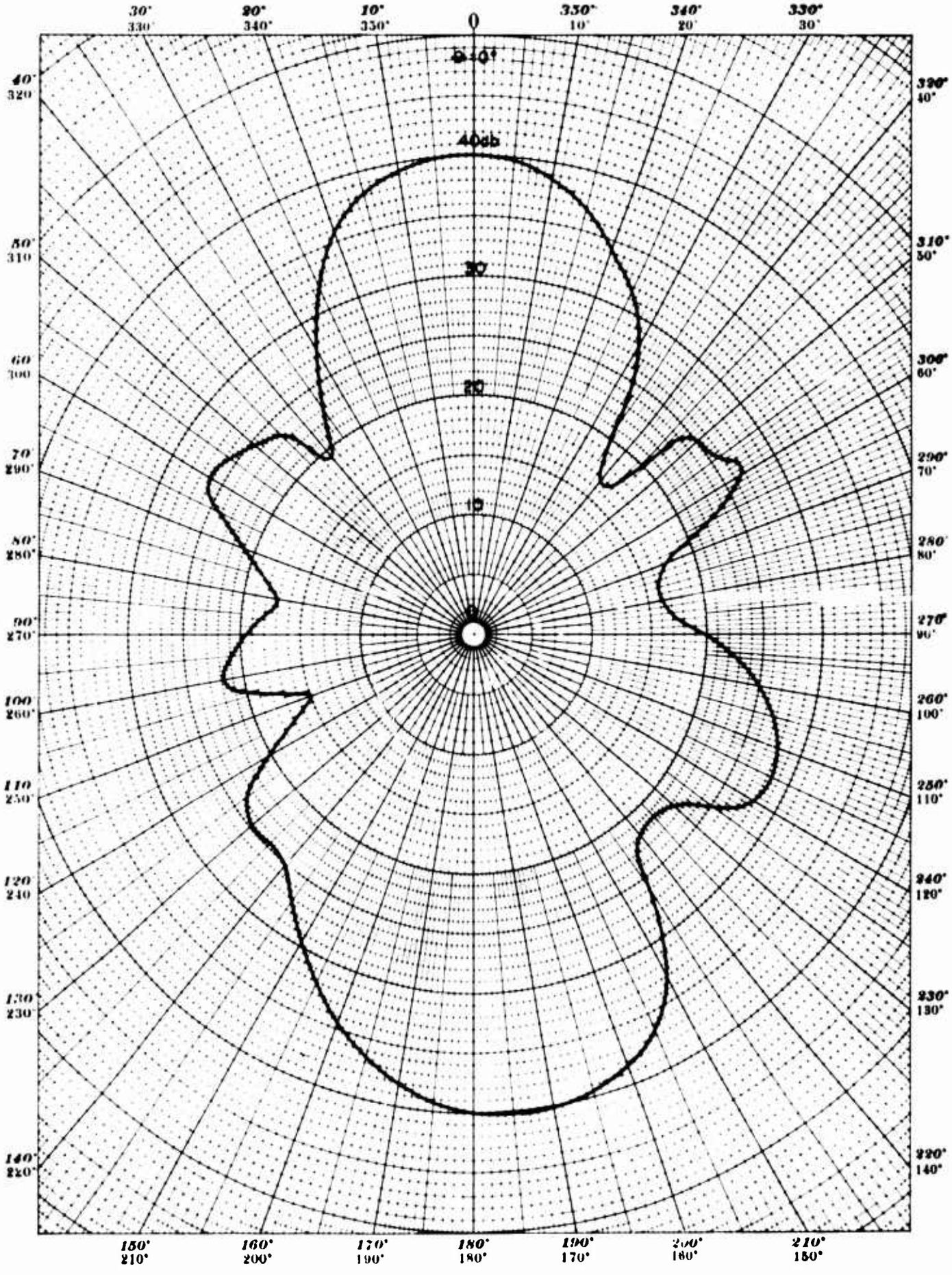

Figure 41. Directivity Pattern - Constant Length Array, 4 Free-Flooded Magnetostrictive Rings

Frequency: 8400 cps—Test Distance: 5 Meters—Depth: 26.5 Meters

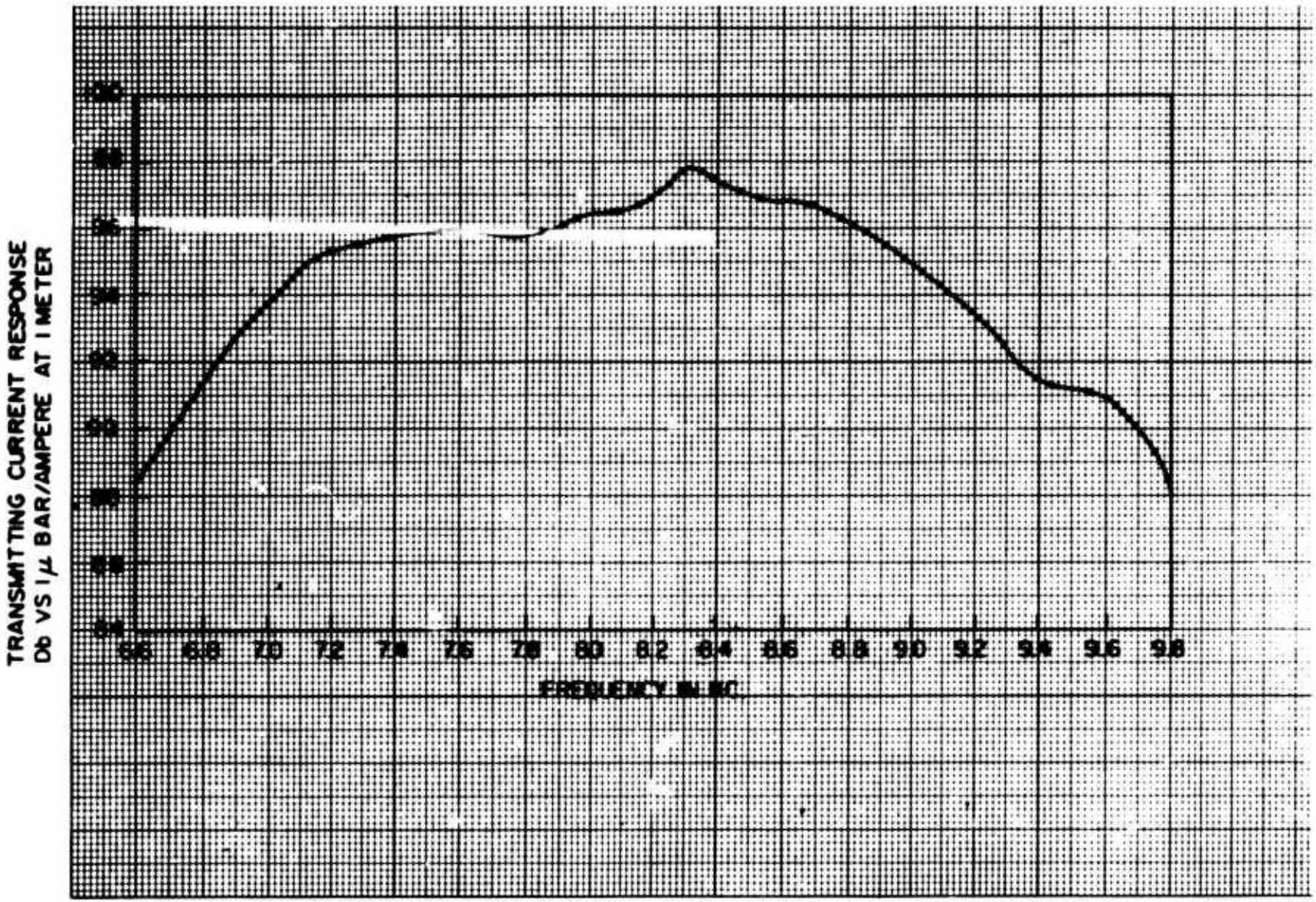

Figure 42. Transmitting Current Response Curve, Array of 5 Magnetostrictive Rings in Series. D.C. = 0.5 Amperes, 87-foot depth. (Distance between rings = 1.218 inches).

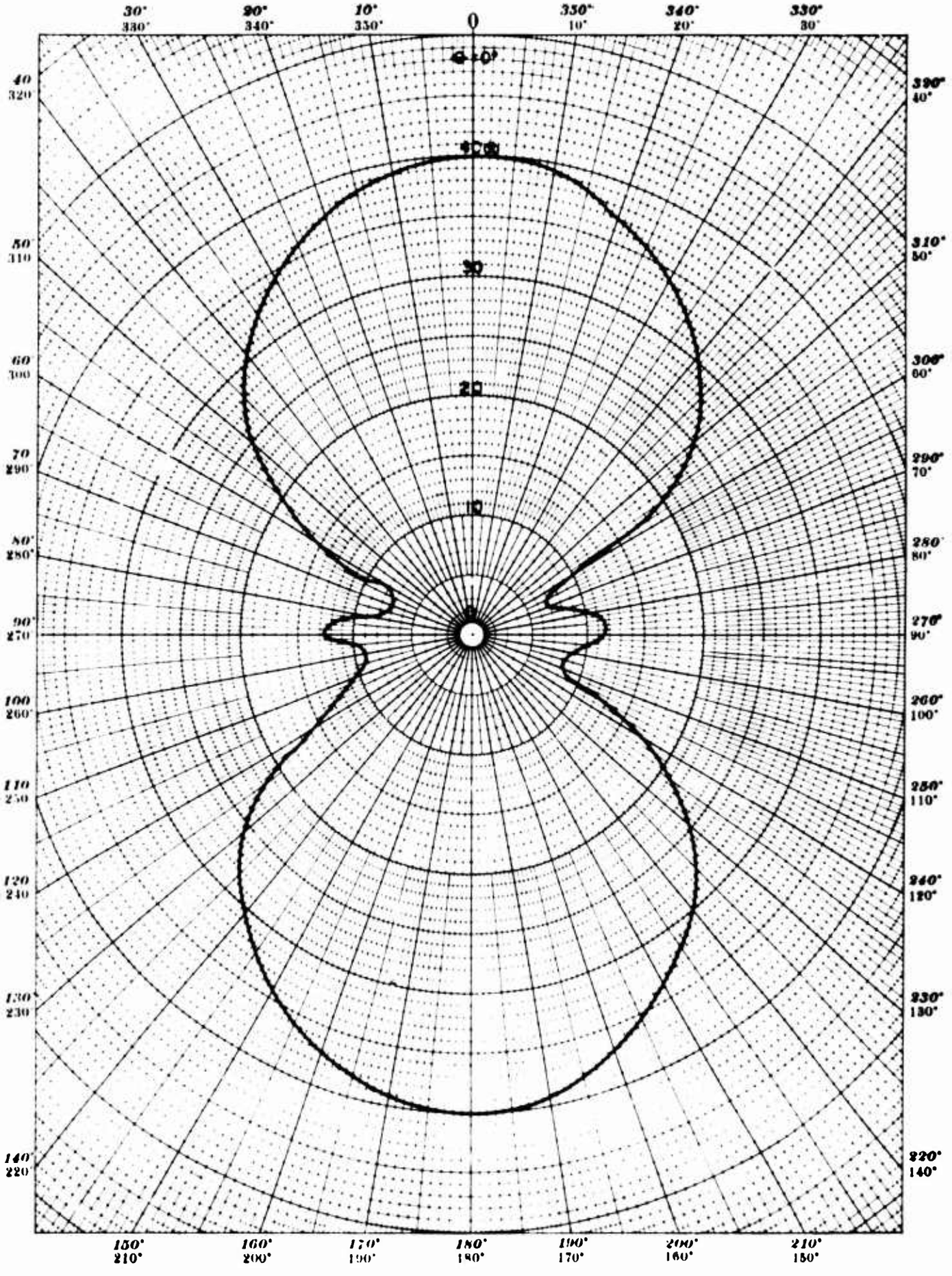

Figure 43. Directivity Pattern - Constant Length Array, 5 Free-Flooded Magnetostrictive Rings

Frequency: 5000 cps—Test Distance: 5 Meters—Depth: 26.5 Meters

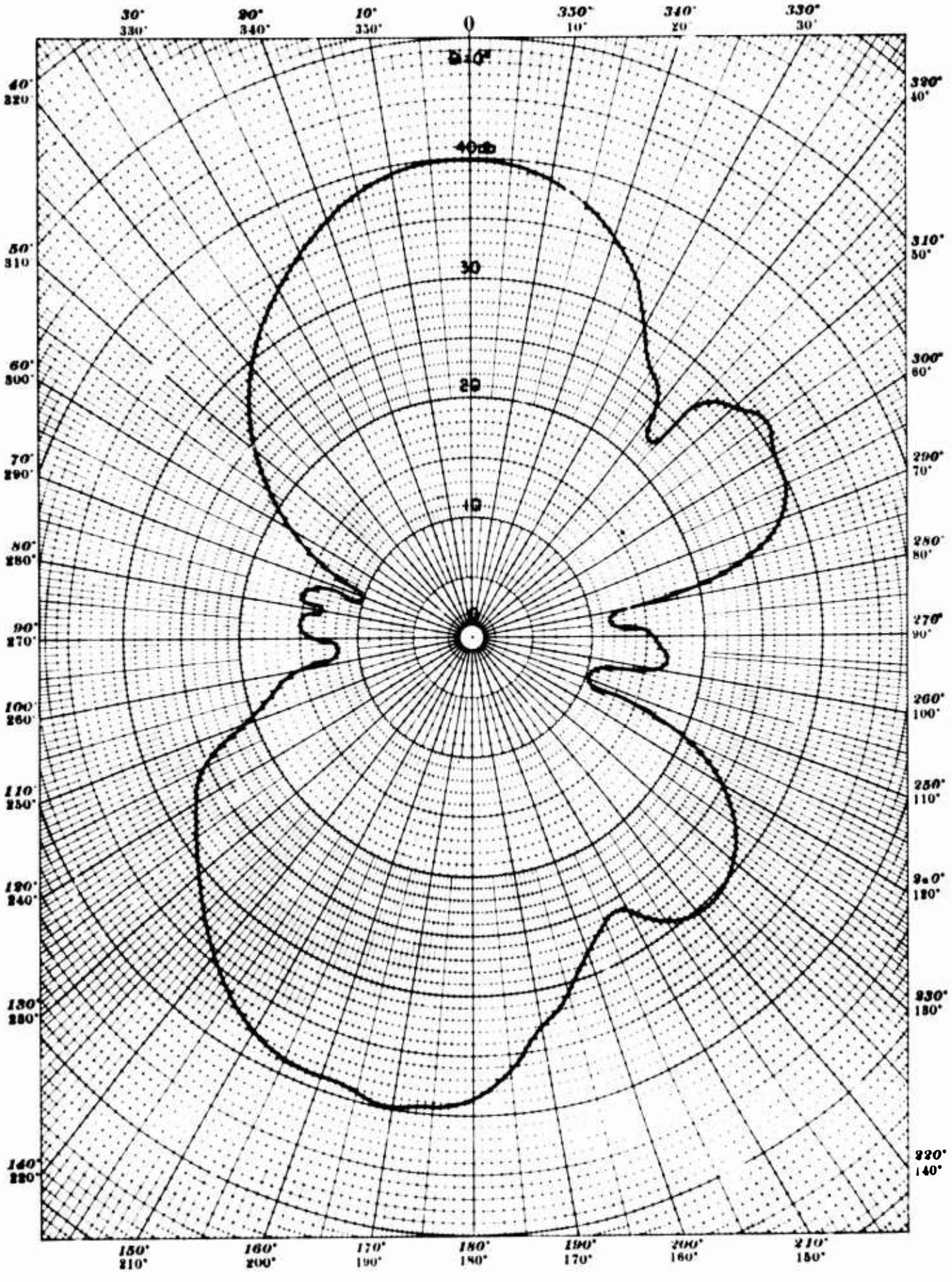

Figure 44. Directivity Pattern - Constant Length Array, 5 Free-Flooded Magnetostrictive Rings

Frequency. 7385 cps—Test Distance: 5 Meters—Depth: 26 5 Meters

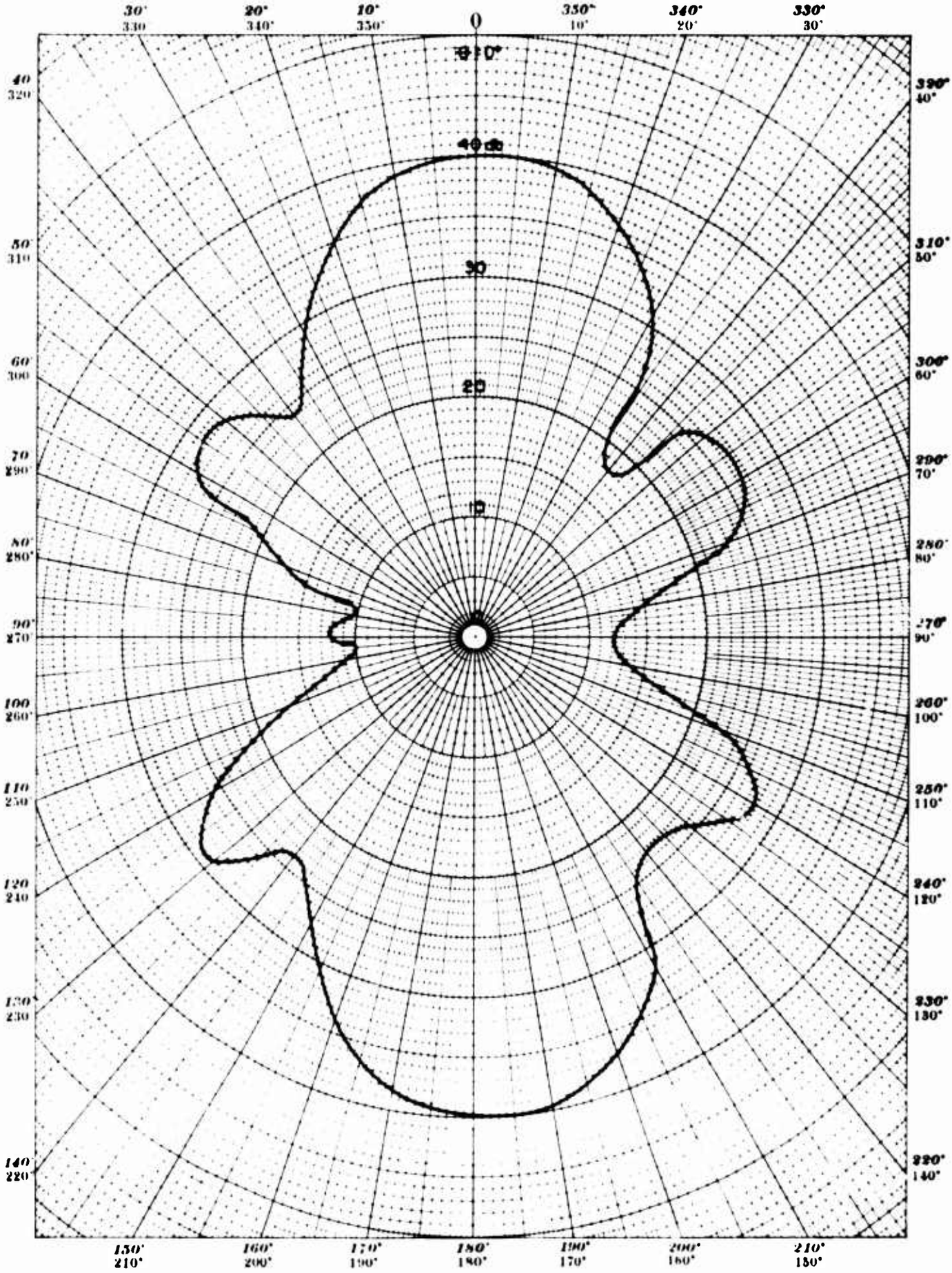

Figure 45. Directivity Pattern - Constant Length Array, 5 Free-Flooded Magnetostrictive Rings

Frequency: 7700 cps—Test Distance: 5 Meters—Depth: 26.5 Meters

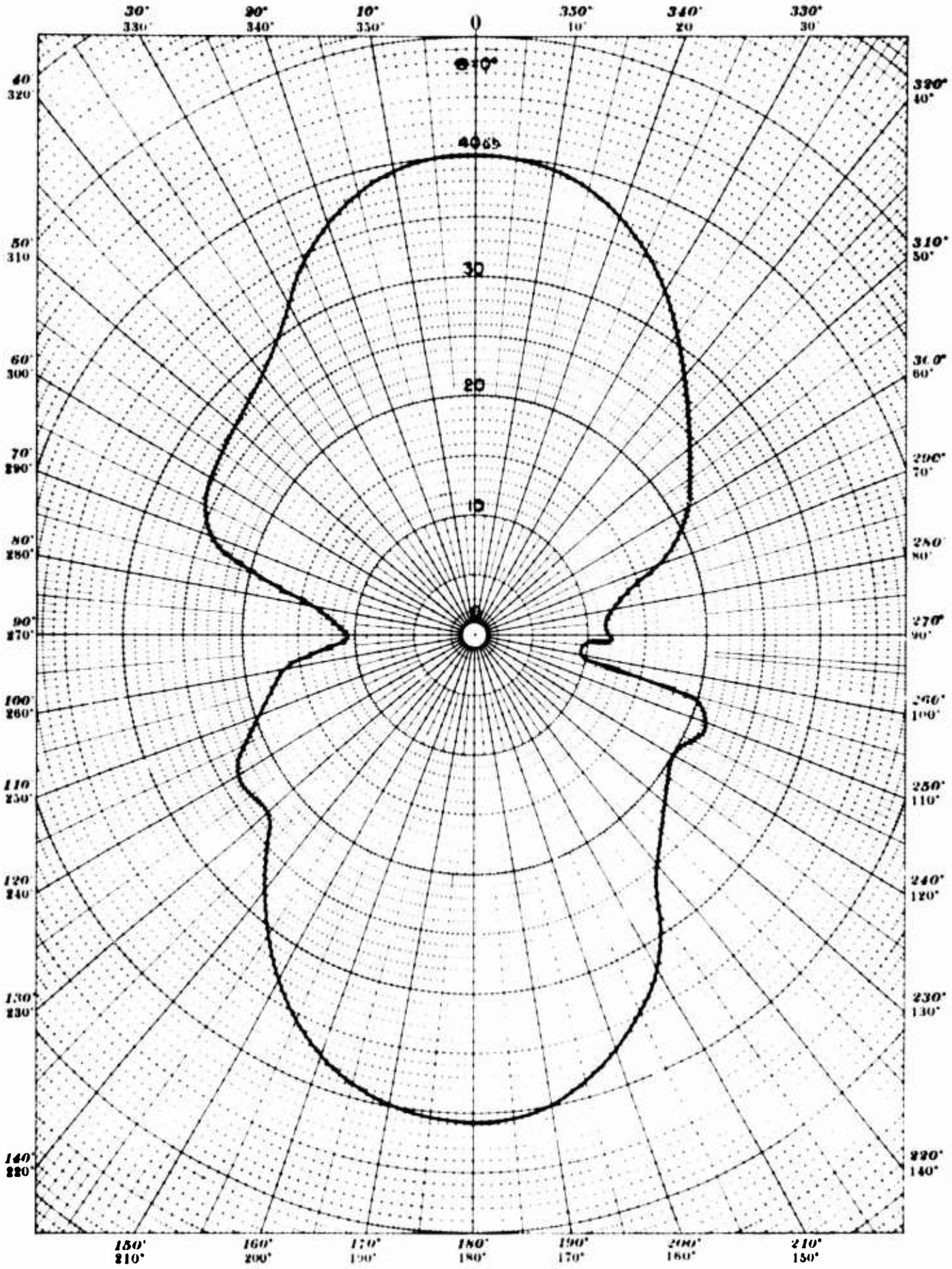

Figure 46. Directivity Pattern - Constant Length Array,
5 Free-Flooded Magnetostrictive Rings

Frequency: 8000 cps—Test Distance: 5 Meters—Depth: 26.5 Meters

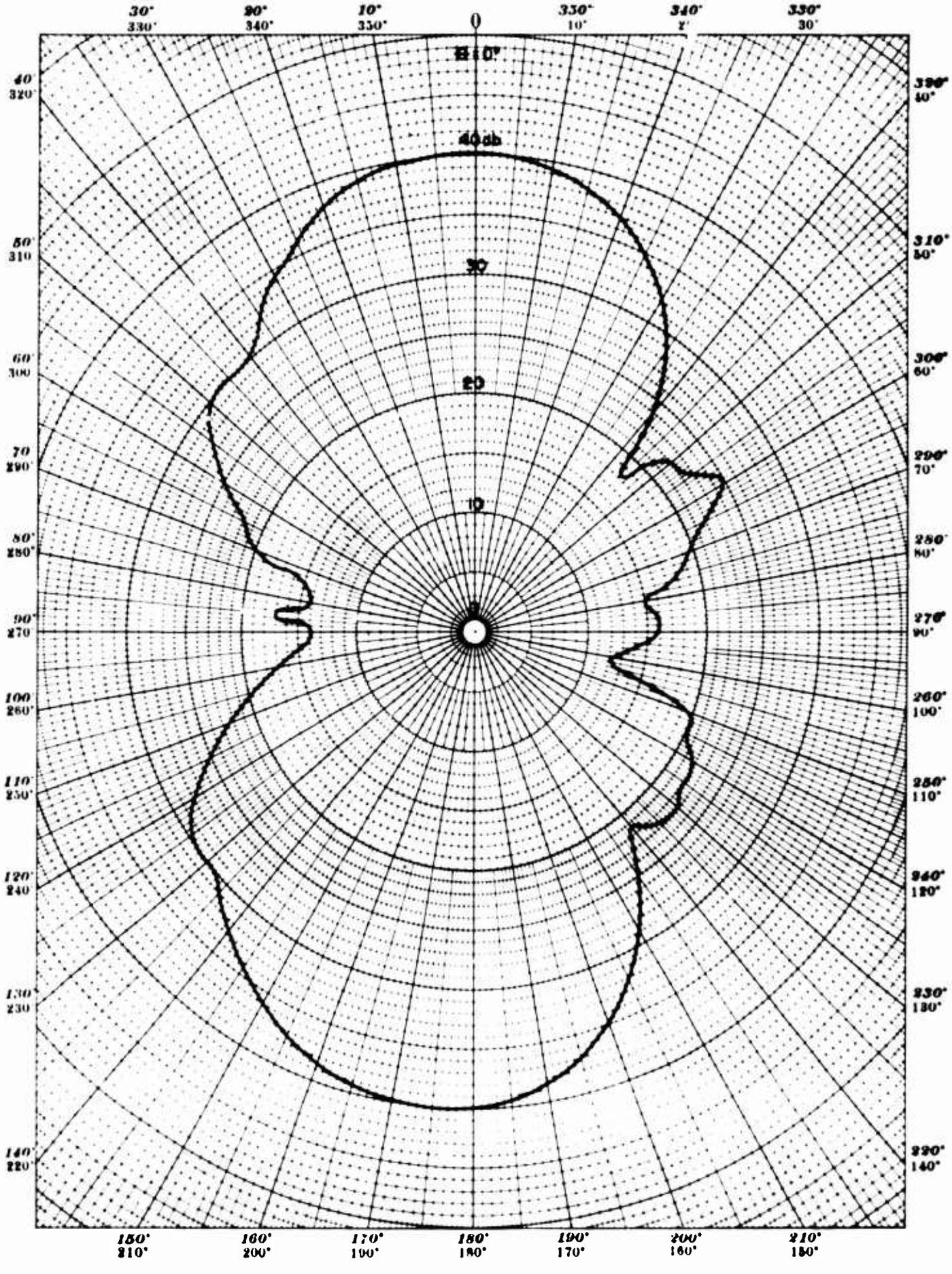

Figure 47. Directivity Pattern - Constant Length Array, 5 Free-Flooded Magnetostrictive Rings

Frequency: 8300 cps—Test Distance: 5 Meters—Depth: 26.5 Meters

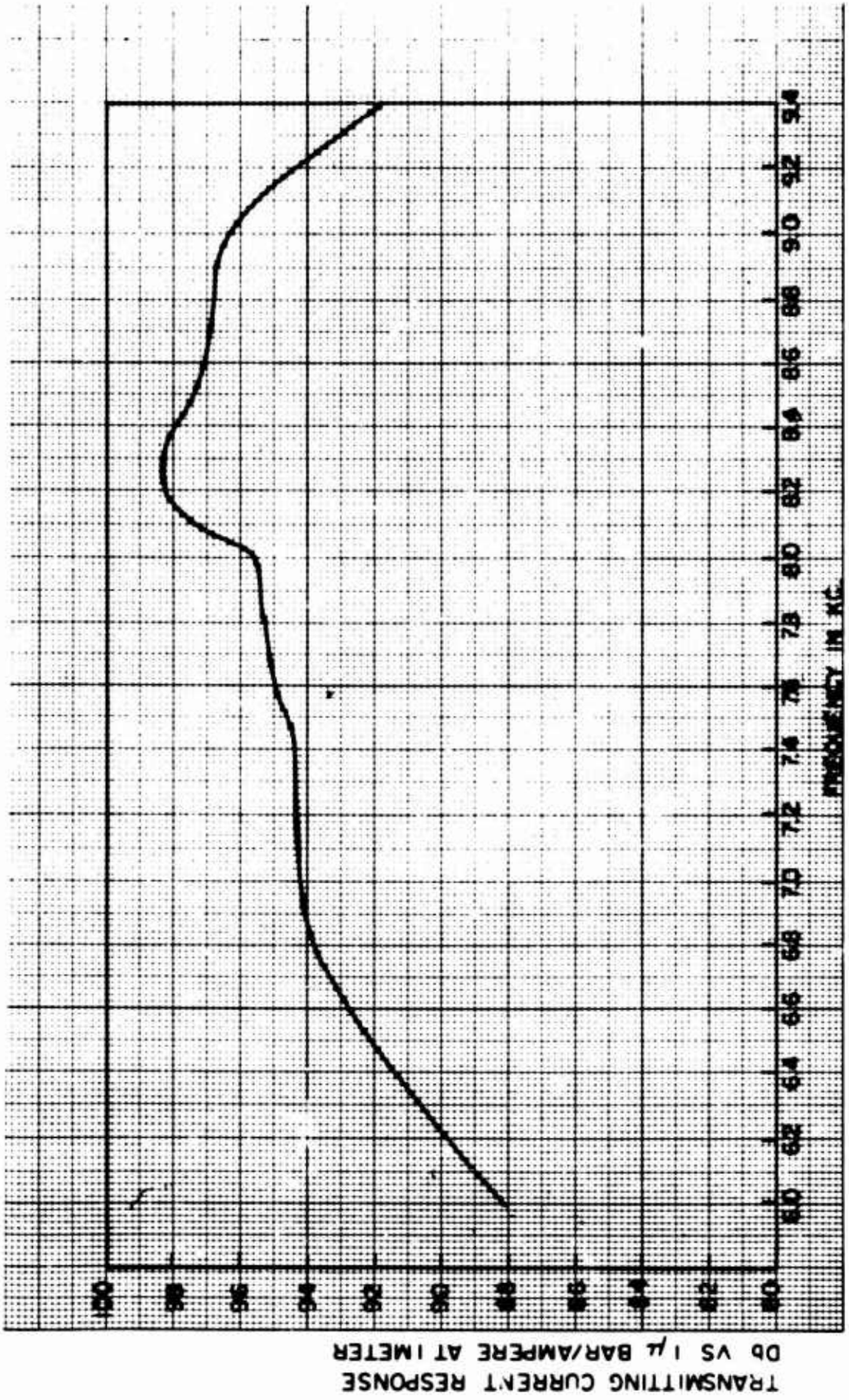

Figure 48. Transmitting Current Response Curve, Array of 6 Magnetostrictive Rings in Series. D.C. = 0.5 Amperes, 87-foot depth. (Distance between rings = 0.850 inches).

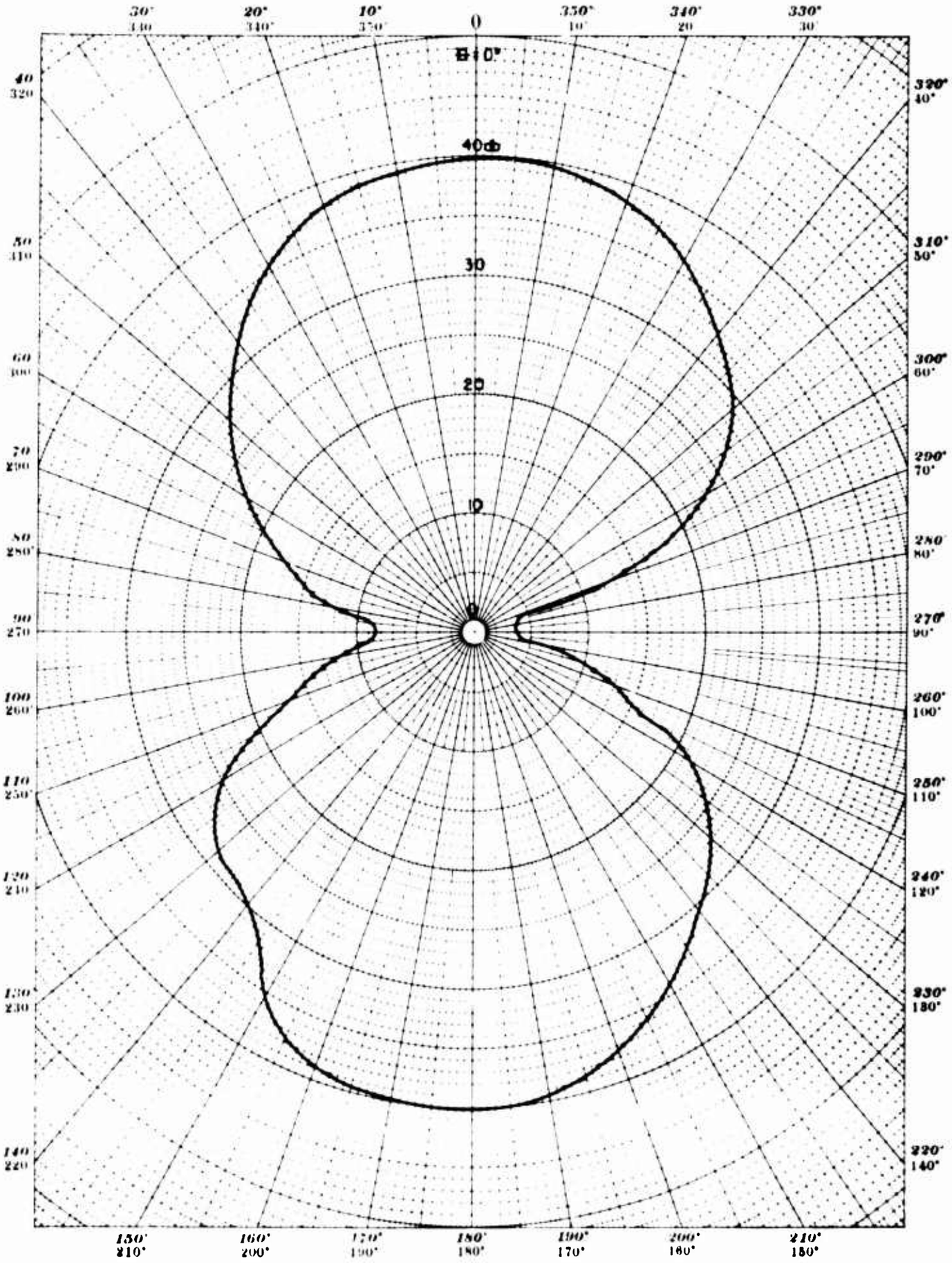

Figure 49. Directivity Pattern - Constant Length Array, 6 Free-Flooded Magnetostrictive Rings

Frequency: 5000 cps—Test Distance: 5 Meters—Depth: 26.5 Meters

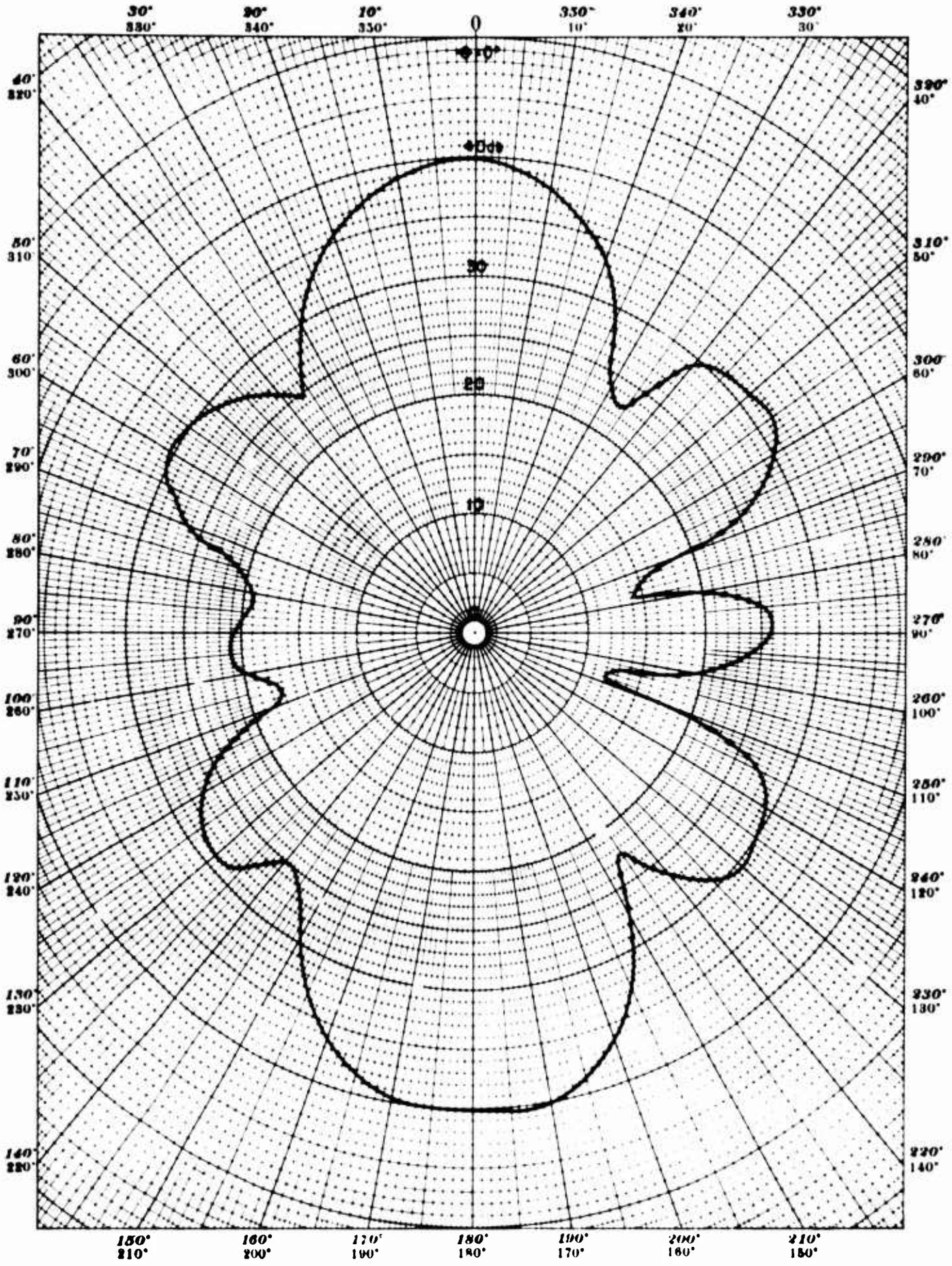

Figure 50. Directivity Pattern - Constant Length Array, 6 Free-Flooded Magnetostrictive Rings

Frequency: 7281 cps—Test Distance: 5 Meters—Depth: 26.5 Meters

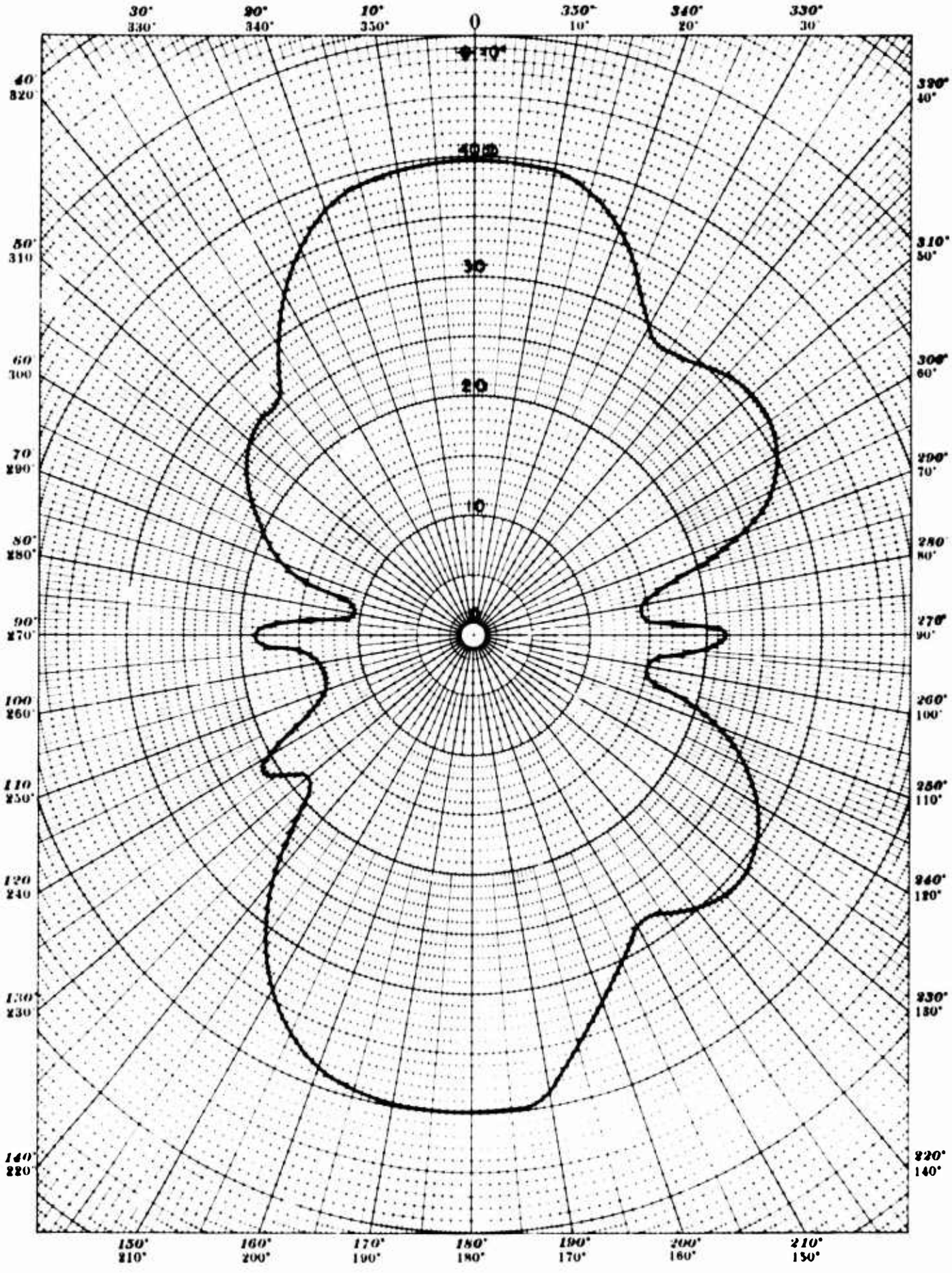

Figure 51. Directivity Pattern - Constant Length Array, 6 Free-Flooded Magnetostrictive Rings

Frequency: 7450 cps—Test Distance: 5 Meters—Depth: 26.5 Meters

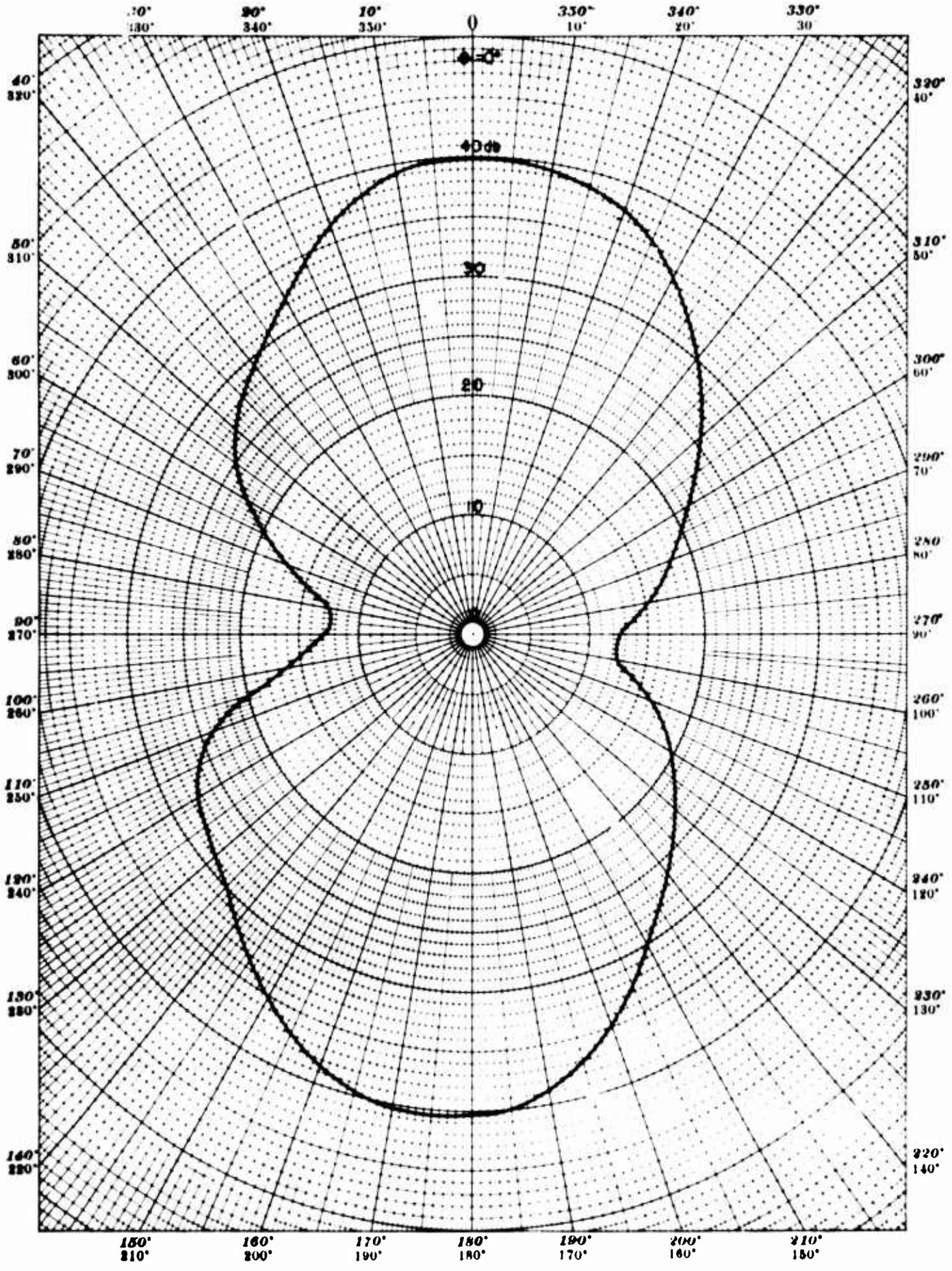

Figure 52. Directivity Pattern - Constant Length Array, 6 Free-Flooded Magnetostrictive Rings

Frequency: 8200 cps—Test Distance: 5 Meters—Depth: 26.5 Meters

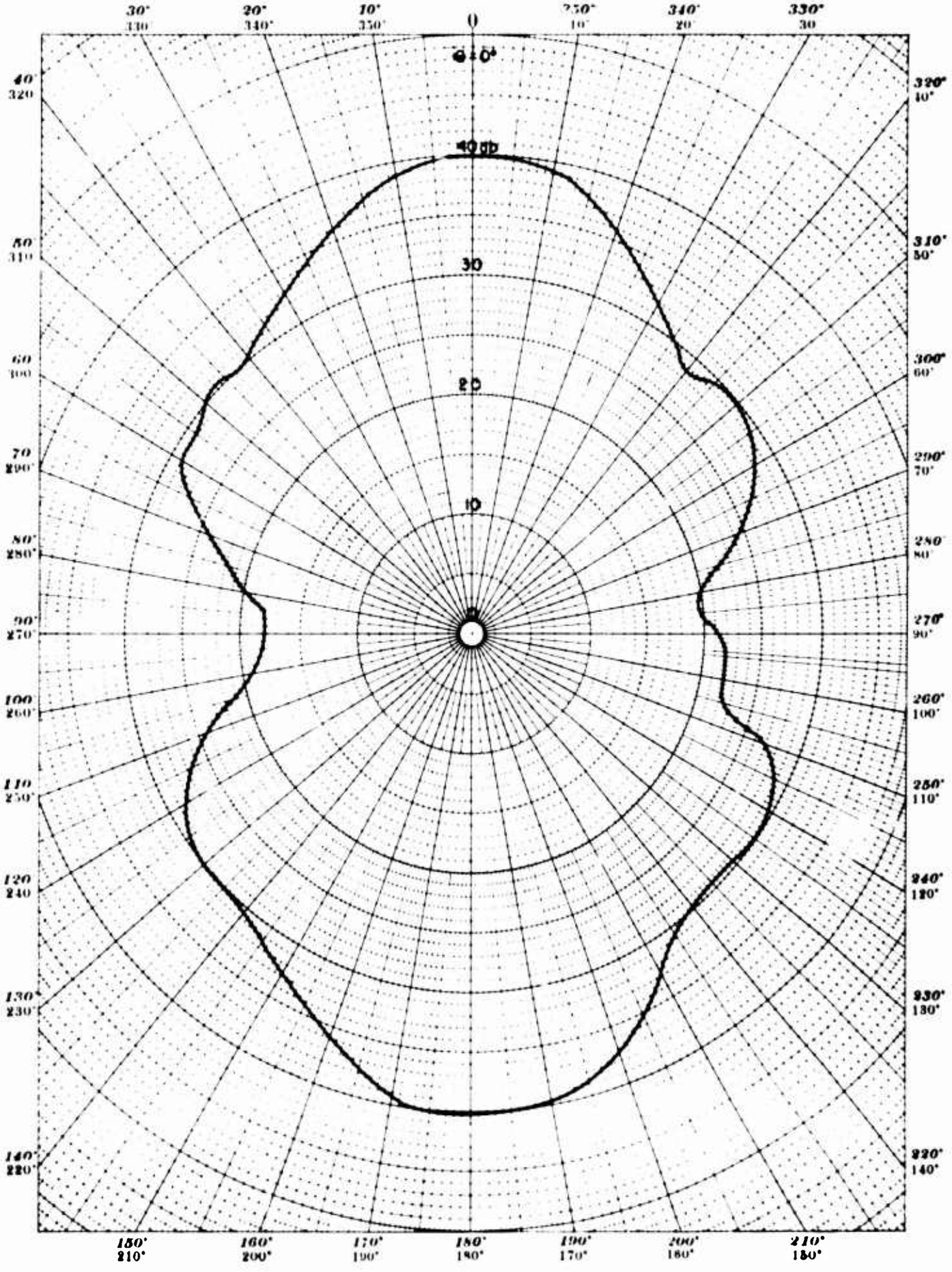

Figure 53. Directivity Pattern - Constant Length Array, 6 Free-Flooded Magnetostrictive Rings

Frequency: 8300 cps—Test Distance: 5 Meters—Depth: 26.5 Meters

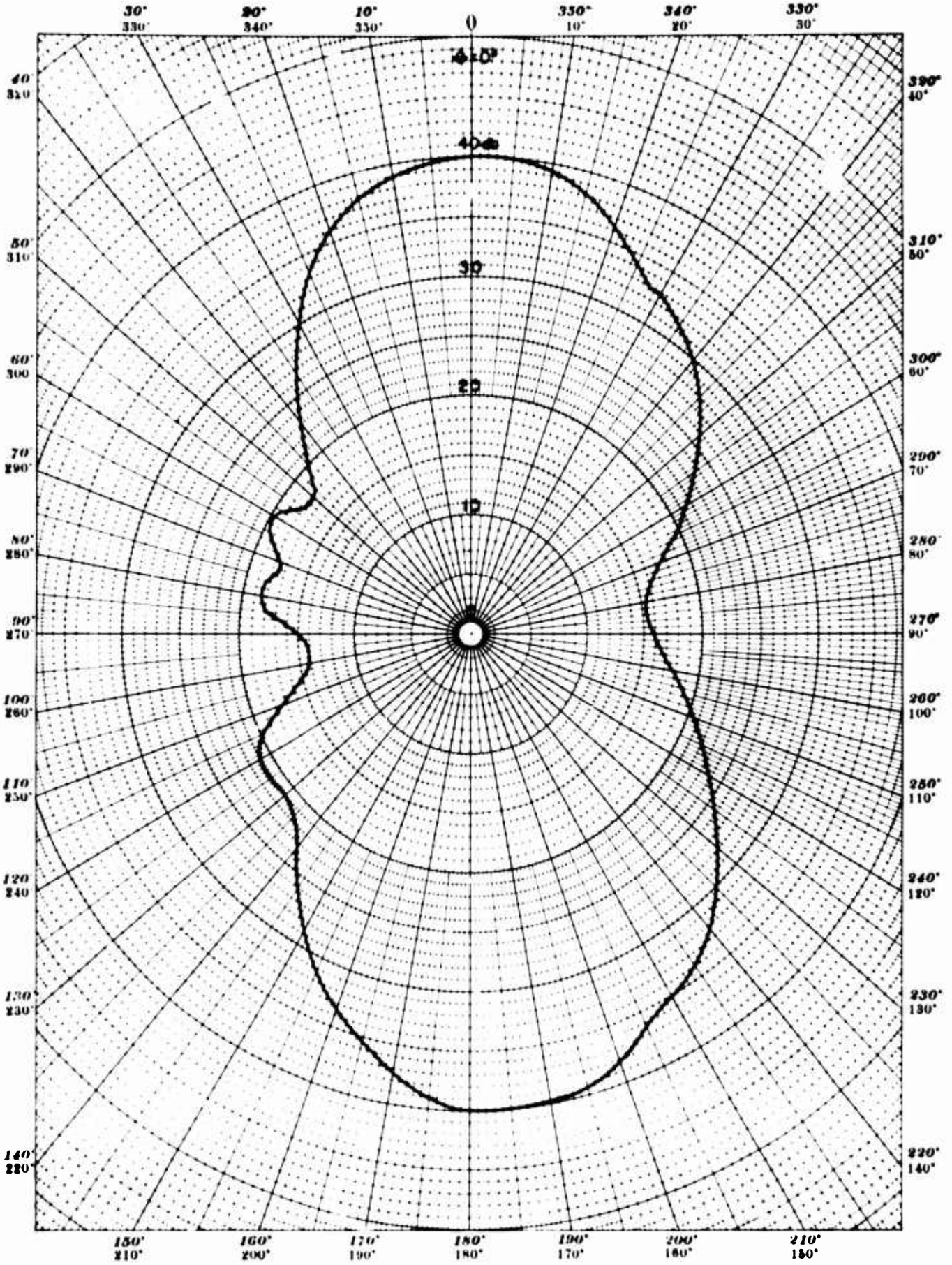

Figure 54. Directivity Pattern - Constant Length Array, 6 Free-Flooded Magnetostrictive Rings

Frequency: 8400 cps—Test Distance: 5 Meters—Depth: 26.5 Meters

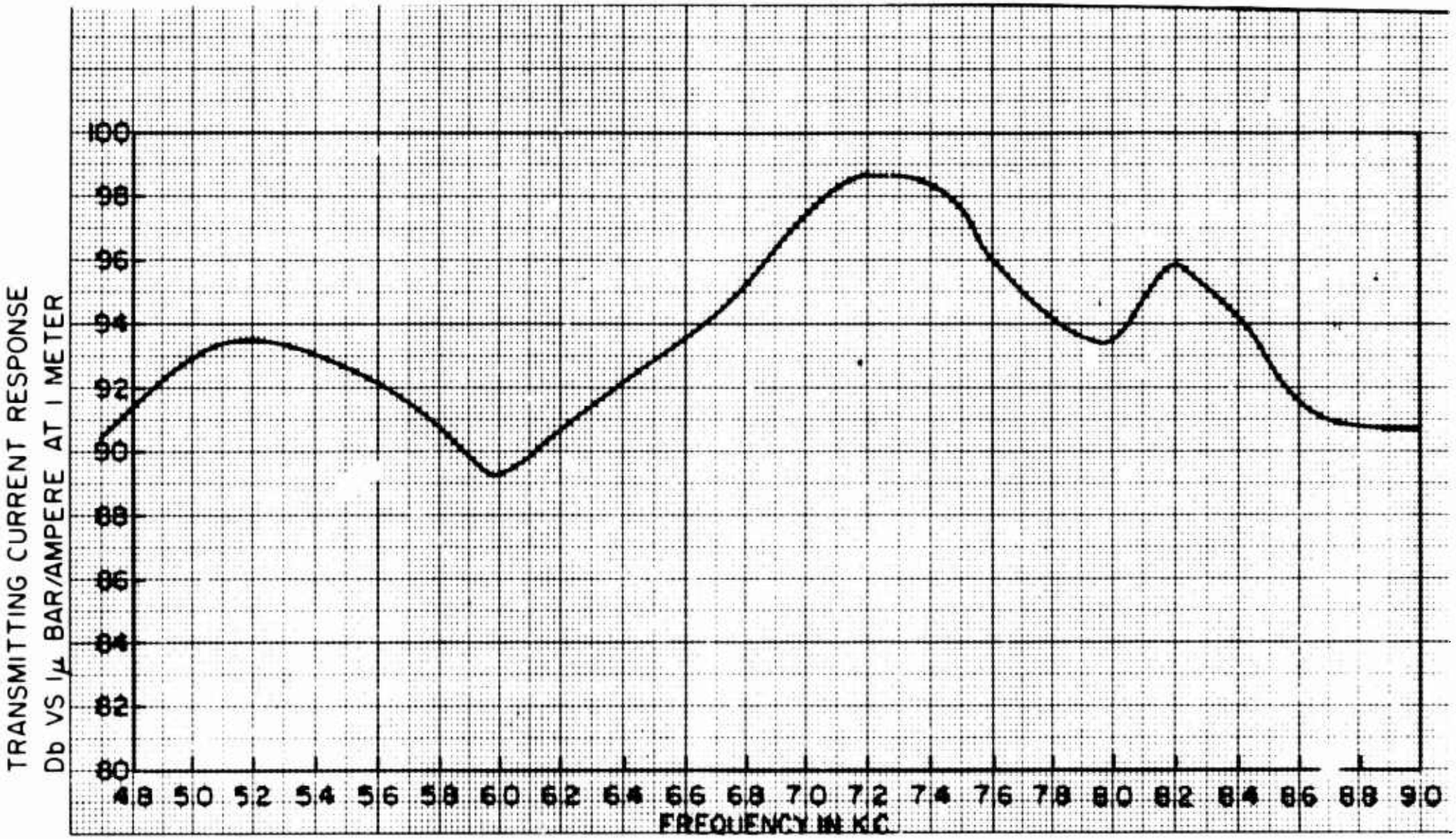

Figure 55. Transmitting Current Response Curve, Array of 9 Magnetostrictive Rings in Series, D.C. - 0.5 Amperes, 87-foot depth. (Distance between rings - 0.297 inches).

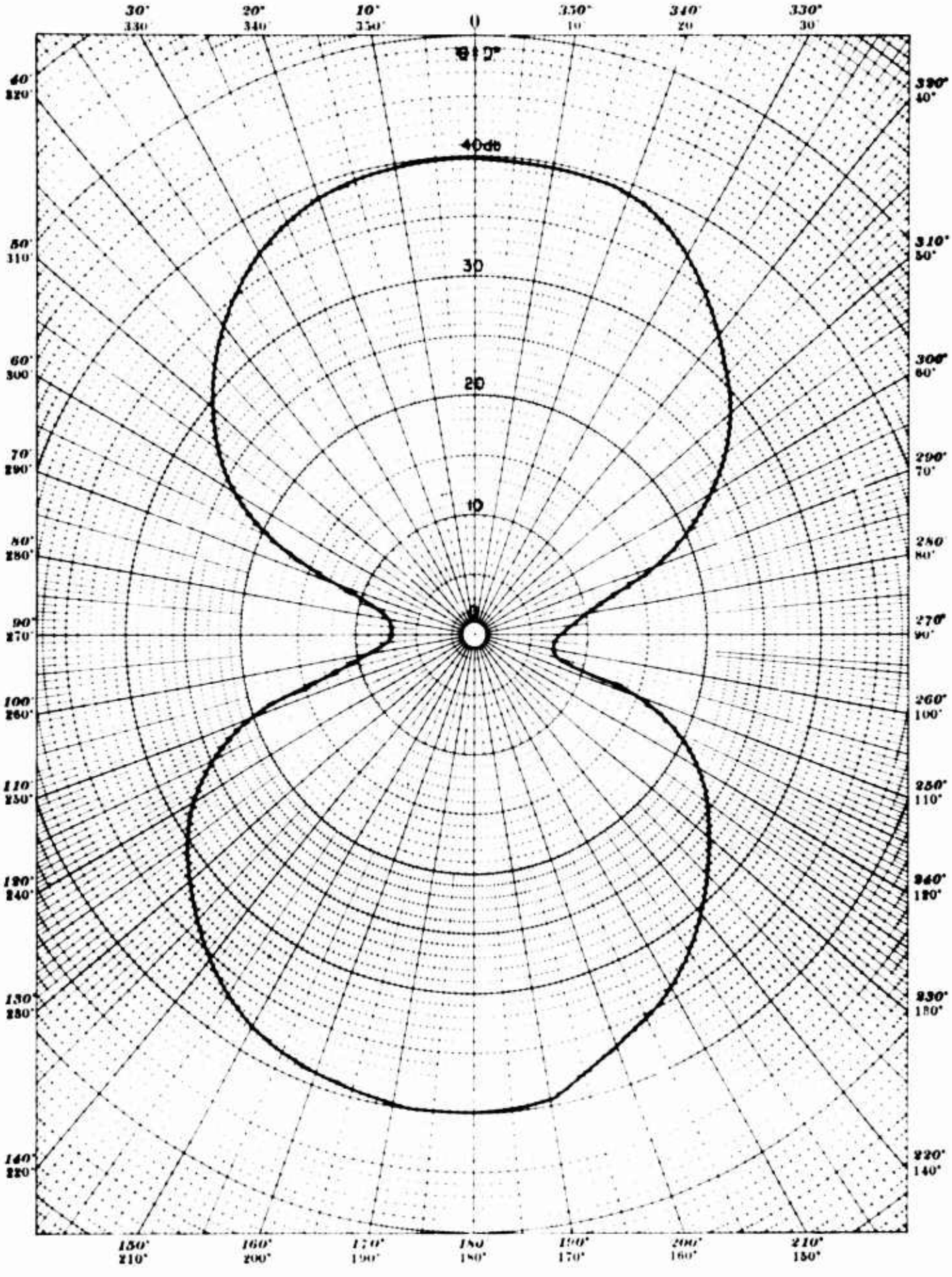

Figure 56. Directivity Pattern - Constant Length Array, 9 Free-Flooded Magnetostrictive Rings

Frequency: 5200 cps—Test Distance: [illegible] Meters—Depth: 26.5 Meters

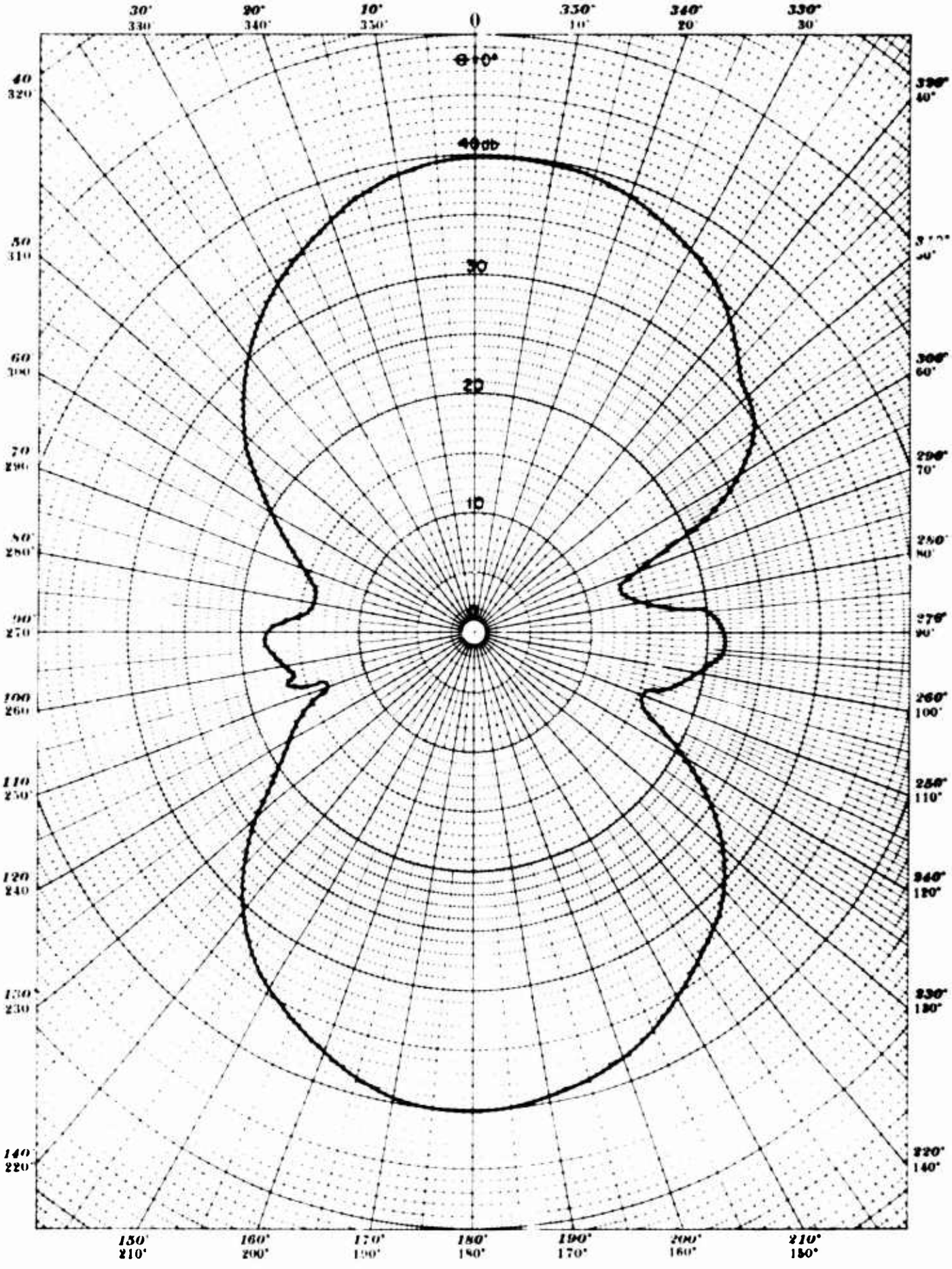

Figure 57. Directivity Pattern - Constant Length Array, 9 Free-Flooded Magnetostrictive Rings

Frequency: 5583 cps—Test Distance: 5 Meters—Depth: 26.5 Meters

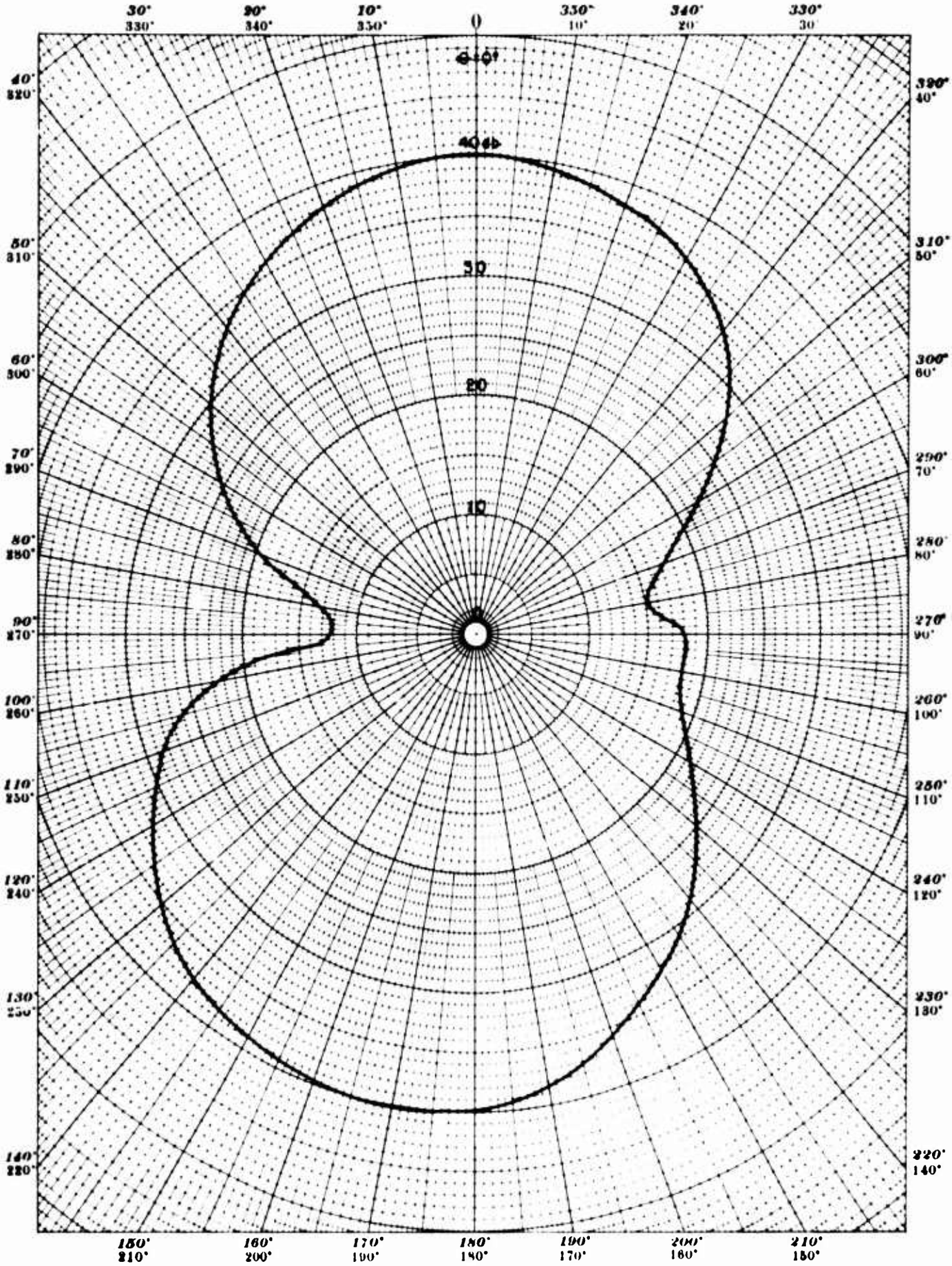

Figure 58. Directivity Pattern - Constant Length Array, 9 Free-Flooded Magnetostrictive Rings

Frequency: 5800 cps—Test Distance: 5 Meters—Depth: 26.5 Meters

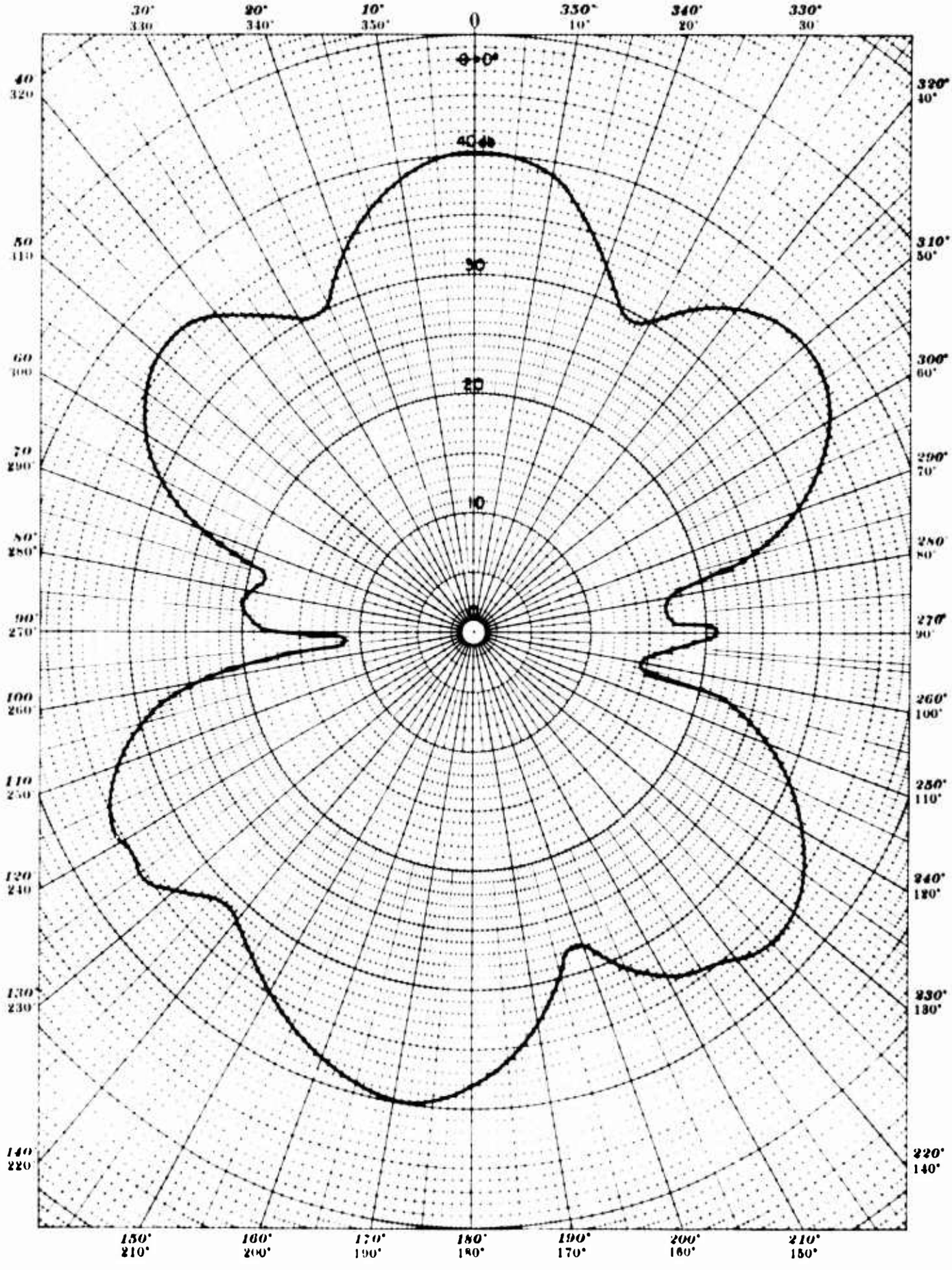

Figure 59 Directivity Pattern - Constant Length Array.
9 Free-Flooded Magnetostrictive Rings

Frequency: 7058 cps—Test Distance: 5 Meters—Depth: 26.5 Meters

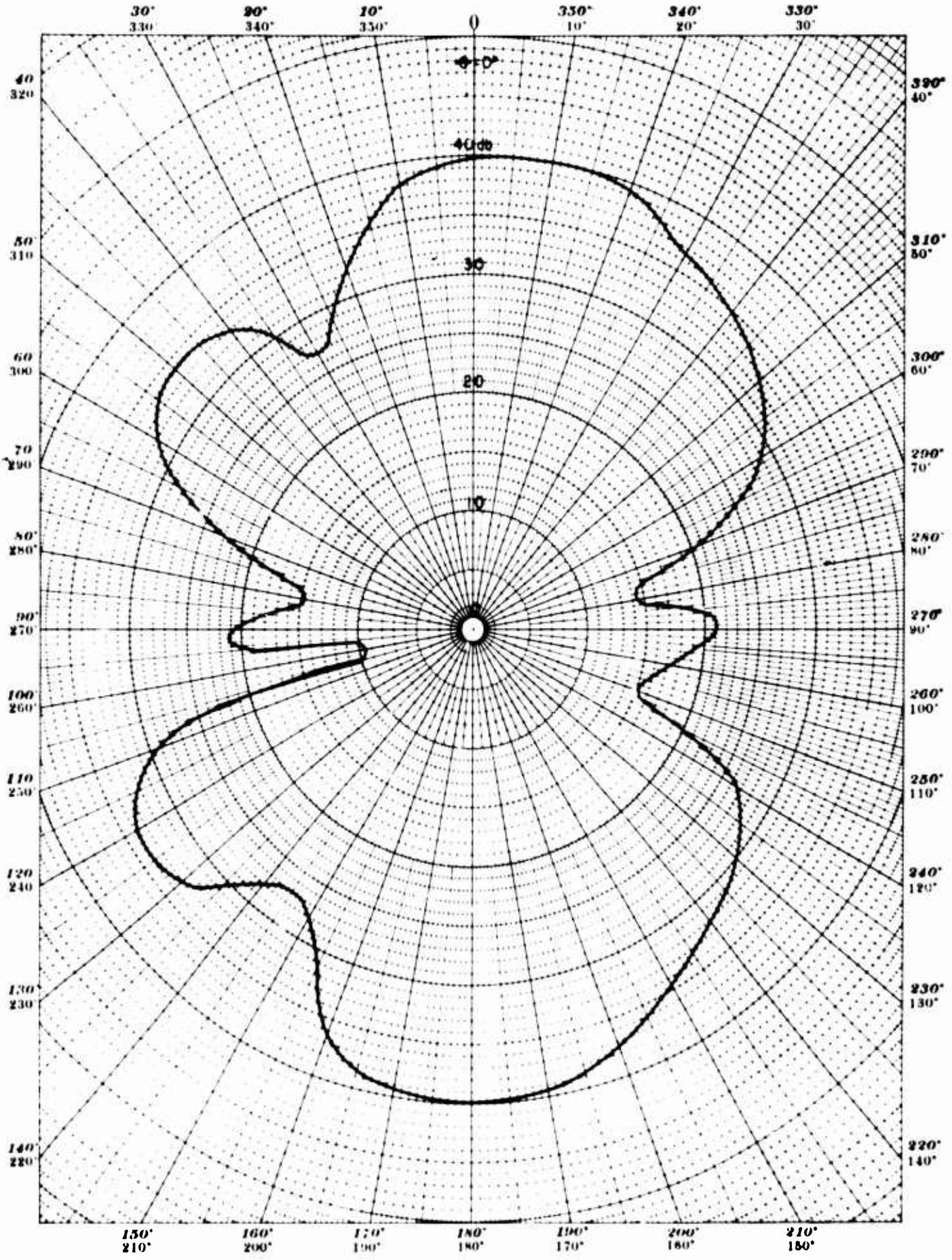

Figure 60. Directivity Pattern - Constant Length Array, 9 Free-Flooded Magnetostrictive Rings

Frequency: 7200 cps—Test Distance: 5 Meters—Depth: 26.5 Meters

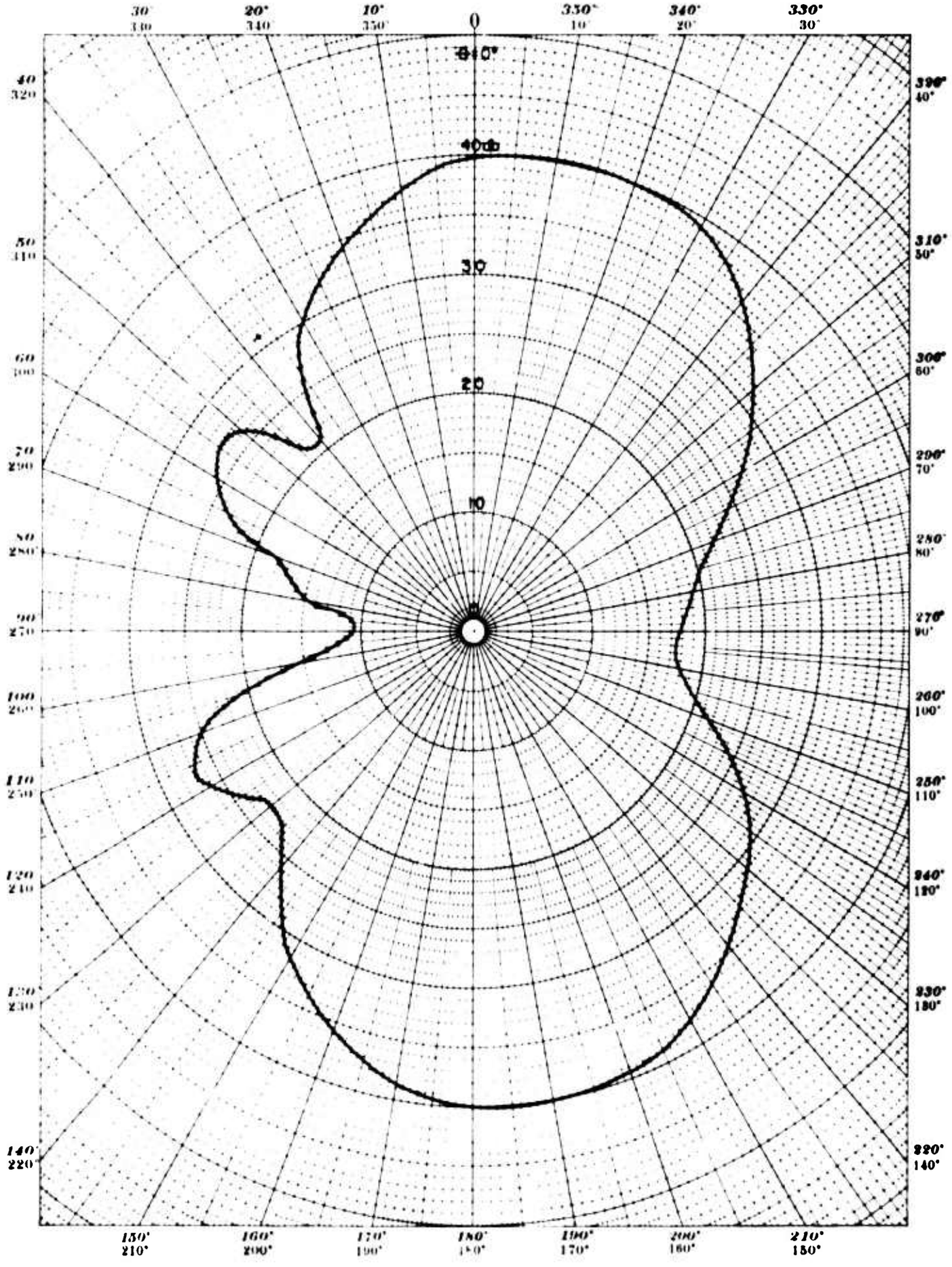

Figure 61. Directivity Pattern - Constant Length Array, 9 Free-Flooded Magnetostrictive Rings

Frequency: 8400 cps—Test Distance: 5 Meters—Depth: 26.5 Meters

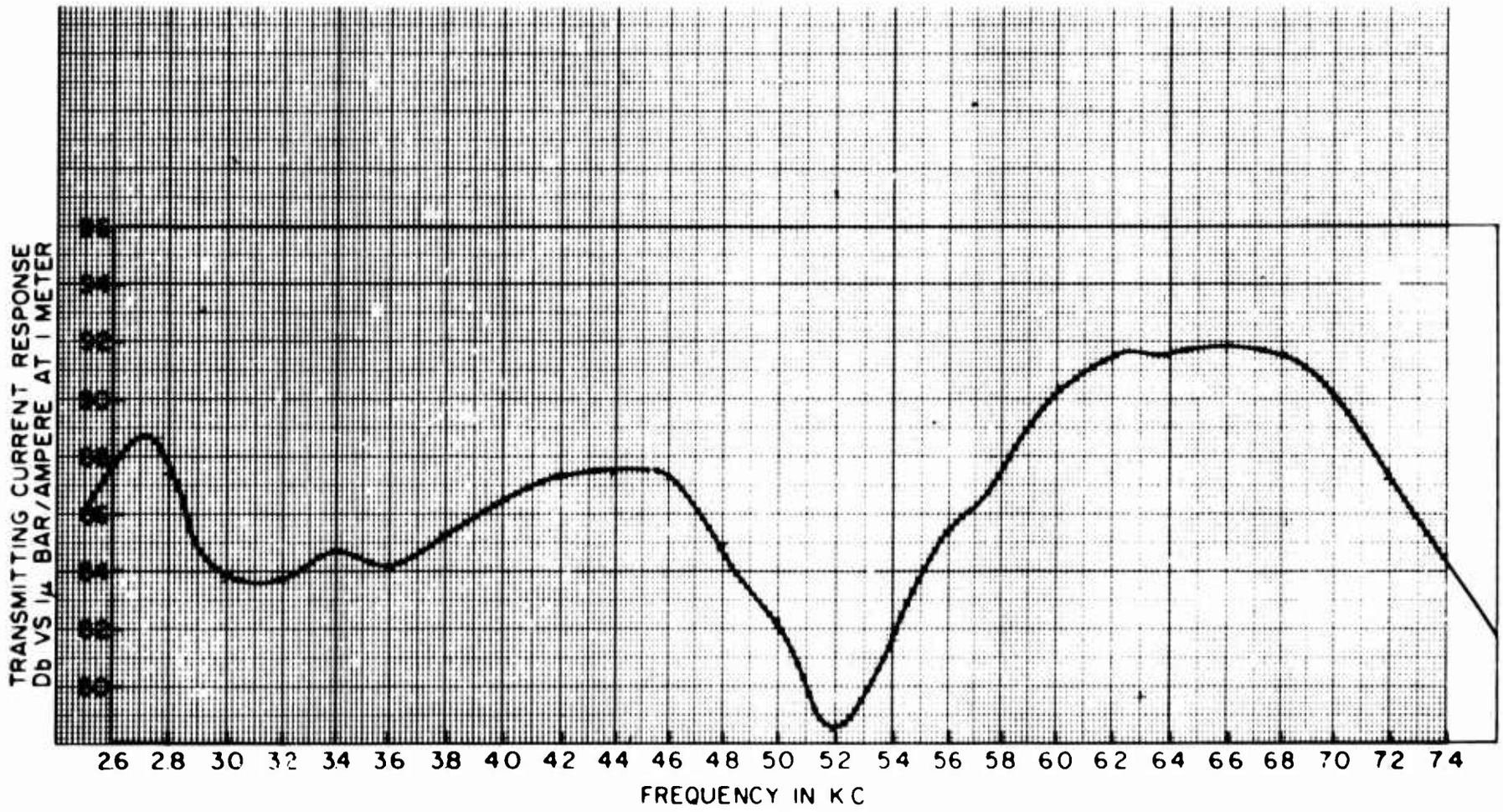

Figure 62. Transmitting Current Response Curve, Array of 12 Magnetostrictive Rings in Series (Rings closely stacked)

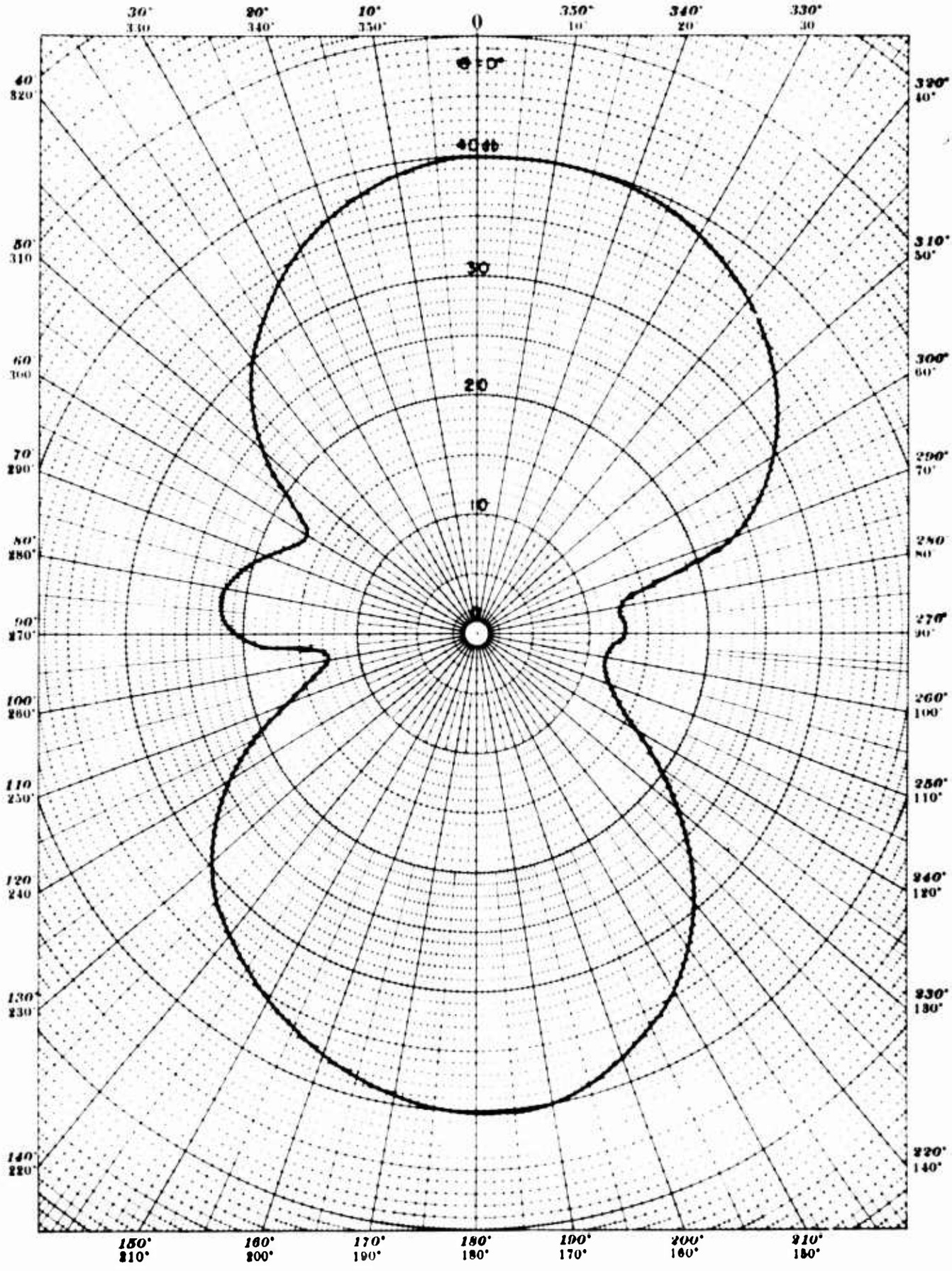

Figure 63. Directivity Pattern - Constant Length Array, 12 Free-Flooded Magnetostrictive Rings

Frequency: 4100 cps—Test Distance: 5 Meters—Depth: 26.5 Meters

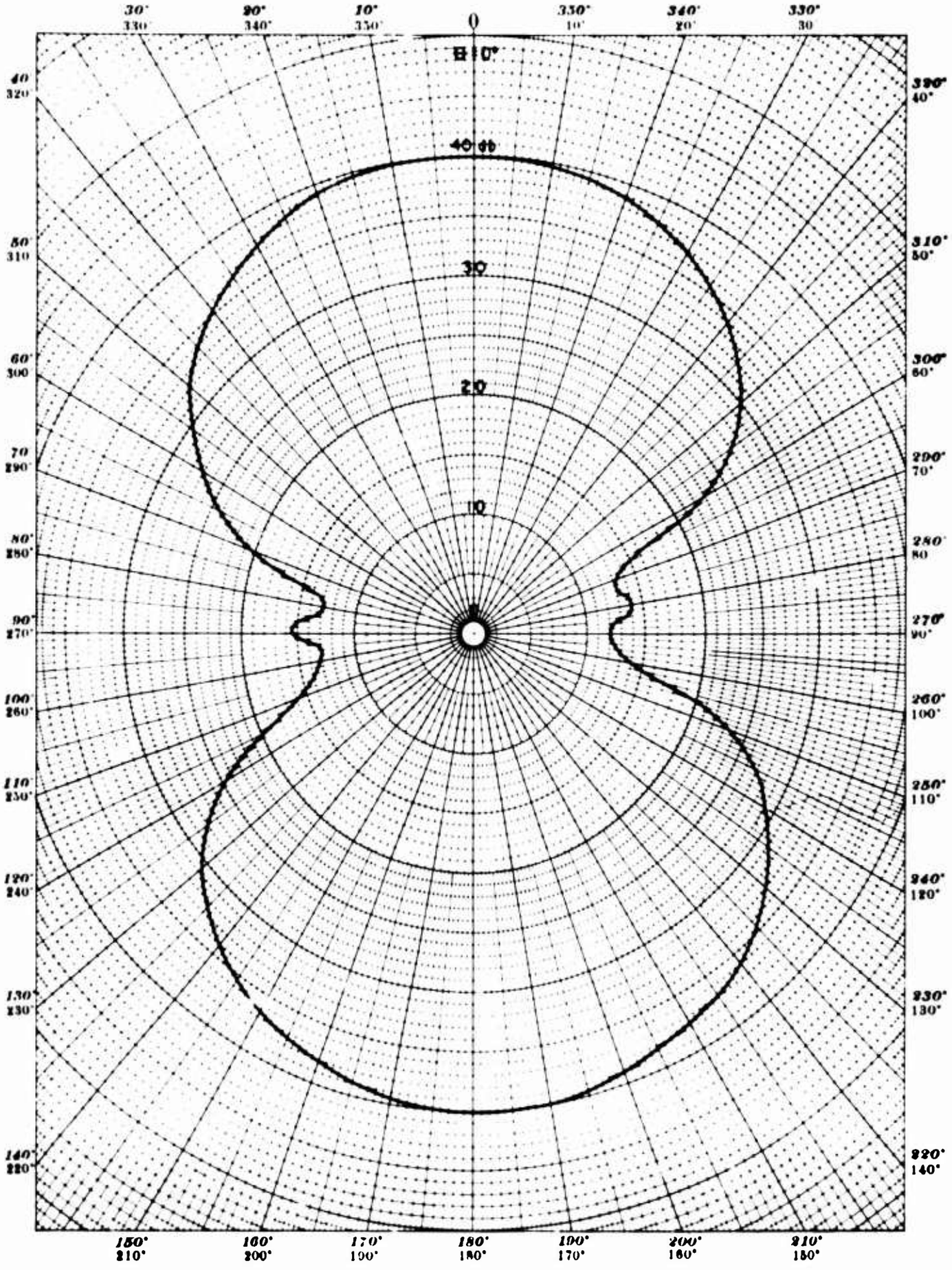

Figure 64. Directivity Pattern - Constant Length Array, 12 Free-Flooded Magnetostrictive Rings

Frequency: 5000 cps—Test Distance: 5 Meters—Depth: 26.5 Meters

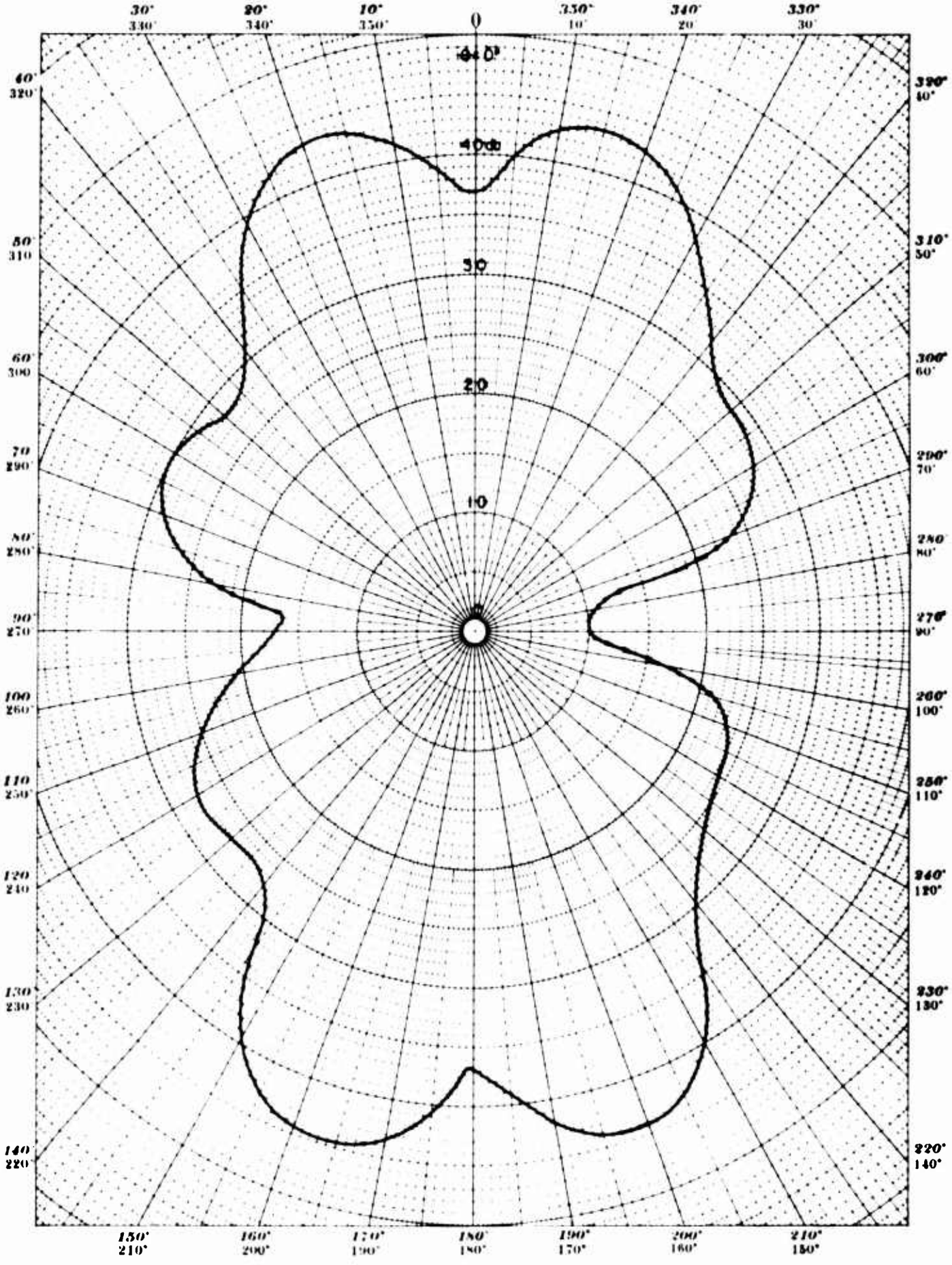

Figure 65. Directivity Pattern - Constant Length Array, 12 Free-Flooded Magnetostrictive Rings

Frequency: 6700 cps—Test Distance: 5 Meters—Depth: 26.5 Meters

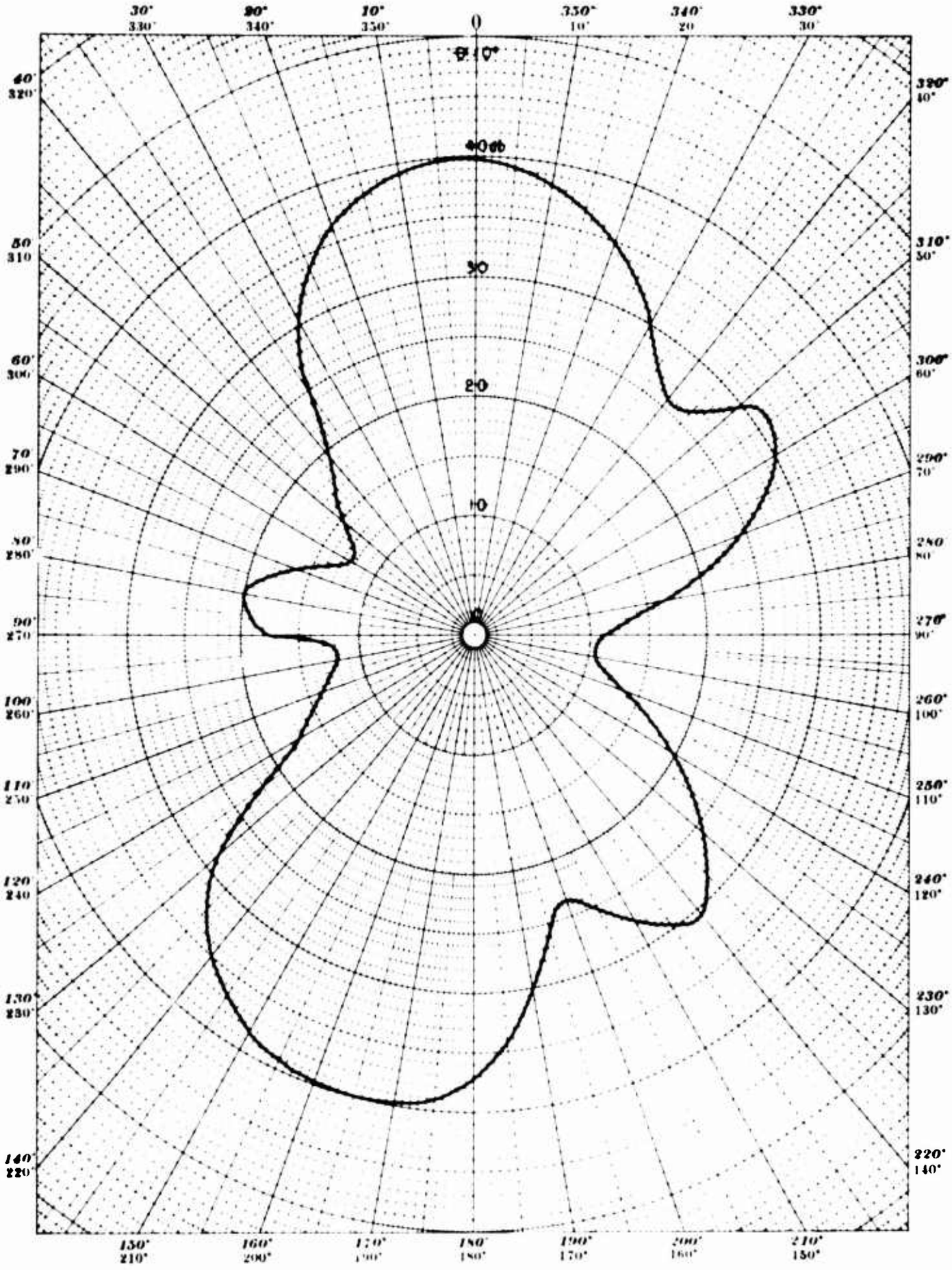

Figure 66. Directivity Pattern - Constant Length Array,
12 Free-Flooded Magnetostrictive Rings

Frequency: 8000 cps—Test Distance: 5 Meters—Depth: 26.5 Meters

Part IV

The array, for the final measurements, consisted of 12 short, series-connected, free-flooded, magnetostrictive rings. The number of rings was held constant throughout the experiment and separation distances between rings were varied from zero to 7-7/16 inches in ten steps. The supporting frame for the array is shown in Figure 67. Data obtained is given in Table V and these results are illustrated graphically by the curves of Figure 68. With the exception of the transmitting current response curves, the results of this and the preceding experiment are generally similar. When the separation distance between rings was 1-3/4 inches, the efficiency was a maximum at 71% but the bandwidth of 550 cps was less than half of the maximum bandwidth measured. The best combination of efficiency (43%), bandwidth (1300 cps), and transmitting current response (96.3 db vs 1 μbar per ampere at 1 meter) was measured when the separation distance between rings was 1 inch or about 1/7 wavelength at the frequency of peak response. Response curves for the 1 inch and 1-3/4 inch separation between rings are given in Figures 76 and 81 respectively. Eight other response curves obtained in the measurements of Part IV are also presented so that relationships between ring spacings and response curves may be observed. Pertinent information relative to efficiency and bandwidth has been extracted from the curves and is presented in Table V. A number of adequately labeled beam patterns are also presented for each array arrangement so that changes in beam forms may be noted. The response curves and corresponding beam patterns are numbered consecutively from Figure 69 to Figure 104.

The impedance circle shown in Figure 105 for a 12-ring array in which the separation distance between rings is 1-3/4 inches is typical of the impedance circles obtained for other spacings. Generally, small circles generated on the principal impedance circle represent undesirable spurious modes of vibration of low efficiency. However, in this particular case, the smaller second circle identified by the 7700 cps frequency point includes the ring

radial resonance at which both transmitting current response and efficiency are a maximum. The bandwidth at the lower resonance near 4400 cps is four times greater than at the 7750 cps resonance, however, the relatively high resistance and low response combine to give an efficiency of just a few percent at the lower frequency. The efficiency at the higher frequency is 71%. Beam patterns taken at 4400 and 7750 cps for the array with 1-3/4 inches separation between rings are shown in Figures 82 and 83 respectively. The acoustic pressure on the ring axis of the first beam pattern is 23 db lower than on the principal acoustic axis. Beamwidth of the principal lobe is 28° at the 10 db down points and the minor lobes shown on either side of the principal lobe are approximately 9 db down. In the beam pattern of Figure 83, suppression of acoustic energy at the open ends of the array is about the same as in the preceding pattern but the principal lobe is much wider. The beam width at the 10 db down points is approximately 96°.

CONCLUSIONS

In comparing all the data for the best combination of efficiency and bandwidth, Table III shows that an efficiency of 65% and a bandwidth of 3900 cps was obtained for 3 short, closely stacked, free-flooded rings which had a resonant frequency of 7000 cps in water. Table IV, for a constant length array, shows that an efficiency of 68% and a bandwidth of 1900 cps was obtained for a 5-ring array which had a resonant frequency of 8300 cps and a 1.2 inch separation between rings. Table V, for a variable length array with a fixed number of rings, shows an efficiency of 43% and a bandwidth of 1300 cps for a 12-ring array which had a resonant frequency of 7900 cps and a 1-inch separation distance between rings. Curves of Figures 28 and 68, plotted from values in Table IV and V respectively, indicate that broad bandwidth was obtained when the separation distance between rings was between 1/2 and 2 inches. If more measurements had been made over this

range of separation distances, broader bandwidths may have been recorded. However, it is doubtful whether a value as high as the 3900 cps bandwidth cited above would have been measured. The data indicates that additional information on broad bandwidth operation at good efficiencies may be obtained by making measurements similar to those made in Part IV but using groups of 3, 4, and 5 closely stacked short rings as elements of the line array.

Finally, the data presented shows that free-flooded magnetostrictive rings suitable for operation at great depths may be arranged to obtain favorable operating characteristics and suggests interesting possibilities for multi-linear planar and multi-planar arrangements of ring transducers.

ACKNOWLEDGEMENTS

The author wishes to acknowledge the fine support and cooperation received from the many people involved in these measurements. Mr. Gus Nordstrom did an excellent job of remodeling the rings which were part of an old array and helped with measurements made in air. Mr. Kerby Kemper, a student trainee, helped with measurements made at the Laboratory and at Lake Seneca. Mr. Paul Rand did a fine job of recording the data obtained at Brighton Dam. Mr. J. G. Larson, Head, Division Services and his group at the Lake Seneca Barge provided many services and necessary aid. Thanks are due to Mr. J. Neeley who was responsible for the measuring equipment aboard the barge and recorded most of the data.

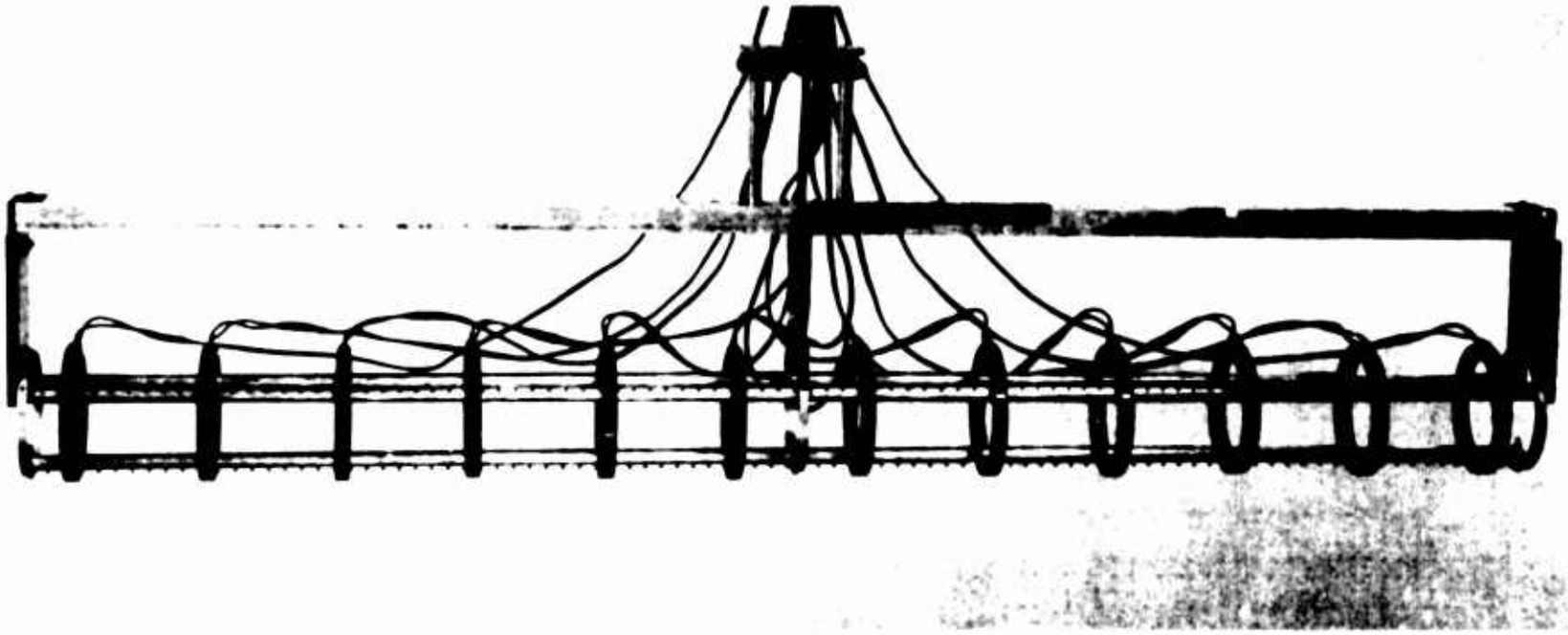

Figure 67. Array of Evenly Spaced Rings

TABLE V

Magnetostrictive Ring Array

12 Rings connected in series

Spacing between rings varied

Measurements made at Lake Seneca Oct. 16-24, 1963

Inches Separation between rings	f_r cps	S db	R ohms	D.I. db	Efficiency %	B. W. cps
0	6600	91.9	300	4.3	16	1200
1/2	7900	94.3	360	3.3	30	400
1	7900	96.3	340	4.1	43	1300
1-3/4	7750	97.7	330	3.4	71	550
2-1/2	7650	97.0	300	3.2	69	450
3-3/8	8200	95.3	210	5.1	44	970
4-3/16	8200	94.8	210	4.6	44	640
5	7900	92.3	230	2.8	34	640
5-13/16	7700	95.1	265	3.2	50	710
7-7/16	7500	97.8	285	5.7	49	770

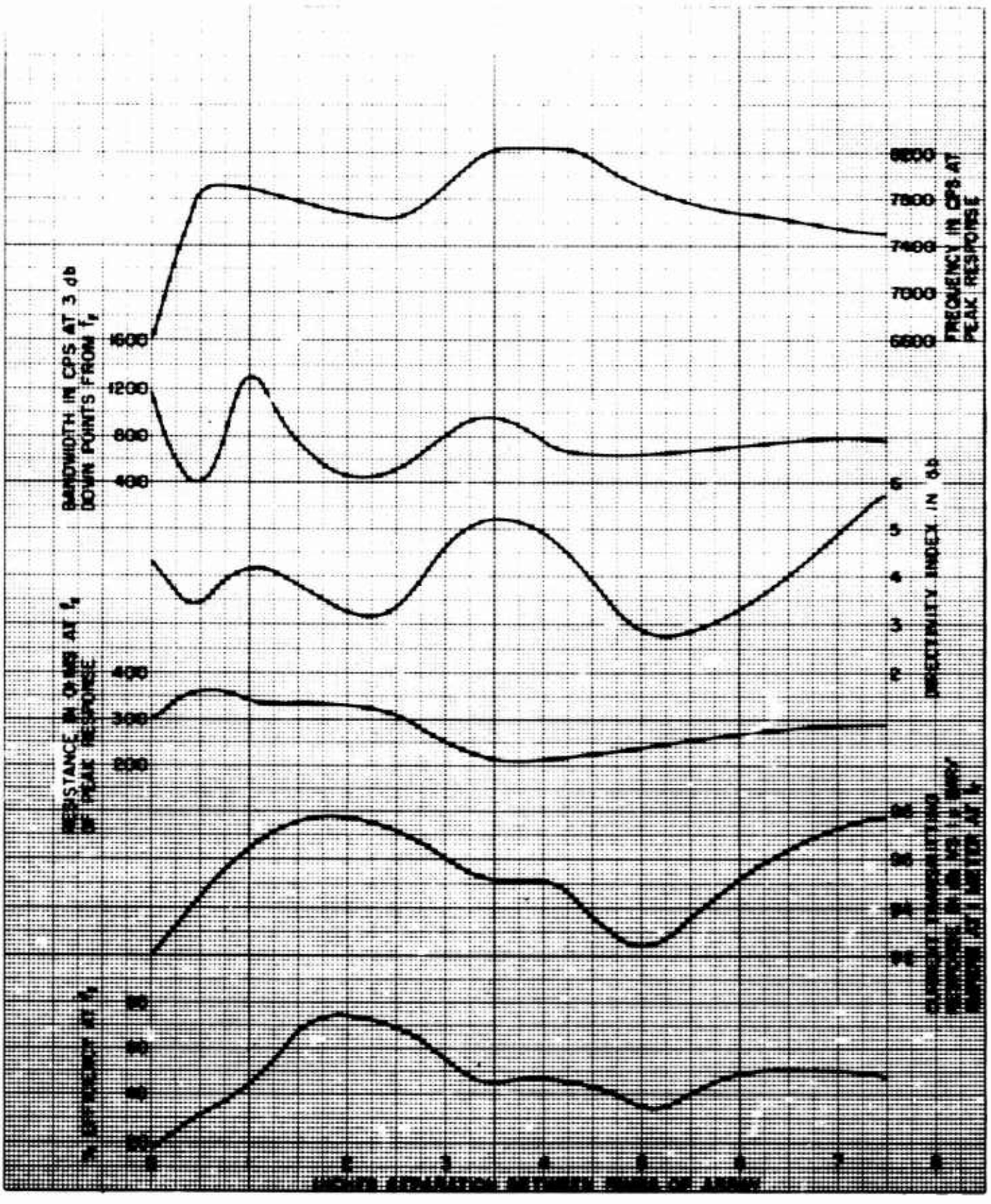

Figure 68 - Array of 12 Magnetostrictive Rings Separation Between Rings Varied

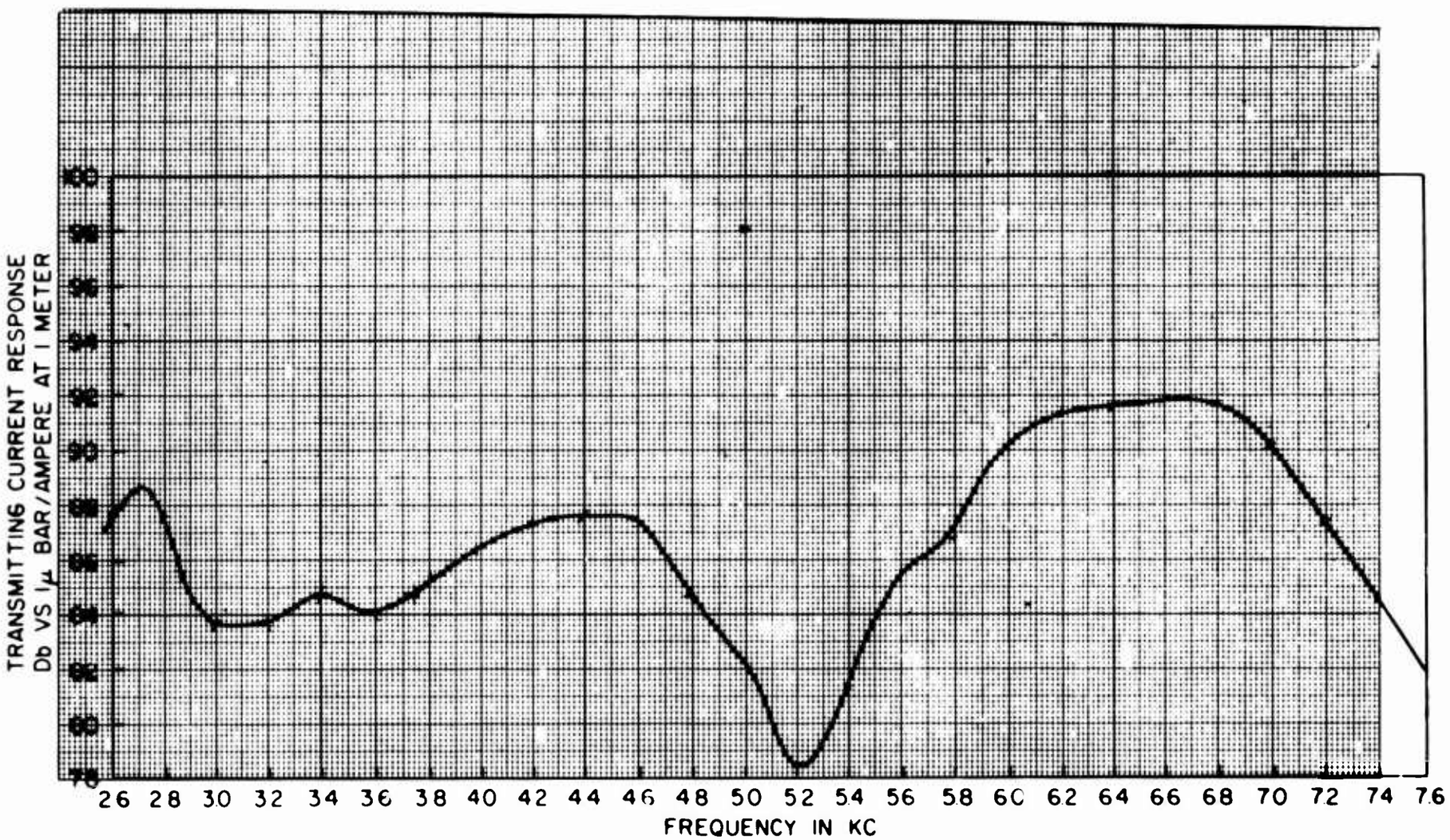

Figure 69. Transmitting Current Response Curve. Array of 12 Closely Spaced Magnetostrictive Rings. Series Connected. D.C. - 0 5 Amp, 87-foot Depth.

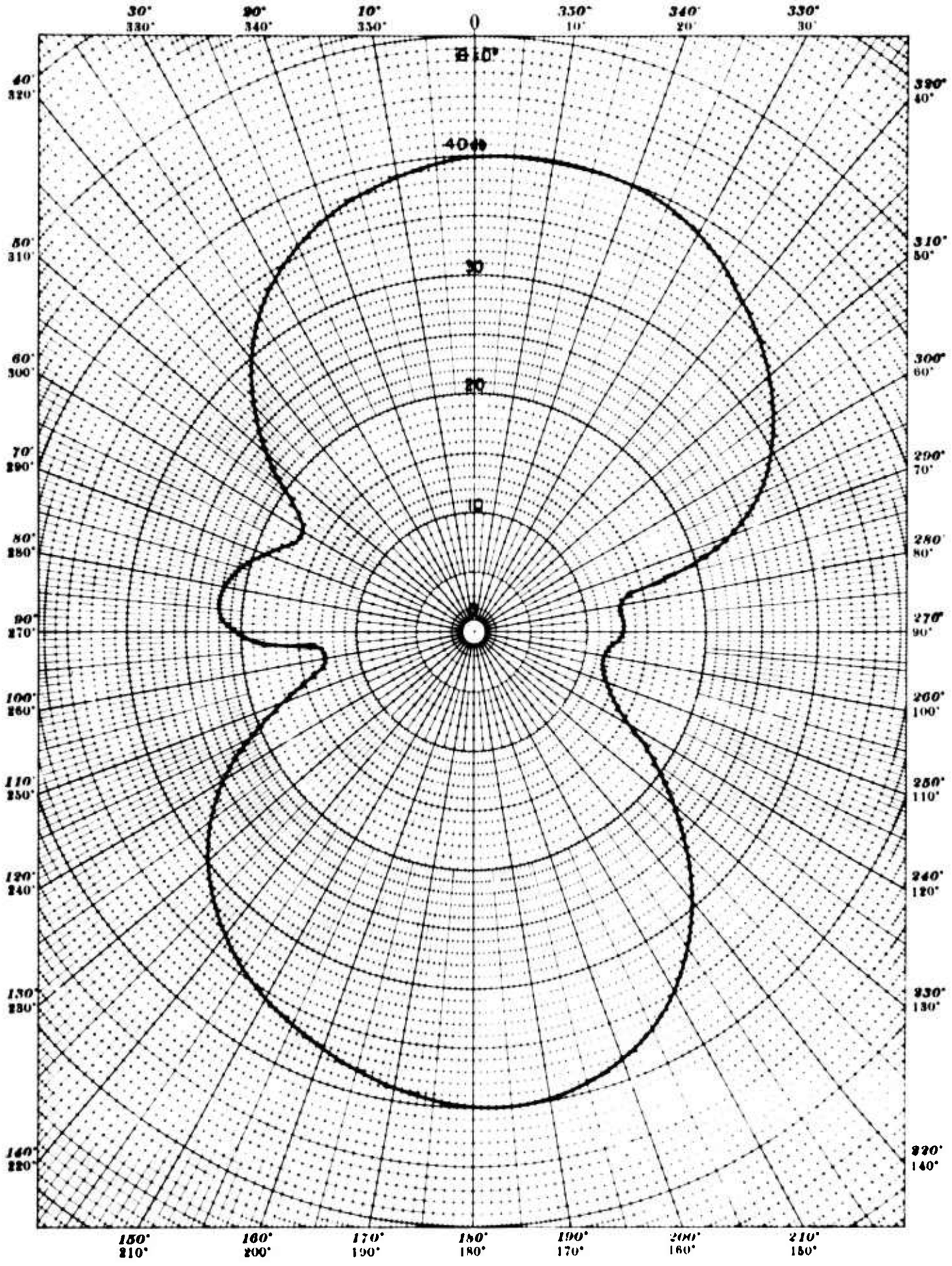

Figure 70. Directivity Pattern - Array of 12 Magnetostrictive Rings, Separation Distance between Rings = 0"

Frequency: 4100 cps—Test Distance: 5 Meters—Depth: 26.5 Meters

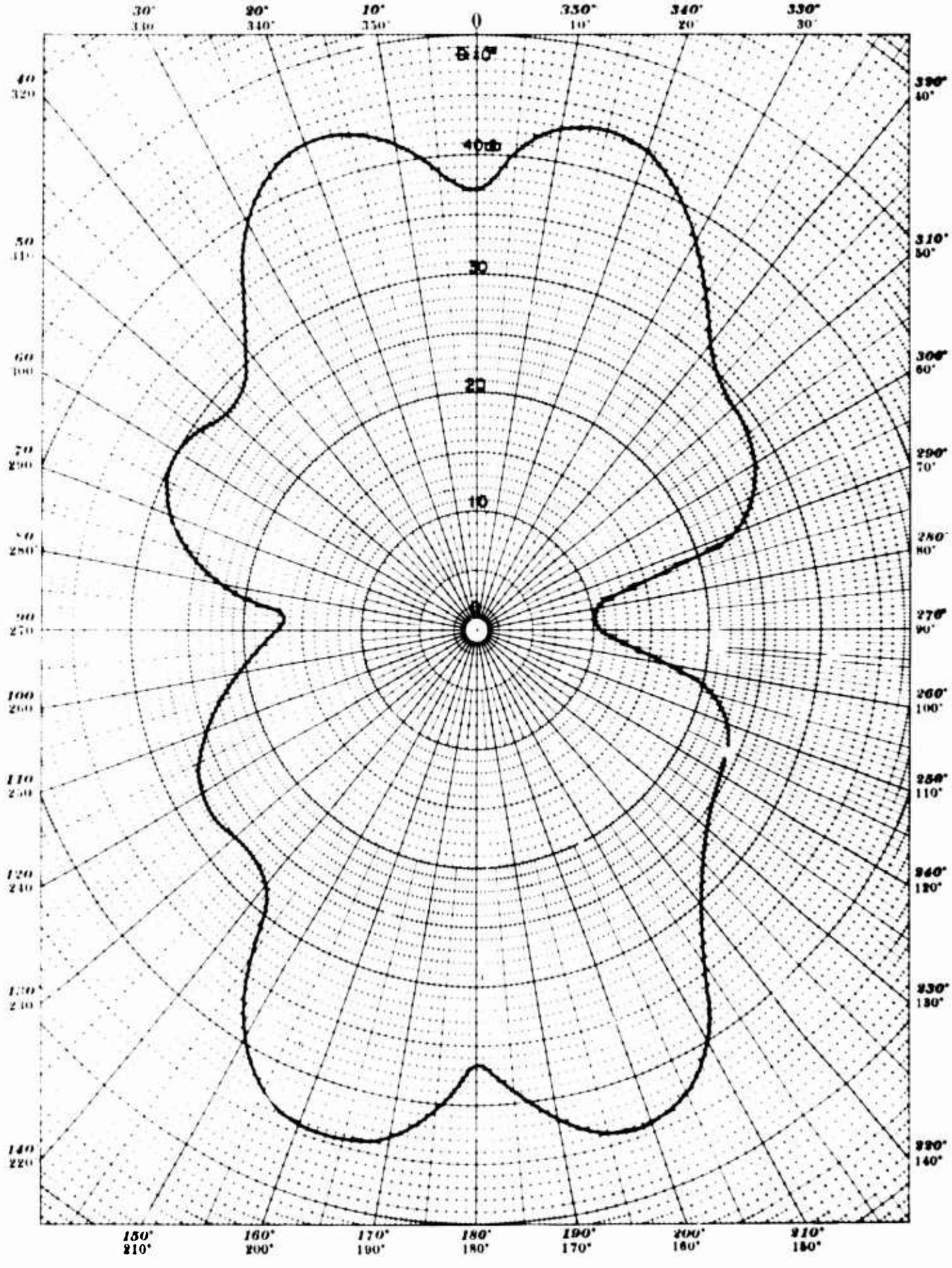

Figure 71. Directivity Pattern - Array of 12 Magnetostrictive Rings. Separation Distance between Rings = 0"

Frequency: 6700 cps—Test Distance: 5 Meters—Depth: 26.5 Meters

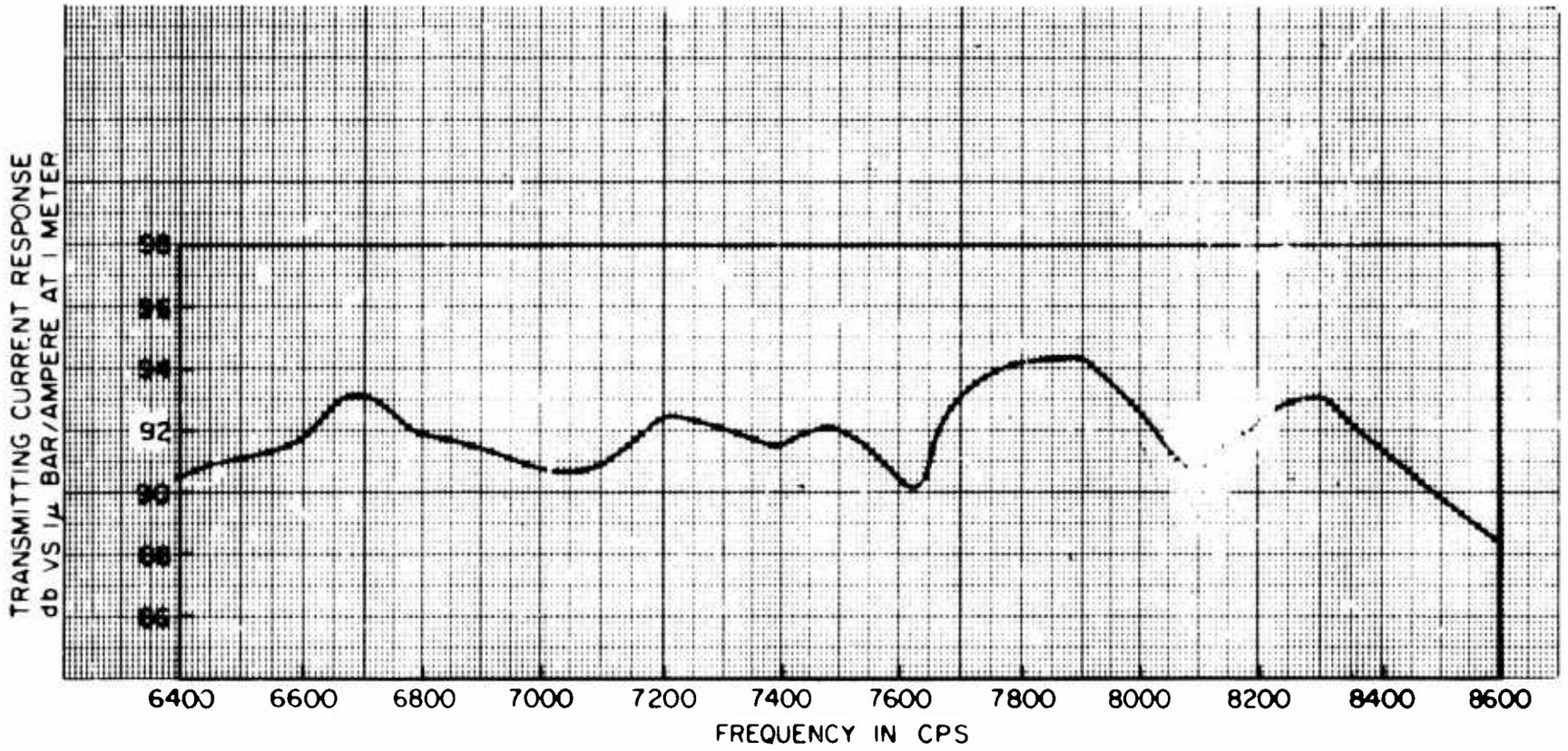

Figure 72 - Transmitting Current Response Curve 1/2 inch Separation between Rings. 12 Magnetostrictive Ring Array Series Connected. D.C. 0.5 Amp.

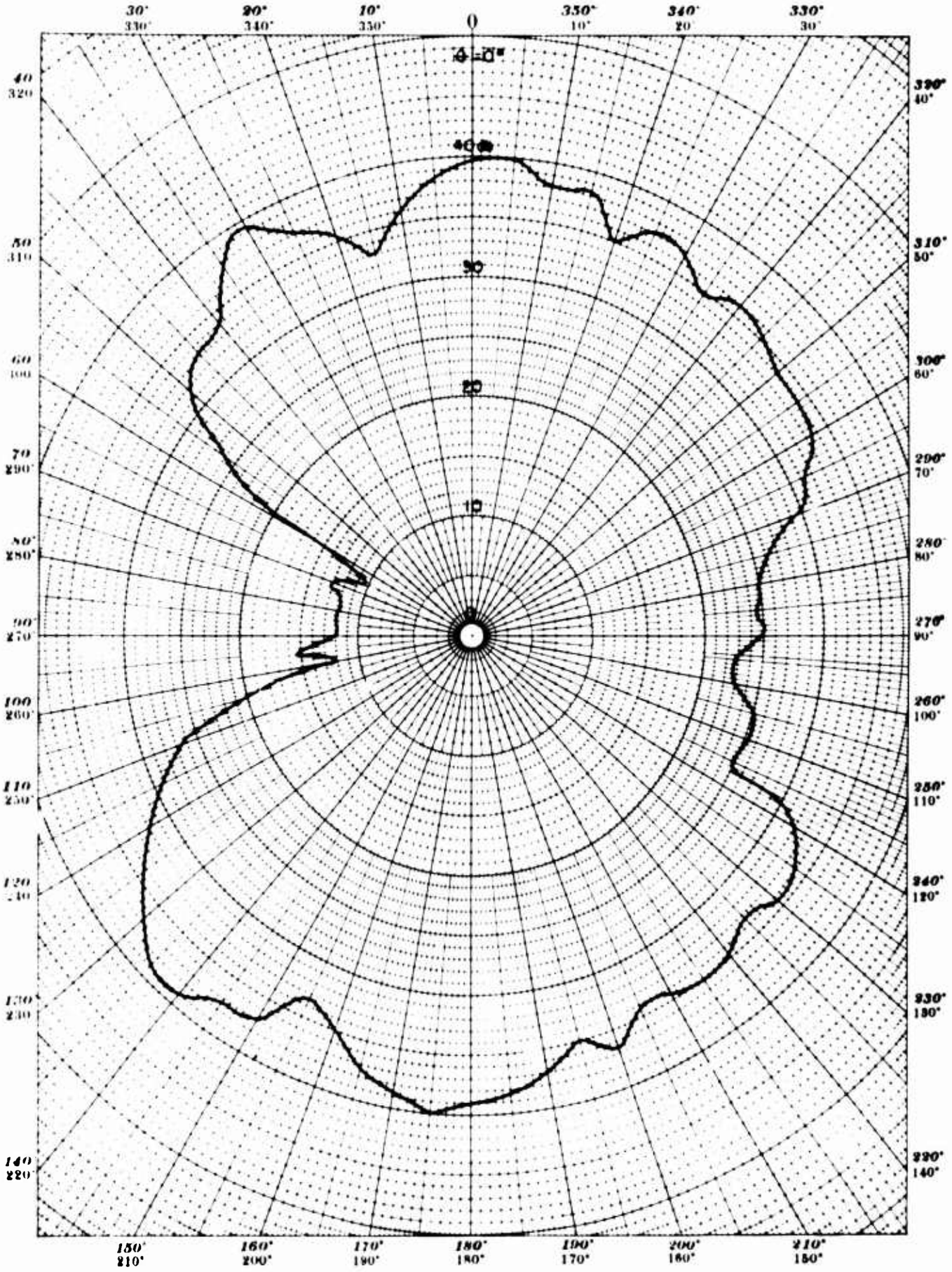

Figure 73. Directivity Pattern - Array of 12 Magnetostrictive Rings. Separation Distance between Rings = 1/2"

Frequency: 7700 cps—Test Distance: 5 Meters—Depth: 26.5 Meters

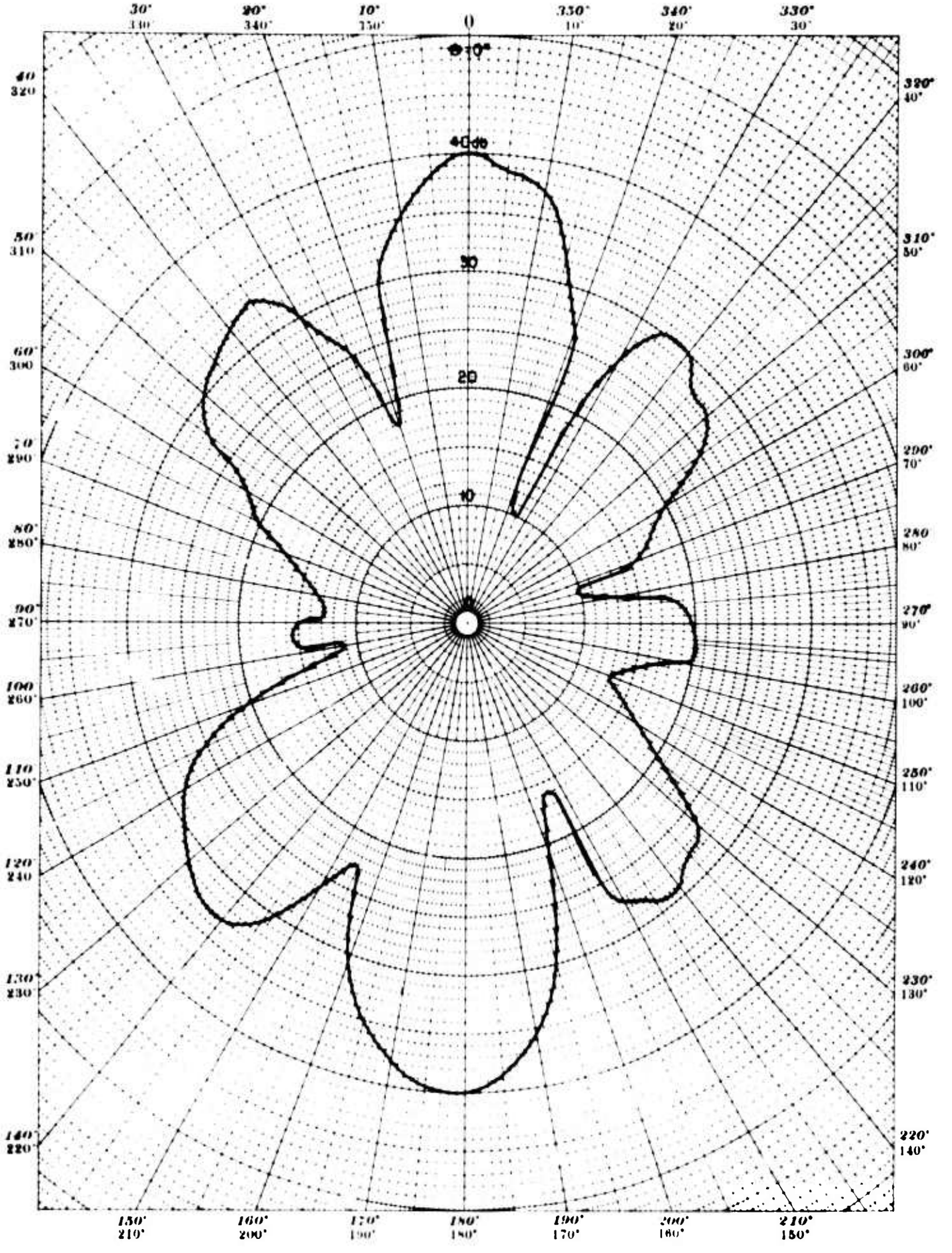

Figure 74. Directivity Pattern - Array of 12 Magnetostrictive Rings, Separation Distance between Rings = 1/2"

Frequency: 6700 cps—Test Distance: 5 Meters—Depth: 26.5 Meters

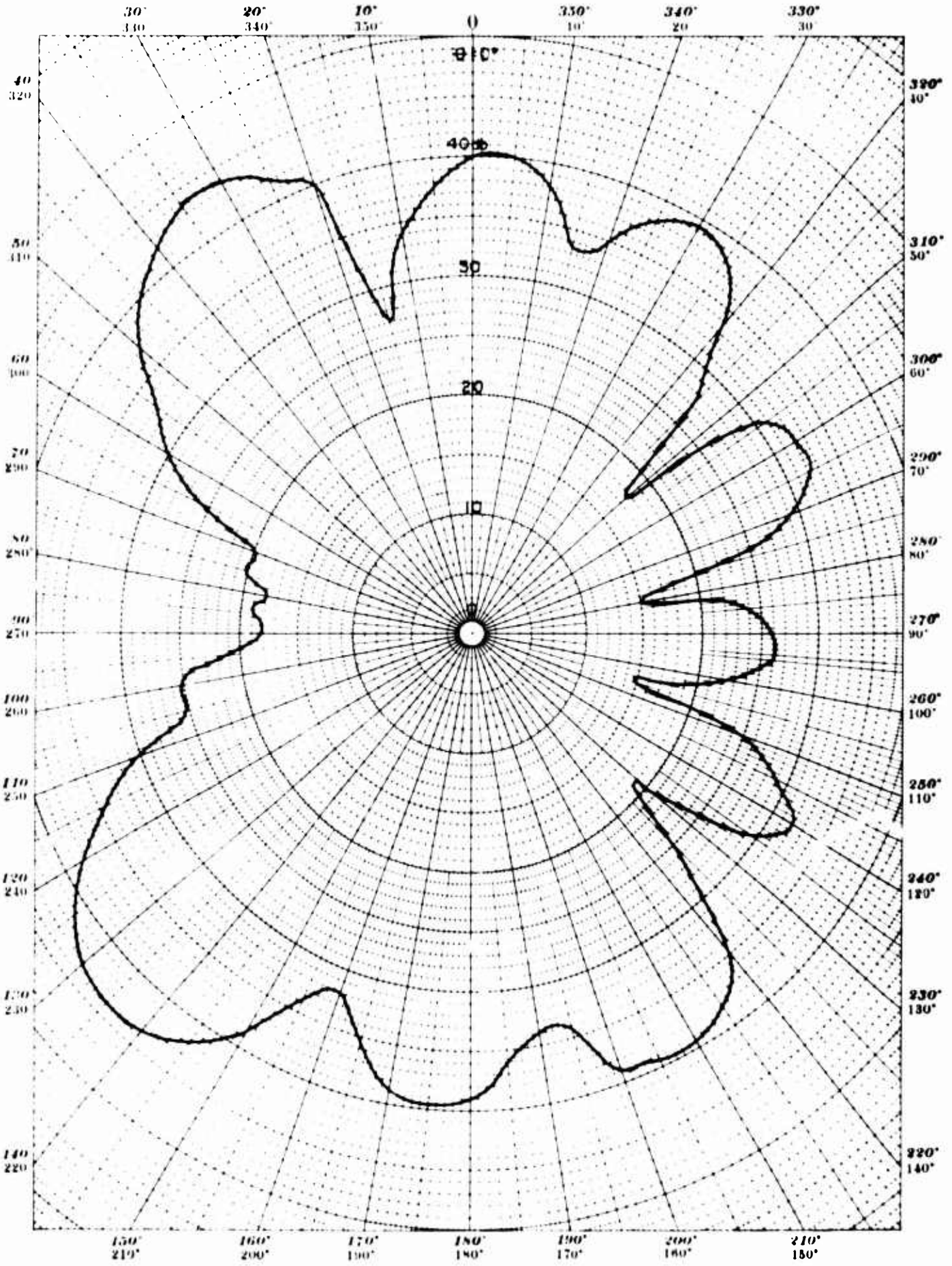

Figure 75. Directivity Pattern - Array of 12 Magnetostrictive Rings, Separation Distance between Rings = 1/2"

Frequency: 7100 cps—Test Distance: 5 Meters—Depth: 26.5 Meters

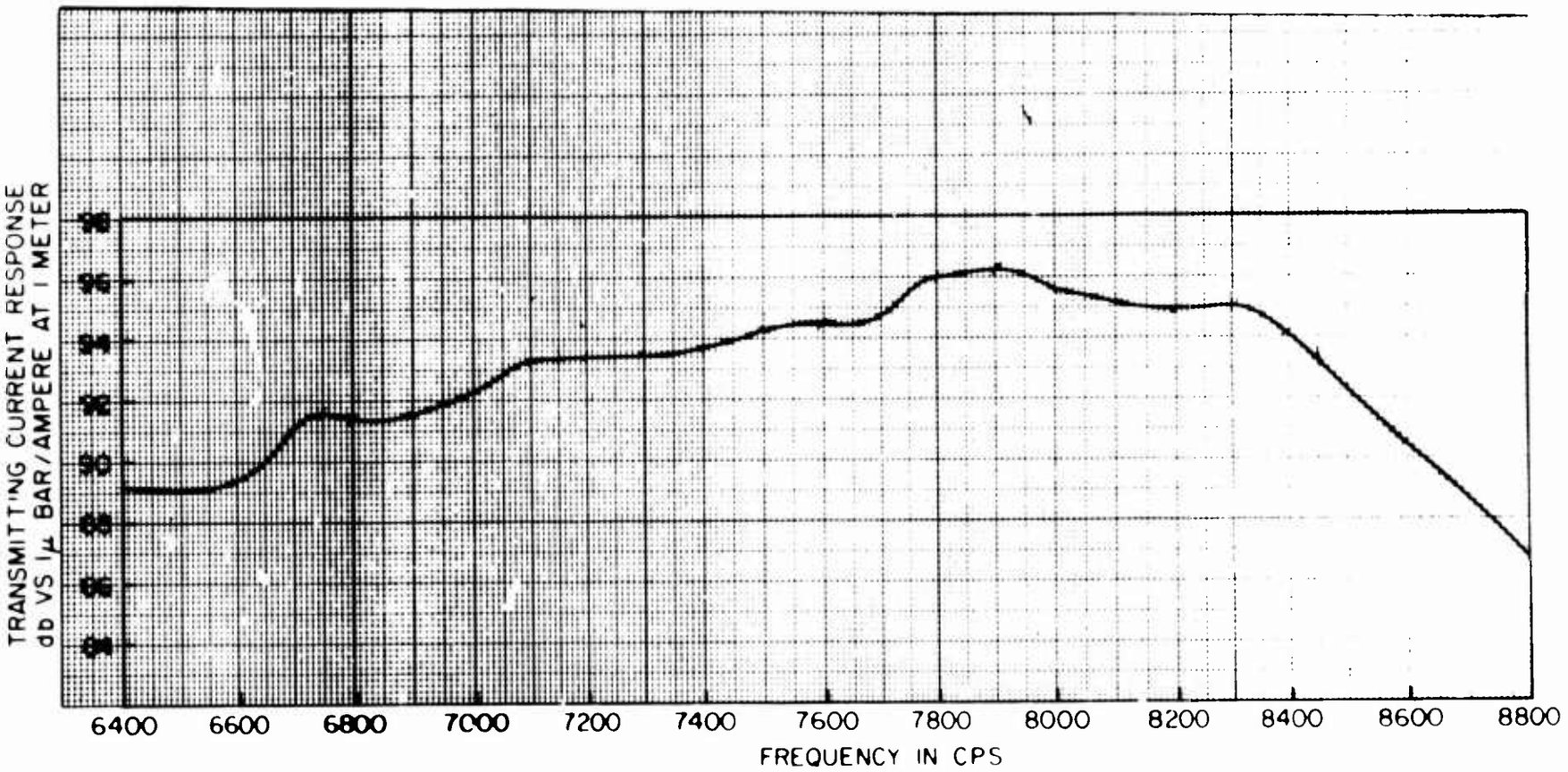

Figure 76 - Transmitting Current Response Curve 1 inch **Separation** between Rings. 12 Magnetostrictive Ring Array **Series** Connected. D.C. 0.5 Amp.

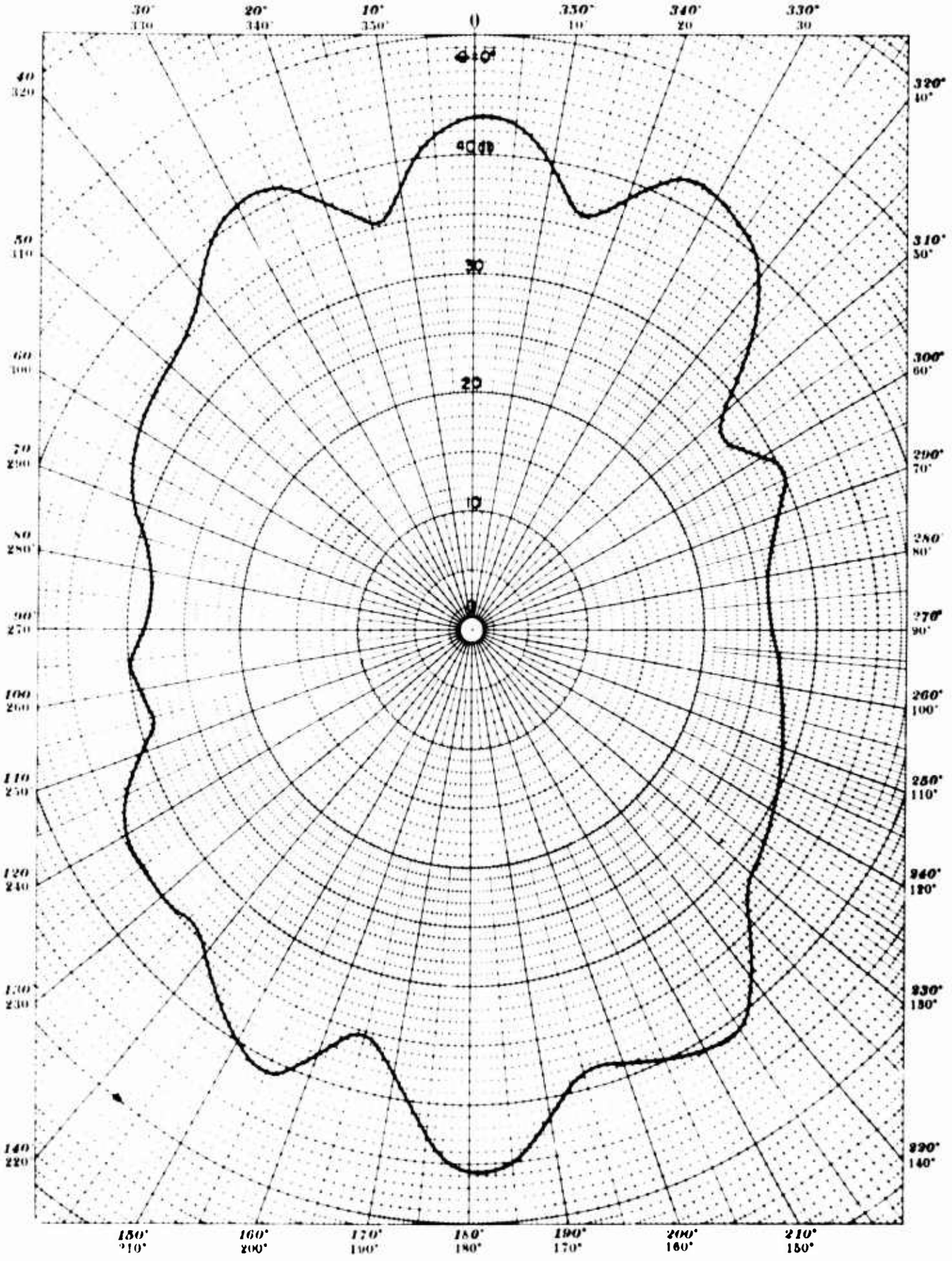

Figure 77 Directivity Pattern - Array of 12 Magnetostrictive Rings, Separation Distance between Rings = 1"

Frequency: 6600 cps—Test Distance: 5 Meters—Depth: 26.5 Meters

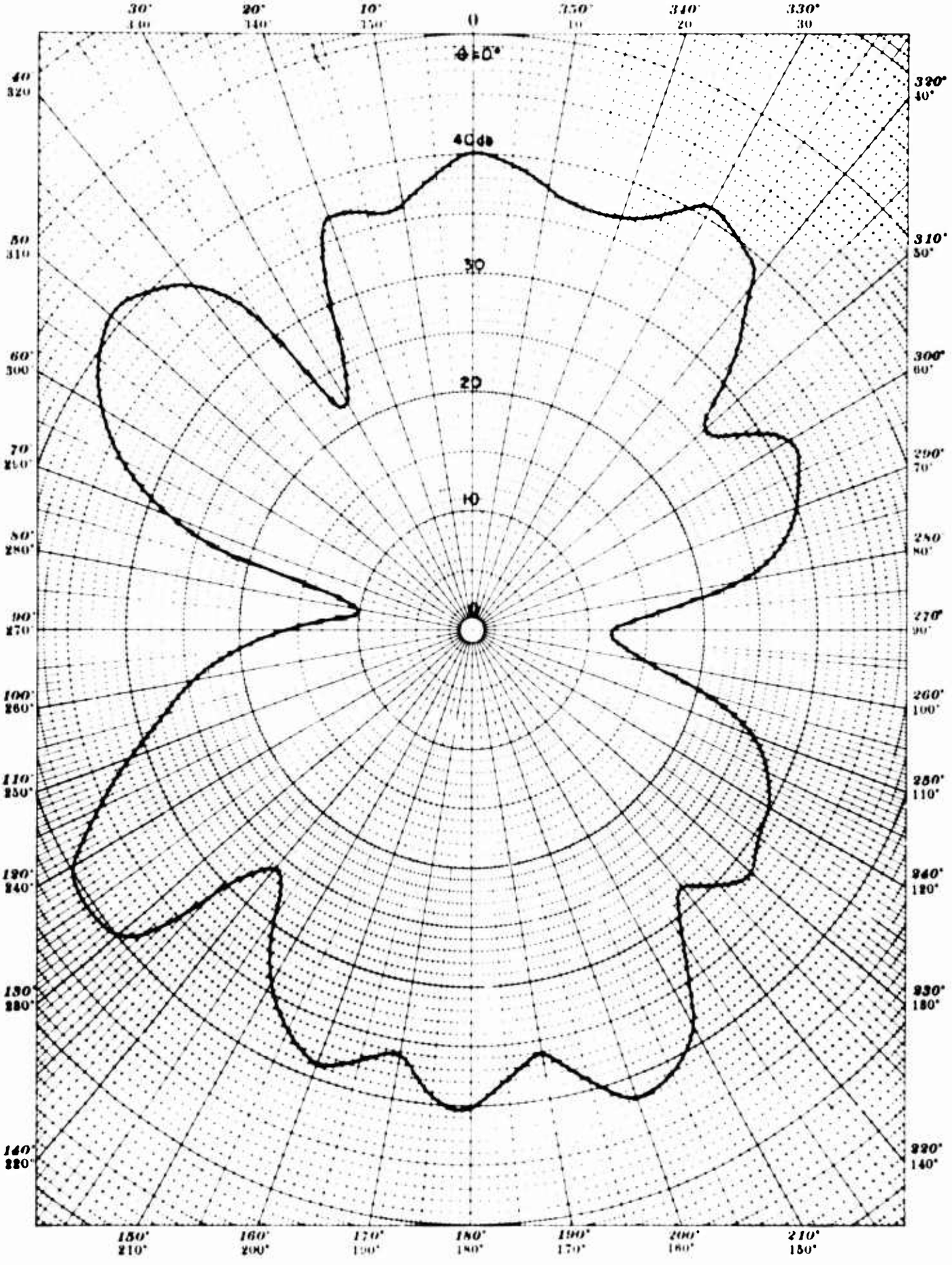

Figure 78. Directivity Pattern - Array of 12 Magnetostrictive Rings, Separation Distance between Rings = 1"

Frequency: 7150 cps—Test Distance: 5 Meters—Depth: 26.5 Meters

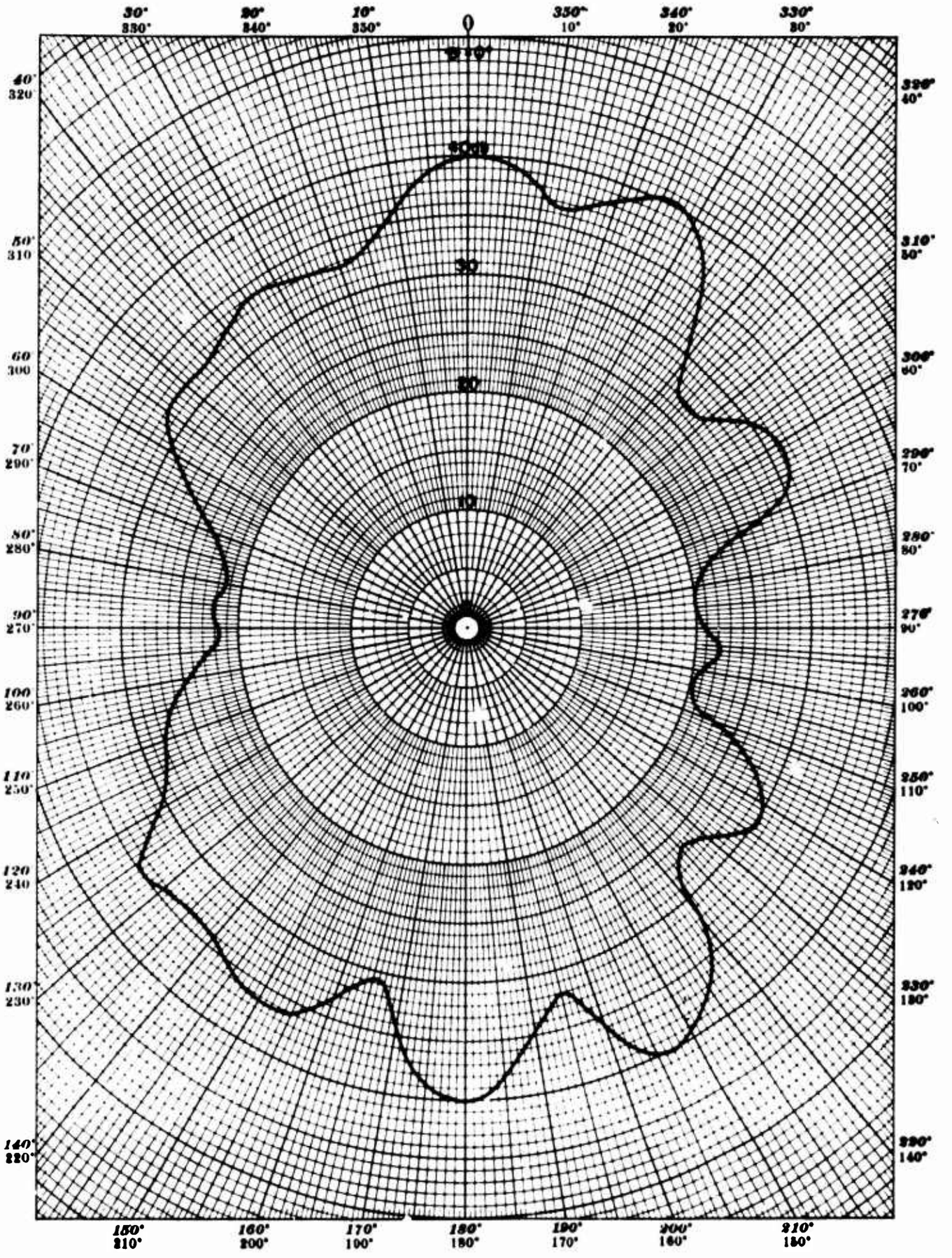

Figure 79. Directivity Pattern - Array of 12 Magnetostrictive Rings, Separation Distance between Rings = 1"

Frequency: 7800 cps—Test Distance: 5 Meters—Depth: 26.5 Meters

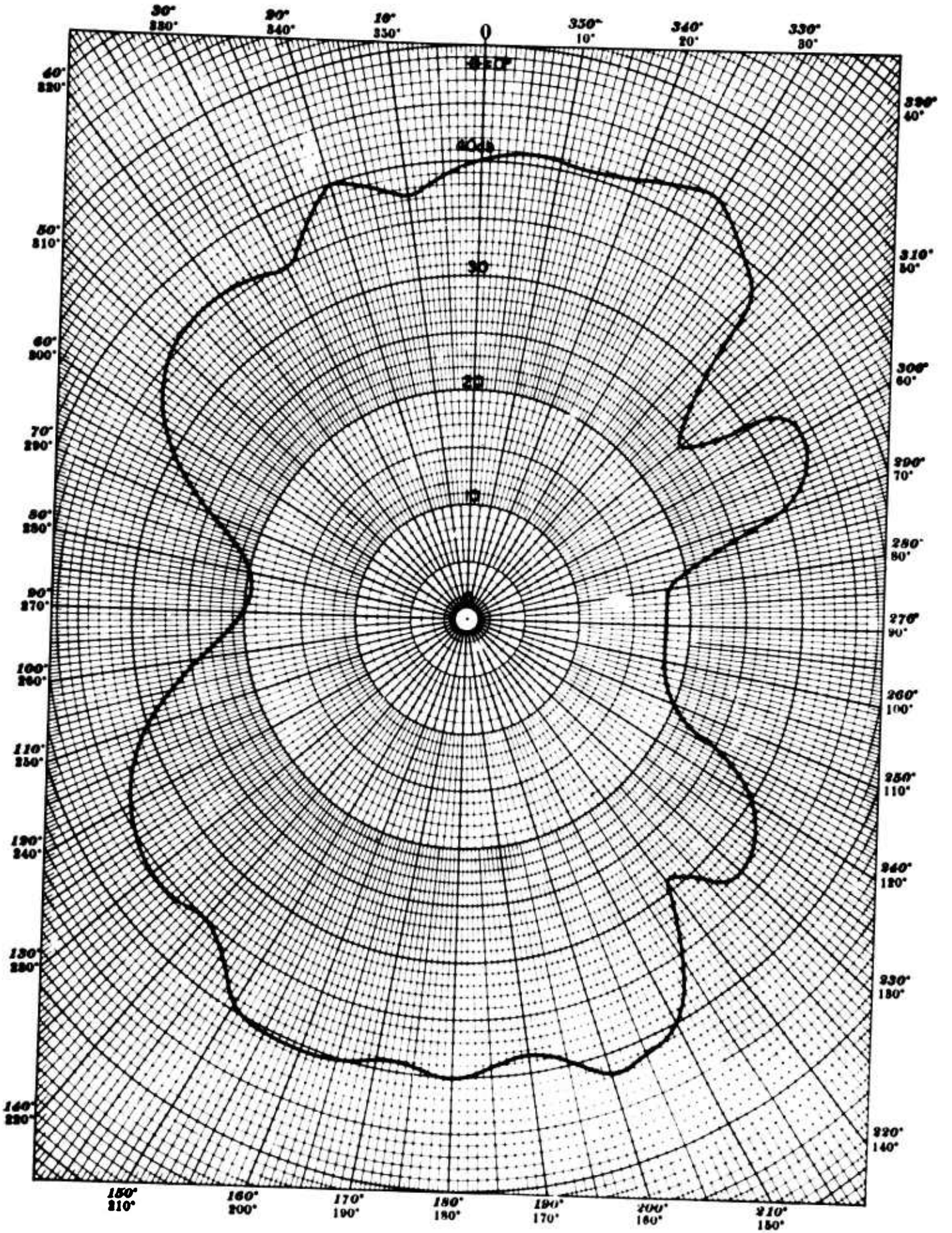

Figure 80. Directivity Pattern - Array of 12 Magnetostrictive Rings, Separation Distance between Rings = 1"

Frequency: 8200 cps—Test Distance: 5 Meters—Depth: 26.5 Meters

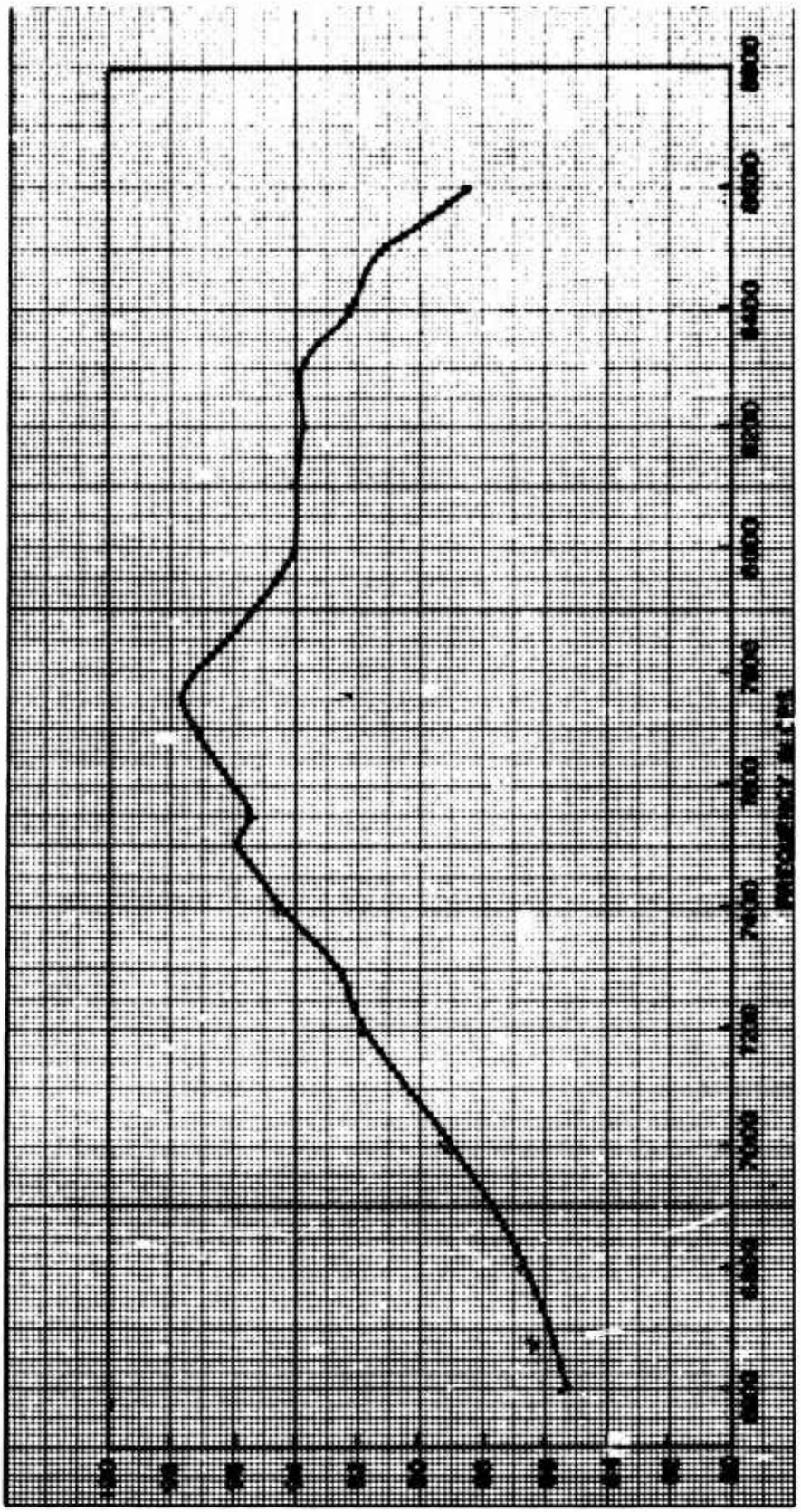

Figure 81 - Transmitting Current Response Curve 1-3/4 inch Separation between Rings. 12 Magnetostrictive Ring Array Series Connected. D.C. = 0.5 Amp.

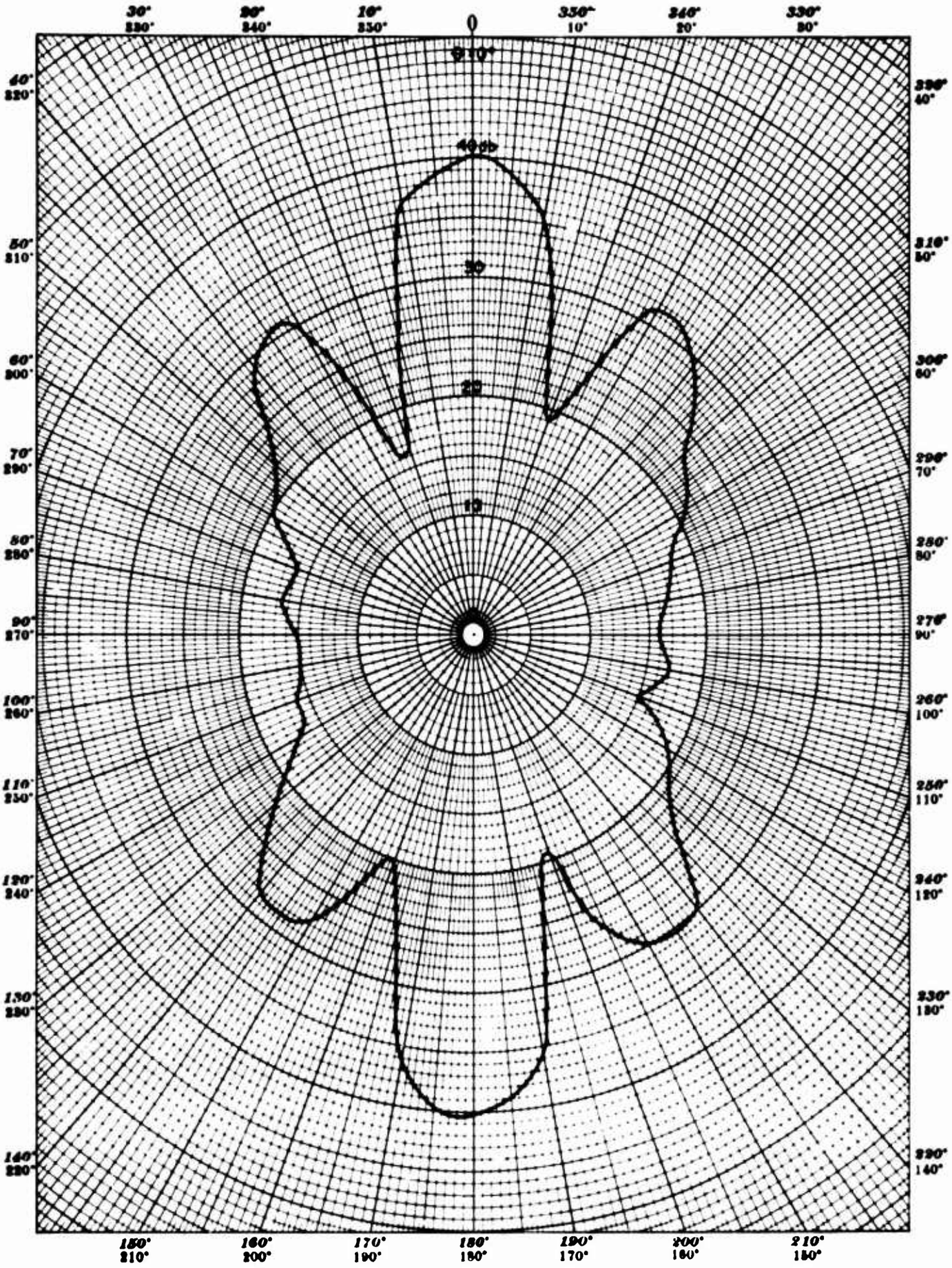

Figure 82. Directivity Pattern - Array of 12 Magnetostrictive Rings, Separation Distance between Rings = 1-3/4"

Frequency: 4400 cps—Test Distance: 5 Meters—Depth: 26.5 Meters

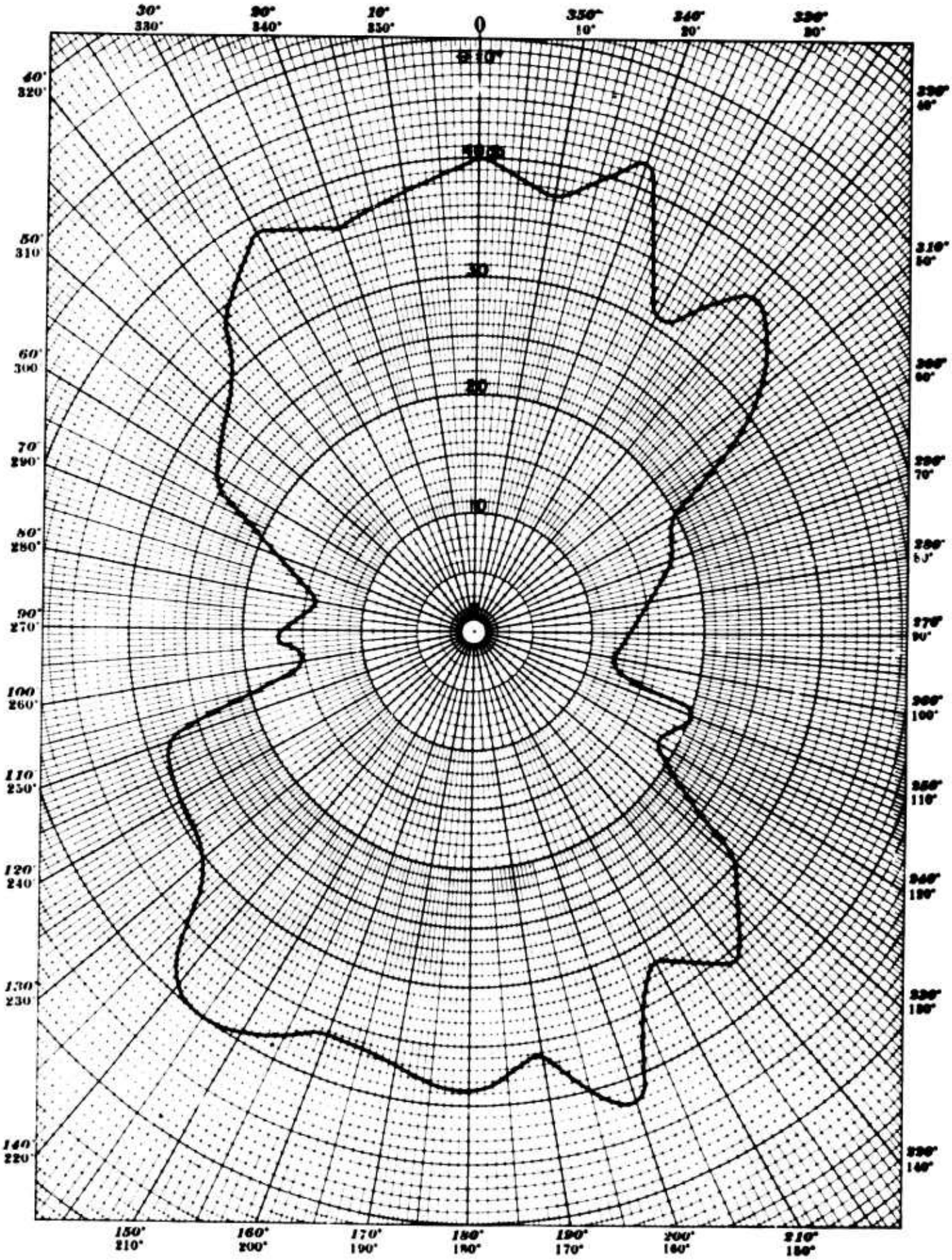

Figure 83. Directivity Pattern - Array of 12 Magnetostrictive Rings. Separation Distance between Rings = 1-3/4"

Frequency: 7750 cps—Test Distance: 5 Meters—Depth: 26.5 Meters

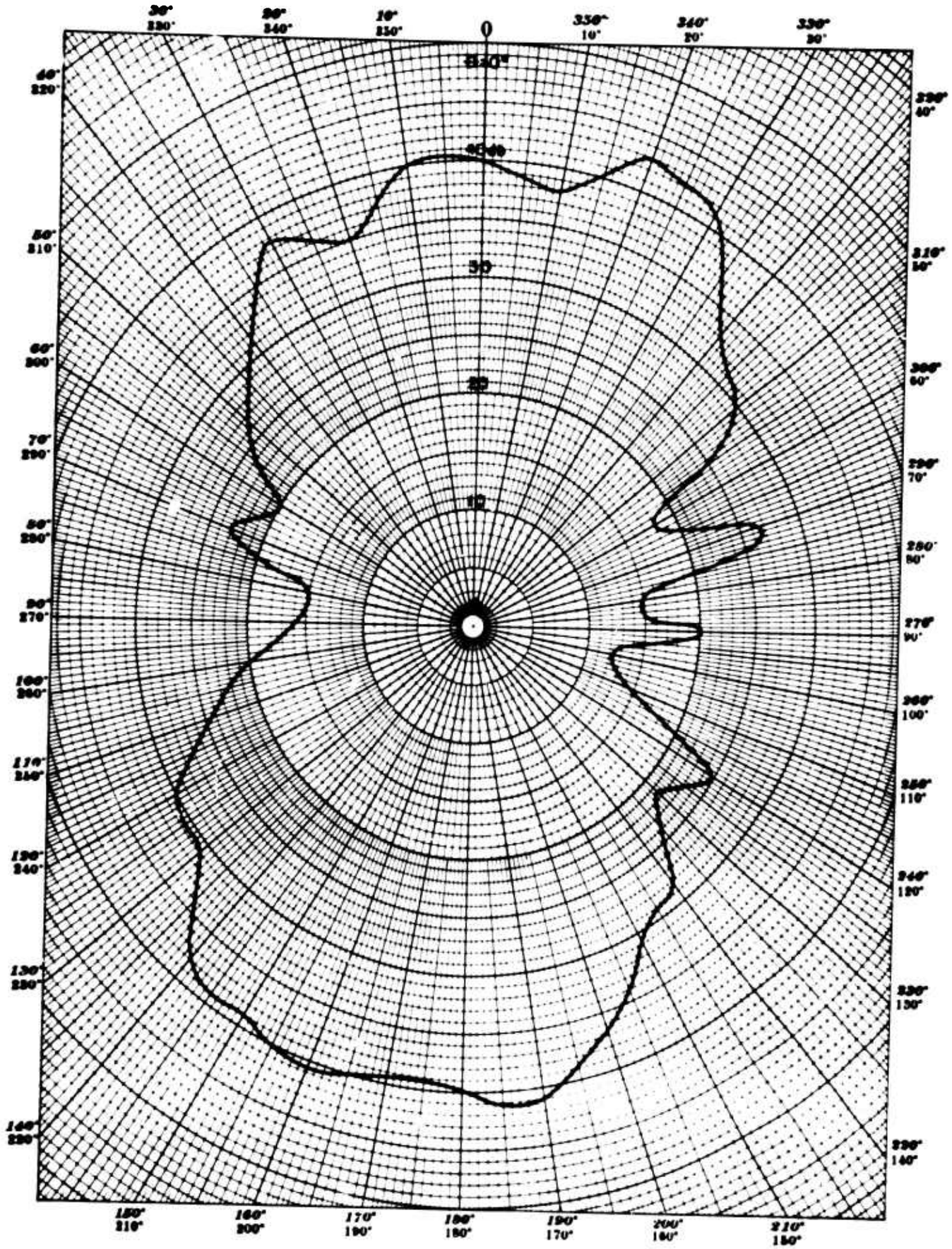

Figure 84. Directivity Pattern - Array of 12 Magnetostrictive Rings. Separation Distance between Rings = 1-3/4"

Frequency: 8200 cps—Test Distance: 5 Meters—Depth: 26.5 Meters

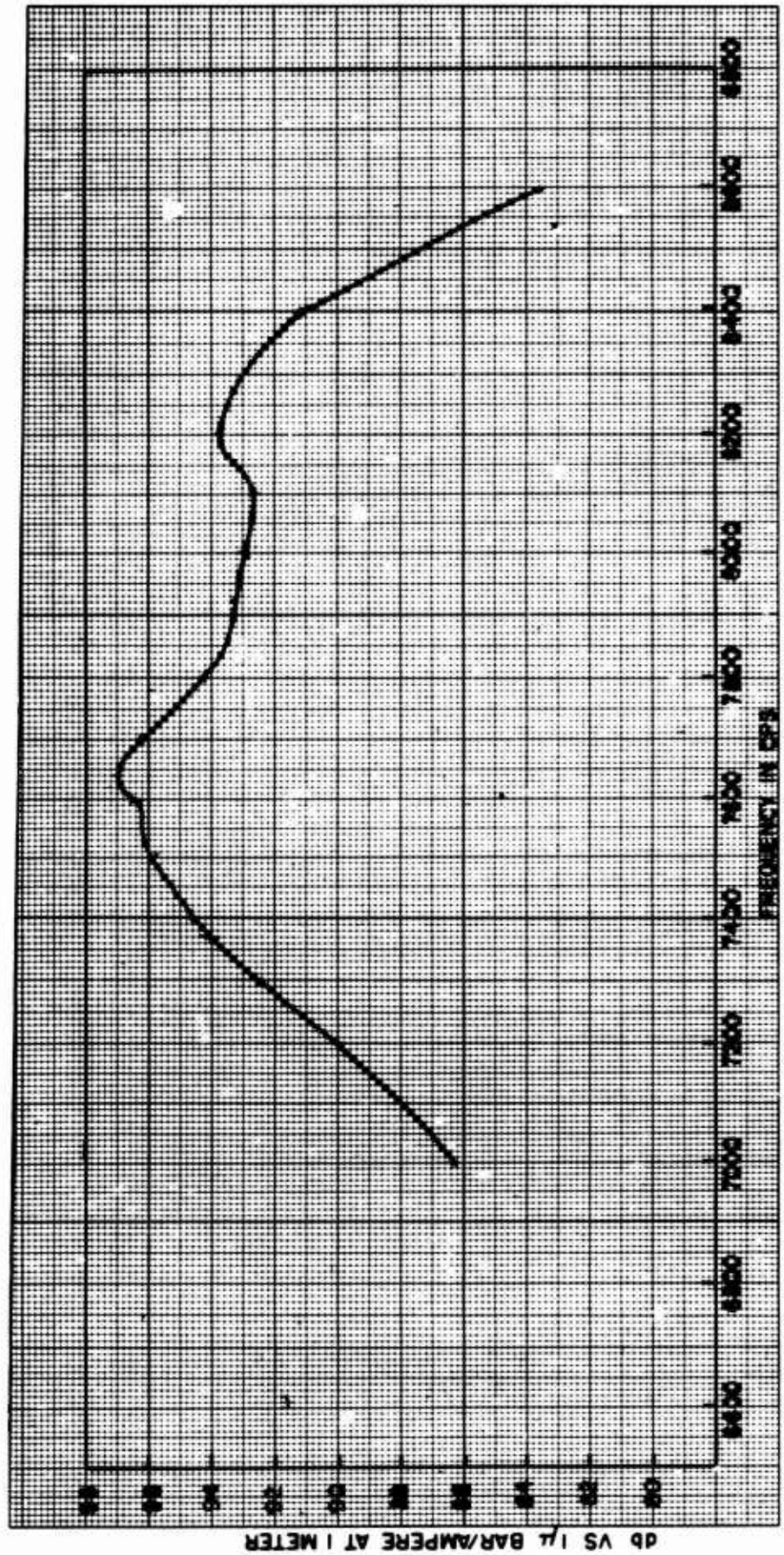

Figure 85 - Transmitting Current Response Curve 2-1/2 inch Separation between Rings. 12 Magnetostrictive Ring Array Series Connected. D.C. = 0.5 Amp.

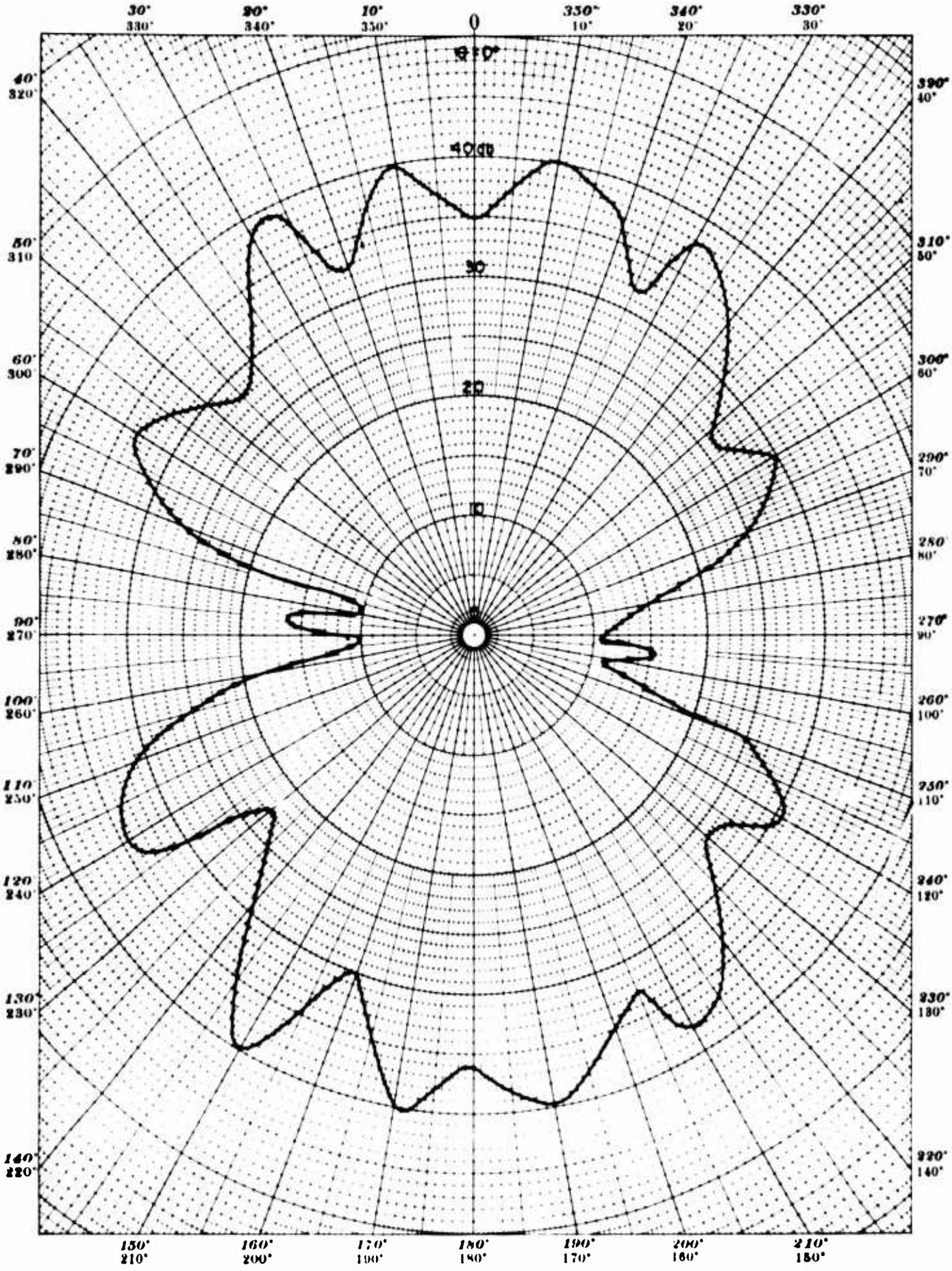

Figure 86. Directivity Pattern - Array of 12 Magnetostrictive Rings, Separation Distance between Rings = 2-1/2"

Frequency: 7100 cps—Test Distance: 5 Meters—Depth: 26.5 Meters

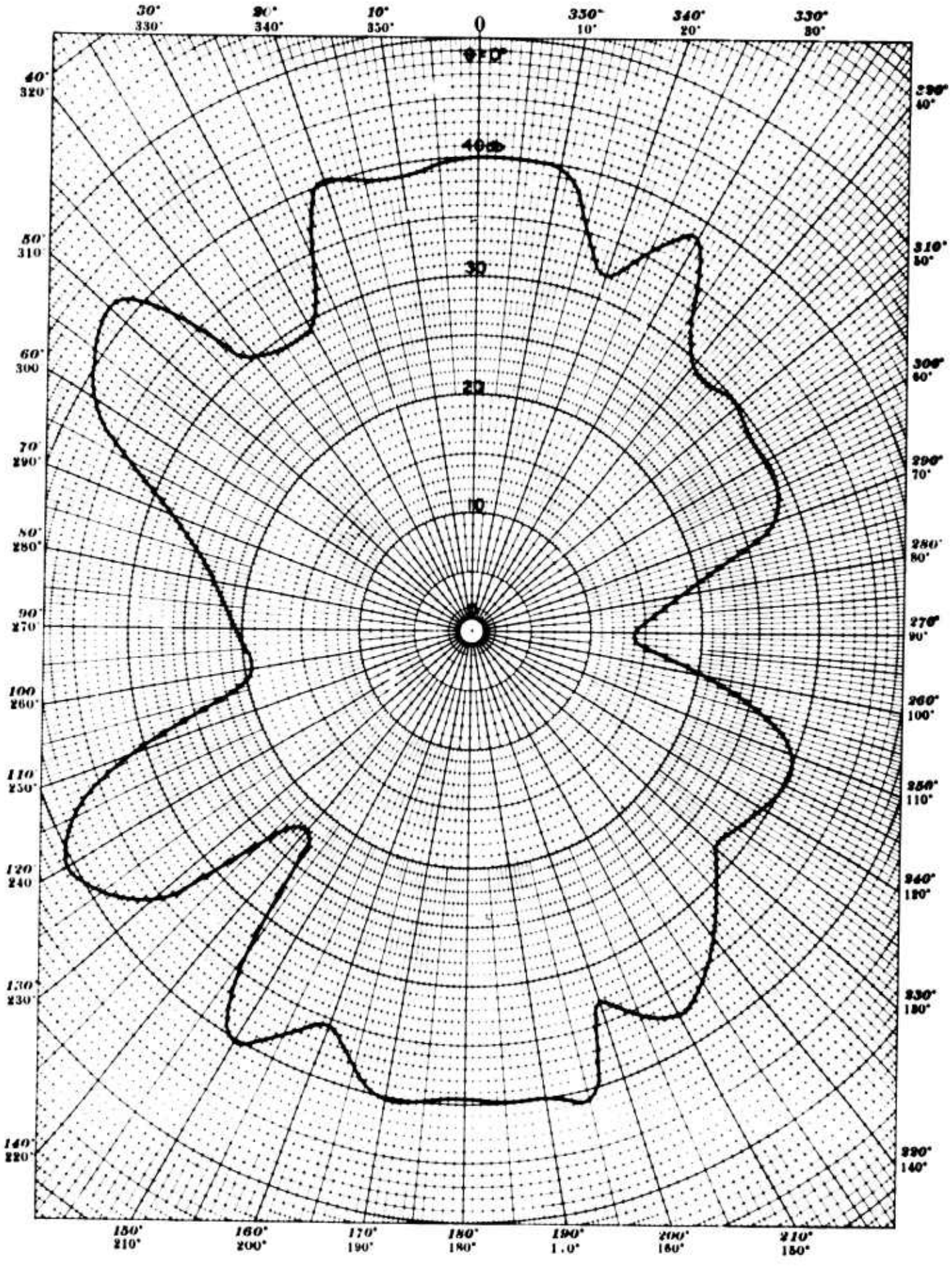

Figure 87. Directivity Pattern - Array of 12 Magnetostrictive Rings, Separation Distance between Rings = 2-1/2"

Frequency: 7600 cps—Test Distance: 5 Meters—Depth: 26.5 Meters

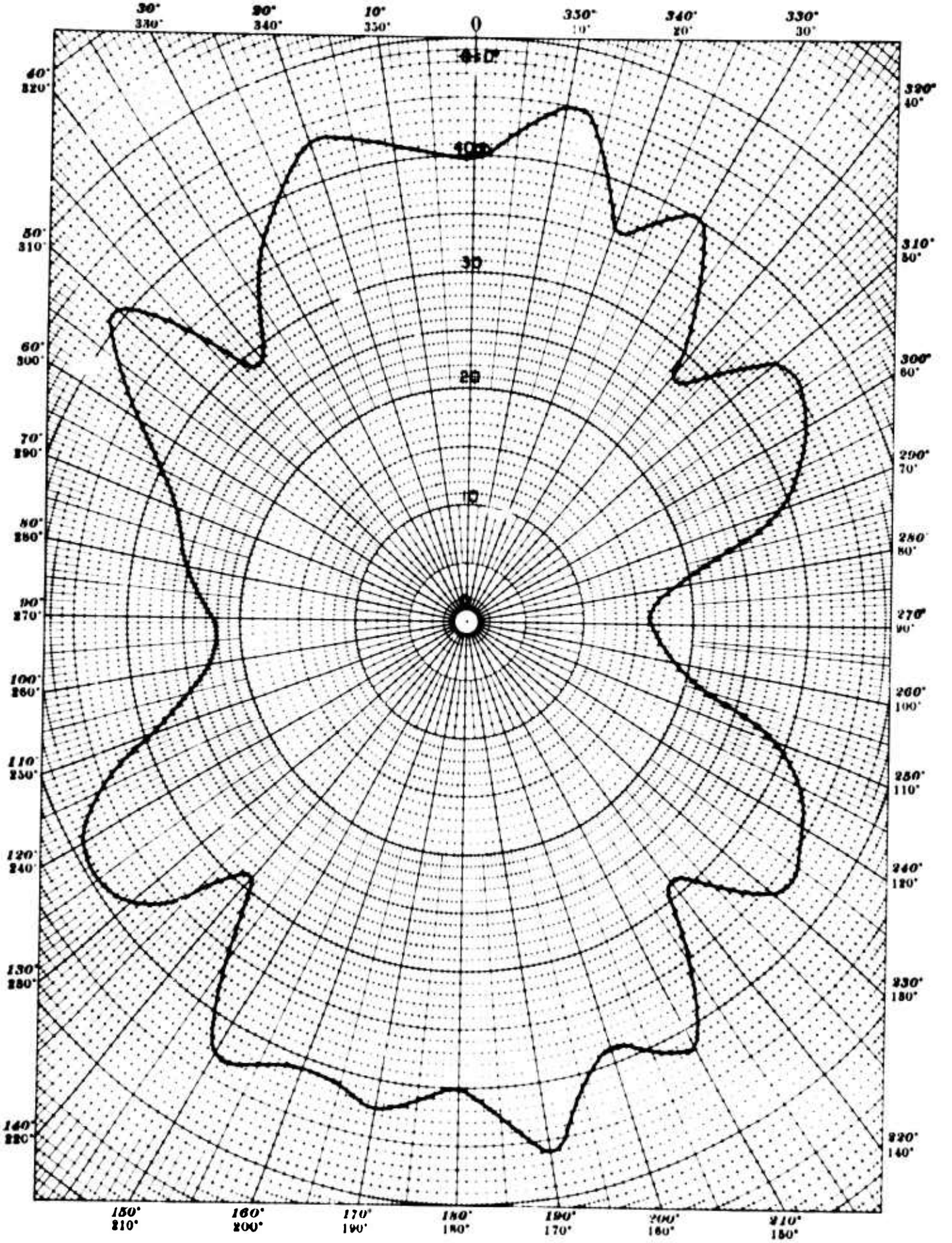

Figure 88. Directivity Pattern - Array of 12 Magnetostrictive Rings, Separation Distance between Rings = 2-1/2"

Frequency: 7800 cps—Test Distance: 5 Meters—Depth: 26.5 Meters

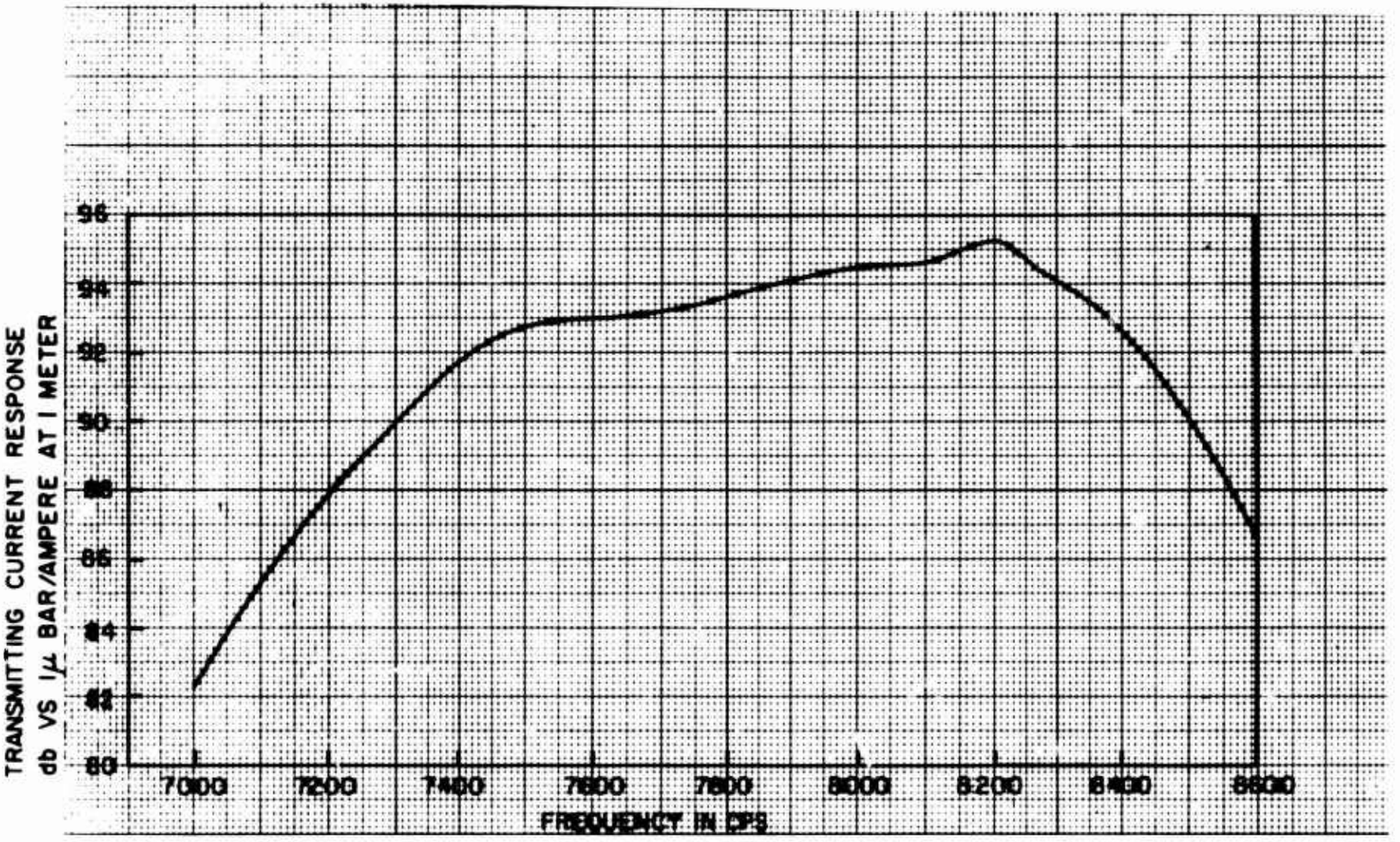

Figure 89 - Transmitting Current Response Curve 3-3 8 inch Separation between Rings. 12 Magnetostrictive Ring Array Series Connected. D.C. = 0.5 Amp.

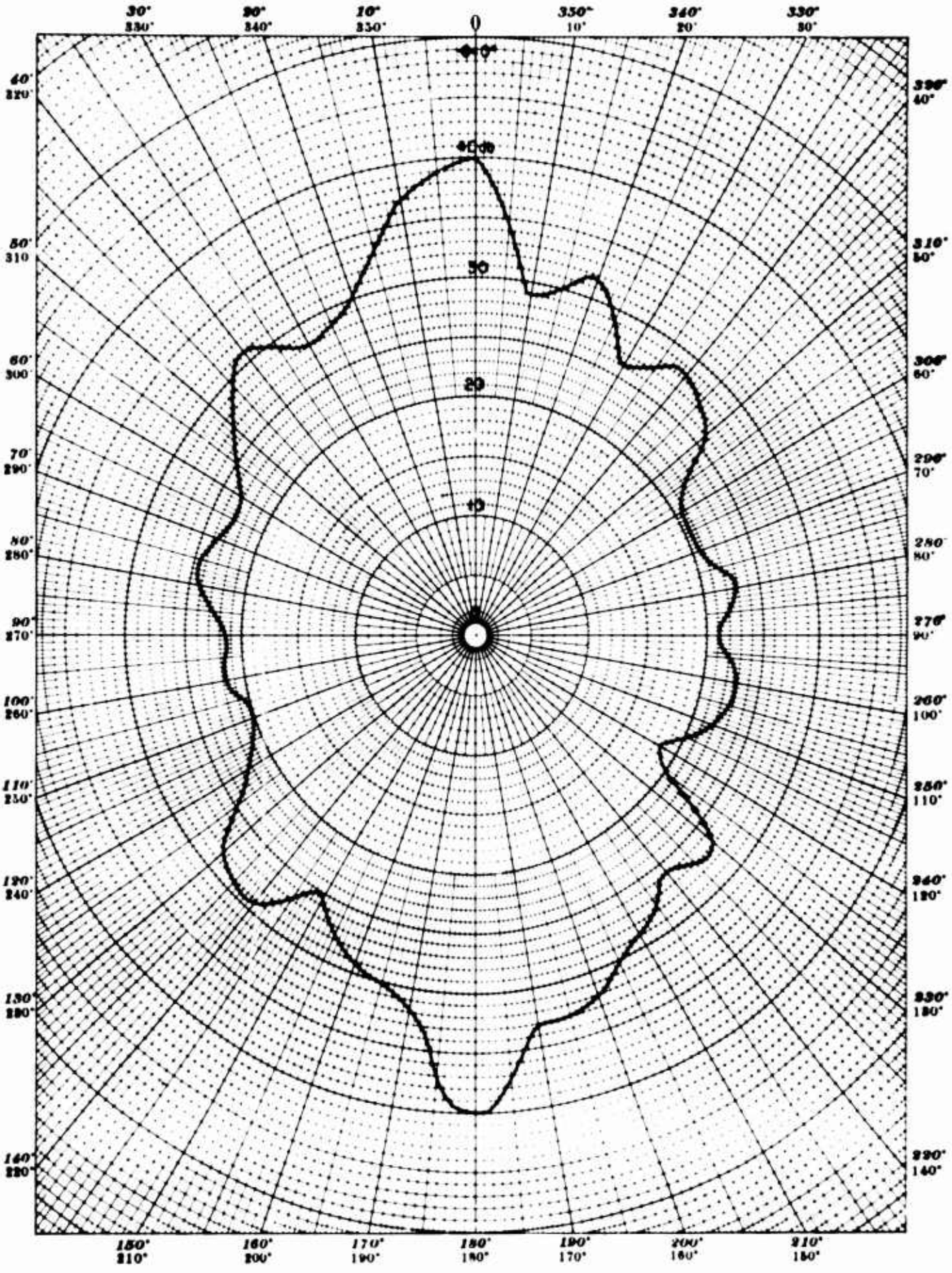

Figure 90. Directivity Pattern - Array of 12 Magnetostrictive Rings, Separation Distance between Rings = 3-3/8"

Frequency: 4100 cps—Test Distance: 5 Meters—Depth: 26.5 Meters

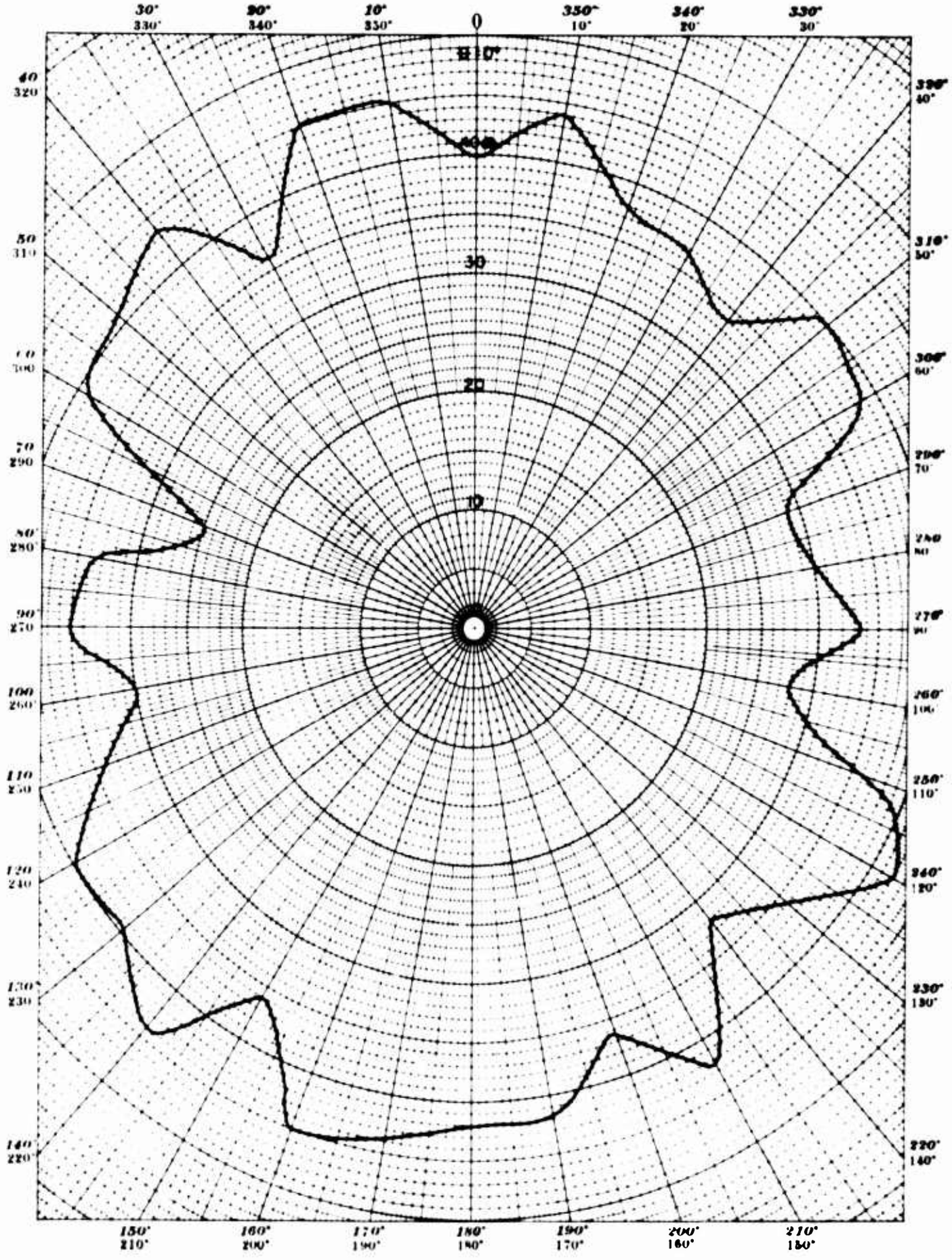

Figure 91. Directivity Pattern - Array of 12 Magnetostrictive Rings. Separation Distance between Rings = 3-3/8"

Frequency: 7500 cps—Test Distance: 5 Meters—Depth: 26.5 Meters

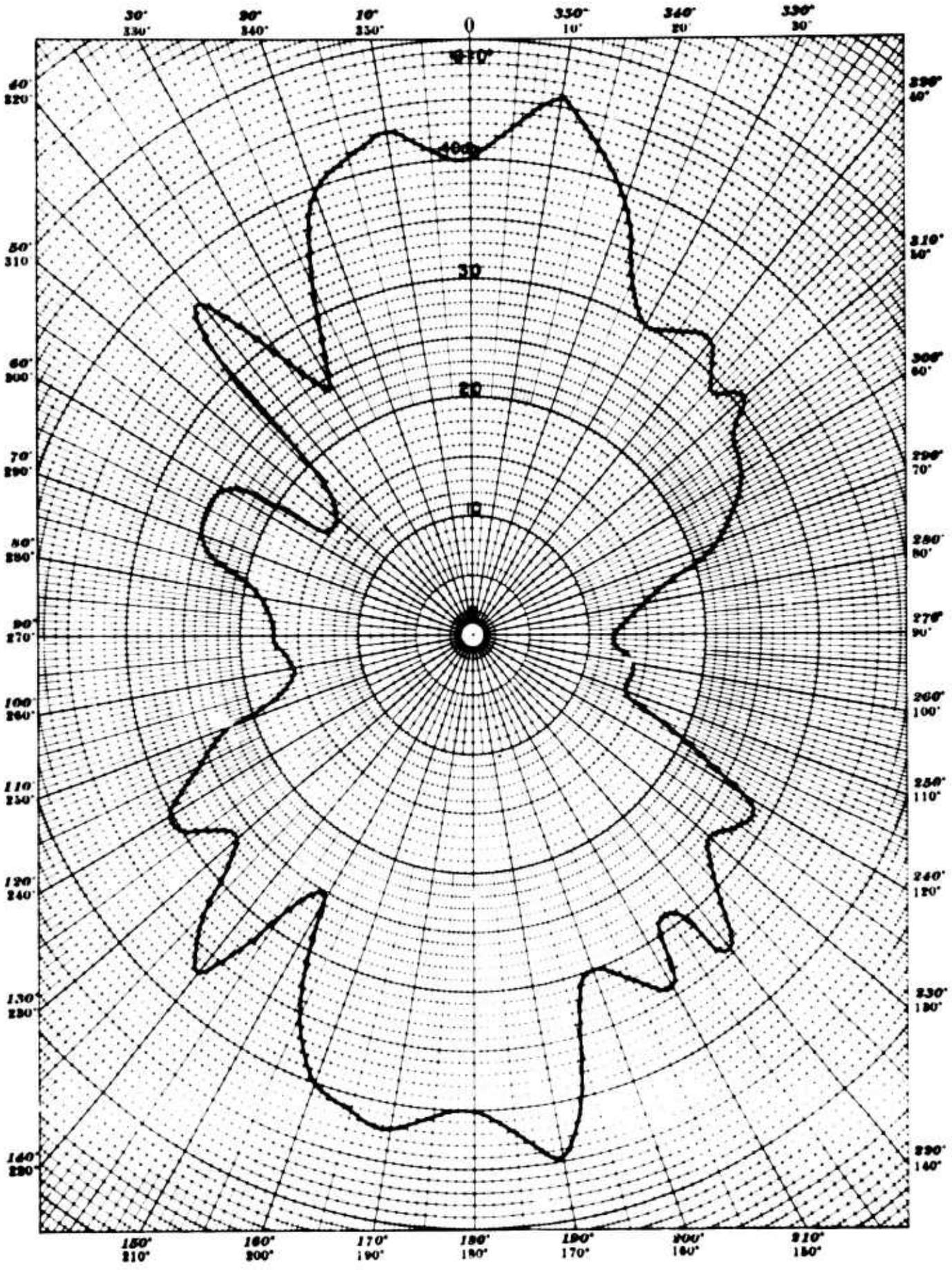

Figure 92. Directivity Pattern - Array of 12 Magnetostrictive Rings, Separation Distance between Rings = 3-3/8"

Frequency: 8200 cps—Test Distance: 5 Meters—Depth: 26 5 Meters

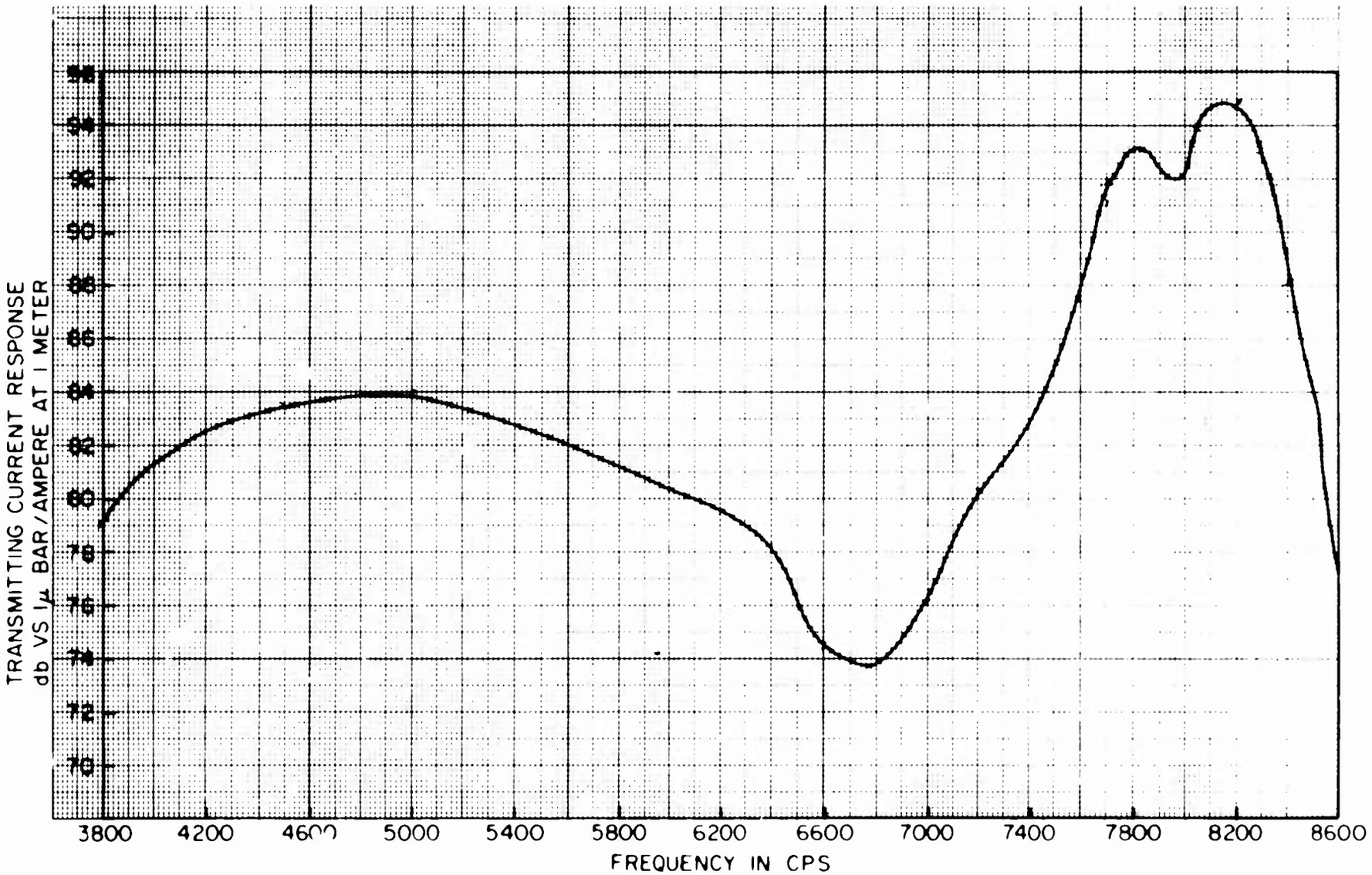

Figure 93. Transmitting Current Response Curves. 4-3/16-inch Separation between Rings. 12 Magnetostrictive Ring Array. Series Connected. D.C. = 0.5 Amp.

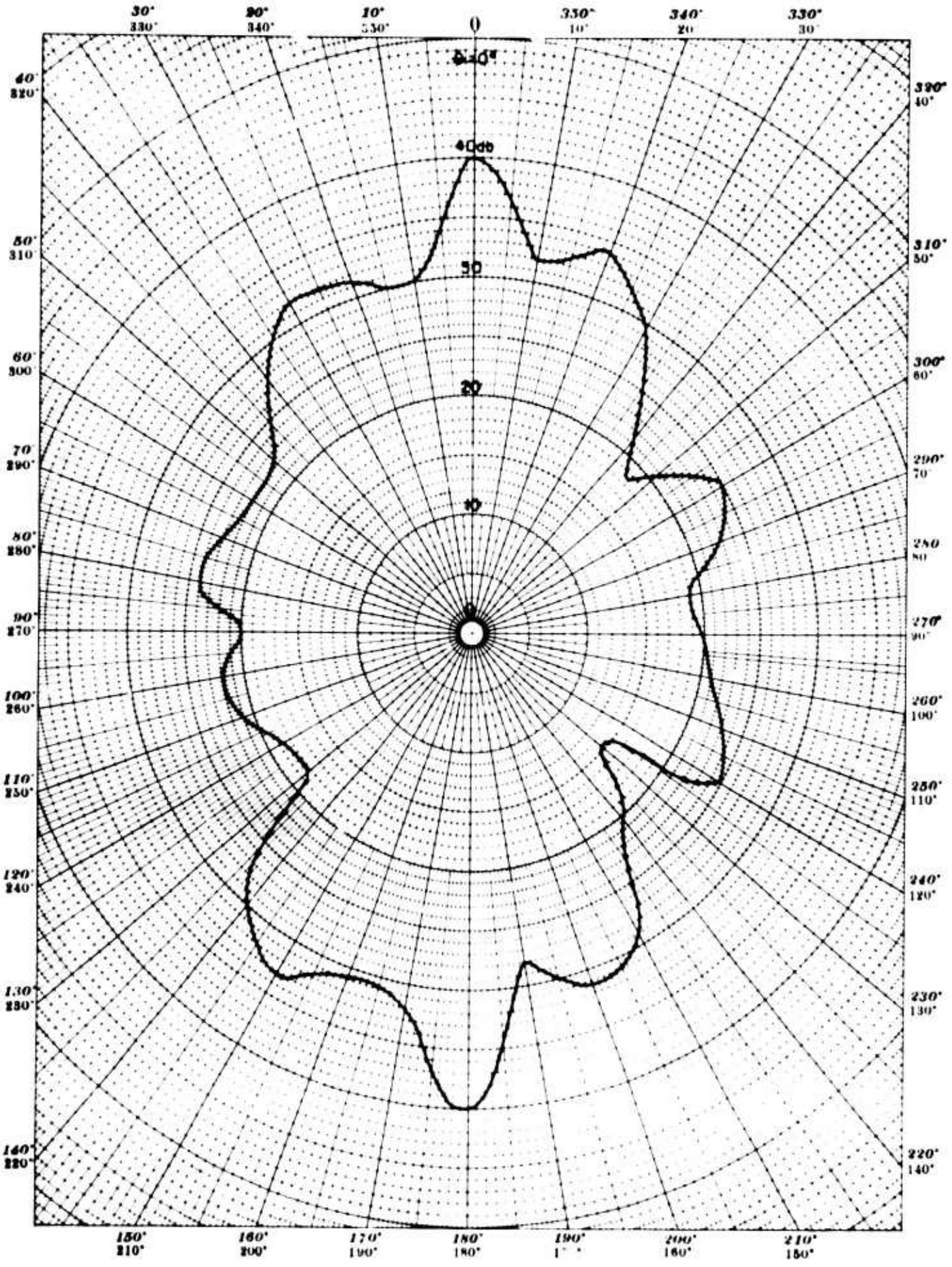

Figure 94. Directivity Pattern - Array of 12 Magnetostrictive Rings, Separation Distance between Rings = 4-3/16"

Frequency: 4400 cps—Test Distance: 5 Meters—Depth: 26.5 Meters

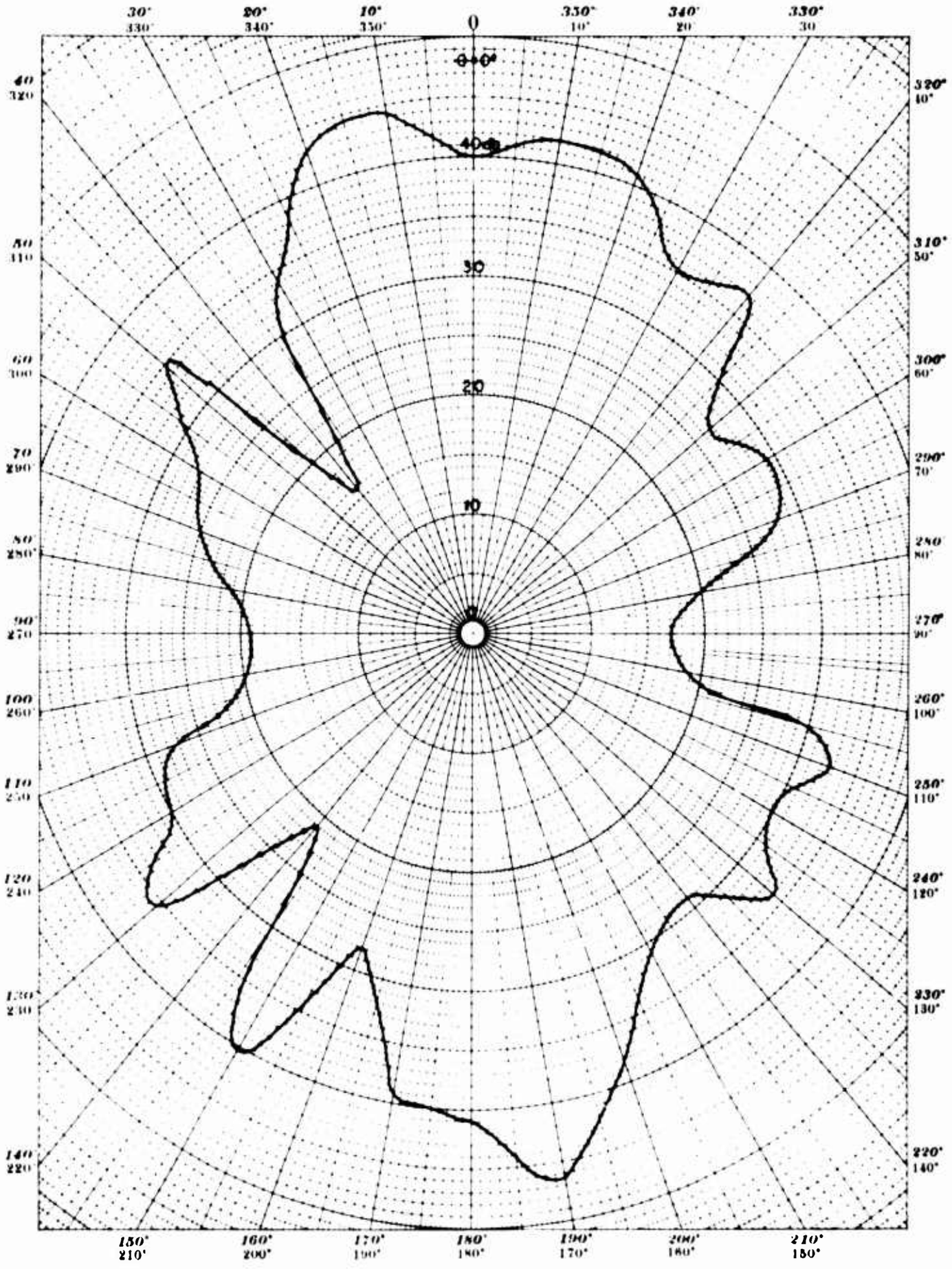

Figure 95. Directivity Pattern - Array of 12 Magnetostrictive Rings. Separation Distance between Rings = 4-3 16"

Frequency: 8200 cps—Test Distance: 5 Meters—Depth: 26 5 Meters

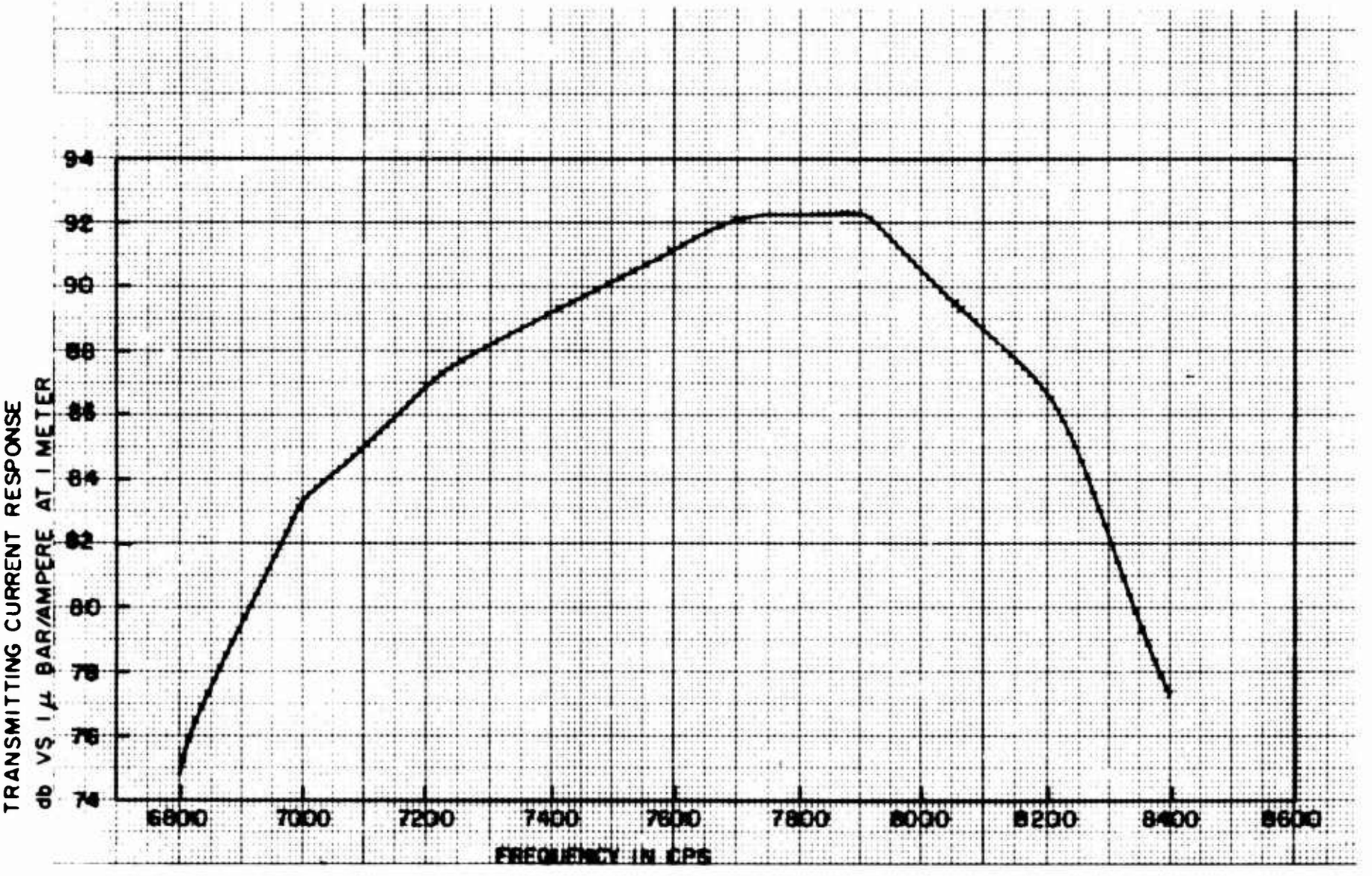

Figure 96. Transmitting Current Response Curves. 5-inch Separation between Rings. 12 Magnetostrictive Ring Array. Series Connected. D.C. - 0.5 Amp.

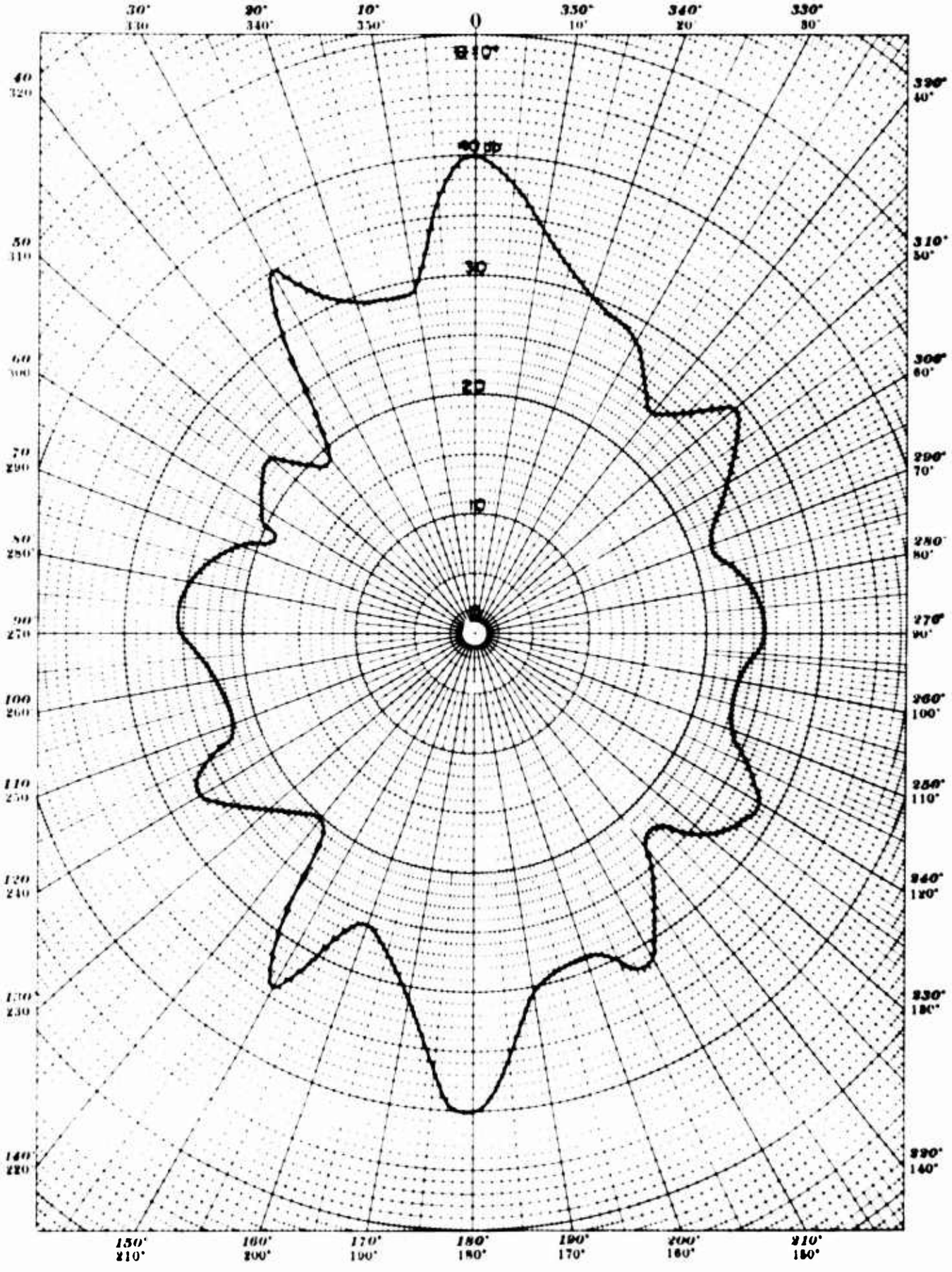

Figure 97. Directivity Pattern - Array of 12 Magnetostrictive Rings, Separation Distance between Rings = 5"

Frequency: 4400 cps—Test Distance: 5 Meters—Depth: 26.5 Meters

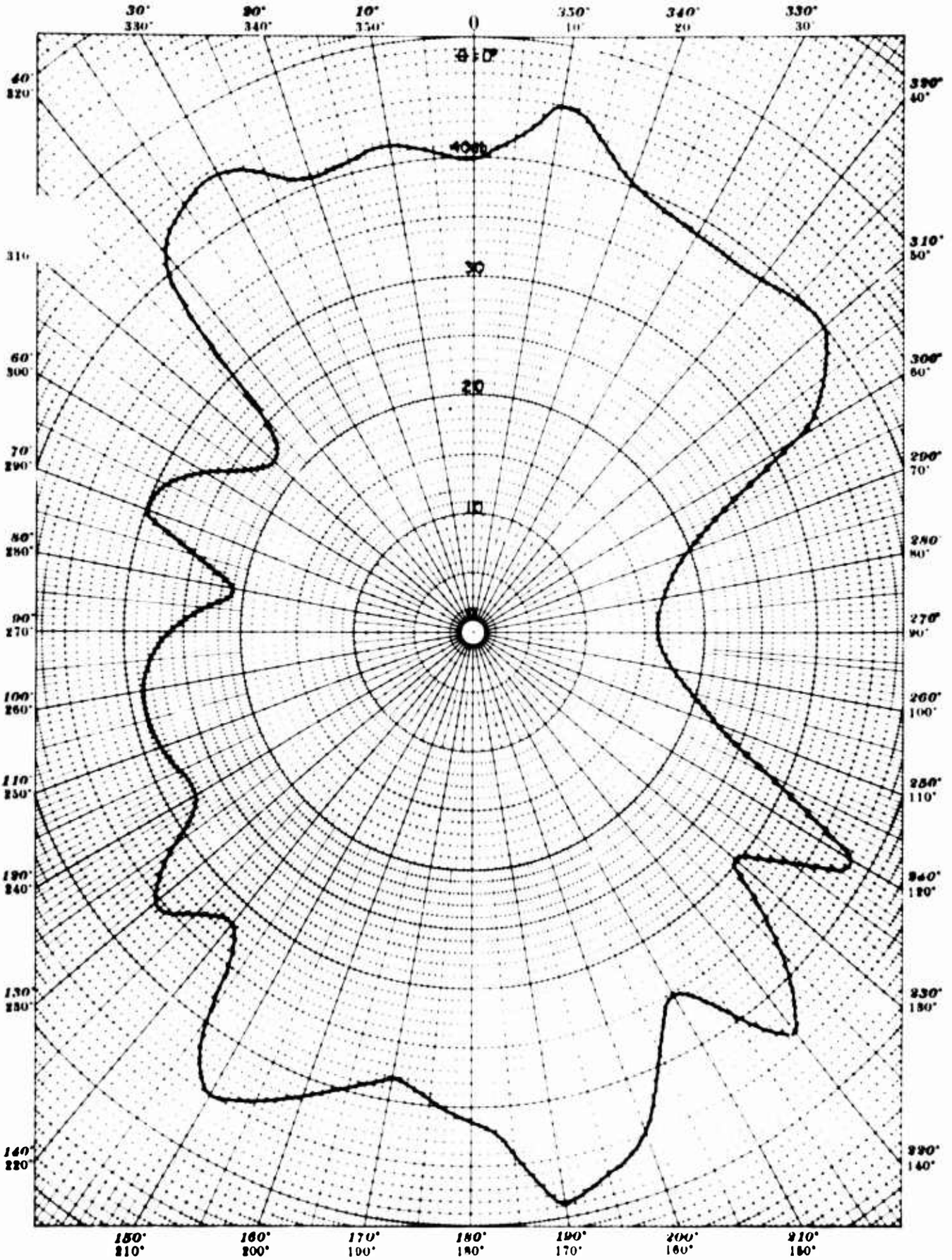

Figure 98. Directivity Pattern - Array of 12 Magnetostrictive Rings, Separation Distance between Rings = 5"

Frequency: 7800 cps—Test Distance: 5 Meters—Depth: 26 5 Meters

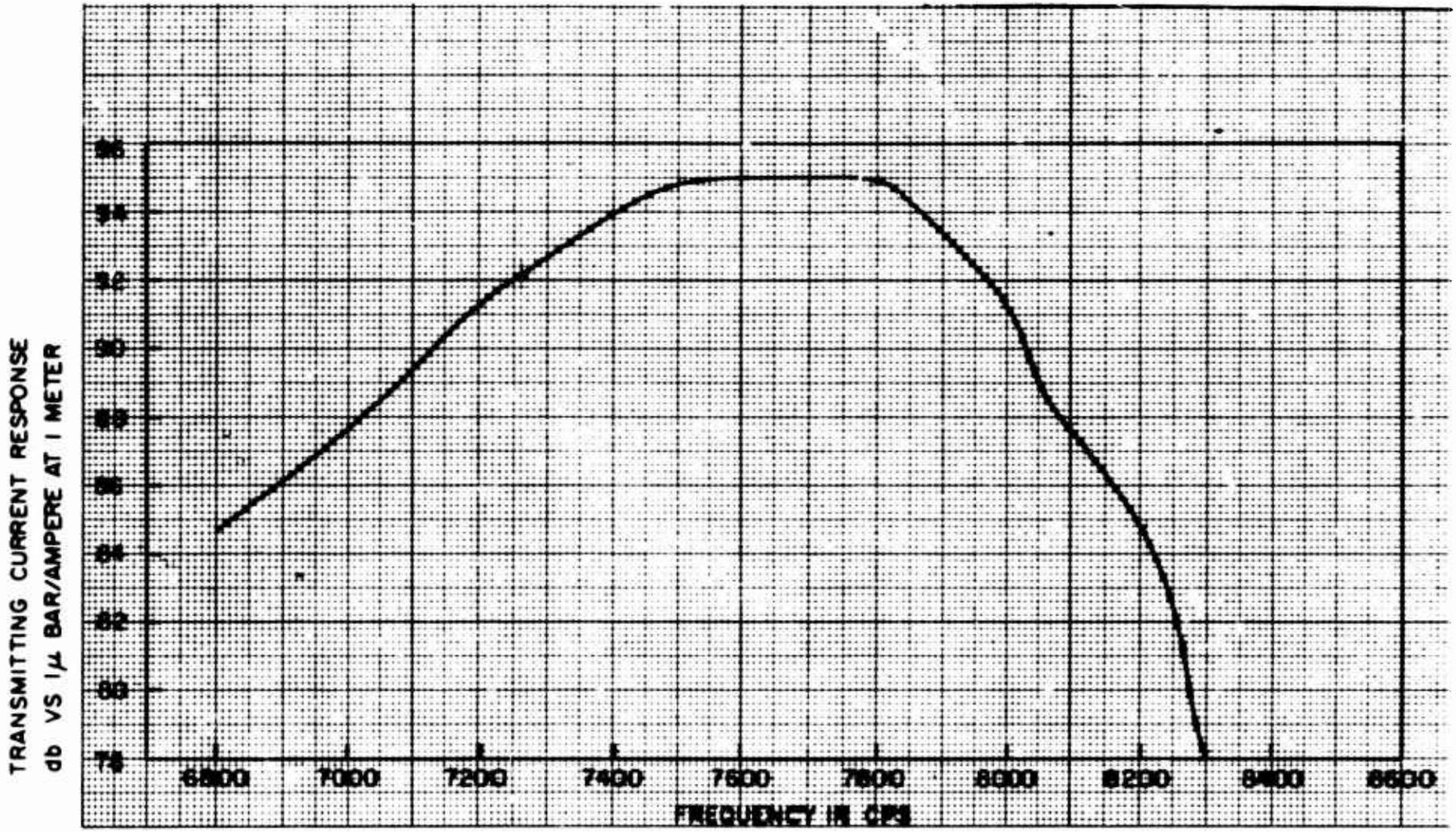

Figure 99 - Transmitting Current Response Curve 5-13/16 inch Separation between Rings. 12 Magnetostrictive Ring Array Series Connected. D.C. 0.5 Amp.

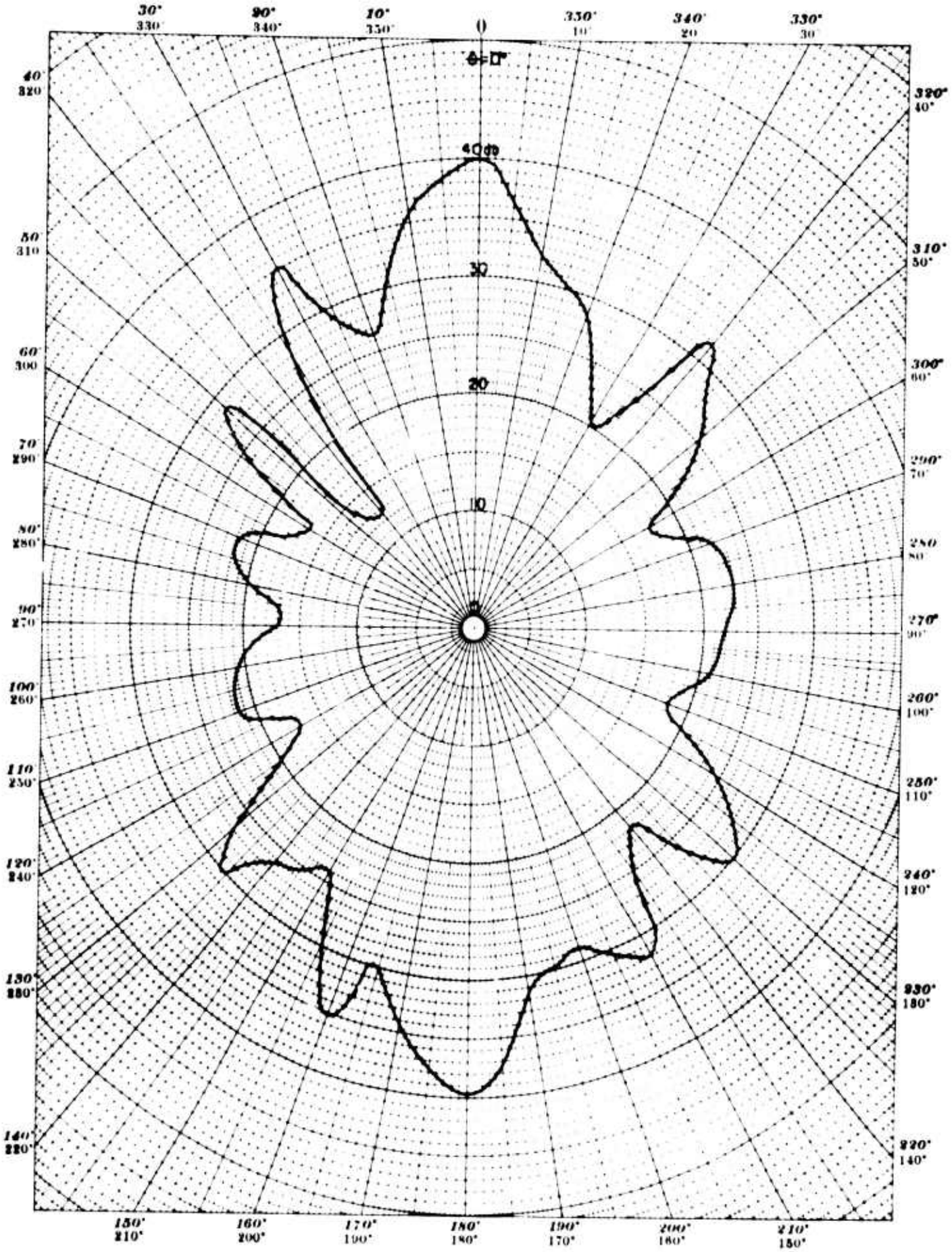

Figure 100. Directivity Pattern - Array of 12 Magnetostrictive Rings, Separation Distance between Rings - 5-13/16"

Frequency: 4400 cps—Test Distance: 5 Meters—Depth: 26.5 Meters

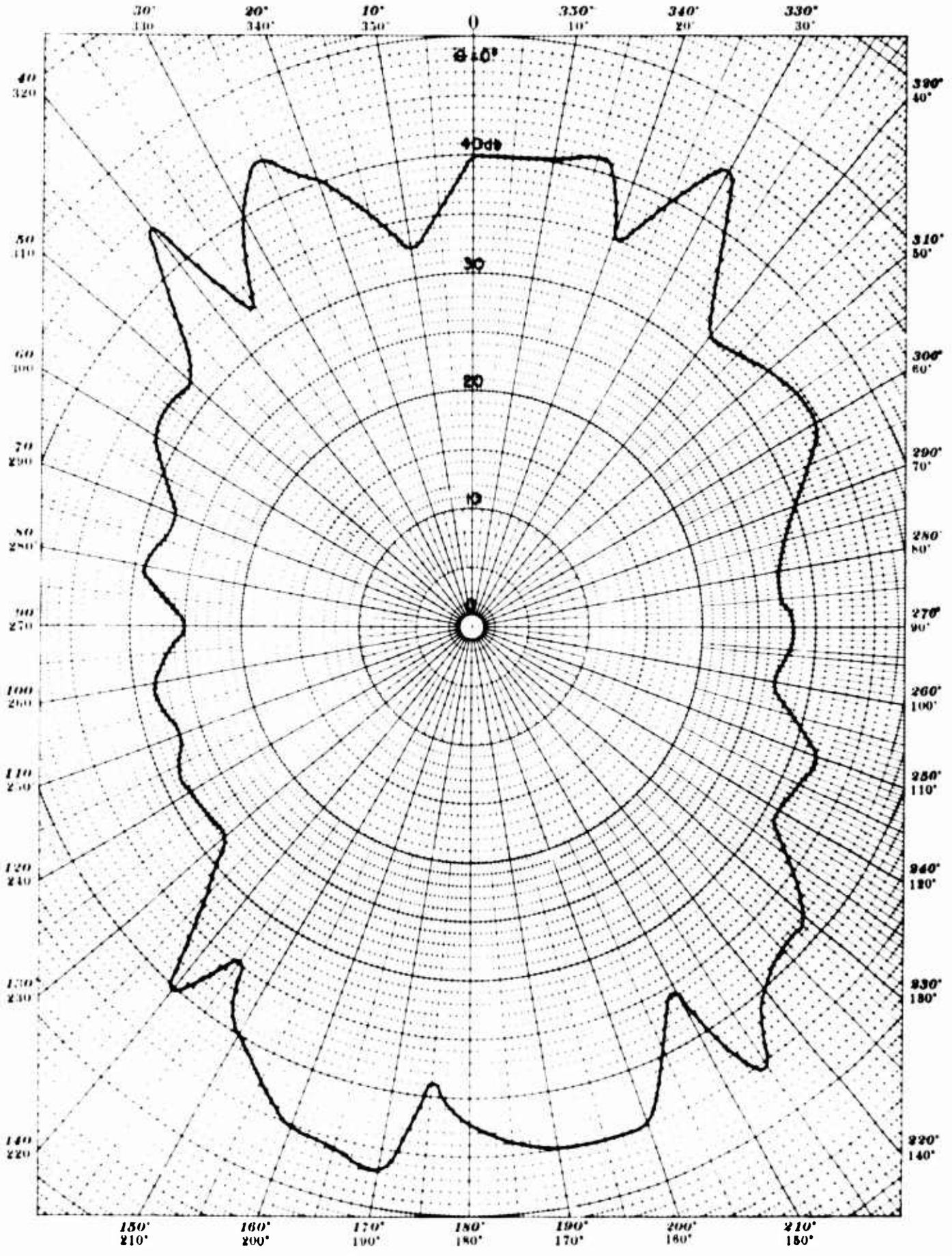

Figure 101. Directivity Pattern - Array of 12 Magnetostrictive Rings, Separation Distance between Rings = 5-13/16"

Frequency: 7600 cps—Test Distance: 5 Meters—Depth: 26.5 Meters

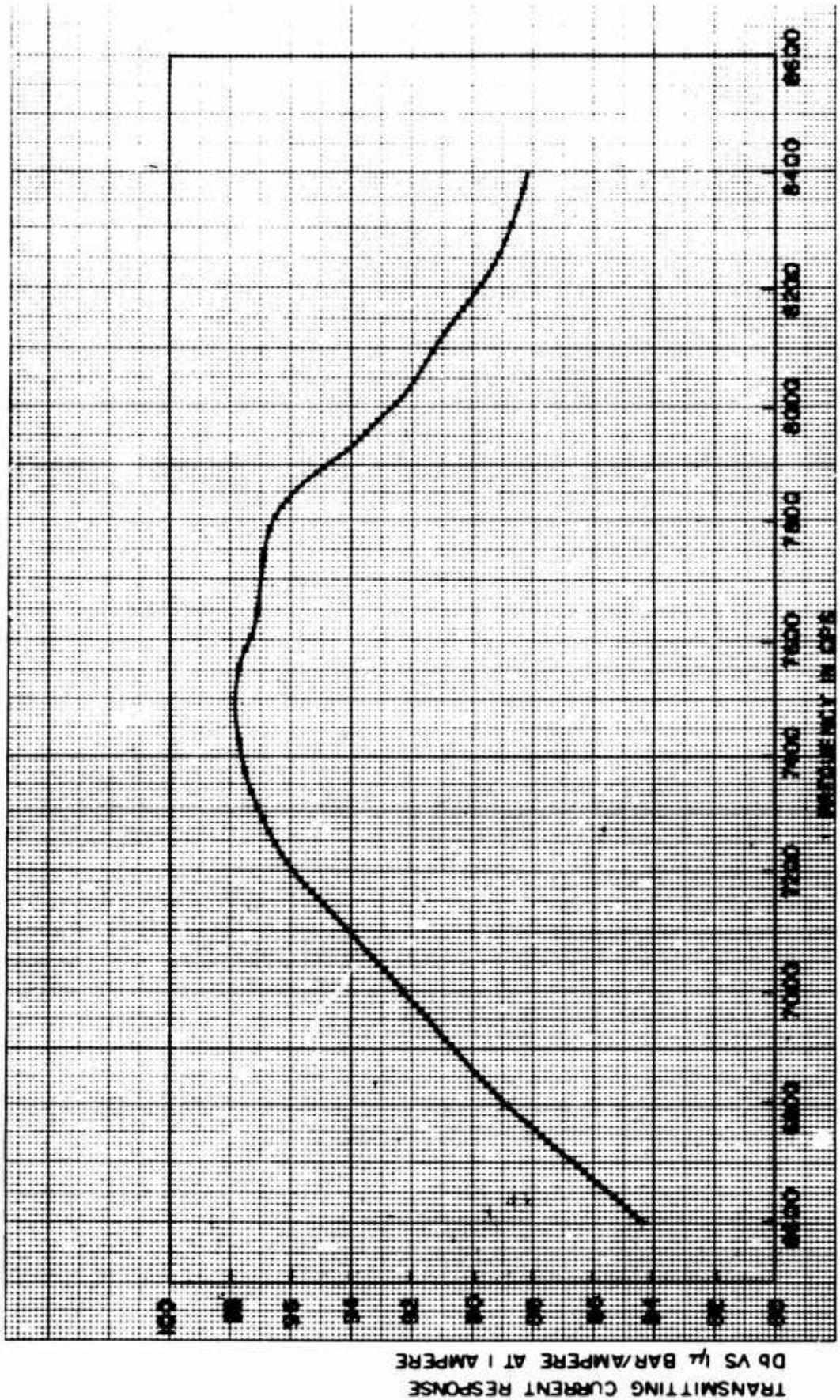

Figure 102 - Transmitting Current Response Curve 7-7/16 inch Separation between Rings. 12 Magnetostrictive Ring Array Series Connected. D.C. - 0.5 Amp.

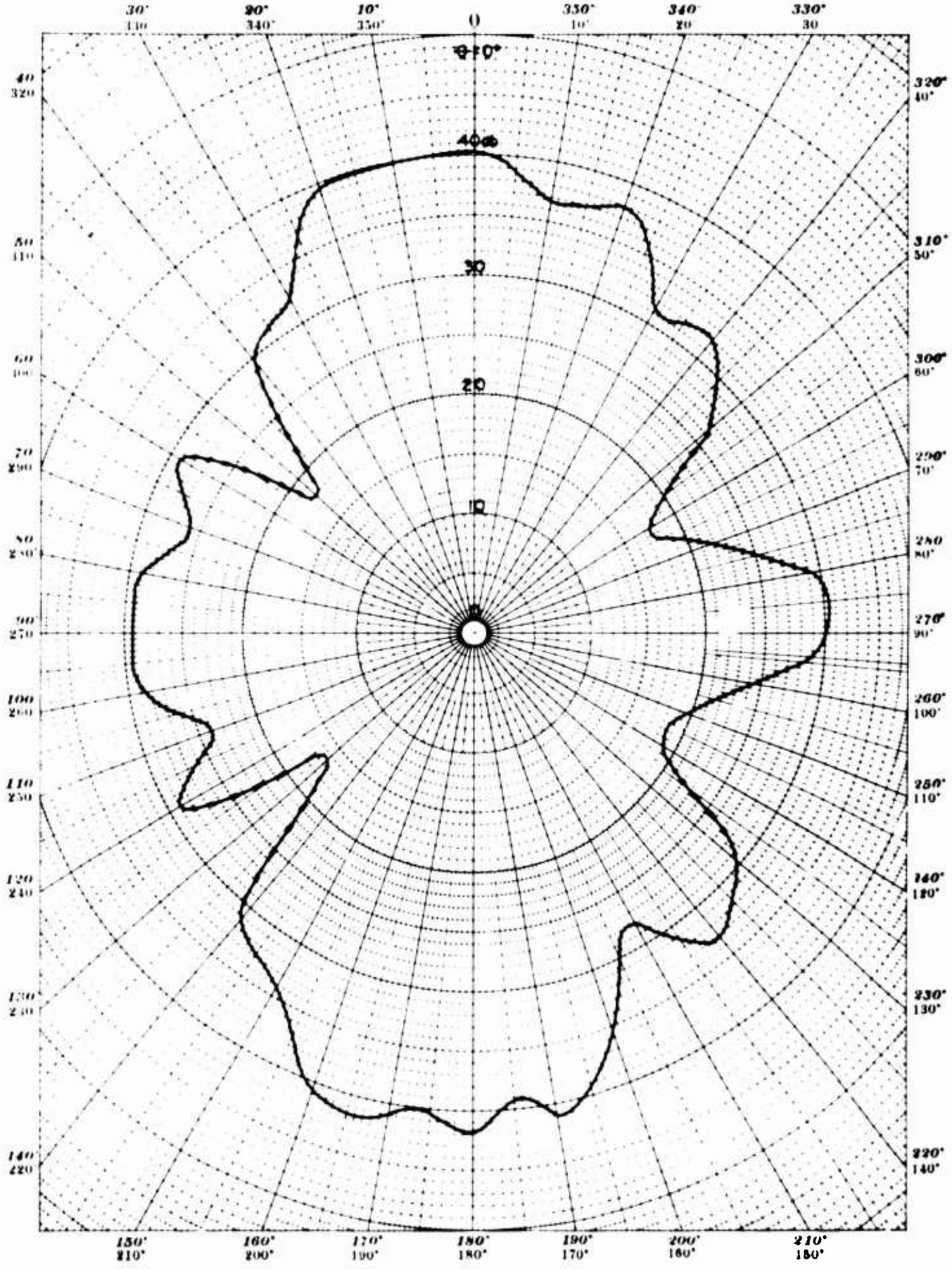

Figure 103. Directivity Pattern - Array of 12 Magnetostrictive Rings, Separation Distance between Rings = 7-7/16"

Frequency: 4400 cps—Test Distance: 5 Meters—Depth: 26.5 Meters

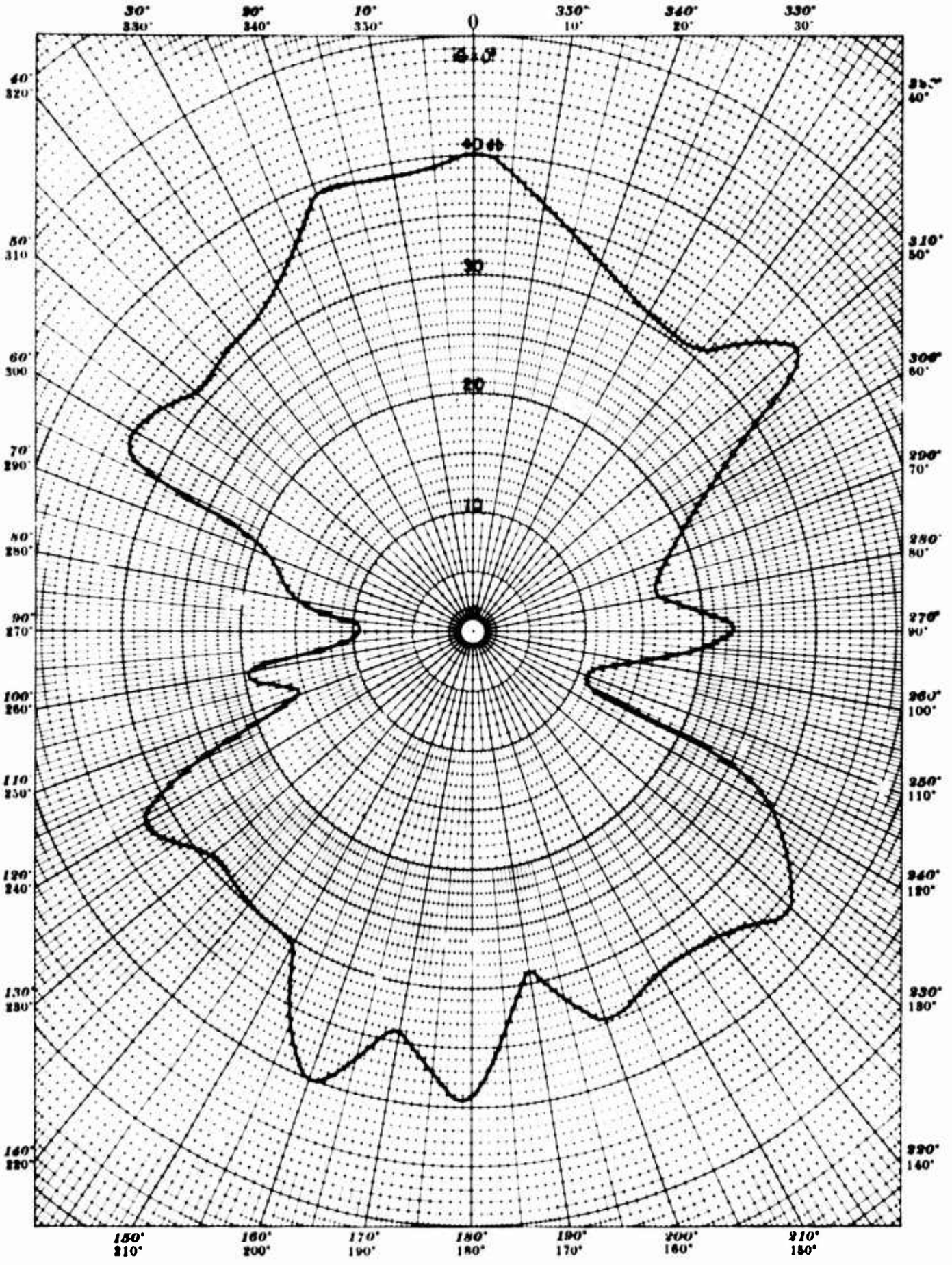

Figure 104. Directivity Pattern - Array of 12 Magnetostrictive Rings, Separation Distance between Rings = 7-7/16"

Frequency: 7350 cps—Test Distance: 5 Meters—Depth: 26.5 Meters

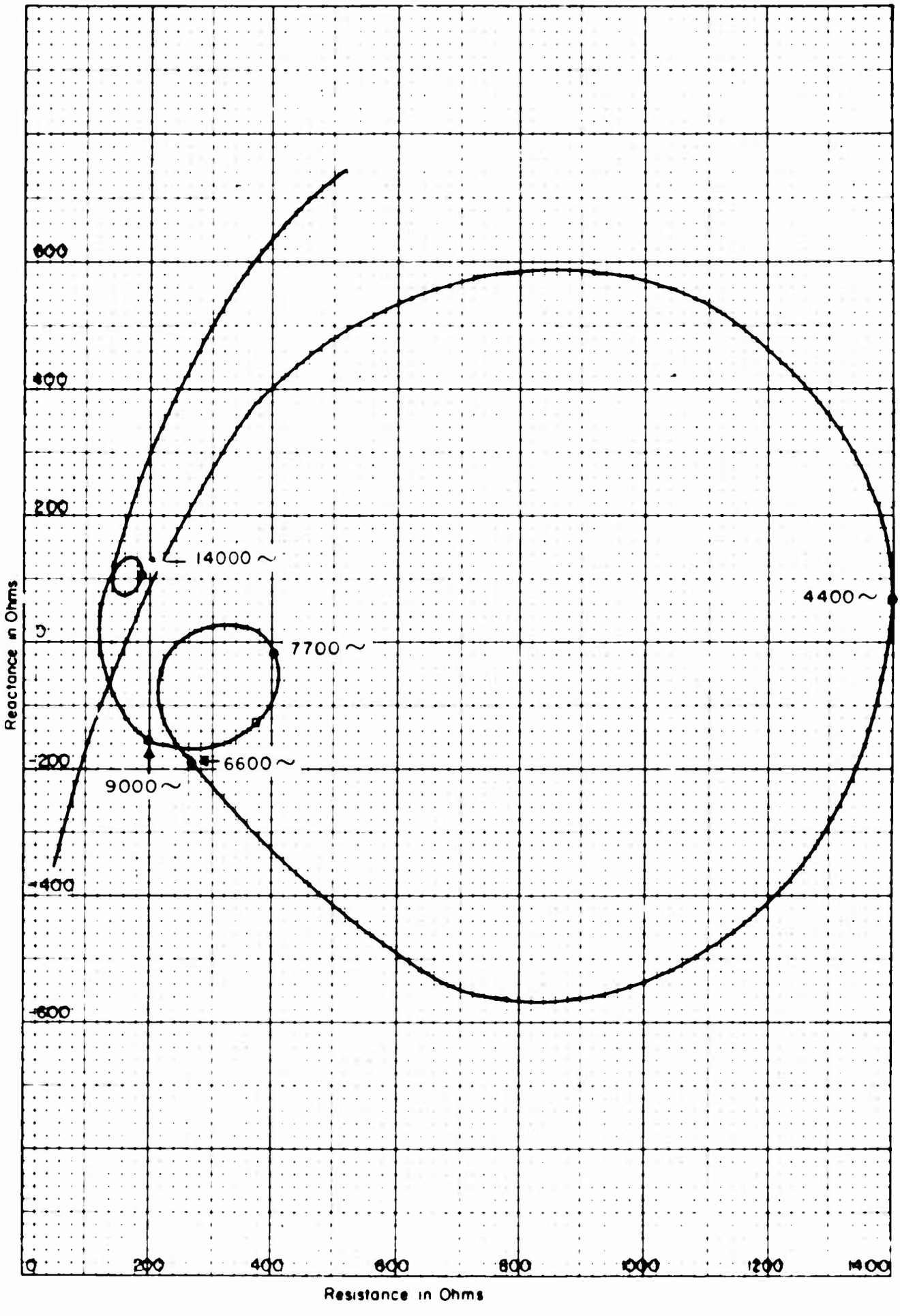

Figure 105 - Impedance Circle - 12 Ring Array - 1-3 4 inch Separation Between Rings

REFERENCES

(1) Camp, L., "Properties of Cylindrical Arrays of Circular Rings"; 65th Meeting of Acoustical Society of America; New York City

(2) Summary Technical Report of Division 6 National Defense Research Committee, Vol. 13, Page 15, Washington, D. C. (1946)

(3) American Standard, Acoustical Terminology, Pg 29, American Standards Association, 10 East 40th St., New York (16), N. Y.